Characterisation and modulation of patterning of mammalian epidermis

Violeta Silva-Vargas

A Thesis submitted for the degree of
Doctor of Philosophy
University College London
2006

ProQuest LLC
789 East Eisenhower Parkway
P.O. Box 1346
Ann Arbor, MI 48106-1346

Declaration

I, Violeta Silva-Vargas, confirm that the work presented in this thesis is my own. Where information has been derived from other sources, I confirm that this has been indicated in the thesis.

Summary

The epidermis is maintained by proliferation of stem cells and differentiation of their progeny. In my PhD thesis I have studied the mechanisms by which these processes are compartmentalised.

β-catenin levels determine lineage commitment in the epidermis. I investigated the role of β-catenin in patterning of the epidermal stem cell compartment and its niche during de novo hair follicle formation. For this I used K14ΔNβ-cateninER transgenic mice. I found that the levels of β-catenin activation determine the number and location of ectopic hair follicles, showing that follicle formation is a threshold-response event. To dissect the downstream effects of β-catenin signalling, I performed microarray analysis and saw that the Hedgehog pathway is upregulated by β-catenin activation. Inhibition of Hedgehog signalling attenuates the effects of β-catenin.

The array also revealed that β-catenin regulates the Eph/ephrin protein family. I found that several ephrin-B ligands and EphB receptors are expressed in distinct zones in mouse skin. In order to study the mechanisms modulating epidermal niche patterning I have analysed EphB2, EphB3 and ephrin-B1 null epidermis. EphB/ephrin-B signalling controls hair follicle spacing, patterning along the radial follicle axis, interfollicular epidermal differentiation and melanocyte localisation. Disruption of EphB/ephrin-B signalling disturbs proliferation, uncoupling expression of K15, CD34 and clonal growth capacity. In culture keratinocytes that differ in EphB/ephrin-B expression segregate from one another, reflecting differences in cell shape, motility and integrin expression. EphB3 and ephrin-B1 are induced on activation of β-catenin and augment β-catenin induced cell clustering. Conversely, EphB/ephrin-B signalling negatively regulates β-catenin activation. Ephrin-B/EphB signalling is a key determinant of epidermal pattern, proliferation and differentiation. In summary, I have elucidated the role of β-catenin, Hedgehog and EphB/ephrin-B signalling in regulating epidermal proliferation, differentiation and morphogenesis.

Para Sebas,

mis padres, mi hermana

y la familia

TABLE OF CONTENTS

Chapter 3- Characterisation of patterning in tail epidermis

Chapter 6- EphB/ephrin-B signalling determines hair follicle patterning

Chapter 7- Mechanisms of Eph/ephrin signalling

Chapter 8- Final Discussion

List of figures

List of Tables

Abbreviations

4OHT	4-hydroxytamoxifen
AM12	gag pol + envAM12 packaging cells
APC	adenomatous polyposis colon
BAMBI	BMP and activin membrane-bound inhibitor
BM	basement membrane
BMP	bone morphogenetic protein
BrdU	5' bromodeoxyuridine
BSA	bovine serum albumin
cDNA	copy deoxyribonucleic acid
CDP	CCAAT displacement protein
cRNA	copy ribonucleic acid
CRUK	Cancer Research UK
C-term	carboxy terminus
DAB	3,3-diaminobenzedene tetrahydrochlodride
DC	dermal condensate
DCS	donor calf serum
Dkk	Dickkopf
DMEM	Dulbecco's modification of Eagles' medium
DMSO	dimethyl sulfoxide
dNTP	deoxynucleotide triphosphate
DP	dermal papilla
DTT	dithiolthreitol
E	embryonic day
ECL	enhanced chemiluminescence
ECM	extracellular matrix
EDTA	ethyldiaminotetraacetic acid, disodium salt
EGF	epidermal growth factor
ER	oestrogen receptor
ERK	extracellular signal-regulated kinase
EST	expressed sequence tag
FAD	F12 + adenine + DMEM
FCS	fetal calf serum
GFP	green fluorescent protein
GSK3-β	glycogen synthase kinase 3-β
H&E	haematoxylin and eosin staining
HBS	HEPES buffered saline
HEPES	N-[2-hydroxyethyl]piperazine-N'-[2-ethanesulphonic acid]
HES	Hairy and Enhancer of Split
HF	hair follicle

HICE	hydrocortisone, insulin, cholera enterotoxin and EGF
HLH	helix loop helix
HMG	High Mobility Group
HRP	horseradish peroxidase
HS	hair shaft
HSC	haematopoietic stem cell
IFE	interfollicular epidermis
Ig	immunoglobulin
IRS	(hair follicle) inner root sheath
JNK	Jun N-terminal kinase
K	keratin
K14	keratin 14
KGF	keratinocyte growth factor
LDL	low density lipoprotein
Lef	lymphoid enhancer factor
LRC	label retaining cell
LRP	LDL-receptor related protein
mRNA	messenger ribonucleic acid
Myc	c-Myc
NFkB	nuclear factor kB
N-term	amino terminus
ORS	(hair follicle) outer root sheath
P	postnatal day
PBS	phosphate-buffered saline
PBST	PBS/Tween
PCR	polymerase chain reaction
PEG	primitive epidermal germ
pen/strep	penicillin/streptomycin
PKC	protein kinase C
Ptc	Patched
RAR	retinoic acid receptor
RNase	ribonucleic acid endonuclease
rpm	revolutions per minute
SC	stem cell
SDS	sodium duodecyl sulphate
S.E.	standard error
SG	sebaceous gland
Shh	Sonic hedgehog
SSC	salt sodium citrate buffer
TAC	transit amplifying cell
TBS	Tris-buffered saline
TBST	TBS/Tween
TCF	T cell factor
TD	terminally differentiated cell
TE	Tris-EDTA buffer

TG/tg	transgenic
TGF	transforming growth factor
TM	transmembrane domain
VDR	vitamin D receptor
WIF	Wnt inhibitory factor
Wnt	mammalian homologue of Wingless
WT/wt	wild type

Acknowledgements

I would like to thank everybody who gave me advice, help and support and have made these pages and years possible!

First of all, I would like to thank Fiona for introducing me to the science world and for giving me this great opportunity to take part of this amazing adventure for the past 4 years.

I would like to start by thanking the past/present members of the Keratinocyte lab (already very many) that have made my time as a 'keratinocyte' memorable. Specially, the other night owls of the lab, Maruta, Lisa, Hector and Josema. 'Que os voy a decir que no sepais ya'! To my baymaties, Rachida, Manela and Simon and before Teresa and Robin and to my other long-term companions Soline, Salva, Ela, Paul and Carrie. I would like to thank Catherine Niemann with whom I did my first whole mount and David Owens for introducing me to world of genotyping during my first months in the lab. To Ro for the greatest teachings on cockney accent! Cheers meaty!

I would also like to thank my great neighbours Susana, Linda and Nando, for always being there!

I would like to thank my collaborators Cristina, Kristin, Adam, Tyler for very long hours of work and thinking with the 'hairy mouse', and Susanne and Ralf Adams and the people in their lab for providing all the mutant mice and advise in the ephrins world.

I would also like to thank Dr Misuzu Seo who inspired me when I was beginning to learn how to make minipreps in Japan.

A very big thank you and muchas gracias to my parents, my sister and my friends for all the support that they always give me. They have really accompanied me and supported me all the time. And Sebas, my love and my life, makes my every day.

Chapter 1- Introduction

Aims

During embryonic development and throughout adulthood a tissue is maintained by replacing the differentiated or damaged cells by new ones and an interplay of pathways is essential to couple differentiation and proliferation to properly maintain the homeostasis of this tissue. The main focus of this study is to use the skin as an experimental model in which to study hair follicle morphogenesis and patterning.

In this Chapter, I will describe how the epidermis and its appendages are structured, how they develop during embryogenesis and how they are maintained through adult life. I will also outline recent advances in the characterisation of the epidermal stem cell compartment and the hair follicle niche. In addition, I will also describe the role of the key pathways involved in regulating and patterning the epidermal stem cell compartment.

1.1- Introduction to the epidermis

The epidermis forms the protective outer covering of mammalian skin providing protection against environmental insults and dehydration, and is an important gateway for sensory input (Millar, 2005). This multilayered epithelium consists of the interfollicular epidermis (IFE) and associated adnexal structures, including the hair follicle and sebaceous and sweat glands (See Figure 1.1).

1.1.1- Development of the epidermis and its appendages

1.1.1.1-Establishment of the stratified skin epithelium

Adult epidermis is a stratified squamous multilayered epithelium in which cells at the basal layer are mitotically active and produce and secrete the extracellular matrix that makes up for the basement membrane (BM) that separates the epidermis from the dermis and the suprabasal layers (Blanpain and Fuchs, 2005; Watt, 2002). At embryonic day (E) E12, the future epidermis consists of a single layer of basal cells of the ectoderm. Between E14 and E17 the stratification process starts and by E18 a fully stratified interfollicular epidermis (IFE) is completed (See Figure 1.2).

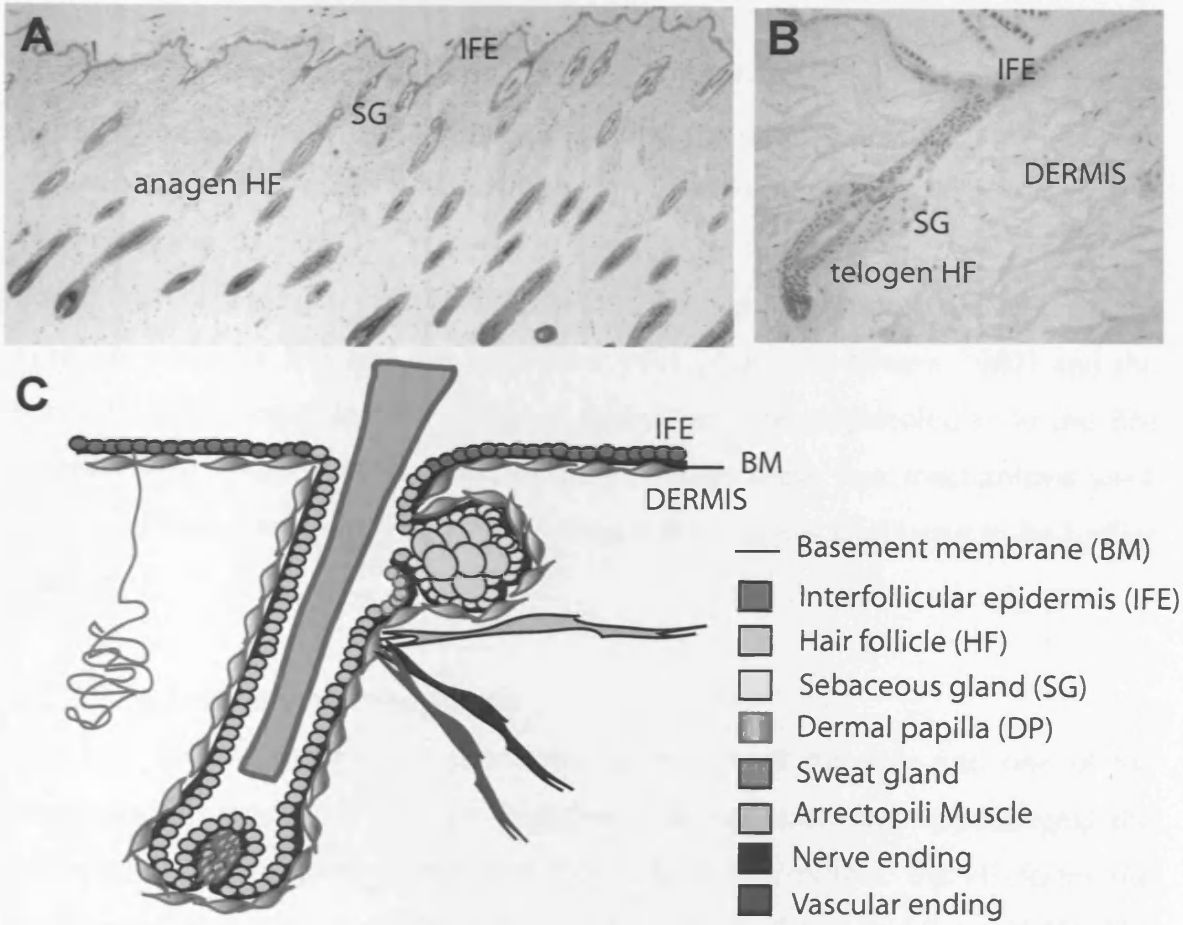

Figure 1.1- Structure of adult mouse skin . (A and B) Sections of mouse back skin stained with haematoxylin&eosin. The main structures are indicated: the interfollicular epidermis (IFE), the anagen hair follicle (HF) in A and telogen HF in B and the sebaceous glands (SG). (C) Schematic diagram representing-adult skin. This consists of, in the upper side the multilayered epidermis, including the IFE and its adnexal appendages the SG, the HF and the sweat gland, next the basement membrane and in the innermost side the dermis, including the dermal cells, the dermal papilla encased at the base of the HF, the arrector pili muscle and the nerve and vascular endings.

Basal cells in the IFE are rich in the α3β1 and α6β4 integrins (Watt, 2002). As basal cells become committed to differentiate, they withdraw from the cell cycle, downregulate integrin expression and they leave the basal layer by moving upwards into the first suprabasal layer to start the programme of terminal differentiation (Watt, 2002). Three types of suprabasal layers can be distinguished: spinous, granular and the stratum corneum (Figure 1.2). Committed cells go through the spinous layer and the granular layer where the programme is further ongoing and finally they become enucleated and flattened when they reach the cornified layer. Finally, squames are shed from the outermost layer, the surface of the skin. Cells that move upwards from the inner layers are constantly replacing shed cells (Figure 1.2).

Basal cells contribute to stratification by two mechanisms: one loosening its contacts with the BM and the neighbour cells (Watt and Green, 1982) and the second one by orienting the plane of mitotic spindle perpendicular to the BM (Lechler and Fuchs, 2005; Smart,1970). Although these two mechanisms were first described a long time ago the molecular basis is just beginning to be further studied.

1.1.1.2-Hair follicle morphogenesis

The hair follicle is the most prominent miniorgan of the skin and one of the features of mammalian species; together with its associated appendages, the sebaceous and apocrine glands and the arrector pili muscle, the HF forms the main component of the pilosebaceous unit (Schmidt-Ullrich and Paus, 2005). The apocrine glands are generated only in non hair-bearing regions. The process of hair follicle morphogenesis arises as a result of a very complex interplay between epidermis and dermis that starts at E13 (See Figure 1.2 and 1.3 for details) and can be divided into three stages: **induction**, **organogenesis** and **cell differentiation** (Schmidt-Ullrich and Paus, 2005). The main signalling pathways involved in this process are shown in Figure 1.3.

The first stage of the **induction** of HF formation, starts with a gradient of inductive signals originating from the epidermis and the dermis in which the message 'make an appendage' is set up by E13 (See Diagram in Figure 1.3). The Wnt/β-catenin

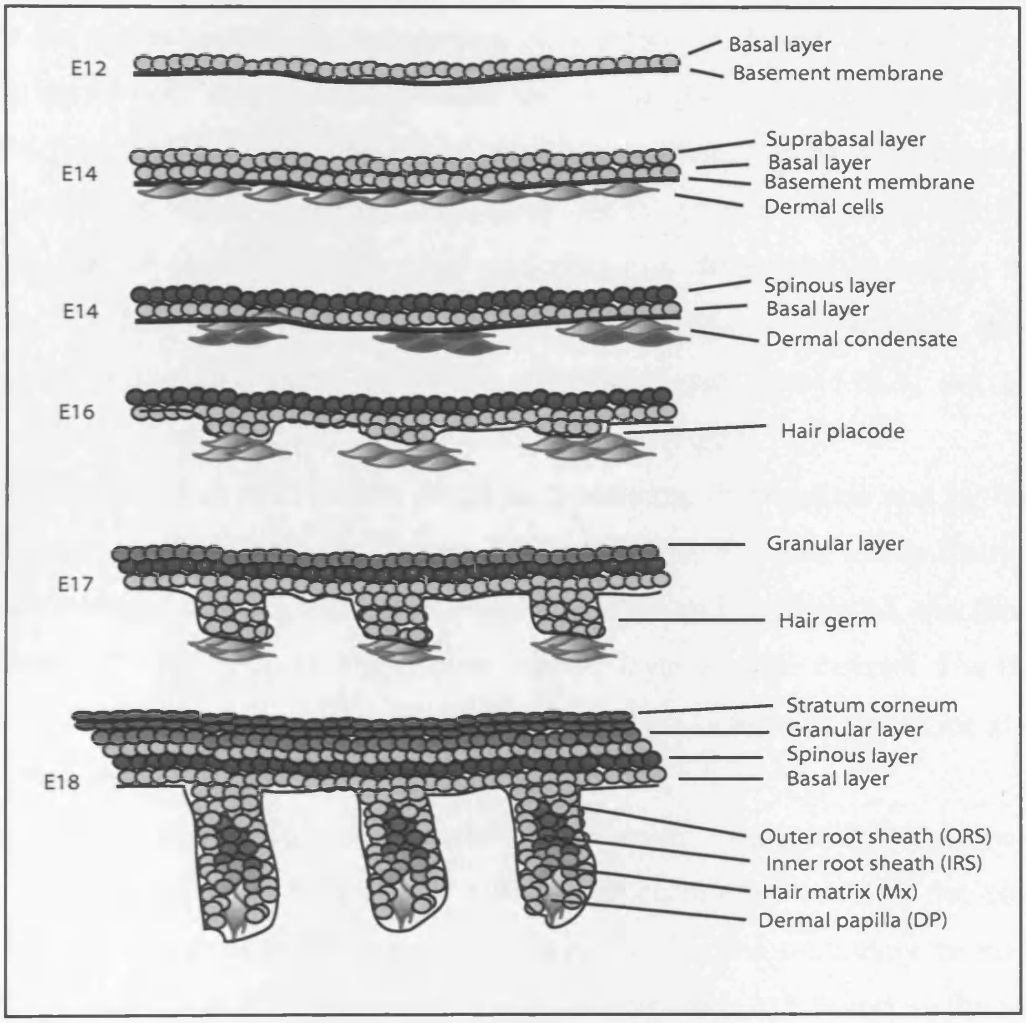

Figure 1.2.- Development and stratification of the epidermis. This diagram illustrates the main stages during development, starting from a single layer of ectodermal cells covering the embryo at E13. As development proceeds, the epidermis progressively is stratified and acquires layers of terminally differentiating cells and by E18 a multilayered stratified epithelium is formed in which the outer differentiated layers constitute the epidermal barrier. E indicates embryonic day. Specific layers are indicated. Taken and adapted from Blanpain and Fuchs, 2006.

pathway has been granted this role by promoting interacting self-organising gradients of stimulatory and inhibitory signals leading to the aggregation of keratinocytes that form the placode by E14. The next step, **organogenesis**, starts by E15.5 and consists of the condensation of specialised dermal fibroblasts, which have inductive properties, underneath the HF placode and the follicular keratinocytes to form the hair germ (Figure 1.3). The crosstalk of pathways between the mesenchymal dermal condensate and the ectodermal placode drives proliferation of both compartments, which allows for the dermal papilla (DP) to be formed and for the downgrowth of the hair placode (Figure 1.3; Schmidt-Ullrich and Paus, 2005; Blanpain and Fuchs, 2005). Another signal at E16.5 is sent from the DP to drive proliferation and elaborate differentiation and in the next step, the hair peg is formed (Figure 1.3). Finally, the **differentiation stage** follows, when the peg starts becoming a bulbous peg from E18.5, the DP becoming surrounded by the most distal keratinocytes (Figure 1.3).

The follicle matures as matrix cells begin to proliferate, differentiate and by day E18.5 to generate the concentrical layers of keratinocytes that give rise to the hair shaft (HS) lineages (hair cuticle, cortex and medulla) and its channel, the Inner Root Sheath (IRS) lineages (Hunxley layer, Henley layer and IRS cuticle). The IRS is surrounded by Outer Root Sheath (ORS), which is the outermost layer (See also Figure 1.4; Hardy, 1992).

There are 4 different types of hair that make up the murine pelage: the major type is the primary or tylotrich (guard) hair follicle that constitutes 10 % of the coat arising from E14 and containing a pad of Merkel cells. The secondary or non-tylotrich includes three hair types: awls (28%) arising from E15.5 and auchenne and zig-zag (70%) arising from E17. In addition to the pelage fibres, the vibrissae or whiskers are very large and highly innervated HF. These are the first follicles to develop, from E12 (Schmidt-Ullrich and Paus, 2005; Hardy, 1992).

Much less is known about the development of the sebaceous gland (SG), which buds from the upper ORS as a terminally differentiating structure that resides above the bulge. Its development begins late in embryonic development from individual keratinocytes that give rise to the sebaceous glands (SG) at around

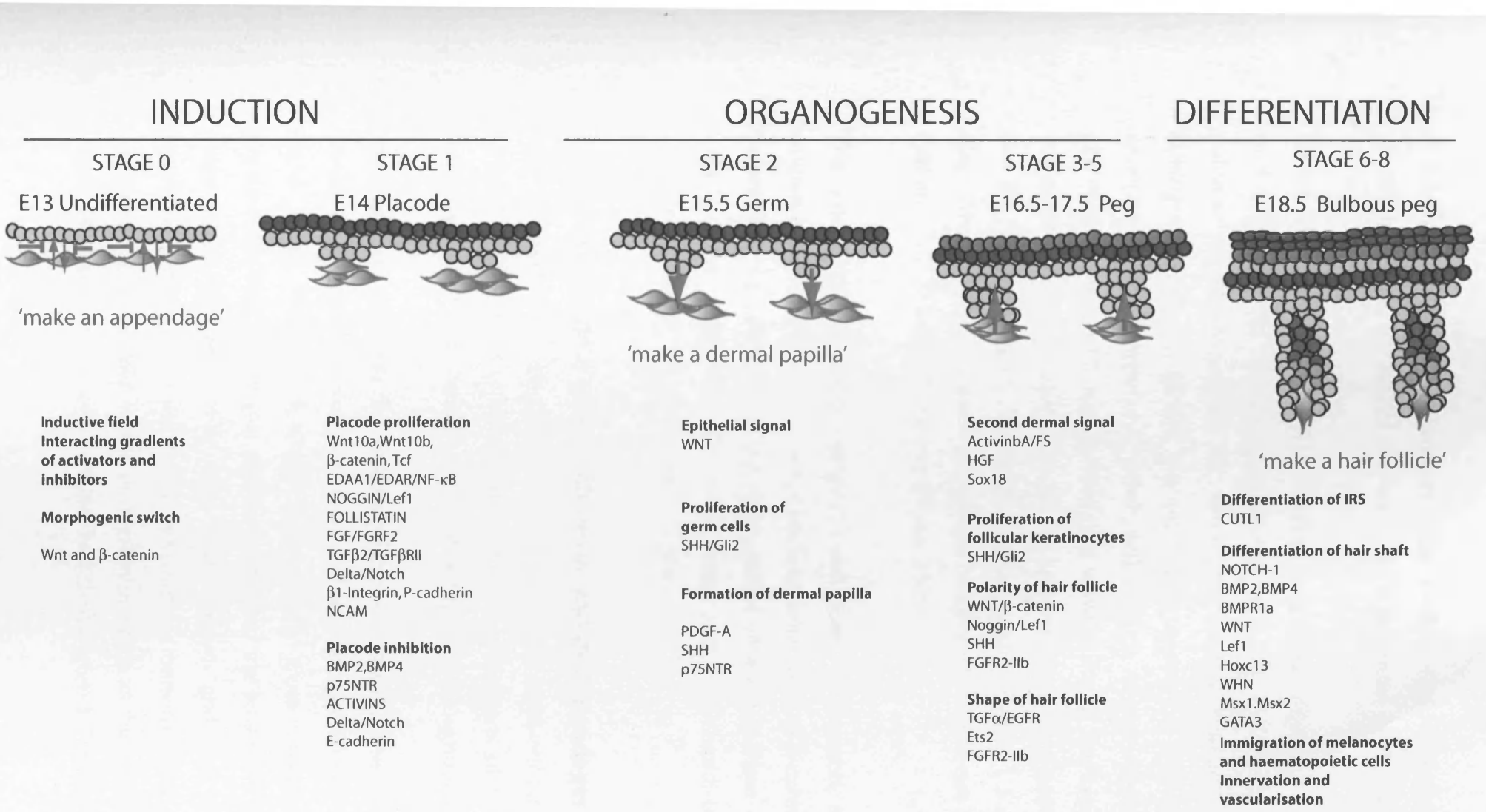

Figure 1.3- Signalling map of the critical steps during hair follicle morphogenesis. This diagram illustrates the process of embryonic HF morphogenesis and depicts a selection of pathways that are involved. During embryonic development, an inductive field of interacting gradients of activators and inhibitors is created between a group of basal cells and the underlying mesenchyme. The outcome of these signals allows for β-catenin activation to switch on a morphogenic programme to make a hair. This triggers a genetic program that will lead to the proliferation of the placode and will trigger the dermis to make a dermal papilla (DP). Then the DP sends a message to the developing follicle allowing it to grow and differentiate to generate discrete lineages to ultimately generate the hair shaft. At this stage non-keratinocyte cell types such as melanocytes and haematopoietic cells immigrate and the HF is inervated and vascularised. Taken and adapted from Schmidt-Ullrich and Paus, 2005.

E17.5 and extending into postnatal life. Differentiated sebocytes produce and secrete lipid-rich sebum into the hair canal that empties out to the skin surface.

Melanoblasts precursors originate in the neural crest, migrate from the dermis and start colonising the developing epidermis from E13. Only at E17.5 they start to colonise the developing the HF, when they become differentiated melanocytes (Steingrimsson et al., 2005). The last step to become a fully mature hair is to generate the pigmentary unit, which will produce melanin to give colour to the HS. At this time the HF is populated by a wave of T cells and Langerhans cells. In addition mast cells also populate the HF and the surrounding dermis. By postnatal day (P) P8, the HF becomes morphological mature (Figures 1.3 and 1.4). At this stage this mini organ is ready to perform its function, to generate a hair shaft (HS) (Millar, 2002; Schmidt-Ullrich and Paus, 2005).

The process of hair morphogenesis is still poorly understood, and although β-catenin is the inductive signal is not yet clear what induces β-catenin stabilisation. Several key signalling pathways are involved in each of these steps, including Wnt/β-catenin, BMP, FGF, EGF, NFKB, Notch and Shh (Schmidt-Ullrich and Paus, 2005; Millar, 2002; See an outline in Figure 1.3).

1.1.2- Maintenance of the epidermis and its appendages

Adult epidermis is a very dynamic tissue, due to the rapid cell turnover in the IFE, HF and SG. Terminally differentiated cells in all regions of the epidermis are continually shed from the skin and must be replaced throughout adult life.

The hair cycle: Hair follicles go through cycles of growth. The different phases are growth (anagen), destruction (catagen), and rest (telogen) (Figure 1.5; Alonso and Fuchs, 2006). When the hair follicle becomes in close contact with the dermal papilla (DP), then the dermal papilla cells signal the bulge and then the anagen phase starts. The responding cells migrate down and start proliferation and expansion to form the bulb, a very dynamic microenvironment or niche, where they continue to expand and then migrate upwards as they differentiate into the several IRS lineages to finally form the hair shaft (Figure 1.5; Millar, 2002)

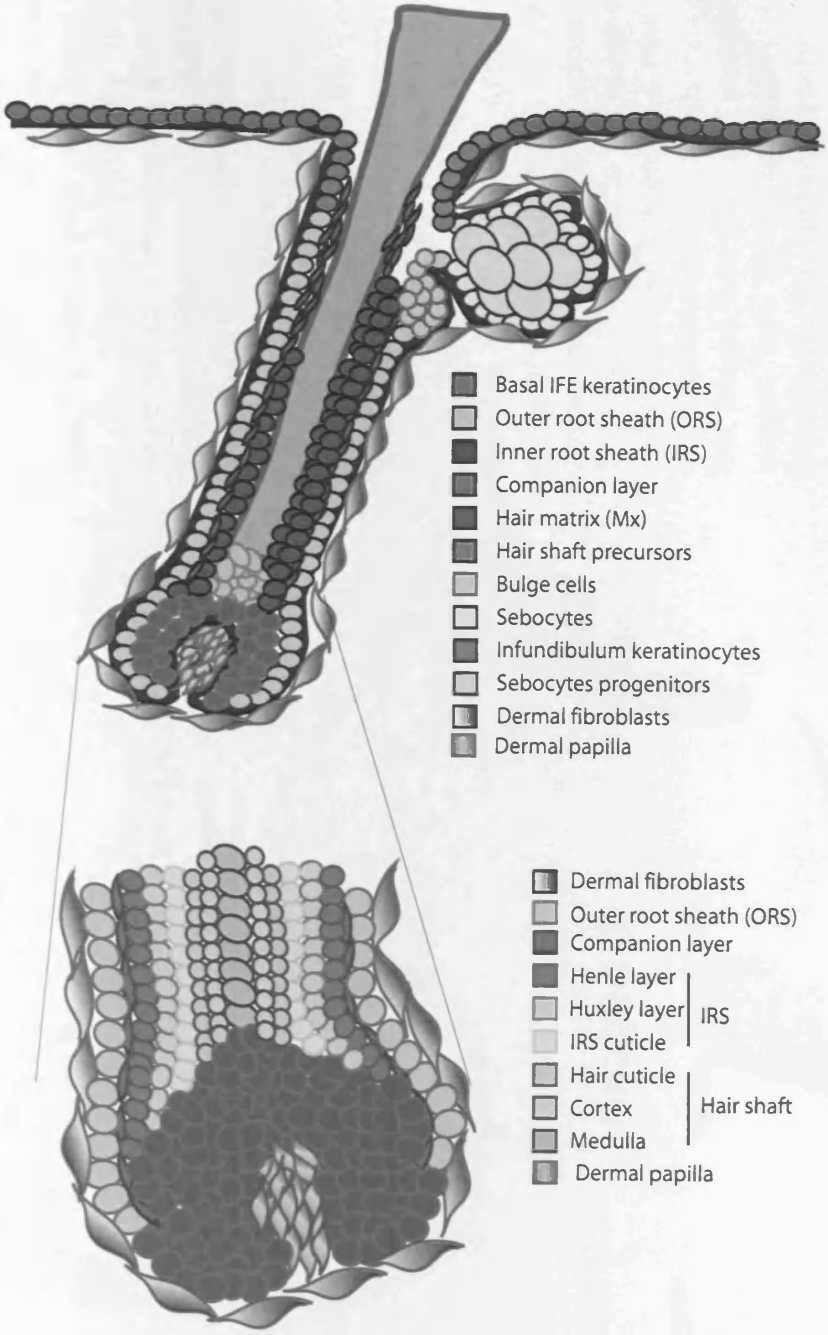

Figure 1.4- Hair follicle lineages. This diagram shows the different hair follicle (HF) lineages that make up the hair shaft (HS). The HF is encased by a basement membrane that separates the basal HF keratinocytes, known as the outer root sheath (ORS) population with the dermal fibroblasts. At the base of the follicle there is the highly proliferative compartment including the matrix population. This population differentiates to form concentric rings of differentiating cells that will give rise to the HS lineages, its channel composed of cells of the inner root sheath (IRS) lineages and the companion layer. HF contain sebaceous glands whose function are to release sebum from the differentiated sebocytes and keep the hair canal and the skin lubricated. Cell types and hair lineages are classified by colours. Taken and adapted from Blanpain and Fuchs, 2006 and Niemann and Watt, 2002.

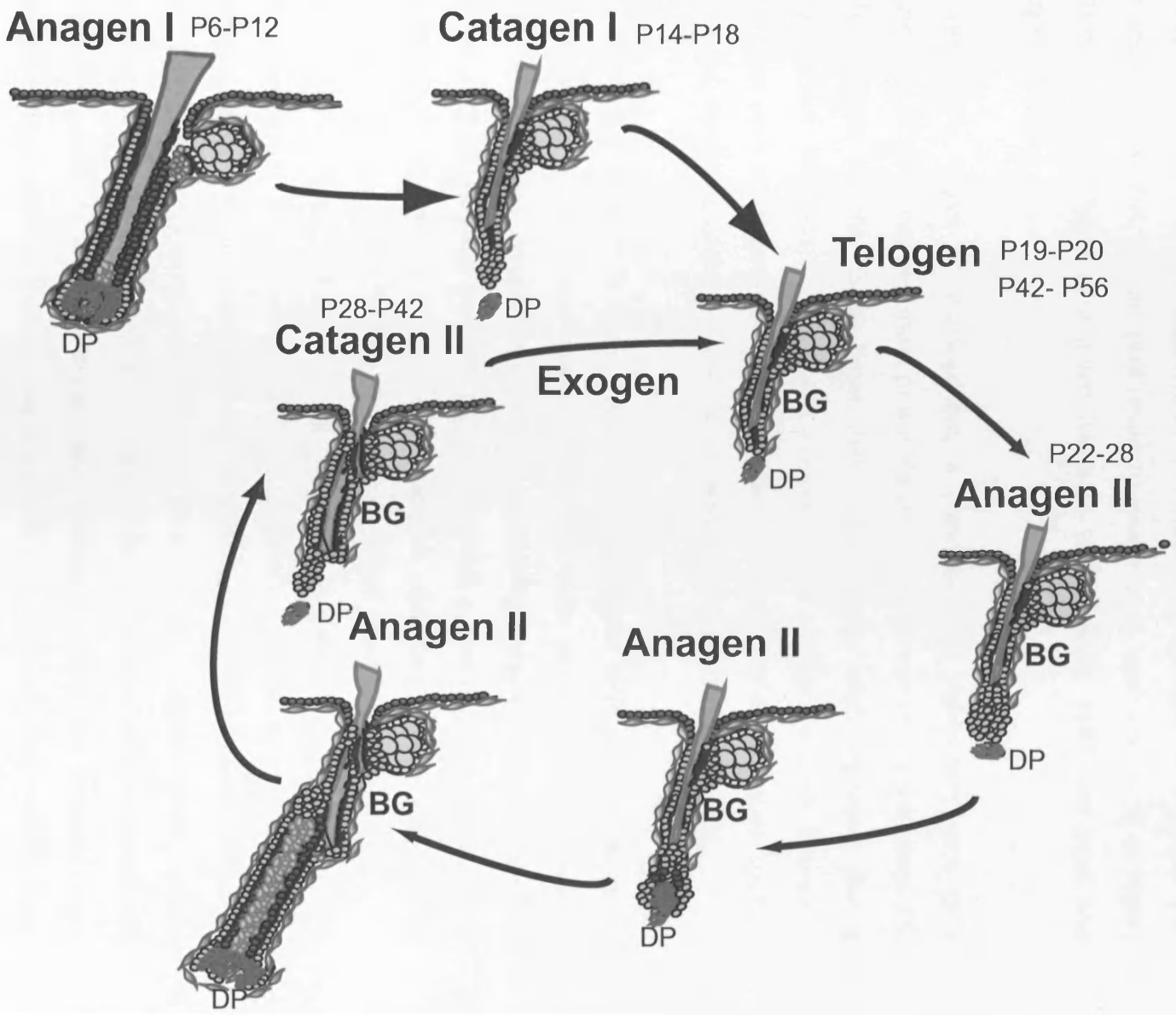

Figure 1.5- The Hair Follicle Cycle. This diagram shows the different stages of the hair follicle cycle. When matrix cells (purple) exhaust their proliferative capacity or the stimulus required for hair growth stops, the follicle enters a destructive phase (catagen) that results in the degeneration of the lower two thirds of the hair follicle. The upper part remains as a pocket of cells surrounding the old hair shaft (club hair). The base of the pocket is the permament portion of the follicle that remains through the whole hair cycle and it is known as the bulge, where the stem cells reside. After the stage of catagen the hair follicle enters a quiescent stage (telogen) in which the dermal papilla (DP) is in close contact. Then the DP signals to the bulge stem cell and the hair follicle enters a new wave of regeneration and hair growth (Anagen). The first telogen lasts for 1 day and the second telogen lasts for approximately 3 weeks, after this the hair cycle is asynchronous. The dates for the first two cycles are indicated and P indicates postnatal day. Taken and adapted from Blanpain and Fuchs, 2006 and Alonso and Fuchs, 2006.

(Alonso and Fuchs, 2006). This phase is followed by a regression phase in which the hair follicle degenerates (Catagen), leading to a resting-phase (telogen). (Figure 1.5; Alonso and Fuchs, 2006).

1.2- Defining a stem cell compartment

The definition of a stem cell must be on a functional basis. Although this question remains contentious after more than 30 years of debate, some consensus has been achieved. The prevailing view is that **stem cells** are cells sitting at the top of the lineage hierarchy with the capacity for unlimited or prolonged self-renewal and are multipotent, this is, can proliferate to produce at least one type of highly differentiated cell types of a given tissue *in vivo* (**Potten, 1997** and Watt and Hogan, 2000).

At very early stages of development, a population of pluripotent stem cells originating in the inner cell mass of the blastocyst, known as embryonic stem (ES) cells produce all the tissue types that make up the adult organism during development. Whereas in adulthood, a population of multipotent cells, known as adult stem cells are responsible for the renewal and repair of adult tissues, such as the blood, the lining of the gut and the epidermis (Watt and Hogan, 2000).

It is important to bear in mind that making functional definition brings some difficulties, as the functional capabilities of the cells can only be assessed by testing their abilities, which themselves may alter their characteristics during the assay procedure. Another problem faced in defining a stem cell population is that the definition can only be relative compared with other cell types (**Potten, 1997**). For instance, as suggested by Potten, et al. a stem cell would be defined as:
a) an undifferentiated cell (i.e. lacking certain tissue specific marker), b) capable of proliferation, c) able to self maintain the population, d) able to produce a large number of differentiated and functional progeny, e) able to regenerate the tissue after injury. These options may be used in a flexible manner. Ideally, these requirements should be satisfied in order to define a population of stem cells (actual stem cell); in practice, experimental limitations exist. For instance, stem cells not expressing these capabilities at a given time, although they possess these

capabilities (potential stem cells) (Potten, 1997). Alternatively, it has been suggested that rather than considering stem cells as undifferentiated cells, it may be more productive to think of them as appropriately differentiated for their specific niches, with perhaps the ability to display more potential phenotypes in alternate niches (Watt and Hogan, 2000a).

After a long debate, several consensus definitions for terms used in the stem-cell biology field have been proposed (Smith, 2006). Defining a **stem cell** as a cell that can continuously produce unaltered daughters and also has the ability to produce daughter cells that have different, more restricted properties and **Tissue stem cell** is defined as a cell derived from, or resident in, a fetal or adult tissue, with potency limited to cells of that tissue. These cells sustain turnover and repair through life in some tissues (Smith, 2006).

When a stem cell divides can give rise to a stem cell daughter and to a non-stem cell daughter that divides a few times before the onset of terminal differentiation. These cells are known as **transit amplifying cells** (TACs) and their role is to increase the number of terminally differentiated cells produced by each stem-cell division (Watt et al., 2006). Although we think of stem and transit amplifying cells as discrete populations, instead there might be gradients of cell behaviour, the transit amplifying cell compartment being in the middle between a cell that has maximum self-renewal capacity and zero differentiation probability, to one that has completed terminal differentiation and can never divide again (Niemann and Watt, 2002).
In the next sections I will introduce what is known about the epidermal stem cell compartment.

1.2.1-Epidermal stem cells

The renewal of the epidermis and its appendages depends on a reservoir of stem cells that is constantly maintained throughout adult life (Figure 1.6). This population of multi-potent stem cells self-renew and generate daughter progenitor cells, the transit amplifying cells (TACs), that undergo a limited number of cell divisions and finally differentiate into hair, interfollicular epidermis (IFE) and

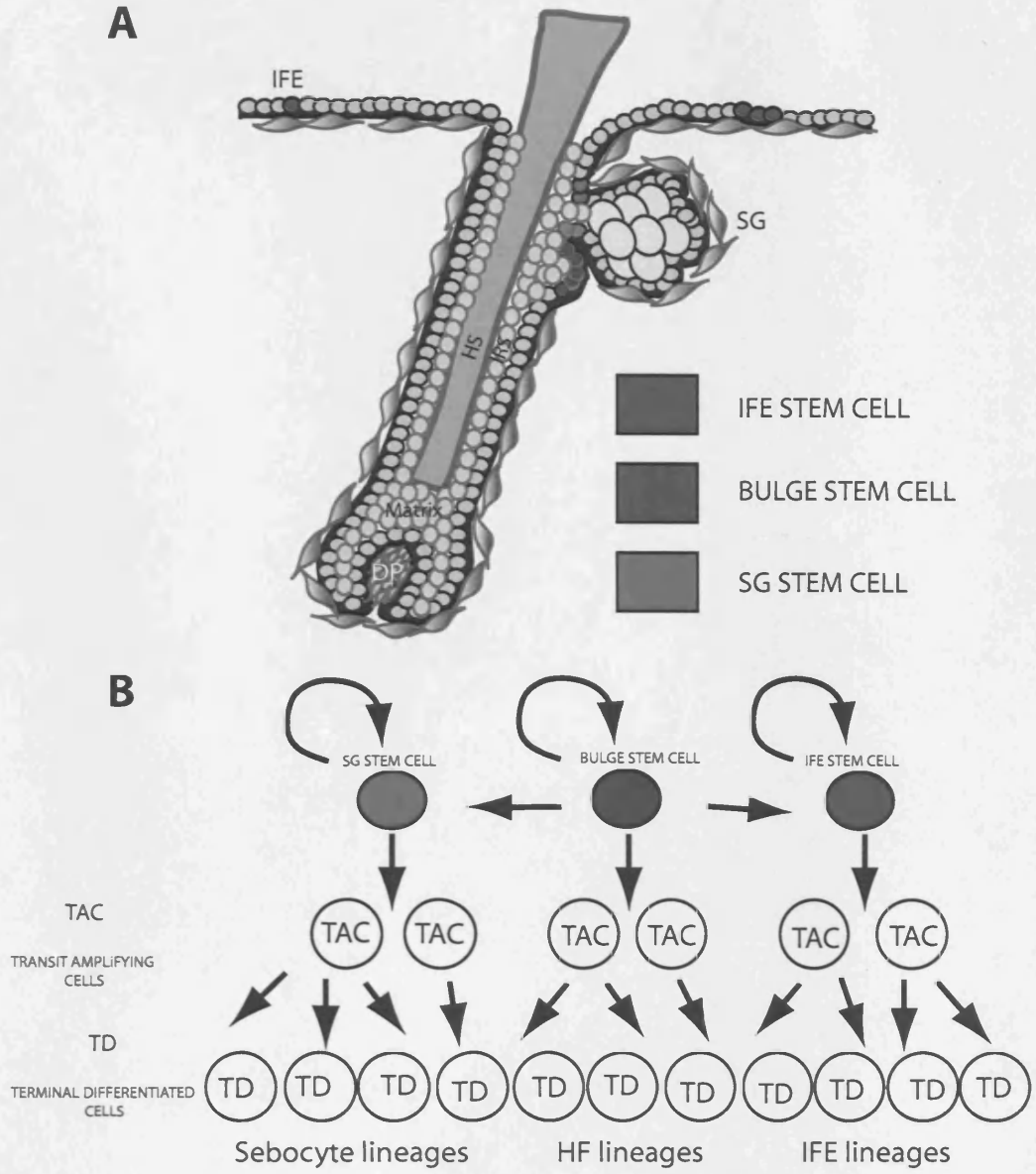

Figure 1.6- Stem cell locations and relationship in mammalian epidermis. (A) There is strong evidence for the existence of stem cells in the hair follicle bulge (blue). Stem cells are known to be present in the basal layer of the interfollicular epidermis (green); however it is not clear whether they are clustered (as shown to the right of the hair follicle) or distributed singly (shown to the left). There is a third progenitor population in the sebaceous gland (red). Cells depicted in bright light green are cells that have not yet initiated terminal differentiation; they comprise transit amplifying cells and cells that have withdrawn from the cell cycle and become committed to terminal differentiation. IFE: interfollicular epidermis; SG: sebaceous gland; HF: hair follicle; HS: hair shaft; IRS: inner root sheath; DP: dermal papilla. (B) Models of lineage relationships within the epidermis. Discrete stem-cell populations coexist, together constituting a multipotent stem-cell compartment. The relationship between the 3 stem cell compartments is not fully understood. Stem cells self renew and they give rise to intermediate populations (transit amplifying or progenitor cells) that go through several rounds of proliferation and they enter the programme of terminal differentiation giving rise to the sebocyte, HF and IFE lineages.

sebaceous lineages, constantly keeping the integrity of the tissue (Figure 1.6; (Niemann and Watt, 2002; Watt, et al.2006). At present, it is unclear whether transit-amplifying cells have multilineage differentiation potential or whether they are lineage-restricted, like for example the committed progenitors in the haematopoietic system (Watt et al., 2006).

1.2.2- Experimental definitions of epidermal stem cells

1.2.2.1-Label retention

Epidermal stem cells and transit-amplifying cells were first identified according to their different proliferative characteristics (Niemann and Watt, 2002; Fuchs, et al.2004; Owens and Watt, 2003; Watt et al., 2006). In the normal epidermis, stem cells are quiescent and tend not to divide, but in response to tissue damage or to being placed in culture they are capable of sustained self-renewal. By contrast, transit-amplifying cells are actively dividing *in vivo,* but in culture they undergo terminal differentiation within a few rounds of division. Therefore, the experimental criteria to identify an epidermal stem cell are based on distinguishing it from its more differentiated progeny. A stem cell has higher proliferative capacity yet divides infrequently, it lacks expression of markers of terminal differentiation and expresses specific cell markers (Flake, 2000; Wagers and Weissman, 2004). Since epidermal stem cells divide infrequently, they can be visualised as Bromodeoxyuridine (BrdU) DNA label-retaining cells (LRC) (Bickenbach, 1981; Braun et al., 2003). Therefore, a DNA label (such as 5-bromo-2-deoxyuridine [BrdU]) is used as an *in vivo* stem cell marker.

LRC are generated in the skin by administering repeated doses of BrdU injections at a stage (P10) in which epidermal cells are highly proliferative, so cells in S phase will take up the label during this pulse period. After a chase period the fate of the cells that incorporate the label can be followed (for details see the Materials and Methods Chapter). After the chase period, cells that have proliferated will dilute and loose the label whereas slow-cycling cells will retain the label (Bickenbach, 1981). In the skin, LRC reside in three confined "niches": 1) clustered in the bulge of the hair follicle scattered in the 2) sebaceous glands and in 3) the basal layer of the IFE (see Figures 1.6 and 3.4; (Bickenbach, 1981); (Braun et al., 2003;Watt et al., 2006). The limitation of the method is that 100%

efficiency of labelling cannot be obtained (López-Rovira et al., 2005; Bickenbach, 1981).

1.2.2.2- *In vitro* clonal growth

We can identify a stem cell by its ability to form and maintain colonies in culture (Flake, 2000; Watt et al., 2006). Early studies by Barrandon and Green showed that when keratinocytes are plated at clonal density can form three types of colonies: **holoclones** (highly proliferative colonies of undifferentiated small round cells that can be passaged for a long term), **paraclones** (abortive colonies of terminally differentiated flat cells) and **meroclones** (small colonies with a heterogeneous population that stop dividing after short passages) (Barrandon and Green, 1985). In addition, cells expressing high levels of β1 integrin give rise to holoclones in culture (Jones and Watt, 1993)

LRC in the bulge, the permanent portion of the follicle can divide *in vivo* (Braun et al., 2003). When they are plated in culture at clonal density, these can yield more and larger colonies, resembling the holoclones, than other portions of the hair *in vitro* (Taylor et al., 2000; Oshima et al., 2001; Ghazizadeh and Taichman, 2001). Recent studies have shown that the double positive CD34/α6 integrin bulge population have a high *in vitro* clonal capacity, giving rise to large proliferative colonies (Tumbar et al., 2004; Morris et al., 2004).

1.2.2.3- Surface markers

For a long time, identification of molecular markers of epidermal stem cells had been through a candidate approach. For instance, the β1 integrin subunit was the first human IFE stem cell marker to be characterised (Jones and Watt, 1993). In recent years, the epidermal biology field has advanced tremendously by the isolation of bulge stem cells based on their expression of surface markers. This has allowed the identification of novel markers by global gene expression profiling. Mouse bulge markers identified by a candidate approach include CD34, keratin 15 (K15) and the α6 and β1 integrin subunits (Lyle et al., 1998; Trempus et al., 2003; Fuchs et al., 2004; Tumbar et al., 2004; Morris et al., 2004; Cotsarelis, 2006). Genes enriched in the bulge identified by microarray analysis include genes that maintain quiescent and undifferentiated states, genes that regulate cell

adhesion, and genes that mediate communication with other cell types, including melanocytes (Tumbar et al., 2004; Morris et al., 2004).

An important issue in skin biology is the correlation and parallels between mouse and human skin in particular for clinical applications. Therefore, the identification of markers that are enriched in human bulge cells is of key importance. A recent study has started addressing this issue by comparing genes upregulated in the bulge of mouse and human hair follicles (Ohyama et al., 2006; Cotsarelis, 2006). For instance, K15 is a bulge marker in both species, however in human follicles CD34 is expressed below the bulge. The Wnt pathway inhibitors, *Dkk3* (*Dickkopf3*) and *Wif1* (*Wnt-inhibiting factor 1*) are expressed in both the mouse and human bulge. A new bulge marker in both species is the CD200 ligand, which has a role in communication with the immune system (Ohyama et al., 2006). The characterisation studies of mouse bulge markers were performed selecting populations FACS sorting according to the expression of markers (Tumbar et al., 2004; Morris et al., 2004).

A novel aspect of the studies of human bulge markers is that the cells were isolated by laser capture micro dissection so cells were compared on the basis of their spatial location rather than relying on existing markers (Ohyama et al., 2006). Very recently, new human epidermal stem cell markers have been identified by generating single cell cDNA libraries from cells expressing high levels of melanoma chondroitin sulphate proteoglycan (MCSP) (stem cells) and expressing high levels of Delta (transit-amplifying cells) (Lowell et al., 2000; Legg et al., 2003). This has led to the identification of Lrig1 as a marker of stem cells in human interfollicular epidermis (Jensen and Watt, 2006).

As mentioned previously, a very important aspect to consider is whether the characteristics that define the stem cell population under study are intrinsic or depend on cues from the microenvironment. For instance, there are two distinct CD34 bulge populations depending on whether they are in contact with the basal layer (α6 integrin positive) or not (α6 integrin negative), they show similar *in vivo* potency, yet they have distinct gene expression profiles (Blanpain et al., 2004). However, other *in vivo* stem cell markers are maintained when bulge cells are

cultured (Claudinot et al., 2005).

Very recently, Fuchs and co-workers have established a distinct population of unipotent progenitors that maintains exclusively the SG (Horsley et al., 2006). This population is localized in the bridge connecting the SG and the HF. Its 'ID' profile is characterized by Blimp1 expression and keratin 5 expression and it is distinct from the more differentiated sebaceous progeny (PPARγ and Nile Red positives) or the proliferative outer layer (Ki67 positive). Lineage marking analysis of Blimp positive cells shows that under steady-state conditions this population feeds the renewal of lost differentiated sebocytes and this unipotent population originates from the CD34/α6 integrin bulge population (Horsley et al., 2006). Further analyses are needed to give more insights about the profile of this newly identified population and what their potency *in vivo* is. This study has opened a door into an area of skin biology that still is in its infancy.

1.2.2.4- *In vivo* potency

In order to maintain both the stem cell and the differentiating cell compartments, epidermal stem cell progeny must exhibit asymmetry of fate. This can be represented as a stem cell giving rise to another stem cell and a differentiated cell. Asymmetry of fate can be achieved on a population basis or at the level of individual cell divisions (Watt and Hogan, 2000). In the population model, a stem cell gives rise to daughter cells that have a finite probability of being either stem cells (50%) or committed progenitors (50%). This strategy might facilitate responses to physiological changes. When cell divisions are asymmetric, a stem cell always divides to produce one stem cell daughter and one non-stem cell daughter. The emerging belief is that the three different LRC reservoirs in the skin can give rise to any epidermal lineage, but under normal circumstances they are restricted by the local microenvironment, the stem cell niche, to give rise to a more limited repertoire of differentiated cells (Figure 1.6; Owens and Watt, 2003). When the epidermis is damaged, it can be completely regenerated by bulge stem cells; conversely, contact with dermal papilla cells can induce the interfollicular epidermis to form hair follicles and sebaceous glands (Niemann and Watt, 2002; Watt et al., 2006).

Until very recently it has been strongly argued that the bulge was the only reservoir of stem cells. However, recent studies have elegantly demonstrated that this notion is no longer valid (Levy et al., 2005; Claudinot et al., 2005 and Ito et al., 2005). Levy *et al.* have shown that cells expressing *Shh* in the embryonic epidermis establish a lineage distinction between what will become, the hair follicle and the surrounding epidermis: cells of the adult bulge are derived from the follicular epidermis, but cells of the interfollicular epidermis are not (Levy et al., 2005).

Claudinot *et al.* have shown that thousands of hair follicles can be generated from the progeny of a single cultured epidermal stem cell. However, the keratinocytes used for transplantation were marked and this revealed that the interfollicular epidermis adjacent to labelled follicles remained unlabelled over many months (Claudinot et al., 2005).

In the third study, Ito *et al.* ablated bulge cells by using the *K15* promoter to express a thymidine kinase suicide gene. Bulge ablation led to complete loss of the hair follicle but survival of the interfollicular epidermis. Using lineage-marking to follow the fate of cells in which the *K15* promoter is active, Ito *et al.* also showed that bulge cells do not normally contribute to the interfollicular epidermis. Following damage to the epidermis, bulge-derived cells contributed to the interfollicular epidermis, but this was temporary and the cells were subsequently lost (Ito et al., 2005). This observation is in agreement with the fact that transplanted bulge stem cells home to the bulge (Claudinot et al., 2005). These studies show that interfollicular and bulge stem cells constitute two distinct populations.

There is already evidence demonstrating that two distinct stem cell populations exist within the bulge (Blanpain et al., 2004). In addition, clonal labelling has revealed distinct populations of self-renewing cells that feed individual lineages at the base of the hair follicle, and distinct clonal organisation along both the proximo-distal and radial axes of the follicle (Legue and Nicolas, 2005). Further studies will be needed to unveil the stem cell hierarchy within the HF, IFE and SG

populations.

1.3- The Stem cell niche

1.3.1-Definition and experimental characterisation

Since 1978, when Schofield proposed the 'niche hypothesis' as a description of the physiologically limited microenvironment that supports stem cells (Schofield, 1978), many investigators have become interested in first identifying the presence of niche in a variety of tissues and more recently in characterising the nature of the niche (Li and Xie, 2005). The definition is still the same after almost 30 years. **Niche** is a 'specific location in a tissue whose microenvironment enables stem cells to reside for an indefinite period of time and produce progeny cells with self-renewing capacities (Nystul and Spradling, 2006). Niches exhibit a complex architecture and they use diverse regulatory pathways (Nystul and Spradling, 2006).

Identification of the signals that regulate stem cell differentiation is fundamental for the understanding of cellular diversity. It is becoming evident that both the extracellular cues from the niche and the cell autonomous or intrinsic genetic characteristics control stem cell function (Li and Xie, 2005). These intrinsic regulators include proteins involved in determining asymmetric cell divisions, nuclear factors controlling gene expression, chromosomal modifications in stem and committed daughter cells, and biological clocks that might set up the number of rounds of division within the TAC population (Watt et al., 2006; Watt and Hogan, 2000). Stem cell niches provide extracellular and intracellular key components that determine the lineage commitment and stem cell self-renewal. Neighbouring cells secrete factors required for differentiation and self-renewal. Cell-cell interactions mediated by integral membrane proteins are also required to direct other signals that control stem cell fate (Li and Xie, 2005).

1.3.2-The hair follicle niche: a city with many 'inhabitants'

The hair follicle is a multi-cellular niche, harbouring several cell types and populations that reside and interact with each other within the niche, and has even been named the 'bone-marrow' of the skin (see Figure 1.7; Schmidt-Ullrich

and Paus, 2005). The HF represents a prototypic neuroectodermal-mesodermal interaction system that is provided by three stem cell sources: epithelial, neural crest and mesenchymal (Schmidt-Ullrich and Paus, 2005). The interaction of these different cell types starts during embryonic development and persists through adulthood, as they are all required to maintain the HF functioning (Millar, 2005). In the HF niche there are also other stem cell populations: such as melanocyte stem cells that reside in the bulge region (Nishimura et al., 2004). Interestingly, their interaction with bulge keratinocytes and secreted factors in the niche are key regulators of the melanocyte fate and function (Millar, 2005). In addition, two studies have shown that the DP constitutes a niche for progenitor cells, known as adult skin derived precursors (SKIPs) (Figure 1.7; Fernandes et al., 2004). Further studies will be important to unveil further the molecular basis of the interaction between these populations and keratinocytes and their relationship with epidermal stem cells.

Many advances have been made in attempting to unveil the nature of the niche. The isolation studies of bulge and their neighbour cells outlined in earlier sections, gave a profile of genes including inhibitors of cell cycle, differentiation and promoters of high adhesion making the bulge a proliferation, and differentiation restricted environment (Fuchs et al., 2004; Tumbar et al., 2004). For example, the expression of the Wnt inhibitors *Dkk3* (*Dickkopf3*) and *Wif1* (*Wnt-inhibiting factor 1*) in the bulge underscores the importance of genes that maintain stem cells in a non-proliferative state and the inhibition of the Wnt pathway, which is crucial for lineage commitment in epidermis.

Recently, the molecular signature of the several cell populations resident in the bulb, the growth-promoting niche in mature hair follicles has been revealed. Rendl and colleagues have combined multicolour tagging with cell specific promoters and surface marker labelling to distinguish between ORS, matrix, dermal fibroblasts, dermal papilla and melanocytes (Figure 1.4 and 1.7; Rendl et al., 2005). For instance, not only several cell types interact with each other but also they express differentially components of key signalling pathways for lineage determination. An example is how the Wnt pathway components are distributed

among these populations: the matrix cells (Wnt10, Wnt11, Wnt5A, Wnt4, Axin2), the ORS (Wnt4, Wnt10), the dermal papilla cells (Wnt5A, Wnt11, Wif1, Srfp2, Frzb, Fzd2, Nkd2, Axin2) and the melanocytes (Dkk3, Nkd1, Nlk, Axin2, Wnt4, Wif1).

In addition, a part of local regulatory pathways, the HF niche is also highly innervated and vascularised and also respond to various hormonal and immune signals (Schmidt-Ullrich and Paus, 2005; Figure 1.7). The hormonal and immune regulation is tightly linked to the hair cycle, making the HF niche one of the unique sites in the body with immune privilege and a peripheral centre for stress (Paus et al., 2005; Paus et al., 2006; Arck et al., 2006). This suggests that the local niche is under a more global control form of systemic regulation that controls the hair and its appendages (Arck et al., 2006).

1.3.3- Pathways modulating the nature of the HF niche

Several pathways are important in regulating the epidermal stem cell compartment, but I will only focus on those related to my Thesis. These include the Wnt, Hedgehog, Notch and Eph/ephrin pathways and their downstream effectors. In addition, I will also include work from our laboratory that has highlighted the importance of integrins, Rac1 and Myc on how the nature of the niche regulates the fate of stem cells.

The niche is important both for population asymmetry and for invariant asymmetry in skin. One way to achieve an asymmetric division is to orient the plane of mitosis so that one cell remains in the basal (undifferentiated) layer and the other in the suprabasal (differentiating) layer. It has recently been shown that in the developing epidermis such vertically oriented mitoses involve asymmetric location of a protein complex containing protein kinase C (PKC)ζ, Par3 (partitioning defective 3) and LGN–Inscuteable (Lechler and Fuchs, 2005). The asymmetric location of this protein complex depends on integrins and cadherins, and does not occur in $p63^{-/-}$ epidermis (Koster et al., 2005; Koster et al., 2006). This study further shows how adhesion of stem cells to the extracellular matrix (ECM), mainly through integrins is also crucial for regulating stem cell behaviour.

Although the role of asymmetric divisions in progenitor differentiation in adult oesophagus is known (Seery and Watt, 2000), the role in adult IFE remains controversial.

Integrin signalling is involved in controlling cell growth, differentiation, migration and survival, either on its own or by cross talking with growth factor signalling (Giancotti and Ruoslahti, 1999). Although integrin-mediated adhesion to the extracellular matrix negatively regulates terminal differentiation of cultured keratinocytes, epidermal deletion of integrins *in vivo* does not lead to a stem cell depletion phenotype (López-Rovira et al., 2005).

This has led to a search for pleiotropic effectors of integrins and other cell surface receptors such as Rho GTPases that might be required to maintain the stem cell compartment and niche *in vivo*.

For instance, Rac1 regulates cell adhesion and growth factor responsiveness, factors involved in niche remodelling and its deletion leads to a failure to maintain the interfollicular epidermis, hair follicles and sebaceous glands, resulting in stem cell depletion (Benitah et al., 2005). Upon deletion of Rac1, there is an initial, transient increase in proliferation and c-Myc expression, followed by loss of proliferating cells and by the onset of terminal differentiation (Benitah et al., 2005). It turns out that Rac1 exerts its effects by negatively regulating Myc, through PAK2 phosphorylation of Myc (Benitah et al., 2005). Activation of Myc causes cells to exit from the epidermal stem cell compartment and stimulates differentiation into interfollicular epidermis and sebaceous glands. Interestingly, one way in which Myc acts is by Miz1-dependent repression of cell adhesion genes, including the α6 and β1 integrin subunits (Gebhardt et al., 2006), thus impacting on the nature of the stem cell niche. Although overexpression of Myc triggers terminal differentiation, ablating Myc from the epidermis results in insufficient expansion of the stem cell compartment (Zanet et al., 2005).

In addition, other Rho GTPases also play important roles in the epidermis. RhoA signalling suppresses differentiation of cultured keratinocytes, as does the Rho effector CRIK (citron kinase) (Grossi et al., 2005). Rho and CRIK might act by

affecting integrin and Notch signalling (Grossi et al., 2005). Recent studies show that deletion of Cdc42 results in progressive hair loss and formation of epidermal cysts (Wu et al., 2006), reminiscent of the consequences of blocking β-catenin signalling (Niemann and Watt, 2002). This shows that Cdc42 is an important regulator of hair progenitor cell differentiation.

Other factors that are important in triggering stem cell proliferation are Tert, the catalytic subunit of telomerase (Flores et al., 2005), which promotes bulge stem cell mobilisation in the absence of changes in telomere length, and β-catenin stabilisation, which promotes the transition from quiescent stem cell to proliferating transit-amplifying cell in the bulge (Lowry et al., 2005). The changes in Rac1, Myc, Tert and β-catenin activity that are found in epithelial tumours (Fuchs et al., 2004; Benitah et al., 2005; Flores et al., 2005) would be consistent with the hypothesis that signals from the niche lead to increased stem cell proliferation predisposing the epidermis to cancer.

1.4- The Wnt pathway a key regulator of lineage commitment in epidermis

There are increasing numbers of pathways involved in the homeostasis and development of the skin, combining changes in gene expression with dynamic changes in cell adhesion and migration. The key signalling pathways involved in lineage commitment, include Wnt/β-catenin, BMP, FGF, EGF, NFKB, Notch and Shh. In this section I will give an overview of the Wnt pathway (Figure 1.8).

1.4.1- Outline of the Wnt pathway

Several members of the Wnt pathway, ligands, receptors and their antagonists are dynamically expressed in all the compartments of the skin (Millar, 2002, 2003; Reddy et al., 2001; Reddy et al., 2004) as shown by expression analysis and profiling of the distinct populations (Millar, 2003; Rendl et al., 2005). Wnt ligands activate three different signalling branches (Figure 1.8; Ciani and Salinas, 2005): canonical Wnt with β-catenin as the main downstream effector (Figure 1.8 A), the planar cell polarity (PCP) which modulates cytoskeleton via interaction with the family of Rho GTPases (Figure 1.8 B) and calcium Wnt pathway which

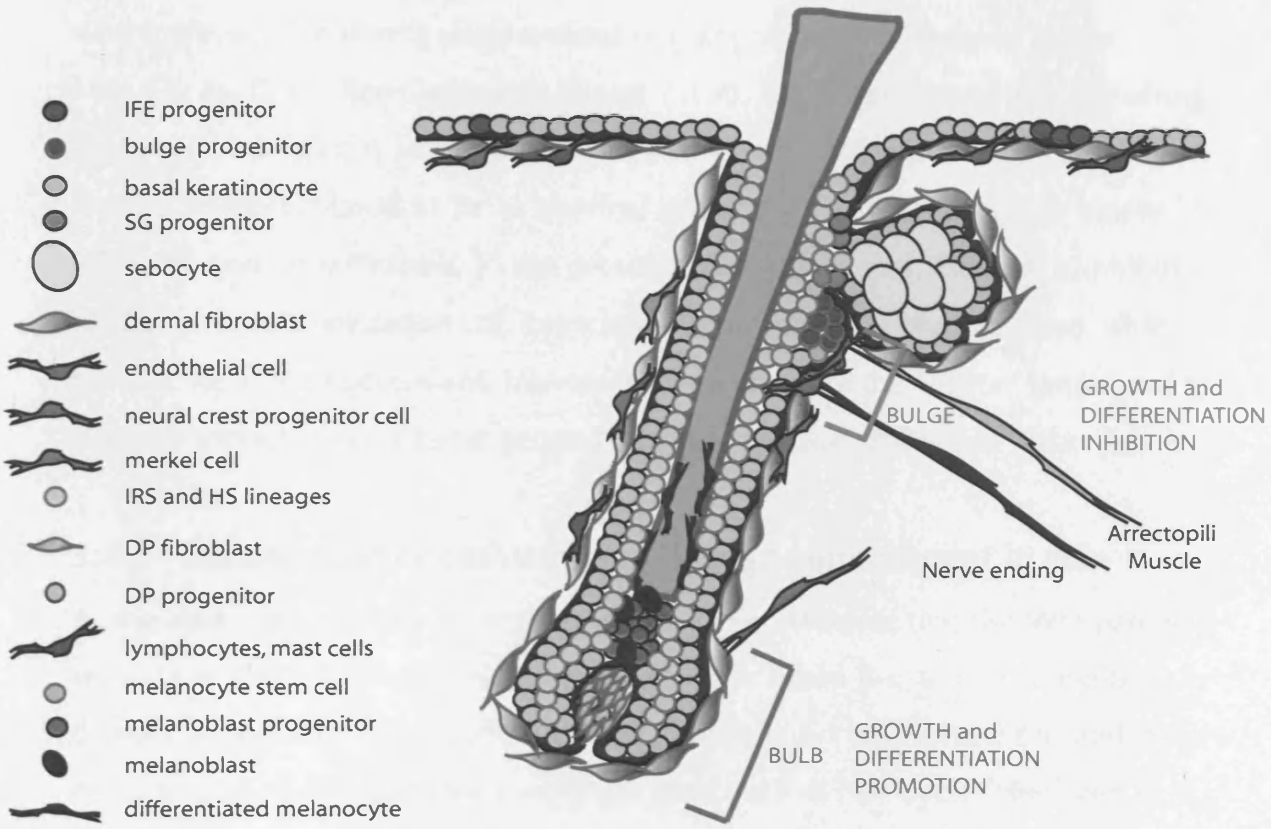

Figure 1.7- The hair follicle niche. This diagram illustrates the large array of cell types that co-exists and composes the hair follicle stem cell niche. Each cell type is explained by the colour code. There are two distinct niches in the hair follicle; one located in the permanent portion of the hair follicle, the bulge, where stem cells reside and the second niche is in the lower portion of the hair follicle, the bulb, where proliferation and differentiation take place.

modulate intracellular calcium and gene transcription via NF-AT (Figure 1.8 C). In this Introduction I will focus in the β-catenin/Wnt branch.

1.4.2- The canonical Wnt pathway

β-catenin is a key effector of the Wnt signalling pathway and a structural component of the adherens junctions, linking cadherins to the actin cytoskeleton, which plays a role during development of many tissues (Nelson and Nusse, 2004; Moon et al., 2002; See diagram in Figure 1.8 A). In the absence of Wnt signalling, the level of β-catenin in the cytoplasm that is not complexed with cadherins is rapidly phosphorylated in its N terminal region by glycogen synthase kinase 3β (GSK-3β) and ubiquitinated. In the presence of a Wnt signal, GSK-3β is inhibited, resulting in accumulation of cytoplasmic β-catenin, which is then able to translocate to the nucleus and interact with members of the TCF/Lef family and to regulate transcription of target genes (Nelson and Nusse, 2004; See Figure 1.8 A).

1.4.3- Canonical Wnt pathway and lineage commitment in skin

At the start of my Thesis, there was considerable evidence that the Wnt pathway regulate epidermal lineage selection (Figure 1.9). When β-catenin is conditionally deleted in the skin during embryogenesis there is no hair formation, and if the deletion occurs after birth the hair is lost after the first hair cycle (Huelsken et al., 2001). When Dickkopf-1, an inhibitor of Wnt action, is ectopically expressed, the development of hair follicle is completely abolished (Andl et al., 2002). When the Wnt pathway is blocked by a dominant negative form of Lef1 mice have a progressive hair loss, develop epidermal cysts with interfollicular differentiation and they also develop tumours with sebaceous differentiation (Figure 1.9; (Niemann et al., 2002; Merrill et al.2001). Epidermal expression of constitutively active β-catenin during embryogenesis leads to hyperproduction of hair follicles and development of tumours similar to human pilomatricomas and trichofolliculomas (Figure 1.9; Gat et al., 1998). Transient activation of β-catenin in adult epidermis induces telogen follicles to enter anagen and the formation of ectopic hair follicles (Figure 1.9; Van Mater et al., 2003; Lo Celso et al., 2004). The levels of β-catenin activation are crucial for lineage commitment in skin; high levels favour hair morphogenesis and blocking the pathway leads to inhibition of

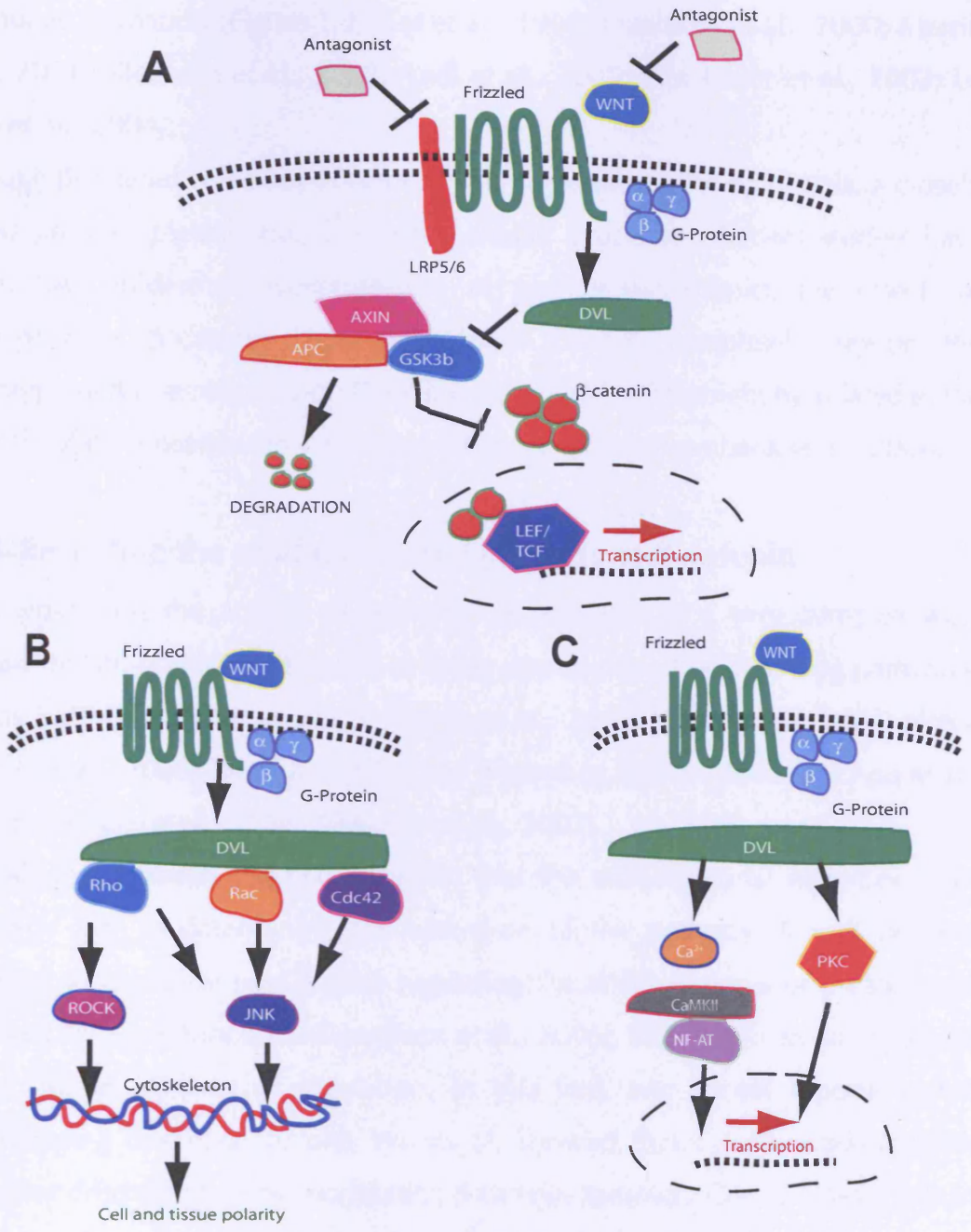

Figure 1.8- The main branches of Wnt signalling pathway. (A) The canonical or Wnt/β-catenin pathway. Binding of Wnt to the Frizzled and low-density lipoprotein receptor 5 (LRP5) or LRP6 complex activates Dishevelled (DVL). Signalling through FZ require G-protein activation. Activation of DVL results in inhibition of glycogen synthase kinase 3β (GSK3β) and accumulation of β-catenin in the cytoplasm by inducing dissassembly of the destruction complex that is formed by adenomatosis polysis coli (APC), Axin and (GSK3β). Subsequently, β-catenin translocates to the nucleus where it activates transcriptional mediated T-cell specific transcription factors (TCF)/lymphoid-enhacing factor (LEF).(B) In the planar cell polarity (PCP) pathway, FZ functions through G-proteins to activate DVL, which in turn, signals Rho GTPases (Rho, Rac or both). Activation of Rac signals through c-Jun amino (N)-terminal kinase (JNK). (C) In the Wnt/calcium pathway, activation of DVL induces the release of intracellular calcium and activation of protein kinase C (PKC) and calcium/calmodulin-dependent protein kinase II (CamKII). This pathway has been implicated in cell fate and cell movement. NF-AT, nuclear factor of activated T cells. Taken and adapted from Ciani and Salinas.2005.

appendage formation (Figure 1.9; Gat et al., 1998; Huelsken et al., 2000; Merrill et al., 2001; Niemann et al., 2002; Andl et al., 2002; Van Mater et al., 2003; Lo Celso et al., 2004).

Although β-catenin is the key effector of Wnt signalling in the epidermis, a closely related protein, plakoglobin, has many similar properties. Recent studies have shown that epidermal overexpression of plakoglobin mimics the effects of overexpressing β-catenin, but plakoglobin cannot completely rescue the phenotype of β-catenin ablation (Teulière, et al.2004). This might be related to the dual role of both proteins in adhesion and transcription (Brembeck et al., 2006).

1.4.4-Revealing the modulators and partners of β-catenin

In the epidermis the activity of β-catenin is regulated in a very complex way, because the Wnt pathway interacts at many levels with other signalling pathways, such as BMP (Jamora et al., 2003; Jamora et al., 2005; Yuhki et al., 2004) Notch (Nicolas et al., 2003; Iso et al., 2003) and Hedgehog (Millar, 2002; Michno et al., 2003; St-Jacques et al., 1998; Niemann et al., 2003).

The balance between the cell adhesion and the transcriptional activities of β-catenin is key in determining the activation of the pathway. It will be very important to elucidate new factors regulating the different pools of β-catenin as they exert different functions (Brembeck et al., 2006), and it is likely to constitute a very important form of regulation. In this line, two recent reports started demonstrating this idea. In one Wu et al. showed that Cdc42 modulate hair progenitor differentiation by modulating β-catenin turnover. Cdc42 plays a role in preventing β-catenin degradation by phosphorylating GSK3β and Axin, two negative regulators of β-catenin stabilization (Wu et al., 2006). This is dependent on an association among Cdc42, PKCζ, Par6 and Par3 (Wu et al., 2006), an important complex for asymmetric division in skin (Lechler and Fuchs, 2005). In the other very recent study, Ganwen et al. show that the Smad antagonist Smad7 determines the lineage choice between HF and SG by modulating Wnt/β-catenin signals. The mechanism is also modulation of the levels of β-catenin by interacting with β-catenin and targeting it to degradation via a novel mechanism dependent on Smurf2 (Han et al., 2006).

Another important aspect will be to elucidate alternative transcriptional partners of β-catenin in skin and to study the intersection between Wnt and other pathways.

1.5- Patterning during development

The simplest pattern observed during development is the spacing pattern. This involves the maintenance of regular distance between neighbouring cells. Examples in which this patterning is observed include teeth, skin appendages, scales and limbs (Wolpert, 1998; **Wolpert L; Beddington R, 1998**). The formation and maintenance of boundaries is a key feature of tissue patterning and results from the outcome of a complex interplay of several pathways leading to differences in cell adhesion and repulsion, cell migration and proliferation and determining whether a boundary will form and separate distinct cell populations or not (Sela-Donenfeld and Wilkinson, 2005; Pasquale, 2005). The Drosophila imaginal disk is the classical model to study patterning (Saburi and McNeill, 2005). In mammals, the limb and feather development are two models that have been widely used to investigate what are the mechanisms that regulate growth and patterning and how they are integrated. These pathways include previously mentioned HH, WNT, TGFβ, BMP, and FGF along with their transducers and modulators. These appear to constitute a kind of ancient 'genetic toolbox' that is constantly being used in most of the developmental programmes that make up tissues (Capdevila and Izpisua Belmonte, 2001). The final result depends on the activity and integration of particular downstream effectors or 'realisator genes' that are expressed (or active) in a particular organ or structure, giving as a result the formation of different structures, i.e. a limb or a hair follicle (Capdevila and Izpisua Belmonte, 2001). Spatially organised cues can function in a graded manner to specify cell movement and cell fate. This can be a mechanism that links cell differentiation and patterning (Pasquale, 2005).

1.5.1- Patterning appendages, lessons from feather development

Feather development has been dissected in great detail. Some parallels can be drawn between hair follicles and feather morphogenesis. In chickens, skin morphogenesis occurs in successive stages (Yu et al., 2004). Firstly, the skin forms

distinct regions, known as macropatterning and secondly, the skin appendages with particular shapes and sizes form in each region, known as micropatterning (Chang et al., 2004; Yu et al., 2004). The spacing of feather buds involves signals from the epidermis to the underlying mesenchyme. The dermis is the main factor determining skin appendage size and spacing. Several Wnt members are dynamically expressed during feather morphogenesis (Chang et al., 2004). Wnt signalling determines the formation skin regions (macropatterning) and of appendages in chicken skin and the shape of individual feathers (micropatterning) (Chang et al., 2004; Yu et al., 2006).

It appears that a positive adjacent ectodermal (horizontal) or dermal (vertical) regulator is concentrated locally, providing the initial signal. This leads to the formation of a circumscribed placode of functionally distinct keratinocytes (Chang et al., 2004). Additionally, members of the Shh, FGF, follistatin, BMP and Eph (EphA4) signalling are expressed during feather bud formation, similar to limb development (Jung et al., 1998; Wolpert, 1998; McKinnell et al., 2004a; McKinnell et al., 2004b; Yu et al., 2004). The fact that both activators (Shh, FGF, Follistatin, EphA4) and inhibitors (BMP) are expressed in the forming feather, favours a model for achieving periodic patterning in which the two signals diffuse at different rates. A periodic pattern can form, the activators having higher potency but a shorter range of action, whereas the inhibitors diffuse further and act over a long range. Through positive feedback (i.e. follistatin expression) and lateral inhibition (BMP, Notch signalling), the competition leads to evenly spaced structures (Jung et al., 1998; McKinnell et al., 2004a; McKinnell et al., 2004b).

Although feathers and hairs evolved independently, recent studies demonstrate remarkable convergence evolution of their stem cell compartment (Yu et al., 2004; Yue et al., 2006); the location of feather stem cells determines feather symmetry and is, in turn determined by the activity of Wnt3A (Yue et al., 2006).

1.6- Ephrin/Eph family

In recent years the role of the family of Eph receptors and their Ephrin ligands have started to account for their role in cell sorting in vascular remodelling and in epithelial systems (Pasquale, 2005). This family of Ephrin ligands and receptors is divided into two sub-types: A and B; ephrin-A ligands are tethered to the plasma

membrane, whereas ephrin-B ligands are transmembrane proteins (See Figure 1.10). Generally EphA receptors interact with ephrin-A ligands and EphB receptors with ephrin-B ligands. Within each class, the receptor-ligand pairs have different affinities and tend to be very promiscuous. EphA4 constitutes an exception, as it not only binds to ephrin-A ligands, but also ephrin-B2 and ephrin-B3 (Pasquale, 2005).

1.6.1- Eph/ephrin signalling

Interaction between ligand and receptor requires cell-cell contact as both are anchored to the plasma membrane. Eph and ephrins can signal bidirectionally (Figure 1.10): this is known as forward signalling in the receptor expressing cell, and reverse signalling in the ligand expressing cell (Kullander and Klein, 2002; Pasquale, 2005). The first step is the formation of an Eph receptor/ephrin cluster. Eph/ephrin complexes can progressively aggregate into larger clusters, depending on the density of receptors and ligands found on the cell surface (Pasquale, 2005). Ligand binding and receptor clustering lead to Eph receptor protein autophosphorylation at the tyrosine residues located in the cytoplasmic tail and at the distal tip of the tail there is a PDZ-binding motif. This acts as docking site for SH2 domain proteins and PDZ domain containing proteins, respectively, including guanine nucleotide-exchange factors of Rho GTPases and signalling adaptors. Examples are: Nck, RasGAP, Fyb, Src, Yes, P85-PI3K, Grb2, Abl, SHEP1, Ephexin, Syntenin, Pick1, Grip, AF-6, Dvl (See Figure 1.10; Kullander and Klein, 2002; Pasquale, 2005)

Although ephrin-B ligands lack catalytic function they become phosphorylated by Src kinases upon receptor binding and clustering. They also contain a PDZ-binding motif (Figure 1.10) that allow for the recruitment of adaptor proteins and cytoskeletal regulators. Examples are: Src/Fyn/yes, Fyn, Grb4, Syntenin, Pick1, Grip, Grip2, FAP-1, PDZ-RGS, PHIP, PTP-BL, Dvl (Kullander and Klein, 2002; Noren and Pasquale, 2004; Pasquale, 2005). In addition, if Eph receptors and ephrins are expressed in the same cells, they can act as heterophilic cell adhesion molecules. However, the physiological significance of these lateral interactions remains to be established (Pasquale, 2005).

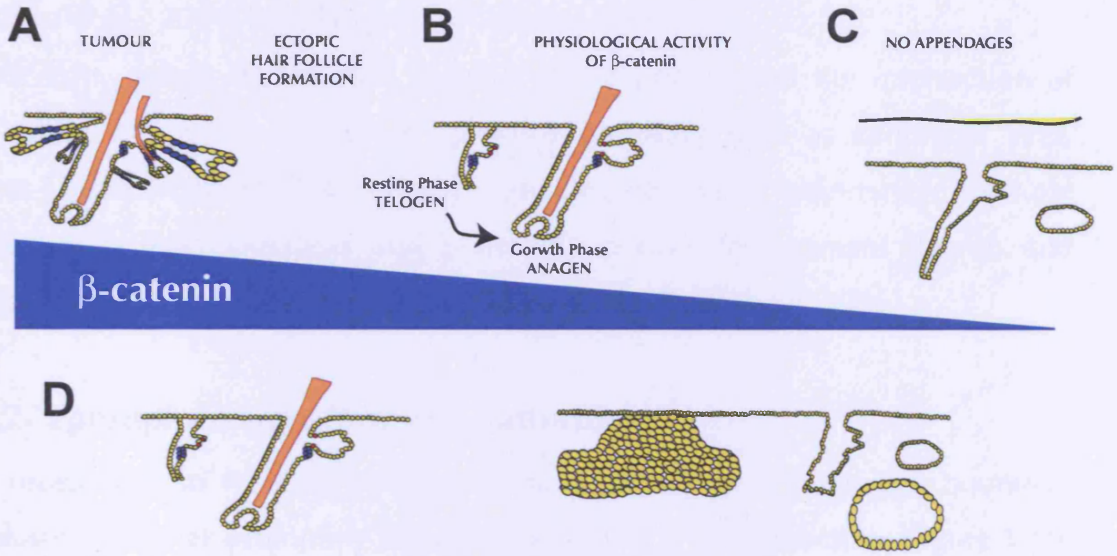

Figure 1.9- Wnt/β-catenin pathway is critical for lineage commitment in mammalian skin. This diagram is a summary of several early studies that illustrate the role of β-catenin activation in lineage commitment. (A) Constitutive activation of β-catenin leads to the formation of tumours of hair origin known as trichofolliculomas (see Gat et al., 1998; Lo Celso et al., 2004). (B) In wild-type skin a pulse of β-catenin activation leads to HF to enter the anagen growth phase (Lo Celso et al., 2004; Van Mater et al., 2003). (C) When β-catenin is blocked by knockout (Huelsken et al.,2001) or by inhibitor overexpression (Andl et al.,2004) a single epithelium forms without appendages or if the deletion occurs later in development the appendages degenerate and are lost. (D) The β-catenin/ Lef 1 interaction is crucial for HF development. When this is blocked HF are lost and instead there is formation of SG and IFE cysts and development of sebaceous tumours (Niemann et

The Eph/Ephrin pathway converges with other well-known tyrosine kinases signalling and ECM modulators pathways and modulate adhesion, proliferation and cytoskeleton dynamics (Kullander and Klein, 2002; Noren and Pasquale, 2004). For instance, it has been shown *in vitro* that Eph/ephrin signalling can either activate or inhibit integrin signalling; inhibit ERK/MAPK pathway and modulate cytoskeletal dynamics via modulation of the activities of Rho GTPases (Rho, Cdc42 and Rac) (Kullander and Klein, 2002; Noren and Pasquale, 2004; Poliakov et al., 2004; Poliakov and Wilkinson, 2006).

In addition, recent studies start to point the importance of the intersection of Eph/ephrin signalling with other signalling pathways such as canonical Wnt, Planar Cell Polarity (PCP) and Notch signalling pathways, important in multiple processes in morphogenesis and patterning during development (Noren and Pasquale, 2004; Poliakov et al., 2004; Poliakov and Wilkinson, 2006).

1.6.2- Eph/ephrin signalling and patterning

Eph receptors and their Ephrin ligands have been shown to control boundary formation by either promoting repulsion or adhesion and attraction (Figure 1.10; (Xu et al., 1999; Mellitzer et al., 1999; Batlle et al., 2002; Cooke et al., 2005). There are several mechanisms resulting in cell repulsion including endocytosis of the adhesive Eph/ephrin complexes from the cell surface, proteolytic cleavage of ephrin ligands or by inactivation of cell-cell and cell-ECM adhesion molecules by Eph receptors. Mechanisms leading to promotion of adhesion and attraction include the result of a poor activation of pathways promoting cell separation, the activity of phosphatases if they are recruited to terminate signalling before cells are separated. In addition to mediating mechanical cell-cell adhesion, Eph/ephrin signalling can activate pathways that promote cell adhesion to the ECM, membrane ruffling and axon extension. Finally, the degree of clustering might also change the balance of opposing signals that regulate the cytoskeleton, cell-cell and cell-substrate adhesion (Pasquale, 2005). Eph/ephrin signalling in addition to determine the position of a cell it also influences on the shape, cell migration, proliferation and differentiation status of a cell (Pasquale, 2005; Poliakov et al., 2004).

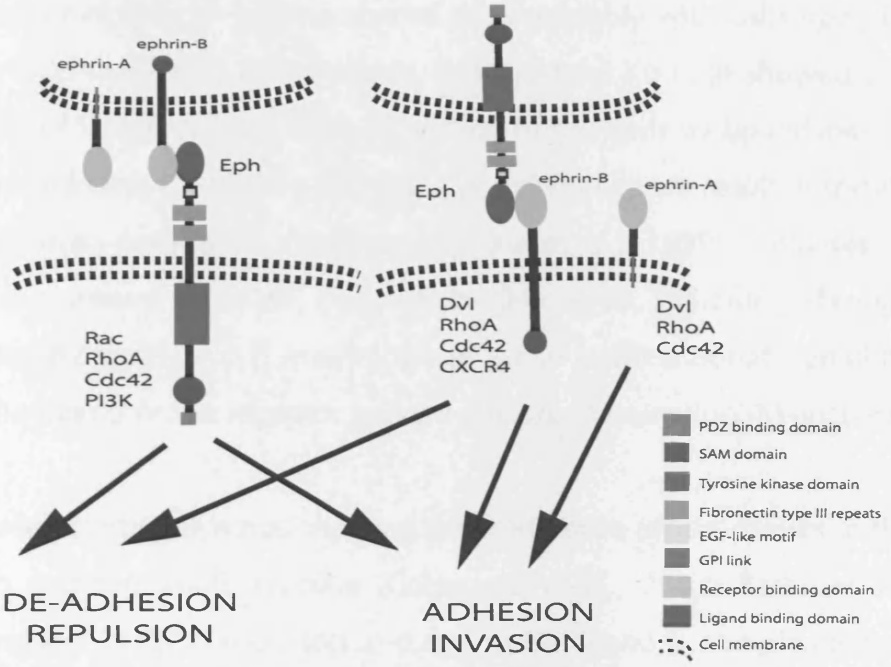

Figure 1.10- EphB/ephrin-B bidirectional signalling. This simplified diagram shows the structure of ligands ephrin-A and ephrin-B and the Eph receptors. Colour codes indicate the main domains of the proteins. Selected downtream effectors are shown. The balance between the outcome of these pathways determine if the outcome will lead to adhesion and invasion or de-adhesion and repulsion. Taken and adapted from Poliakov et al., 2005; Noren and Pasquale, 2004 and Pasquale, 2005)

Several studies have shown that EphB/ephrin-B signalling is sufficient to block cell mixing and it is required for boundary formation. A good example of the involvement of Eph/ephrin signalling in the formation of sharp interfaces during development is the segmentation of rhombomeres in the hindbrain (Sela-Donenfeld and Wilkinson, 2005). The formation of rhombomers also relies on activation of Eph/ephrin signalling by modulation of adhesive or migratory properties of cells. Eph/ ephrin molecules are expressed complementarily in rhombomeres and cells from an odd-numbered mix preferably with cells from the same or another odd-numbered rhombomere. Interestingly, Xu et al showed that mosaic activation of Eph receptors leads to sorting of the cells to boundaries in odd-numbered rhombomeres. Mosaic activation of ephrin ligands result in sorting to boundaries in even-numbered rhombomeres (Xu et al., 1999). Analyses in zebrafish cell cap assays revealed that the bi-directional signalling through ephrin-B2 and EphB2 restricts cell intermingling, while unidirectional signalling through either the ligand or the receptor prevent cell communication (Mellitzer et al., 1999).

Further evidence supporting this notion has come from more recent studies in the developing limb and the small intestine (Compagni et al., 2003; Batlle et al., 2002). The expression of EphB receptors and ephrin-B1 ligand is complementary in the developing limb. In addition, mosaic expression of ephrin-B1 shows that ephrin-B1 expressing cells segregate from ephrin-B1 null cells. This suggests a role of ephrin-B1-EphB interaction signalling in the segregation of chondrocytes (Compagni et al., 2003).

Analyses of the intestinal architecture revealed that there are opposing gradients of expression along the crypt-villus axis of the receptors EphB2/EphB3 and the ligands ephrin-B2/ephrin-B1 (Batlle et al., 2002). These allow cell positioning to regulate progenitor fate. Progenitors sit on top of the Paneth cells at the bottom of the crypt, where there are high levels of receptor expression and where β-catenin is active. As the proliferative cells start migrating upwards they start the programme of differentiation and they downregulate the expression of receptors and instead they start expressing high levels of the ligands. In addition, they show that Wnt signalling modulates the expression of Eph/ ephrin molecules and thus can regulate the balance of stem cell renewal versus differentiation and fate

determination in a spatially regulated manner (Batlle et al., 2002; van de Wetering et al., 2002). Analysis of mutant mice reveal that the EphB/ephrin signalling prevents intermingling of proliferating cells into the zone of differentiating cells (Batlle et al., 2002).

1.7- Patterning in the epidermis and HF

Little is known about how pattern is controlled in mammalian skin: both the placing of individual hair follicles within the epidermis, and patterning of undifferentiated cells along the hair follicle outer root sheath or inner root sheath during development and how these are maintained during the hair cycle. The molecular basis for follicle pattern formation is not yet fully understood. The regulatory pathways involved in morphogenesis, such as, FGF, Wnt, BMP, hedgehog, are likely to play a role in determination of the pattern. In addition, homeobox transcription factors previously described as key regulators in limb patterning (Capdevila and Izpisua Belmonte, 2001) are also expressed in gradients in distinct compartments of the follicle and are likely to play a role (Hardy, 1992). A very recent example has started giving some clues as to how the primary hair follicle pattern might be set during embryogenesis by looking at the Edar/BMP pathway (Mou et al., 2006). The Edar/BMP had been shown previously to be key for primary hair development by inhibiting responsiveness (Schmidt-Ullrich et al., 2006). In this study, Mou et al., from a culture system suggest a model in which Edar determines the localisation of stabilised β-catenin, thus where the follicle will be formed, by inducing a feedback loop between the dermis expressing BMP4/7 (inhibitor of HF) and the epidermis expressing CTGF (BMP4/7 inhibitor) (Mou et al., 2006). Further molecular and *in vivo* analyses are needed to understand how these and other pathways involved in HF morphogenesis are intersecting to generate HF pattern. It is likely that the pattern is set out as a complex interplay of pathways rather than a single one on its own.

In addition, not only we need to solve how the pattern is set up during embryonic development, but also how is maintained during the hair cycle. Regulation of pattern during anagen development is likely to include pathways involved in cell-cell interaction, migration and invasion such as cadherins, integrins, GFs and their downstream counterparts.

Aims

In this Thesis I set out:

1- To optimise and use the whole mount technique to obtain quantitative and spatial information about epidermal stem cells and their progeny without relaying on sections.

2- To study how β-catenin induces ectopic hair follicle formation in adult epidermis.

3- To us a model of inducible ectopic hair follicle formation, control β-catenin signal timing, strength and duration and analyse the impact of the β-catenin signal on the stem cell compartment and how this impacts hair follicle formation.

4- To identify pathways that intersect with β-catenin.

Chapter 2- Materials and Methods

2.1- K14ΔNβ-cateninER mice

2.1.1- Experimental treatment of mice

The D2 and D4 lines of K14ΔNβ-cateninER transgenic mice were generated as described previously (Lo Celso et al., 2004). The Clare Hall Animal Unit carried out all animal care and breeding. All mouse husbandry and experimental procedures were conducted in compliance with the protocols established by the Cancer Research UK animal ethics committee, following the Home Office regulations. All mice were killed with CO_2 following Humane killing regulations under The Animal Act 1986, Home Office.

K14ΔNβ-cateninER mice were maintained heterozygote and kept in C5-7BL/6 background.

For my experiments I used mice that were 6-8 weeks old, and therefore in the resting phase of the hair cycle (Stenn and Paus, 2001). Wild-type, non-transgenic littermates were used as controls. The ΔNβ-cateninER transgene was activated by topical application of 4-hydroxytamoxifen (4OHT; Sigma) dissolved in acetone. 4OHT was purchased from Sigma either 99% pure Z-isomer (biologically active) or minimum 70% pure Z-isomer. The doses indicated always refer to the amount of Z-isomer, and were always applied to the skin in a maximum of 200μl. Tail skin was treated by applying 4OHT with a paintbrush (0.5, 1.5 or 3 mg per mouse every second day). For back skin treatment (0.5, 1.5 or 3 mg per mouse) 4OHT was applied with a Gilson micropipette to a clipped area of dorsal skin.

In order to study the interaction between β-catenin and Shh pathways, mice received daily topical applications of Cyclopamine (Biomol, 50 μM in ethanol), and 1mg 4OHT once per week (D2 line) or every second day (D4 line). 4OHT was applied 30 minutes after Cyclopamine.

Typically, each experiment was designed so that each condition group was analysed in triplicate, this is, and 3 animals were used per condition.

For each experiment two controls were always included. These were transgenic mice treated with vehicle alone, in this case it was acetone, named Untreated. A

second group of wild type mice treated with 4OHT or cyclopamine alone, named Wild type treated.

2.1.2- Genotyping procedure

2.1.2.1-DNA extraction

For genotyping the Clare Hall Animal Unit (CRUK, London, UK) took a small ear snip from each animal. Each ear snip was incubated in 50µl of ear buffer containing 50mM Tris-HCl pH 8.0, 20mM NaCl, 0.1% SDS supplemented with 2.5 µl of 25mg/ml proteinase K (Sigma) solution at 55°C for one hour, vortexed, and incubated at 55°C a further two hours. 150µl of dH_2O were added and the tubes were incubated for 10 min at 95°C and subsequently briefly centrifuged to collect condensate from the lid. The DNA content per sample was measured by spectrometry using a Nano Drop reader (Nano Drop Technologies) in order to optimise the PCR reaction.

2.1.2.2- PCR reaction

The following primers (supplied by DNA Technology AIS) were used for genotyping PCR of K14ΔNβ-cateninER mice: β-cat [ATGCTGCTGGCTATGGTC AG] and for ER [GCACACAAACTCTTCACC]. In a 50µl reaction, 1µl of each primer (25µM) was added to 25µl of 2xPCR master mix (Promega), 1µl of DNA preparation and 22µl of dH_2O. The following PCR conditions were used: 1 cycle [94°C, 1min], 32cycles [94°C, 30sec], [50°C, 30sec], [72°C, 1min] and 1 cycle [72°C, 7min]. 10µl of the PCR product were run on a 2% agarose TAE gel following standard procedures (**Sambrook, 1989**). The PCR product of the transgene ΔNβ-cateninER was a 0.6kb fragment.

2.2- Eph mice

Ephrin-B1-deficient animals were generated in Ralf Adams laboratory (London Research Institute,CRUK, London, UK) by breeding conditional (Lox/+ or Lox/Lox) mutants to PGK-Cre transgenic animals (Compagni et al., 2003). Homozygous EphB2 and EphB3 null mice were bred by Ralf Adams laboratory as described previously (Orioli et al., 1996). Wild-type mice of the same background and age,

or EphB2 and EphB3 heterozygous or Cre-negative littermates were used as controls. I also examined mice in which the EphB2 cytoplasmic domain has been replaced by a β-galactosidase gene (Henkemeyer et al., 1996). This mice line was also kept and bred by Ralf Adams laboratory.

2.2.1-Genotyping procedure

All mice strains were genotyped by the Ralf Adams laboratory as previously described (Compagni et al., 2003); (Henkemeyer et al., 1996); (Orioli et al., 1996).

2.3- BrdU labelling

2.3.1- Pulse for labelling S phase cells

To achieve short-term labelling of cells undergoing DNA synthesis, adult mice received an intraperitoneal injection of 100mg/kg body weight 5-bromo-2'-deoxyuridine (BrdU; Sigma) 1hour prior to sacrifice.

2.3.2- Generation of LRC *in vivo*

To generate label-retaining cells (LRC), the protocol described by Bickenbach and colleagues (Bickenbach, 1981) was used. Ten-day-old mice were injected with 50mg/kg bodyweight 5-bromo-2'-deoxyuridine (BrdU; 20 µl of 12.5 mg/ml BrdU) every 12 hours for a total of four injections to label mitotic cells. An extremely high percentage of keratinocytes incorporate the BrdU label because the epidermis is hyperproliferative in 10-day-old mice (López-Rovira et al., 2005). Normally, mice were maintained for a minimum of 70 days after the final BrdU injection in order to detect LRC. In some experiments, the localisation of cells containing the BrdU label was assessed after a chase period of less than 70 days. Braun et al have shown that 28 days is the minimum chase period required to detect LRC in mouse skin (Braun et al., 2003). For an outline of the experimental design see Figure 3.3 and 3.4).

2.4-Antibodies

The primary antibodies used in this study are listed in Table 2.1. The secondary antibodies used were anti-goat, anti-rabbit, anti-mouse or anti-rat (H+L) IgG Alexa

633, 488, 594 conjugated secondary antibodies and they were purchased from Molecular Probes.

2.5-Tissue sections immunofluorescence

2.5.1-Tissue processing for paraffin sections

To collect skin for paraffin sections, the back of the mouse was shaved before removing the skin and stretching out onto a backing card (dermal side down). In order to get a good cross-section of the skin, it is important that the direction of the hair shafts is parallel to the card. Small rectangles of skin, (tail, back, whiskers, ears) were cut out and placed into neutral buffered saline overnight before transferring to a 70 % ethanol solution. The CRUK Histopathology Unit mounts the supported skin in paraffin blocks. 5mm sections are then cut from the blocks using a microtome and mounted onto glass slides.

2.5.2-Paraffin tissue sections staining

Sections were deparaffinised by washing twice in Xylol followed by rehydration through four washes in isopropanol solutions of decreasing concentration (100 %, 96 %, 75 %, 50 %) by the Histopathology Unit.

Standard staining procedure

Typically, a staining would be performed 3 times on 3 independent samples. For each set of stainings a section is always included with a secondary antibody only as a negative control. The normal protocol would include a first step of antigen retrieval: tissue sections would be microwaved in 10 mM sodium citrate (pH 6.0) for 5-20 minutes, incubated for another 15 minutes in the hot solution and rinsed in 1xPBS. If the protein to be analysed was a transcription factor then a subsequent step of permeabilisation was required. Sections were either incubated in a 0.3% TritonX-100/PBS solution for 5-10 minutes or for Ki67 and BrDU staining in 2 M HCl at 37°C, washed in borate buffer, and digested in 0.01% trypsin in 0.05 M Tris buffer for 3 minutes at 37°C. After antigen retrieval, sections were usually blocked in a freshly prepared Super Block Buffer, consisting of 2% bovine serum albumin, 5% fetal calf serum and 2.5% fish skin gelatin in PBS, for 2 hours. After blocking sections were incubated with the primary antibody in

Super Block solution at 4°C overnight. The next day sections were rinsed three times for 10 minutes each with PBS/0.2% Tween.

For immunofluorescence staining, secondary antibody conjugated to a fluorophore (see secondary antibodies list) was incubated with the section, for 45 minutes at room temperature. A counter stain would be included in order to visualise and localise he protein under study. For this, sections were incubated with Phalloidin (either conjugated to TRITC (red channel), FITC (green channel), 633 (blue channel) to visualise polymerised actin (Sigma) and DAPI to stain nuclei (Molecular Probes) simultaneously in dH_2O for 10 minutes. Sections were rinsed with dH_2O and then carefully dried and mounted in Mowiol (Calbiochem) or Vectashield (Vector).

Immunostained sections were kept at 4^0C protected from the light.

For **immunohistochemistry**, the DAKO visualisation systems were used.

Sections were deparaffinised by washing twice in Xylol followed by rehydration through four washes in isopropanol solutions of decreasing concentration (100 %, 96 %, 75 %, 50 %) by the Histopathology Unit. Next, sections would be blocked with H_2O_2 for 5min. The following steps would be the same as described above.

After incubation with the primary antibody and subsequent washings, sections were incubated with HRP conjugated secondary antibodies and then reacted with DAB substrate according to the manufacturer's instructions. Following incubation with the secondary antibody sections were washed twice in PBS and incubated for 30 min at room temperature with streptABComplex/HRP (DAKO) prepared according to the Manufacturer's instructions. Slides were washed twice again in PBS and then developed in di-amino-benzydine The DAB solution was either supplied already prepared or it was prepared by adding one tablet of DAB to one tablet of hydroxyurea in a total volume of 10ml dH_2O. After 3 washes in dH_2O sections were dehydrated and counterstained with haematoxylin and mounted by the CRUK Histopathology Unit.

When labelling sections of mouse skin with mouse primary antibodies, Mouse on Mouse kit (Immunofluorescence or Immunohistochemistry kits, Vector Laboratories) was used according to the Manufacturer's instructions. This kit

worked well for both immunofluorescence and immunohistochemistry procedures.

2.5.3-Cryosections sections

To prepare frozen sections of mouse skin, small rectangles of skin sample were placed on nitrocellulose membrane for support and subsequently in a plastic mould containing O.C.T compound (BDH) and then frozen on dry ice. Frozen blocks were stored at -70^{0}C before cutting 6-10μm sections with a cryomicrotome (Reichart-Jung) and mounting onto slides (Superfrost Plus, BDH).
When staining sections I followed the method described for paraffin sections from the blocking step onwards.

2.6- **Whole mount preparation**

The method to prepare mouse tissue was developed by Uffe Jensen and Kristin Braun (Braun et al., 2003; Jensen et al., 1999) by modifying a method originally described to prepare human epidermal whole mounts (Jensen et al., 1999).

To prepare whole mounts of mouse tail epidermis, a scalpel was used to slit the tail lengthways. Skin was peeled from the tail, cut into pieces (0.5x0.5 cm^2) and incubated in 5 mM EDTA in PBS at 37°C for four hours. Forceps were used to gently peel the intact sheet of epidermis away from the dermis and the epidermal tissue was fixed in 4% formal saline (Sigma) for 2 hours at room temperature. Fixed epidermal sheets were stored in PBS containing 0.2% sodium azide at 4°C for up to 8 weeks prior to labelling.

2.6.1-Immunolabelling of tails skin whole mounts

Typically, every staining will be performed a minimum of 3 times on 3 independent samples. For an experimental outline see Figures 3.1 and 3.3.

Epidermal sheets were blocked and permeabilised by incubation in PB buffer for 30 minutes. PB buffer consists of 0.5% skim milk powder, 0.25% fish skin gelatin (Sigma) and 0.5% Triton X-100 in TBS (0.9% NaCl, 20 mM HEPES, pH 7.2). Primary antibodies were diluted in PB buffer and tissue was incubated overnight at room temperature with gentle agitation. Epidermal whole mounts were then

washed for at least 4 hours in PBS containing 0.2% Tween 20, changing the buffer several times. Incubation with secondary antibodies was performed in the same way. Samples were rinsed in distilled water and mounted in Gelvatol (Monsanto, St Louis, MO) containing 0.5% 1,4-Diazabicyclooctane (DABCO) (Sigma) or with Vectashield mounting medium (Vector).

A negative control was always included and these would determine the settings for confocal microscopy analysis (For an example see figure 3.3).

To detect BrDU or transcription factors, after permeabilisation and prior to incubation with primary antibodies, epidermal sheets were incubated for 20-30 minutes in 2M HCl at 37°C.

2.6.2- Visualisation of sebocytes in tail whole mounts

Lipid-containing cells, including sebocytes, were detected by performing Nile Red staining on frozen sections. A stock solution of Nile Red (x1000, 10μg/ml in methanol) was normally diluted 1/1000 in PBS. Whole mounts were incubated in 1x Nile Red for 15 minutes and washed with PBS or washing buffer for up to 4 hours to remove excess stain. Then cells were mounted and visualised by confocal microscopy. When I performed Nile Red staining together with antibody immunolabelling, I first carried out the normal procedure for antibody labelling and immediately after the secondary staining I added the Nile Red for 15 minutes and washed with washing buffer for up to 4 hours to remove excess stain. When I performed double labelling I always used a secondary antibody conjugated with 633 fluorophore to avoid bleed through between the green (488) and the red (594) channels.

2.6.3-Visualisation of apoptotic cells in tail whole mounts

Apoptotic cells were detected in epidermal sheets by using the DeadEndTM Fluorometric TUNEL System (Promega). Prior to performing the TUNEL assay whole mounts were immunolabelled with a keratin 14 antibody in order to

visualize basal cells. The analysis were performed in 3 independent samples (0.5x0.5cm^2/each). FITC positive cells then would be counted under a microscope.

2.6.4-Melanocyte visualisation in tissue sections and whole mounts

To visualise melanocytes, epidermal sheets were incubated with 0.2% L-Dopa diluted in dH_2O at 37° C in the dark for 6h to overnight. L-Dopa was handled under the fume hood to avoid inhalation or skin contact. Solutions were prepared freshly each time, always under the fume hood.

Before mounting slides were rinsed with dH_2O several times and mounted with Mowiol (Calbiochem) or Vectashield (DAKO).

Epidermal sheets harvested from albino mice were used as a negative control of each experiment.

Paraffin sections were dewaxed prior to L-Dopa labelling. Before mounting they were de-hydrated. A light counter stain with Hematoxylin was also performed to facilitate visualisation of the epidermal structures.

2.6.5-Optimisation of the whole mount labelling

When I performed immunolabelling with a new antibody I always used the standard whole mount immunolabelling procedure with a different range of antibody concentrations. However, if a staining did not work properly I customised the protocol for the antibody staining. The following steps were modified in order of importance when changing the procedure: 1- Order, 2- Temperature, and 3-Agents and 4- Incubation time.

1- **Order:** Start with permeabilisation, followed by immunolabelling and fixing at the end.
2- **Temperature:** Perform all procedures at 4°C (including fixation, permeabilisation and staining).
3- **Fixative agents:** The following options would be tried: No fixation. Different concentrations of formaldehyde (i.e. 4%, 0.4%). Different concentrations of fresh paraformaldehyde (i.e. 4%, 0.4%). This proved to be the most adequate. Try methanol, acetone or methanol/acetone (1/1) for

30 min to overnight at 4°C. Bouin's fixative 2hours at room temperature. Zinc containing fixative overnight at 4°C.

4- **Permeabilising agents:** PB buffer with 0.5% Triton-X100, or with 0.05% Triton-X100 or 0.5% Saponin; or PBS with 0.5% Saponin.
5- **EDTA treatment:** Decrease the incubation time or use Dispase (Invitrogen) instead as previously described (Rendl et al., 2005).
6- **Use Phosphor free buffers:** for phospho antibodies.

2.6.6- Protocol for visualising Eph and ephrins in skin sections and whole mounts

When ephrin-B/ EphB immunolabelling was performed on tail whole mounts a modified version of the protocol described by Batlle et al. was used (Batlle et al., 2002).

Whole mounts were processed normally and fixed with 4% paraformaldehyde for 2 hours at 4°C. However, they were developed using a combination of a HRP conjugated secondary antibody (ENVision®System-HRP (DAB) from DAKO) and Tyramide-FITC (Molecular Probes) following the manufacturers instructions.

When ephrin-B/EphB immunolabelling was performed in back skin DAB substrate was used in the developing step, as described for the protocol of immunohistochemistry.

Knockout tissue and omission of primary antibodies were always used as negative controls.

2.6.7-X-gal staining in whole mounts

Tail whole mounts were fixed with 4% PFA for 1hr at room temperature. The following stock solutions were prepared and combined as shown to give 10 ml X-gal substrate solution.

Solution	[Stock]	[Working]	[For 10 ml]
$K_3Fe(CN)_6$	0.5M	5mM	100 ml
$K_4Fe(CN)_6$	0.5M	5mM	100 ml
$MgCl_2$	0.5M	2mM	40 ml
Nonidet P40	10%	0.02%	20 ml
Sodium deoxycholate	5%	0.01%	20 ml
1xPBS	10x	1x	1 ml
X-Gal	40mg/ml	1mg/ml	250 ml
dH_2O			8.47 ml

Whole mounts sheets were incubated with the substrate solution in wells of a 24/well plate on a rocking table at 37°C for 6 hours to overnight. The reaction was terminated by fixing the whole mounts again for 4 hours at 4°C with 4% formaldehyde solution. Whole mounts were mounted with Mowiol and kept at 4°C.

2.6.8- Confocal microscopy of epidermal sheets

Images were acquired using a Zeiss LSM 510 confocal laser scanning microscope (Carl Zeiss) with an argon laser at 488nm and 568nm and a helium-neon laser at 633nm. Approximately 30 optical sections of each epidermal sheet were captured with a typical increment of 1-3 μm. Scans are presented as *z*-projections. Objectives used were Zeiss 10/NA 0.45, Zeiss 20/NA 0.75 and Zeiss 40/NA 1.2. The samples were scanned from the dermal side towards the epidermal surface to a total thickness of 40-80 μm, which encompassed the epidermis from the hair follicle bulb to the basal layer of interfollicular epidermis. For comparison, images of different conditions labelled with the same antibodies were taken using the same settings.

For each set of staining omission of the primary would be always included as a negative control. This would be used for determining the setting of the confocal microscope as it would show the background staining given by the secondary antibody.

Typically, one analysis would start by taking several low power images (x10) of each epidermal sheet. This would allow visualisation of large areas of tissue and

would be performed for all the mice and conditions of the experiment. Next, closer images would be taken (x20), first comparing several follicles and epidermal units within on sample. Next, these would be compared with other samples. These steps would help assessing the analysis of patterns of expression or changes rising in different conditions or genotypes (See Figure 3.3).
Typically, mice of the same background, sex, and age would be compared. These factors must always be taken into account when performing analysis. In addition, changes during the hair cycle could only be analysed between littermates during the synchronous stage of the hair cycle.

2.6.9-Whole mount quantification

In order to perform quantifications in whole mounts, normally 30-50 units per tail were scored in three separate mice for each experimental condition.

2.7- Immunofluorescence staining of cultured cells

Cells were cultured on tissue culture plastic microscope slides (Nunc) or on glass coverslips (Chance Propper Ltd.) prepared by the CR-UK Washing Room. The cell medium was aspirated and cells were washed once with 1xPBS. Cells were fixed with 4% paraformaldehyde for 20 minutes, rinsed twice with PBS and kept at 4^0C until used. Cells were permeabilised either with cold acetone or 0.3% Triton X-100 for 5 minutes. Then, they are blocked for 1 hour with 4% BSA. Primary antibody incubation was performed overnight at 4^0C. Secondary antibodies were incubated for 30 minutes at room temperature. Cells were incubated with Phalloidin-TRITC (1/500) to visualise polymerised actin (Sigma) and DAPI (1/10000) to stain nuclei (Molecular Probes) simultaneously in dH_2O for 15 minutes, prior to mounting cells were rinsed with dH_2O.
For each set of staining omission of the primary would be always included as a negative control.

2.8-Cultivation of Mouse Epidermal Keratinocytes

2.8.1- Cells

Primary adult epidermal keratinocytes or spontaneously immortalised keratinocytes lines were used for experiments. Both types of cells were normally cultured on a feeder layer of J2-3T3 cells (Rheinwald and Green, 1975).
The Methods I describe are based on (Silva-Vargas et al., 2005) for primary cells and (Romero et al., 1999) for immortalised cells.

2.8.2- Cell solutions distributors

Calcium-free F12 and calcium-free DMEM are bought from Invitrogen. Adenine can be purchased from Sigma Aldrich Co. Ltd. Penicillin, streptomycin, trypsin (0.25%), and (0.02% EDTA) can be obtained from Invitrogen. A suitable supplier of foetal calf serum (FCS) and newborn calf serum (NCS) is PAA Laboratories. Hydrocortisone and Cholera enterotoxin are purchased from Merck Biosciences (UK) Ltd. Epidermal growth factor (EGF) is purchased from Peprotech EC Ltd. Insulin and Mitomycin C are purchased from Sigma Aldrich Co Ltd. Mikrozid is purchased from Schulke & Mayer UK Ltd. Dimethyl sulfoxide (DMSO) is obtained from VWR International Ltd. Collagen I coated dishes are purchased from BD Biosciences.

2.8.3-Cell culture solutions and media

Solutions

Trypsin-EDTA: For passaging cells, mix 1 part 0.25% trypsin and 4 parts 0.02% EDTA. 0.25% trypsin is used to isolate keratinocytes from adult mouse skin.

Phosphate-buffered saline (PBS): To make 1 litre, dissolve 0.2g KCl, 0.2g KH_2PO_4, 8.0g NaCl, and 2.16g Na_2HPO_4. $7H_2O$ in 900 ml distilled water. Adjust pH to 7.4, add distilled water to 1-litre final volume, autoclave, and store at room temperature.

Mitomycin C in PBS: Prepare a stock solution of 0.4 mg/ml in PBS, filter sterilize and store in aliquots at -20°C.

Hydrocortisone: Prepare a 5-mg/ml stock in absolute ethanol. Store at -20°C.

Cholera enterotoxin: Prepare a 10^{-5} M stock in distilled water. Store at 4°C.

EGF: Prepare at 100-μg/ml stock in FAD medium + 10% FCS. Store at -20°C.

Insulin: Prepare a 5-mg/ml solution in 5 mM hydrochloric acid. Store at -20°C.

2.8.4-Culture media for keratinocytes

2.8.4.1- FAD medium preparation

The basic medium consists of three parts of calcium-free DMEM and one part calcium-free F12 supplemented with 1.8 x 10^{-4} M adenine (Calcium-free FAD), 100 IU/ml penicillin, and 100 μg/ml streptomycin. Store at 4°C.

Calcium-free FAD is supplemented with 10% batch-tested FCS. The serum batches that are optimal for keratinocytes tend to be completely unsuitable for fibroblastic cells or hybridomas. FCS is stored at -20°C before use.

Calcium-free FAD + FCS are further supplemented with a HICE cocktail, consisting of hydrocortisone (0.5μg/ml), insulin (5 μg/ml), cholera enterotoxin (10^{-10} M), and EGF (10 ng/ml) (all final concentrations).

Complete medium, or low-calcium FAD/Complete (calcium-free FAD + FCS + HICE) is stored at 4°C and used within 2 weeks.

2.8.4.2-Keratinocyte Serum Free medium (KSFM)

KSFM was obtained from GIBCO-Invitrogen and was used when culturing keratinocytes in a feeder-free system. KSFM basal medium was supplemented with 0.2 ng/ml recombinant human Epidermal Growth factor (EGF) and 30 mg/ml Bovine Pitutary Extract. When this medium was used for Wnt3a or Eph/ephrin-Fc stimulation assays no supplements were added.

2.8.4.3-Culture medium for 3T3 J2 feeder cells

J2 cells were cultured in DMEM supplemented with 100 IU/ml penicillin, 100μg/ml streptomycin, and 10% calf serum.

Stock feeders were normally passaged at 1:5/1:10 weekly and the culture medium was changed every 2 days.

2.8.5-Preparing J2 feeder Layers for keratinocyte cultivation

4 μg/ml mitomycin C was added to confluent flasks of 3T3 J2 and incubated for 2 hr at 37°C. This irreversibly inhibits proliferation of the J2 cells. At the end of the

incubation period cells are rinsed with 0.02% EDTA, and then harvested in trypsin-EDTA. J2 from a 75 cm flask are used to provide feeders for three $25cm^2$ dishes or three $60cm^2$ dishes. If possible, it is better to seed the feeders prior to the keratinocytes, so that they can attach properly.

2.8.6-Primary mouse keratinocyte isolation and culture

2.8.6.1- Isolation of mouse keratinocytes

Keratinocytes can be isolated from either the dorsal or tail skin. Mice are killed following U.K. Schedule I of the 1986 Animal Act. The hair of the back is shaved, and then skin is excised from the rest of the body with the aid of scissors and forceps and stored on ice until use for up to few hours. The following steps are the followed under sterile conditions.

1)- Wash the skin for approximately 1min in 10% Betadine (iodine) solution in sterile water agitating constantly.

2)- Wash skin 2x in 70% ethanol solution for approximately 10 seconds each.

3)- Complete washing by immersing the skin in sterile PBS for 10 seconds to remove excess ethanol.

4)- Transfer the tissue to a 100-mm-diameter petri dish, dermis facing upwards. Using sterile scalpel and forceps, remove excess fat and muscle.

5)- Transfer the skin to a fresh dish containing 0.25% trypsin so that the tissue floats with the epidermis-side up.

6)- Incubate the tissue at 32° C or 37° C for two hours. Alternatively, tissue may be left to digest overnight at 4° C.

7)- Scrape epidermis away from dermis using a scalpel and forceps.

8)- Cut pieces of epidermis into small (1x1mm) pieces using two scalpels, and dice tissue into very fine pieces using a scalpel.

9)- Suspend epidermal slurry in 10ml complete FAD medium, and filter through 70μm nylon mesh (Falcon) into a 50ml conical tube. Repeat this process several times to ensure that a single cell suspension is formed.

10)- Centrifuge isolated keratinocytes at 1200rpm, 5 minutes to pellet isolated cells, and discard supernatant. Resuspend pellet in complete FAD medium.

11) Count the number of cells in the supernatant with haemocytometer using Trypan blue dye to exclude dead cells from the count.

12)- Resuspend cells at desired concentration in complete FAD medium.

13)- Seed cells onto the confluent J2-3T3 feeder layer at desired density.

14)- Feed the cells with fresh complete FAD medium three times per week. Cultures are typically grown for 14 days.

For the generation of each line, adequate experimental controls should also be prepared.

2.8.6.2- Passage of Keratinocytes

It is important to passage keratinocytes before they reach confluence, as they hard to disaggregate once large numbers of differentiated cells accumulate.

In order to passage keratinocytes, first aspirate the medium. Rinse the cultures several times with 0.02% EDTA and remove the remaining feeder cells by gentle aspiration, as they are EDTA sensitive. Next, add 0.25% trypsin to the culture dish and incubate at 37°C for about 10 minutes. This will allow the keratinocytes to detach. Add medium containing serum to inactivate the trypsin. Transfer the cells by pippeting to a tube and centrifuge at 900 rpm for 3 min at RT.

Aspirate the supernatant and resuspend the pellet in completed FAD medium. Count cells using a haemocytometer, and resuspend in complete medium at desired density. Seed the single keratinocyte suspension onto confluent, mitomycin-treated J2 3T3 feeders.

For standard culture of all primary epidermal keratinocytes or immortalised lines I used the complete FAD medium without calcium (named Medium Calcium) with the exception of the ΔNβ-cateninER D2 and D4 keratinocyte lines that were cultured with complete FAD medium including calcium (named High Calcium).

2.9-Mouse Keratinocyte immortalisation

Spontaneously immortalised keratinocyte lines were generated by serial passaging as described in Romero, et al.1999. These were cultured with a feeder layer, essentially as described in the previous section. In early passages cells were passaged at 1:1 ratio. After 6-10 passage cells were passaged at a 1:5 ratio.

2.10- Keratinocyte clonal growth assays

For clonal growth assays, 10^3 – 5 x 10^3 primary adult keratinocytes were plated on pre-coated collagen I coated 35 mm dish containing confluent J2 feeder layer. Medium was changed every other day. After 14 days the cultures were fixed with 4 % paraformaldehyde and stained with 1% Rhodamine B. Colonies were defined as clusters of 5 or more keratinocytes.

2.11- Keratinocyte motility

To examine cell motility in the absence of proliferation, spontaneously immortalised keratinocytes were plated without feeder layer on collagen coated 35 mm glass-bottom Petri dishes (MatTek). Prior to analysis, cells were first rinsed with pre-warmed Versene and then treated with Mitomycin C for 2 hours.
To analyze motility, cells were cultured in complete FAD medium. The cells were kept humidified at 37°C with 5% CO_2. Fields of cells were monitored and recorded by low-light video microscopy, at a 10 min lapse interval on inverted Olympus microscopes IM or IMT-2 equipped with 10× NA 0.25 or 4× NA 0.1 phase-contrast objective lenses and driven by Broadcast Animation Controllers (BAC 900; EOS Electronics [AV], Ltd.) and fitted with monochrome charge-coupled device cameras and video recorders (models M370 CE and PVW-2800P, respectively; Sony). Recordings were digitized and the sequence of all frames was run on a PC. Experiments were performed at least 3 independent times.

2.12- Keratinocyte Retroviral infection

Retroviral supernatants were generated by transient transfection of Phoenix packaging cells and stable infection of AM12 cells. Phoenix cells ($5x10^6$) were plated in a 10 cm dish, incubated for 24 hr, and then transfected by calcium-phosphate precipitation with 20 μg of the retroviral plasmid pBABE-EGFP (Lowell et al., 2000) for15 hr at 37°C. After 48 hr, the virus-containing medium was filtered (0.45μm filter, Millipore) and supplemented with 4μg/ml polybrene (Sigma) (first supernatant). Viruses were collected for an additional 8 hr as before (second supernatant). One plate of Phoenix cells produced sufficient virus for one

to two plates of target cells. The packaging cell line AM12 were infected two rounds of incubation culture with retroviral supernatant produced by the Phoenix cells. After 2days, the selection step with was started. GFP positive cells were selected by a combination of puromycin resistance (2μg/ml puromycin, Sigma-Aldrich).

Immortalised mouse keratinocyte lines were plated at 10^5 cells/cm^2 and cultured for 2–3days until they reached 60% confluency. Keratinocytes were infected by two rounds of incubation culture with previously filtered retroviral supernatant from the infected and selected AM12 packaging cells for 7 h rinsed two times with PBS, and placed in keratinocyte medium. After 2 days the selection with was started. GFP positive cells were selected by a combination of puromycin resistance (2 μg/ml puromycin, Sigma-Aldrich and FACS sorting.

2.13- Keratinocyte sorting experiments

Mixing experiments were performed at close to confluent cell densities on collagen coated dishes with J2-3T3 feeders (Lowell et al., 2000). 10^5 or 10^4 GFP labelled cells were combined with 10^4 or 10^5 unlabelled cells per 60 mm dish. Each condition was performed at least in triplicate. The cultures were fixed 5 days after plating and labelled with Phalloidin to detect polymerised actin.

Analysis of these experiments would include the analysis of several fields of each sample. There is variability between experiments so it is important to perform several times.

2.14- FACS and flow cytometry

For two colour FACS analysis, keratinocyte suspensions prepared from adult skin were incubated with FITC or biotin conjugated primary antibodies for 30 min on ice and then washed twice for 10 min at 4^{0}C. The subsequent incubation with streptavidin PE (BD Bioscience) was performed in the same way. The cell viability was assessed by 7AAD staining (BD Bioscience). Cells were analysed with a FACS Vantage sorter (Silva-Vargas et al., 2005); (Morris et al., 2004), after gating out dead cells and cells with high forward and side scatter.

Omission of the primary antibody, single stainings , unstained and an adequate isotype control should always be performed.

2.15- Ephrin/Eph stimulation assays

Recombinant ephrin-B1-Fc, ephrin-B2-Fc, EphB2-Fc or EphB3-Fc (R&D systems) was pre-clustered with 0.2 μg of goat anti-human IgG (Jackson Laboratories) per 1 mg Eph/ephrin for 30 min at room temperature. Keratinocytes were treated with a final Eph/ephrin concentration of 2 μg/ml.

Keratinocytes were plated on collagen-coated surfaces at the desired cell density and transferred to basal FAD medium three hours prior to treatment with recombinant EphB and ephrin-B proteins. One hour prior to treatment cells were incubated with 20 μg/ml human IgG (Antibodies Inc.) in order to block any FC receptor present on the keratinocytes. Eph/ephrin stimulation was carried out at 37^{0}C for between 10 min and overnight, depending on the experiment.

Each condition is performed in triplicate.

2.16- Wnt pathway activation assays

TOPFLASH activity was measured by a luciferase assay in the presence or absence of Wnt3A or Wnt5A (R&D) in basal KSFM (GIBCO). The CRUK Protein Facility purified recombinant mouse Wnt3A or Wnt5A as described previously (Willert et al., 2003)and (Mikels and Nusse, 2006), respectively).

In order to perform luciferase assays, keratinocytes were transfected with the Lipofectamine 2000 method. Cells were transiently transfected with the following constructs: pRL (Renilla luciferase control, Promega), Topflash or Fopflash (firefly luciferase) (van de Wetering et al., 1997). 0.5x 10^5 keratinocytes were plated in quadruplicate in 24-well plates and left overnight to settle on KSFM with additives at 37°C. The next day 0.5μg of DNA were transfected per well (0.08 μg pRL and 0.12μg Topflash or Fopflash) following the manufacturer's instruction. Cells were incubated with the transfection mixture overnight on KSFM. The next day cells were incubated either with Wnt3A or Mock (buffer alone) or in combination with recombinant EphFc. When Eph treatment was combined with Wnt stimulation, the second day I incubated the cells with human IgG for 2hours in order to block

any Fc receptors. Then, cells were rinsed and the recombinant EphFc were added for 1 hour. The last step was to add the Wnt3A or 4OHT accordingly. These were left for 24 hours prior analysis.

Cell lysis was performed using passive lysis buffer from the Dual-Luciferase Reporter Assay Kit (Promega). Cells were washed twice with PBS, 200µl of 1x buffer were added to each well and lysis was performed using a rubber cell scraper. Lysates were collected in eppendorf tubes, put on dry ice with ethanol, and then subjected to four freeze/thaw cycles. The clear lysates were transferred to fresh tubes and either stored at -20°C or used immediately for luciferase analysis. Renilla and firefly luciferase activities were detected in enzymatic reactions prepared using the Dual-Luciferase Reporter Assay Kit (Promega) according to the Manufacturer's instructions. 10µl of each lysate were analyzed using a BioOrbit 1251 luminometer connected to an automated capillary system that automatically added the two luciferase substrates to the lysates. Renilla luciferase activity was used to normalise the data for transfection efficiency.

2.17- Cell lysis and Western blotting

2.17.1- Protein isolation

Cells were lysed in RIPA buffer (50 mM Tris-HCl pH 7.4, 1% NP40, 0.25 % sodium deoxycholate, 150 mM NaCl, 1 mM EGTA). To analyse the soluble pool of β-catenin, keratinocytes were lysed in hypotonic buffer at 4°C (20 mM Tris-HCl pH 7.5, 1 mM $MgCl_2$, 1 mM sodium orthovanadate, 25 mM β-glycerophosphate with protease inhibitors) and centrifuged at 600 g for 10 min to remove nuclei. The supernatant was centrifuged at 100,000 g for 1 hr at 4°C; the particulate fraction was discarded and the soluble fraction was used for analysis.

2.17.2- BCA protein assay

The concentration of protein in samples was determined using a BCA protein assay kit (Pierce). The kit is based upon the Biuret reaction involving the reduction of Cu^{2+} ions to the Cu^{1+} (cuprous) ion by protein in alkaline medium. Chelation of the cuprous ion to bicinchoninic acid (BCA) molecules provides a sensitive colorimetric detection method with the reaction product exhibiting a strong

absorbance at 562nm. The absorbance is linear over a 20-2000 mg/ml protein concentration range. A protein standard curve was produced from 0 to 2 μg/μl protein by making dilutions of a 2 mg/ml BSA solution (Pierce) into PBS according to the Manufacturer's instructions. Protein samples to be assayed were diluted 1:4 to 1:5 in PBS to minimise interference of lysis buffer detergent and supplements with the reaction and also to place the protein concentration within the standard curve. The assay was set up on a 96-well plate (DYNEX Technologies) according to the Manufacturer's instructions and all standards and samples were assayed in triplicate wells. The plate was incubated at 37°C for 30 min and the absorbance at 562nm was then read on a Titertek Multiscan MCC/340 MKII spectrophotometer. The protein concentration of each sample was determined against the standard curve.

2.17.3- Immunoprecipitation of Eph and ephrin proteins

To detect Eph and ephrin proteins from cell lysates I had to perform immunoprecipitation (IP) of the Eph and ephrin proteins and then immunoblot with the same antibody. This step increased the western blot (WB) quality.

The day before, cells were plated on Collagen I pre-coated dishes at near to confluency density and they were further incubated with KSFM media without additives in order to starve cells.

Cells were harvested and lysed with a cell scrapper in ice-cold IP buffer that consisted in (0.15 M NaCl; 0.05 M Tris; 5mM EDTA; 0.5% NP-40; including a cocktail of protease inhibitors: PMSF 200μg/ml final concentration and Aprotinin 25μg/ml) and leave on ice for 30 minutes. Put aside a small volume (50 μl for total lysate control sample and 50 μl for protein concentration measurements). Centrifuge at 12000 rpm for 15 minutes at 4°C and transfer the supernatant to a new tube. For IP, 10μl of primary goat antibody (all the anti-ephrin/eph antibodies used were raised in goat from R&D Systems) were added (Stock 100μg/ml) and cell lysates were incubated rocking for 2 hours to overnight at 4°C. Then 50 μl of Protein G slurry were added and further incubated for 2 hours at 4°C, if the IP was performed with a rabbit antibody, I used Protein A instead. Centrifuge at slow speed 1200 rpm for a minute at room temperature. Aspirate supernatant and add

wash by adding 1ml ice-cold PBS, centrifuge and aspirate 3 times. Boil and add sample buffer to the beads. Store at -20°C.

2.17.4- Laemmli sample buffer

2x Laemmli sample buffer (reducing) comprised 125mM Tris-HCl, pH6.8, 2% SDS, 20% glycerol, 0.02% bromophenol blue and 10% (v/v) β-mercaptoethanol (Sigma). The sample buffer was aliquoted and stored at –20°C.

2.17.5- SDS-PAGE

A vertical mini-gel electrophoresis apparatus (Atto) was used. Gels were prepared between the glass plates using the method of Laemmli (Laemmli, 1970). Table 2.1 describes the gel compositions. Immediately after pouring the resolving gel solution, 0.5 ml of dH_2O was carefully applied to ensure a level interface as well as to eliminate an air-acrylamide interface. Gels were allowed to polymerise at room temperature for approximately 30 min. The dH_2O layer was discarded from the top of the resolving gel and the stacking gel solution was then poured. An 8 or 12 well comb was inserted to create wells and the gel was left to polymerise. After the gel had set, the comb was removed and the wells were flushed with SDS-PAGE running buffer which comprised 50mM Trizma base, 384mM glycine and 0.1% SDS.

Equal amounts of protein from each sample (typically 10-20μg total protein) were diluted into Laemmli sample buffer and placed in a 100°C hot block for 5 min before being briefly spun down in a bench top centrifuge and applied to the wells using capillary pipette tips. 10μl pre-stained rainbow molecular weight markers (Amersham) were added to 10μl Laemmli sample buffer, boiled for 5 min and loaded into one of the wells. Samples were electrophoresed at 120V until the dye front had run off the bottom of the gel and the gel was then removed and prepared for Western blot.

2.17.6- Preparation of SDS-PAGE gels

Stock solutions

40 % acrylamide mix (37.5:1 acrylamide to bis-acrylamide ratio) (Amresco), 3M Tris-HCl, pH 8.8 (BDH), 10 % SDS in dH_2O, 2M Tris-HCl, pH 6.8 (BDH), APS

10 % ammonium persulphate (Bio-Rad) in dH_2O, aliquots stored at –20°C, TEMED N,N,N',N'-tetramethylethylenediamine (Bio-Rad).

Resolving gels (15 ml)

% GEL	40 % Acrylamide mix	3M Tris-HCl, pH 8.8	10 % SDS	dH_2O	APS	TEMED
8 %	3 ml	1.9 ml	0.15 ml	9.8 ml	0.15 ml	9 ml
10 %	3.75 ml	1.9 ml	0.15 ml	9.05 ml	0.15 ml	6 ml
12 %	4.5 ml	1.9 ml	0.15 ml	8.3 ml	0.15 ml	6 ml
15 %	5.625 ml	1.9 ml	0.15 ml	7.715 ml	0.15 ml	6 ml

Stacking gel (10 ml)

Solutions	40 % Acrylamide mix	3M Tris-HCl, pH 8.8	10 % SDS	dH_2O	APS	TEMED
	1.275 ml	0.1 ml	0.625 ml	7.85 ml	0.1 ml	10 ml

2.18- Western blotting

After electrophoresis, proteins were transferred onto PVDF membrane (Millipore), which had been pre-wet in absolute methanol. Mini-Trans Blot Cells (Bio-Rad) were used to transfer the protein and were set up according to the Manufacturer's instructions. Transfer took place at 4°C overnight at 30 volts. The blot was then rinsed briefly in TBS containing 0.1 % Tween-20 (TBST) before blocking with 5 % Marvel milk powder (99 % fat free, Premier Brands UK Ltd.) dissolved in TBST for at least 1 hour at room temperature.

2.18.1- Transfer buffer

The transfer buffer for Western blotting was made up freshly each time: 8.75g Trizma base and 43.5g glycine were dissolved in 500 ml dH_2O to which was added 15 ml of a 10 % SDS solution. The buffer was made up to 1.2 l before the addition of 300 ml of methanol and was then thoroughly mixed.

2.18.2- Probing blots with antibodies and ECL detection

Blocked membranes were incubated with primary antibody typically diluted in 5 % milk powder solution in TBST. Some antibodies (according to manufacturers instructions) were diluted in 5 % BSA in TBST. Incubation with primary antibody was at 4°C overnight with gentle agitation. After 3 x 20-30 min washes with TBST, the blots were incubated for 1 hour at room temperature with HRP-coupled

secondary antibody (Amersham) diluted 1:5000 in 5 % milk, TBST. Membranes were then washed 3 or 4 times with TBST again. To detect bound HRP, a chemiluminescence kit was used according to the Manufacturer's instructions (ECL, Amersham). X-ray films (Kodak) were exposed in autoradiography cassettes. Densitometry of bands produced on films was carried out using NIH Image v1.58.

2.19- Oligonucleotide arrays and data analysis

2.19.1- RNA preparation

Back skin samples were prepared for RNA isolation using a combination of methods previously developed in the lab (Arnold and Watt, 2001)and (Owens et al., 2003). The portion of dorsal skin that had been previously clipped and where the treatment was applied was cut into 4 pieces of about 1cm^2 of size. These were put into cryo-vials and flash frozen in liquid nitrogen. Processing of the skin to obtain RNA was performed with care using standard RNA techniques (for standard references on molecular biology see (**Sambrook, 1989**). The square of dorsal skin from each mouse was weighted so that they were around 50mg. They were then placed into 12ml of TRI reagent (Helena Biosciences) in a 50ml polypropylene tube (Nalgene) and homogenised at room temperature for 1 min using a Polytron homogenizer set to a high speed. The tubes were left at room temperature for 5 min and then kept on ice until the next step. 1.2ml 1-bromo-3-chloropropane (BDP, Helena Biosciences) was then added to each tube, mixed by shaking very vigorously for 15 sec and incubated at room temperature for 15 min. The samples were centrifuged at 11400rpm in a Beckman J-20 centrifuge for 30min at 4°C. The upper, aqueous phase containing the RNA was carefully removed into brand new polypropylene tubes (Nalgene). 12ml isopropanol were added and the samples were mixed by vortexing. Samples were placed at -20°C for one hour to precipitate the RNA, which was then pelleted by spinning again at 11400rpm in a Beckman J-20 for 30min at 4°C. The isopropanol was discarded appropriately and the pellet was left to dry and then resuspended in RNase-free dH_2O. For a second run of RNA purification, I used the Qiagen RNeasy Mini Columns according to the Manufacturer's instructions and resuspended in 100µl of RNase-free dH_2O. The RNA was quantified by spectrometry and the quality

controlled by running samples on formaldehyde/agarose/ethidium bromide gels following the standard procedure (Sambrook, 1989).

2.19.2- cDNA and cRNA preparation

Double-stranded cDNA was generated from 10 μg total RNA using Superscript Double Strand cDNA Synthesis Kit (Invitrogen) according to the Manufacturer's instructions, with a T7-polyT primer (Affymetrix). The cDNA was purified using the GeneChip Sample Cleanup Module (Affymetrix) and used to generate biotinylated cRNA by *in vitro* transcription using the Enzo BioArray High Yield Transcript Labelling Kit (Affymetrix). cRNA was purified using the GeneChip Sample Cleanup Module (Affymetrix) following the Manufacturer's instructions and quantified as described before. 25 μg of cRNA were fragmented in Fragmentation buffer provided with the GeneChip Sample Cleanup Module by incubating it at 94°C for 35 min exactly in a heating block.

The quality of cDNA, cRNA and fragmented cRNA was checked by running an aliquot of each on formaldehyde/agarose/ethidium bromide gels. The molecular weight markers used were 0.24-9.5 Kb RNA Ladder (Invitrogen) for cDNA and cRNA, and RNA Century Size Markers (Ambion) for the cRNA.

2.19.3- Microarrays hybridization and scanning

The hybridization and scanning of the arrays were performed by the Cancer Research UK Affymetrix Facility located in the Paterson Institute for Cancer Research, Manchester (UK). 10 μg of fragmented cRNA were hybridized to the GeneChip Mouse Expression Set 430 (A and B chip) oligonucleotide arrays (Affymetrix), comprising 45037 probe sets. Complete annotations and spotting patterns can be found online at http://www.affymetrix.com. The hybridization was performed following the Manufacturer's instructions using an Affymetrix GeneChip Instrument System. The arrays were washed and stained with streptavidin-phycoerythrin before being scanned on an Affymetrix GeneChip scanner.

2.19.4- Normalization and Filtering of the Array Data

Unscaled raw data were loaded from a text file on Genespring (Version 6.1, Silicon Genetics). Measurements less than 0.001 were set to 0.001. The normalization was set as follow: per chip normalization to the 50th percentile, per gene normalization to the median.

Spearman correlation was used to generate a condition tree and cluster all the chips as a quality control. As a result, one replicate for the conditions wt7 and wt0 (B chip) were removed.

All the data that passed the quality control were filtered using the Genespring advanced filtering tool. I identified probes with present or marginal flags in at least one out of 6 conditions, t test p value less than 0.05 in at least one condition, standard deviation less than 1.45 in at least 2 out of 6 conditions, and a change in relative expression levels of at least 2-fold in the 4OHT-treated transgenic samples compared to untreated transgenic and all the wild-type samples.

Unscaled raw data were analyzed using GeneSpring™ software (Silicon Genetics, version 6.1). Normalized data were filtered to select for genes showing a fold change greater than 3 with t-test p-values less than 0.05 and a standard deviation less than 1.45 upon activation of the transgene.

2.19.5- Normalization and filtering of the array data

Unscaled raw data were loaded on Genespring (Version 6.1) with measurements less than 0.001 set to 0.001, per-chip normalization to the 50th percentile and per-gene normalization to the median. A condition tree based on Spearman correlation was used to cluster all the chips as a quality control. All the data from the chips that passed the quality control were filtered using the Genespring advanced filtering tool. We identified probes with present or marginal flags, t-test p-value less than 0.05, standard deviation less than 1.45 and a change in relative expression levels of at least 3-fold in the 4OHT treated transgenic samples compared to untreated transgenic and the all the wild-type samples.

Most of the 103 upregulated genes could be classified into distinct functional groups (Table 1A). Proteins involved in signalling or transcription were the largest category (29.1%), followed by proteins involved in cellular metabolism (15.5%)

and keratins (14.6%). Representative genes in each group are listed in Table 1B, with their fold induction indicated in brackets.

The lists shown in this study contain no repeated probes and only the known genes.

Antibody	Specificity	Species	Originator	Dilution
AC40	Actin	Mouse	Sigma	
OBT0030	Bromodeoxyuridine	Rat	Oxford Biotechnology	1:100
	β-catenin	Mouse	BD	1:100
C20	c-Myc	Rabbit	Santa Cruz	1:100
	CDP	Rabbit	gift from M. Busslinger	1:600
RAM34	CD34	Rat	BD Pharmingen	1:50
	Dishevelled 2	Rabbit		1:100
AF473	EphrinB1	Goat	R&D	1:50
	Ephrinb2	Goat	R&D	1:25
	EphB2	Goat	R&D	1:25
BAF 432	EphB3	Goat	R&D	1:25
	EphB4	Goat	R&D	1:25
Ab 4389	EphA4	Rabbit	Abcam	1:100
MC-20	Estrogen receptor	Rabbit	Santa Cruz Biotechnology	1:100
ab7523	Gli 1	Rabbit	Abcam	1:100
	Gli 2	Rabbit	gift from R. Toftgård	1:50
MB 1.2	β1 integrin	Rat	gift from B Chan	1:100
	Keratin 17	Rabbit	gift of P. Coulombe	1:100/1:500
AF 64	Keratin 14	Rabbit	Covance	1:5000
LHK15	Keratin 15	Mouse	gift from I. Leigh	1:100/1:50
NCL-Ki67p	Ki67	Rabbit	Novocastra	1:600
01902-D	c-kit	Rat	Pharmingen	1:10
2D12	Lef1	Mouse	Upstate	1:100
C-19	N-Myc	Rabbit	Santa Cruz	1:100
nestin 130	Nestin	Rabbit	gift from R. McKay	1:100
ab12053	Sox4	Rabbit	Abcam	1:50
GOH3	α6 integrin	Rat	BD Biosciences	1:100
05-591	pAkt	Rabbit	Biosource	1:100
	Keratin 10	Rabbit	MK10 DAKO	1:2500
	Caspase 14	Rabbit	Abcam	1:500
	keratin 6	Rabbit	Babco	1:5000
11796	pSMAD2/3	Goat	Santa Cruz	1:250
Ly-6A/E	Sca1	Rat	BD	1:250
2B8	c-Kit (CD117)	Rat	BD	1:50
Sox2	Sox2	Rabbit	Gift from R Lovellbadge	1:500
AB5603	Sox2	Rabbit	Chemicon	1:250
AB5772	Sox3	Rabbit	Chemicon	1:100
AB5811	Sox13	Rabbit	Chemicon	1:100

Table 2.1- List of selected primary antibodies used in the work presented in this Thesis.

2.20- List of selected suppliers

Abcam, Cambridge,UK.

Acros organic, Netherlands.

Affymetrix Inc. Santa Clara, California, USA.

Ambion Inc. Austin, Texas, USA.

Amersham Biosciences, Amersham, Buckinghamshire, UK.

Amresco, Solon, Ohio, USA.

Antibodies Inc.; Davis, California,USA.

Atto, supplied by BioRad.

Beckman Instruments, Palo Alto, California, USA.

BD Biosciences, Erembodegen, Belgium.

BD PharMingen, San Diego, California, USA.

BDH Laboratory Supplies Inc. Hemel Hempstead, Hertfordshire, UK.

Becton-Dickinson, Lincoln Park, New Jersey, USA.

Biochrom, Berlin, Germany.

Biomol International, LP.Hamburg, Germany.

Biorad Laboratories Inc. Hemel Hempstead, Hertfordshire, UK.

Boehringer Mannheim UK Ltd. Lewes, East Sussex, UK.

Calbiochem – Novabiochem (UK) Ltd. Nottingham, UK.

Carl Zeiss Ltd. Welwyn Garden City, Hertfordshire, UK.

Chemicon (Millipore), Harrow, Middlesex,UK.

DAKO A/S, Glostrup. Denmark.

Difco aboratories, Manston, Wisconsin, USA.

DNA Technology AIS, Aharus, Denmark.

Eppendorf, Histon, Cambridge, UK.

Falcon, part of Nunc A/S, Roskilde, Denmark.

Fischer Scientific, Loughborough, Leicestershire, UK.

Gibco BRL/Life Technologies Ltd. Paisley, Renfrewshire, UK.

Helena Biosciences, Sunderland, Tyne & Wear, UK.

IBL, Hamburg, Germany.

ICN Pharmaceuticals Ltd. Thame, Oxon, UK.

Imperial Laboratories (Europe) Ltd. Andover, Hampshire, UK.

Invitrogen, Paisley, UK.

Jencons, Leighton Buzzard, Beds, UK.

Jackson Laboratories, Maine,USA.

Merck Biosciences, Darmstadt, Germany.

Millipore, Harrow, Middelsex, UK.

Molecular Probes, Leiden, Netherlands.

Monsanto Chemicals, Springfield, Massachusetts, USA.

Nalgene Nunc International, Rochester, New York, USA.

Novagen, Madison, Wisconsin, USA.

New England Biolabs (NEB). New York, USA.

Nunc A/S, Roskilde, Denmark.

Oxford Biotechnology, Kidlington, Oxfordshire, UK.

Peprotech, Rocky Hill, New Jersey, USA.

Pharmacia Biotech, Uppsala, Sweden.

Pierce, Rockford, Illinois, USA.

Premier Brands UK Ltd. Knighton, Stafford, UK.

Promega UK Ltd. Southampton, UK.

Qiagen Ltd. Crawley, UK.

Roche, Lewes, East Sussex, UK.

R&D Systems, Minneapolis,USA.

Santa Cruz Biotech Inc. Santa Cruz, California, USA.

Savant supplied by Life Sciences International, Basingstoke, Hampshire, UK.

Schleicher and Schuell, London, UK.

Sera-Lab, Crawley Down, Sussex, UK.

Sigma Chemical Co. Poole, Dorset, UK.

Silicon Genetics, part of Agilent Technologies UK Ltd. South Queensferry, UK.

Stratagene, LA Jolla, California, USA.

Vector Laboratories, Burlingame, California, USA.

Zymed, San Francisco, California, USA.

Chapter 3- Characterisation of patterning in tail epidermis

Aims

An interesting question in biology is how patterning arises during development and how it is maintained throughout adulthood. The epidermis constitutes an ideal model to start unveiling this question. The epidermis is a highly compartmentalised tissue, which contains domains where proliferation and differentiation are inhibited, in which stem cells reside and domains where the lineage choice of the stem cell progeny occurs. Patterning allows for coupling of differentiation and proliferation by separating progenitor populations from their more differentiated progeny. In this Chapter I sought to define further the compartments of tail epidermis and characterise markers of LRC and their committed progeny.

3.1- Introduction to the tail whole mount system to assess patterning in epidermis

The tail whole mount system is a technique that although is dated to the 1800s (Schweizer and Marks, 1977), it was being further developed in our laboratory at the time I joined the laboratory (Braun et al., 2003). The work that I performed that contributed to its further development is presented in this Chapter.

Whole mounts of several parts of the furry body can be prepared, however the hair follicles of the tail are quite large compared to those in the back and the IFE is thicker. This makes the skin of the tail quite resistant as it remains intact and can be peeled off the dermis and thus ideal to work with. The diagram in Figure 3.1 shows a step-wise protocol that is described in detail in the Materials and Methods section. The benefit of this system is that allows of 3-D visualisation, screening of large areas and quantification of changes occurring or patterns in the epidermis. In wild-type skin the hair follicles are arranged in rows and clustered in groups of three (triplets) (see Figure 3.2). Each follicle has a pair of prominent

sebaceous glands. In order to make quantification consistent, we defined one triplet and the adjacent interfollicular epidermis as one epidermal unit (See red dotted line in Figure 3.2).

A typical experiment is depicted in Figure 3.3.

For each set of staining omission of the primary would be always included as a negative control. This would be used for determining the setting of the confocal microscope as it would show the background staining given by the secondary antibody.

Typically, the analysis of a tail skin whole mount would start by taking several low power images (x10) of each epidermal sheet. This would allow visualisation of large areas of tissue and would be performed for all the mice and conditions of the experiment. Next, closer images would be taken (x20), first comparing several follicles and epidermal units within on sample. Next, these would be compared with other samples. These steps would help assessing the analysis of patterns of expression or changes rising in different conditions or genotypes (See Figure 3.3).

Typically, mice of the same background, sex, and age would be compared. These factors must always be taken into account when performing analysis. In addition, changes during the hair cycle could only be analysed between littermates during the synchronous stage of the hair cycle.

The observations and the results obtained in tail whole mounts should be backed up by analysis of conventional histology of tail skin and also compared with back skin.

3.2- LRC compartment

One characteristic of stem cells is that they are slow-cycling cells with a high proliferative capacity. Taking advantage of this feature, they can be detected by labelling the tissue at a stage in which is highly proliferative, this is, so that cells will take up the label (Bickennbach, 1981; Braun et al., 2003). In mouse, the skin is highly proliferative around 10 days after birth (P10) (Figure 3.4 A, B). After a chase period of minimum of 40 days, only the slow-cycling cells will retain the label (see Figure 3.4 A and C). The more proliferative cells will dilute the label after a few divisions. I used this assay to detect the label retaining cells (LRC) in epidermis. At P50, LRC were clustered in the permanent portion of the hair

follicle, known as the bulge (See Figure 3.4). There were a few scattered LRC in the SG and in IFE (See Figure 3.4 C and D). There were no big differences between a chase period of 40 days or 60 days (See Figure 3.4 C and D). When I joined the laboratory this technique was being developed and I contributed to the optimisation of this technique to screen for new bulge LRC markers (Braun et al., 2003) and markers of differentiation and signalling pathways involved in lineage commitment that will be described in the Chapter.

3.3- Characterisation of the epidermal stem cell compartment *in situ:* 'Candidate-approach' screen of stem cell markers

Since the whole mount technique allows us to visualise and characterise the stem cell compartment of mouse tail epidermis *in situ*, we can use this approach in combination with LRC experiments to locate slow cycling cells and to assess the expression of several putative stem cell and differentiation markers by immunolabelling (Figure 3.5). The whole mounts are analysed by confocal microscopy.

3.3.1- Well-known bulge markers

On a candidate-approach basis, we carried out a screen for several putative stem cell markers in this system (see Figure 3.5). In particular, we have shown that keratin 15 is expressed in label-retaining cells in the tail epidermis confirming that is a good stem cell marker like in the back (Figure 3.5 E,H,J,K; Lyle et al., 1998; Braun et al., 2003). It was later confirmed by studies of Morris, Costarelis and colleagues that keratin 15 expression is a bonafide marker of bulge stem cells that under steady-state conditions replenish the hair follicle lineages (Morris et al., 2004).

Based on the literature, I also assessed in this system, known markers of bulge stem cells like the HSC and HF marker CD34 (Trempus et al., 2003). I confirmed that CD34 is expressed in LRC of the bulge of mouse tail follicles (Figure 3.5 D,G).

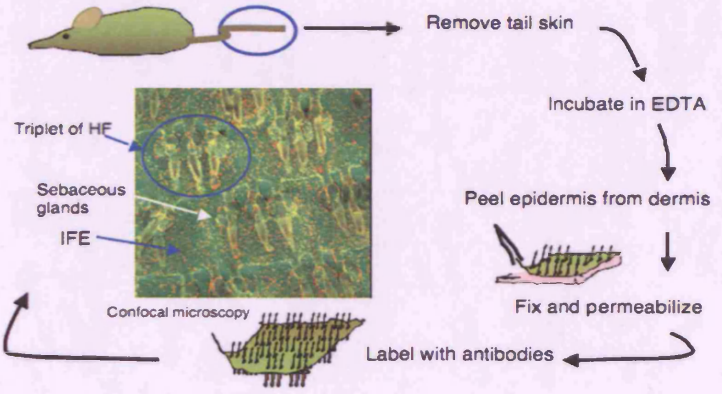

Figure 3.1 - Tail skin whole-mount labelling technique . This diagram shows the steps carried out to isolate and process tail epidermis from tail skin (See Materials and Methods for detailed explanation). This technique allows visualisation in 3-D of basal cells from sebaceous glands (SG), hair follicle (HF) and interfollicular epidermis (IFE). The whole-mount shown was immunolabelled for Ki67 (red) and β1 integrin (green) and visualised by confocal microscopy.

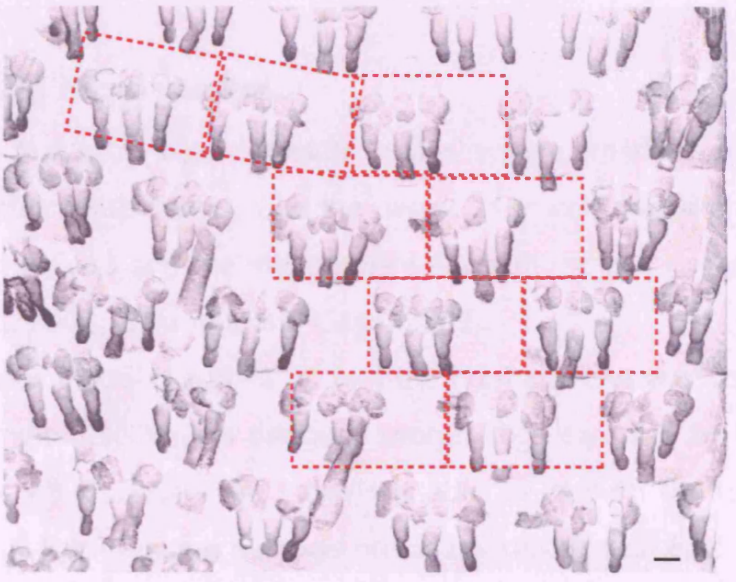

Figure 3.2 - Tail skin whole-mount allows quantification of large areas. Whole mount of wild type epidermis immunolabelled with anti-keratin 14 antibody was processed with LSM software and the color shown is the saturation of the original image. Hair follicles in tail epidermis are arranged in staggered rows of triplets. Dashed red line indicates the epidermal units which will be used as a measure for quantification in later chapters. Scale bar: 100 μm.

Tcf-3 has been reported to be expressed in the bulge, where it acts as a repressor of the Wnt pathway (DasGupta and Fuchs, 1999; DasGupta et al., 2002; Merrill et al., 2001). I have confirmed in this system that this is indeed a good marker (Figure 3.5 E).

pSMAD2 was revealed in a screen for bulge markers (Tumbar et al., 2004), and the immunolabelling shows that is expressed in the bulge of tail follicles (Figure 3.5 F). When I did double labelling with BrDU, I could see that a large proportion of the cells pSMAD2 positive were CD34 positive (Figure 3.5 G) and keratin 15 positive (Figure 3.5 H).

3.3.2- Candidate bulge markers

Based on the literature, I also assessed in this system, markers of stem cells reported from other adult tissues, like the neural stem cell markers, such as the transcription factor Sox2 and the intermediate filament protein, nestin (Marvin et al., 1998;Li et al., 2003; D'Amour and Gage, 2003).

Nestin is expressed in cells resident of the bulb normally clustered and a second population of single cells with a dendritic morphology can also be found along the ORS (Figure 3.9 B). However, I was not able to confirm the expression of nestin in the bulge keratinocytes that was previously reported (Li et al., 2003).

P63 was also a good candidate, as it is critical for the stratification of epithelia (Koster et al., 2004). The antibody recognises all the 7 isoforms and labelled all cells in ORS, SG and IFE, so it was discarded further as a good bulge marker (Figure 3.5 D).

In the case of Sox2, LRC at the top of the bulge, express high levels of cytoplasmic Sox2 (Figure 3.5 I, L, M). These cells are keratin 15 and CD34 negative. (See Figure 3.5 I,L,M). Interestingly, the keratin 15 positive population of the HF is only formed after postnatal day 5 (Figure 3.5 K).

After I completed this screen, two groups reported the identification and genetic profiling of bulge LRC (Tumbar et al., 2004 and Morris et al., 2004). In agreement with my findings they reported that label retaining cells in the bulge express keratin 15 and that CD34 is a good marker to isolate bulge LRCs.

Their studies provide new markers that will be tested in the future.

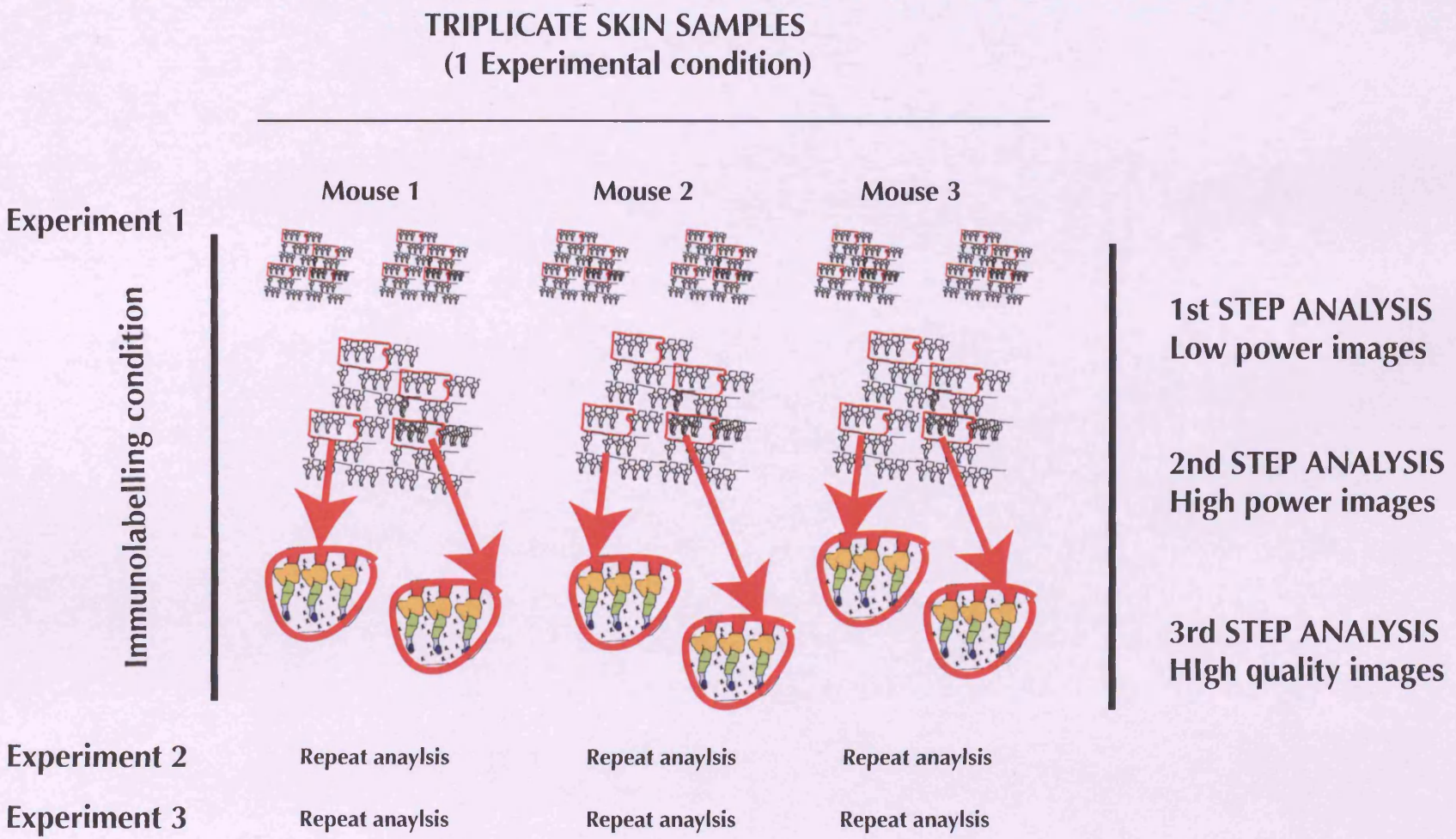

Figure 3.3- Stepwise protocol of tail skin whole mount analysis. Typically, each staining will be performed a minimum of 3 times on 3 independent samples. For each set of staining omission of the primary would be always included as a negative control. This would be used for determining the setting of the confocal microscope as it would show the background staining given by the secondary antibody. For comparison between experimental conditions, images of different conditions labelled with the same antibodies were taken using the same settings. Typically, the first step of the analysis would start by taking several low power images (x10) of each epidermal sheet. This would allow visualisation of large areas of tissue and would be performed for all the mice and conditions of the experiment. The second step will consist in taking closer images at higher magnification (x20), first comparing several follicles and epidermal units within on sample. Next, these would be compared with other samples. These steps would help assessing the analysis of patterns of expression or changes rising in different conditions or genotypes.

Since the screen was performed, a new population positive for the thymic progenitor cell surface marker MTS24 has been described which is above the keratin 15/CD34 double positive population that resembles the Sox2 population (Nijhof et al., 2006).

3.4-Visualisation of lineage commitment in tail epidermis

3.4.1-Patterning in the IFE

The epidermis of the tail is highly patterned, as can be appreciated in whole mount preparations. In wild type skin, hair follicles are arranged groups of three (triplets) and are organised in rows, such that the hair follicle triplets in one row are staggered relative to those in the rows on either side (See figure 3.2). Single scattered LRC positive cells are also localised in IFE (Figure 3.4 C, D). After comparing various samples, their localisation does not appear to follow a fixed pattern, however they are normally confined to the parakeratotic scale region. In addition, within tail IFE two types of differentiation can be distinguished (see Figure 3.6; López-Rovira et al., 2005). The IFE that encircles each hair follicle triplet, known as the parakeratotic scale, expresses caspase 14 (Figure 3.6 A) but does not express keratin 10 (Figure 3.6 B). The remainder of the tail IFE is keratin 10 positive and caspase 14 negative (Figure 3.6 A, B). When looking at a section of tail skin the areas devoided of basal keratin 10 expression demark the parakeratotic scale area (Figure 3.6 C and D).

Interestingly, when looking at dermis whole mounts a similar pattern of expression like parakeratotic scales is found when immunolabelling with several basement membrane markers like collagen IV (Manuela Ferreira, personal communication).

3.4.2- Patterning along the follicle in tail epidermis

Patterning is also observed along the length (proximo-distal axis) of individual hair follicles, including the sebaceous glands (Figure 3.7) with different expression domains that correspond to areas in which either differentiation or proliferation are inhibited (like the bulge) or differentiation and proliferation are promoted (like the bulb).

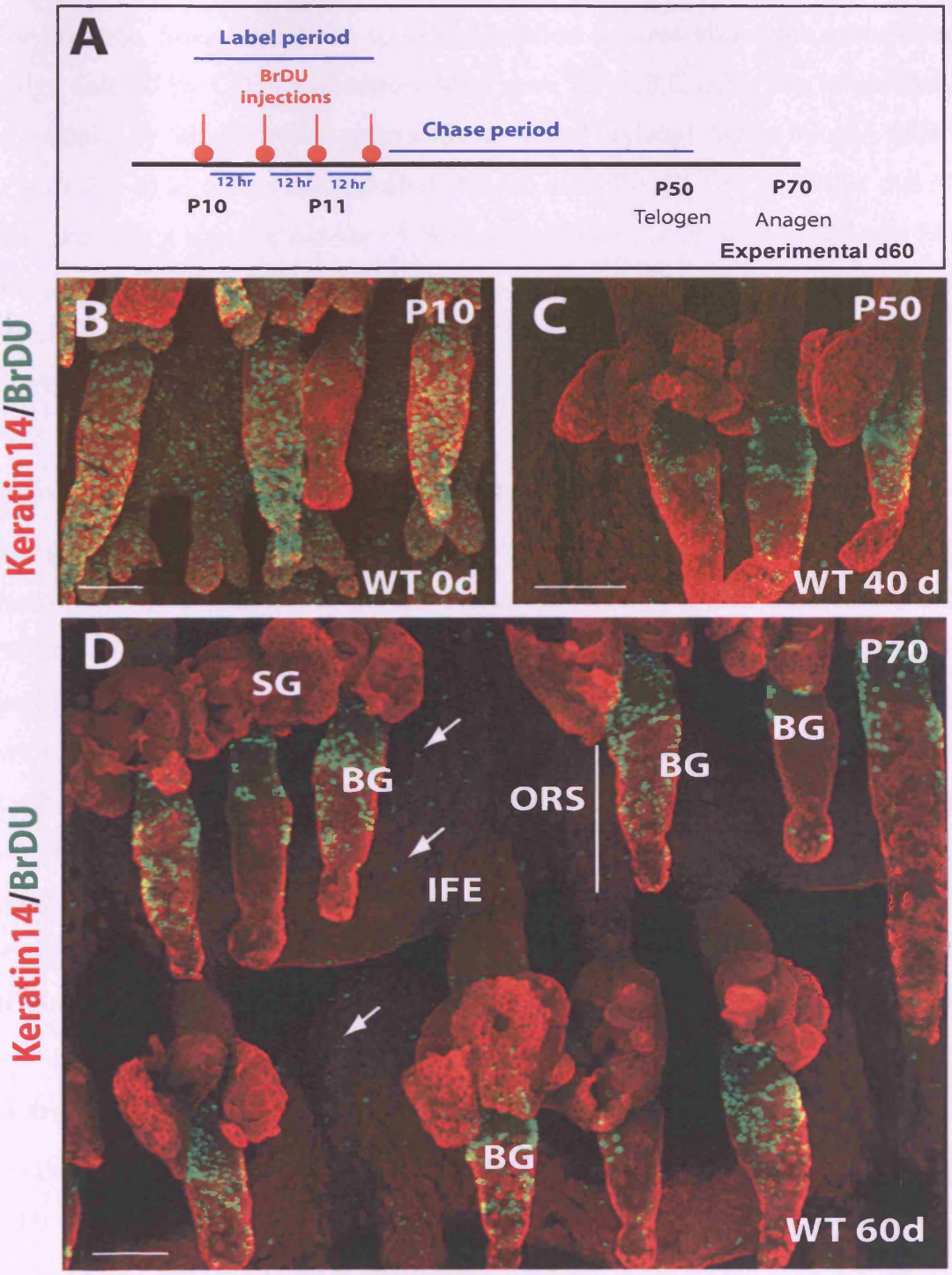

Figure 3.3- Generation of Label Retaining Cells to study the stem cell compartment (A) Diagram shows the time line of the LRC experiment to label slow-cycling cells. (B-D) Tail epidermal whole mounts of wild type skin of the indicated ages were immunolabelled with antibodies to keratin 14 to visualise basal cells and BrdU. In D locations of sebaceous glands (SG), bulge (BG) and outer root sheath (ORS) and interfollicular epidermis (IFE) are indicated. Arrows in (D) show LRC cells. Scale bars: 100 μm.

I focused on the markers that have discrete domains of expression in the follicle. For instance, Sox2 expression specifically labels an area above the conventional bulge defined by CD34 expression (see Figure 3.7 A,B,C,D,E). The infundibulum is specifically labelled with antibodies to phosphorylated Akt in telogen follicles (Figure 3.7 B) as previously reported (Alonso et al,.2005). The lipophilic dye Nile Red provides a specific marker of sebocytes (Figure 3.7 F), while CDP and FABP are highly expressed in the bulb of anagen follicles (Figure 3.7 G, H). Interestingly, the expression of the Planar Cell Polarity protein, Dishevelled2, also marks the bulb (Figure 3.7 I).

3.5-The proliferation pattern in tail epidermis

As previously mentioned in Figure 3.4, quiescent cells are visualised by label retention after a long chase period (30 days) and they are located in the bulge portion of the HF and scattered in the SG and IFE (Figure 3.4 and 3.8 A). The proliferative compartment can be visualised by immunolabelling S-phase cells with a 1h pulse of BrDU. In addition Ki67 can be used as a marker of actively cycling cells. A large number of proliferating cells can be seen in the basal layer of IFE, in the outer layers of the SG and at the base of the hair follicle, the bulb, in anagen follicles (Figure 3.8 B-D). We can also visualise proliferative cells with a marker for lipid rafts, which normally are enriched in highly proliferative cells (Figure 3.8 E and F; Gniadecki and Bang, 2003).

3.6- Cell types resident in the HF

As described in the Introduction, the skin niche is very complex and multiple cell types coexist. I analysed several of these populations in tail epidermis (Figure 3.9 A-F). I analysed Neural crest derivatives such as Nestin positive cells (Figure 3.9 A), which are known to include a progenitor population of the dermal papilla (Fernandes et al., 2004) and melanocyte stem cells (positive for c-Kit) (Figure 3.9 B). Nestin positive cells are not keratinocytes as they are negative for keratin 14 (Figure 3.9 C). Keratin 16, marker for Merkel cells, the skin mechanoreceptors, defines a row of three or four cells on either side of the upper part of the bulge (Figure 3.9 D). Differentiated melanocytes can be visualised by L-Dopa staining,

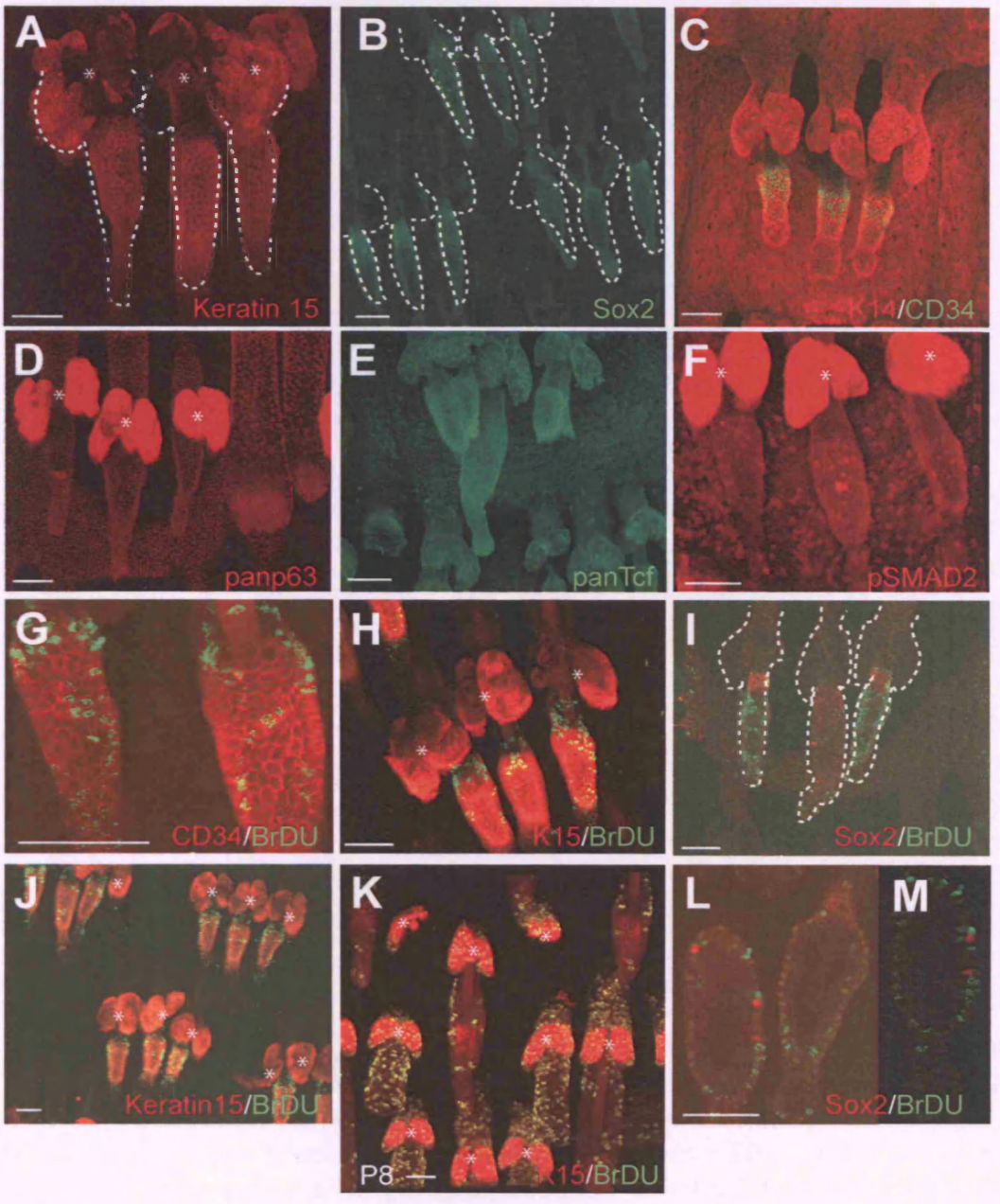

Figure 3.5 - Screen for bulge markers. A candidate approach to search for markers of the bulge compartment of tail epidermis was performed using the whole mount system. (A-M) Examples of some of the proteins tested are shown. (A-M) Whole-mounts of wild type epidermis immunolabelled with antibodies to the proteins shown. Asterisks indicate non-specific staining in sebaceous glands. Epidermis in K is from P8 mouse. Epidermis in other panels is from adult mice. Scale bars: 100 μm.

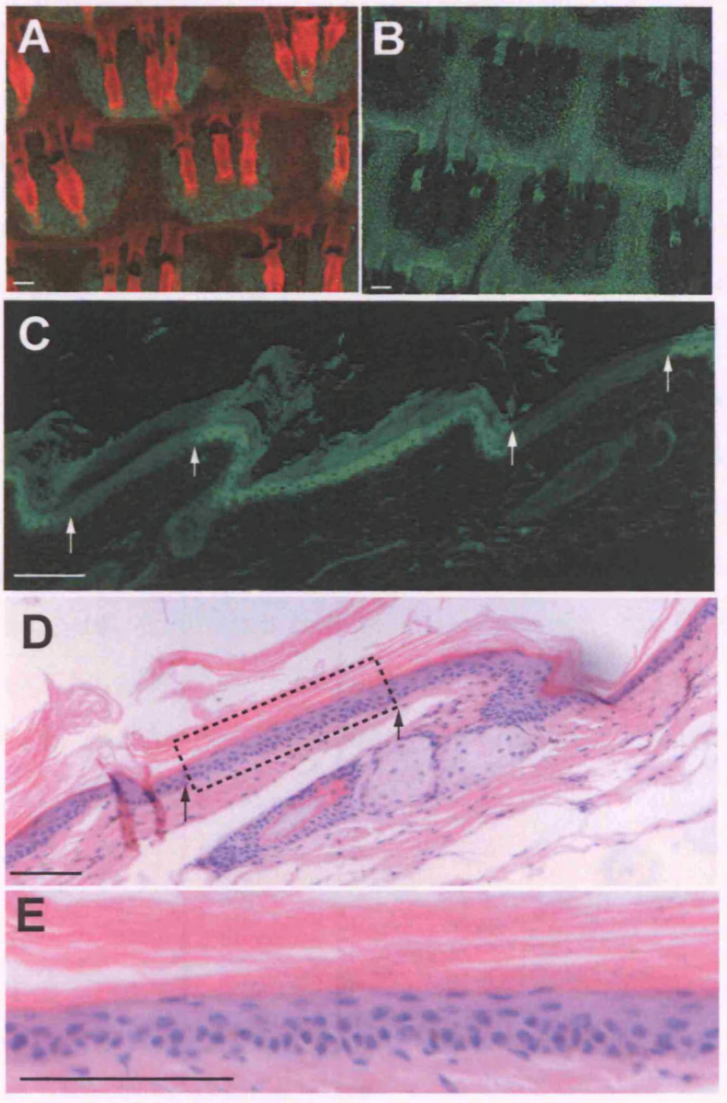

Figure 3.6- Patterning within the interfollicular epidermis
(A-B) Tail epidermal whole mounts of wild type skin immunolabelled with anti-caspase 14 antibody (A) or anti-keratin 10 antibody (B). (C) Tail skin section immunolabelled for keratin 10. Arrows indicate the boundaries of the parakeratotic scale (keratin 10 negative).(D) Section of tail skin stained with Haematoxylin and Eosin. (E) is an enlargement of the box in D, which correlates to the parakeratotic scale. Scale bars: 100 μm.

and in tail epidermis are localised at the bulb of hair anagen follicles and in the parakeratotic scale area of IFE (Figure 3.9 E).

Several types of immune cells reside within the epidermis and the dermis (Stenn and Paus, 2001), including Langherhans cells which I visualised by expression of the DEC205 marker (Figure 3.9 F).

3.7- Sox2-GFP a tool to analyse stem cells in mouse skin

A transgenic line driving GFP under the promoter of Sox2 was obtained from Dr Fred Gage (Salk Institute, San Diego, USA). The GFP expression allows isolation of the Sox2 population to characterise it *in vitro* and *in vivo*. It is very encouraging to see that GFP expression confirms the staining observed with the antibody (see Figure 3.10 A and B). This population is negative for the known bulge marker CD34 (Figure 3.10 C). FACS isolation of GFP positive cells show that Sox2 positive cells are very rare and represent a 0.02% of total keratinocytes (Figure 3.10 D). FACS analyses confirmed that they are negative for CD34 and only 0.015% of the Sox2 population is positive for α6 integrin (Figure 3.10 D). It will be very interesting to analyse how this population changes in situations in which the nature of the niche is altered.

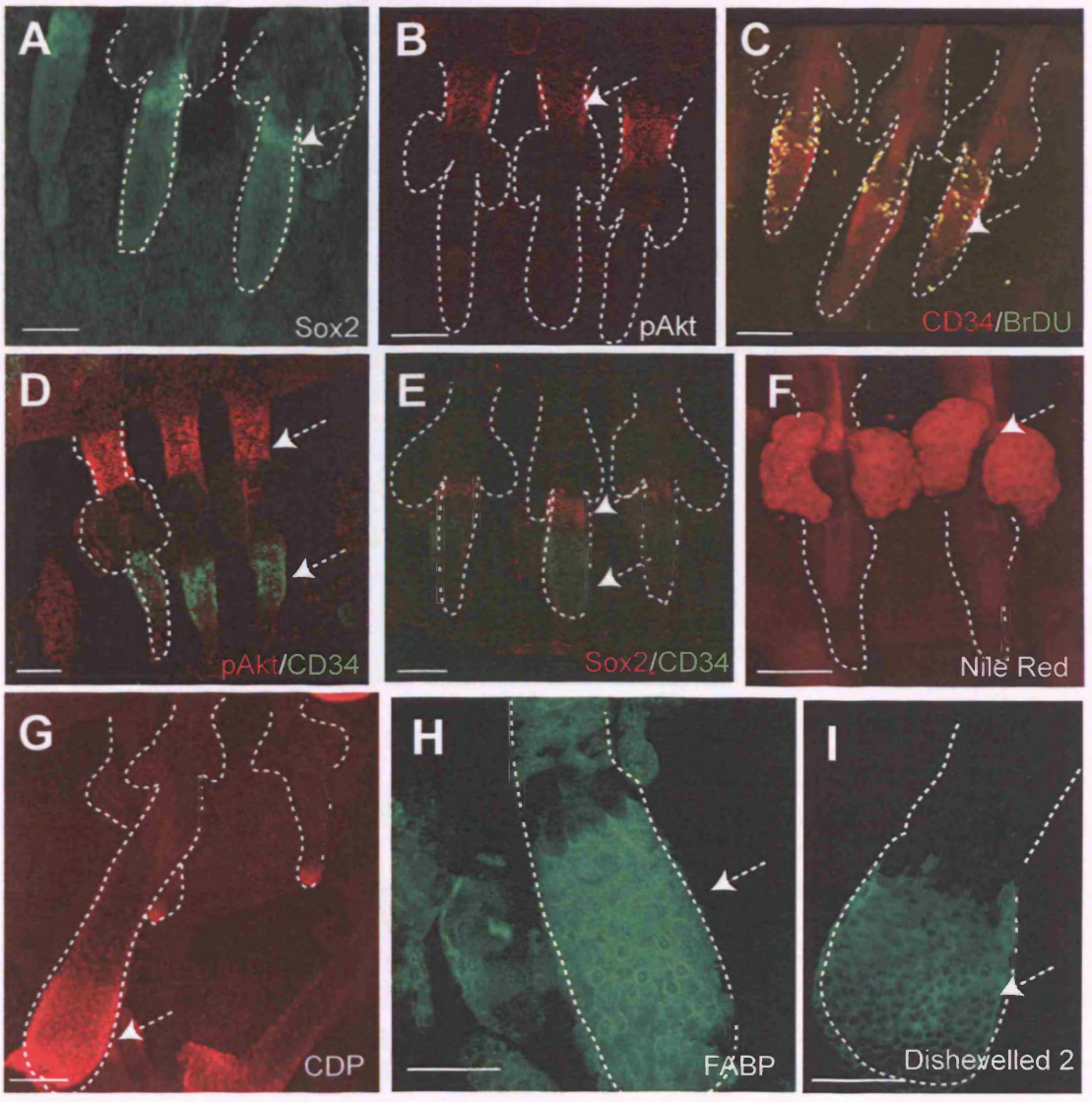

Figure 3.7 - Patterning along the distal-proximal axis of the hair follicle. (A-I) Wild-type whole-mounts were immunolabelled with antibodies to the proteins indicated. Scale bars: 100 μm.

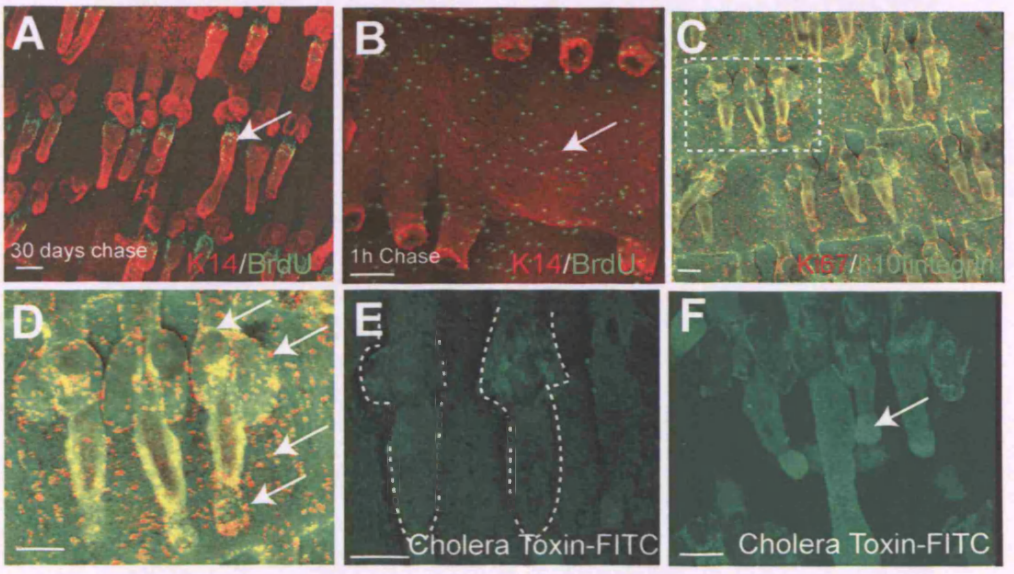

Figure 3.8 - Proliferation within tail epidermis (A-F) Tail whole mounts of wild type epidermis immunolabelled with antibodies to the proteins shown. (A) LRC were generated by 4 BrdU injections as shown in Figure 3.3A. After 30 days chase, Label Retaining Cells (LRC), quiescent cells are located clustered in the bulge, and a few scattered in the IFE and SG. (B-D) Proliferative cells are located in IFE, the bulb of HF and periphery of the SG. (E-F) Cholera Toxin labelling reveals the transit amplifying compartment which are the proliferative cells. Dotted lines in E demarcate HF and SG. Arrows indicate LRC in A, proliferative cells in B,D and Lipid rafts in F. HF in E are in telogen and in F are in anagen. Scale bars: 100 μm.

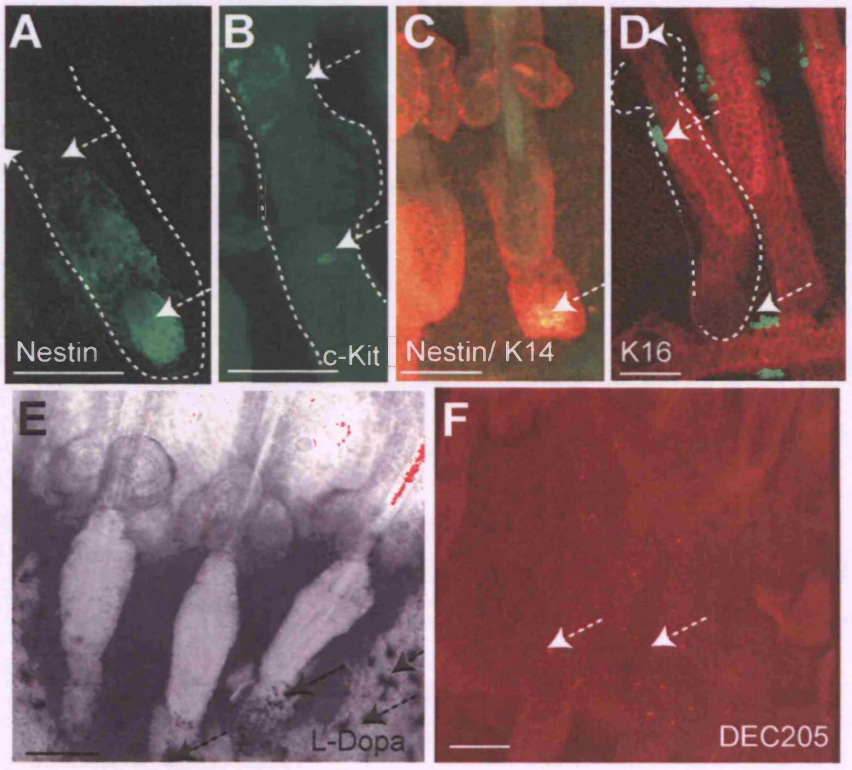

Figure 3.9 - Neural crest cells and immune cells reside in skin
(A) Wild-type whole-mounts were immunolabelled with antibodies to the proteins indicated (A-D,F) or stained with L-Dopa (E). Scale bars: 100 μm.

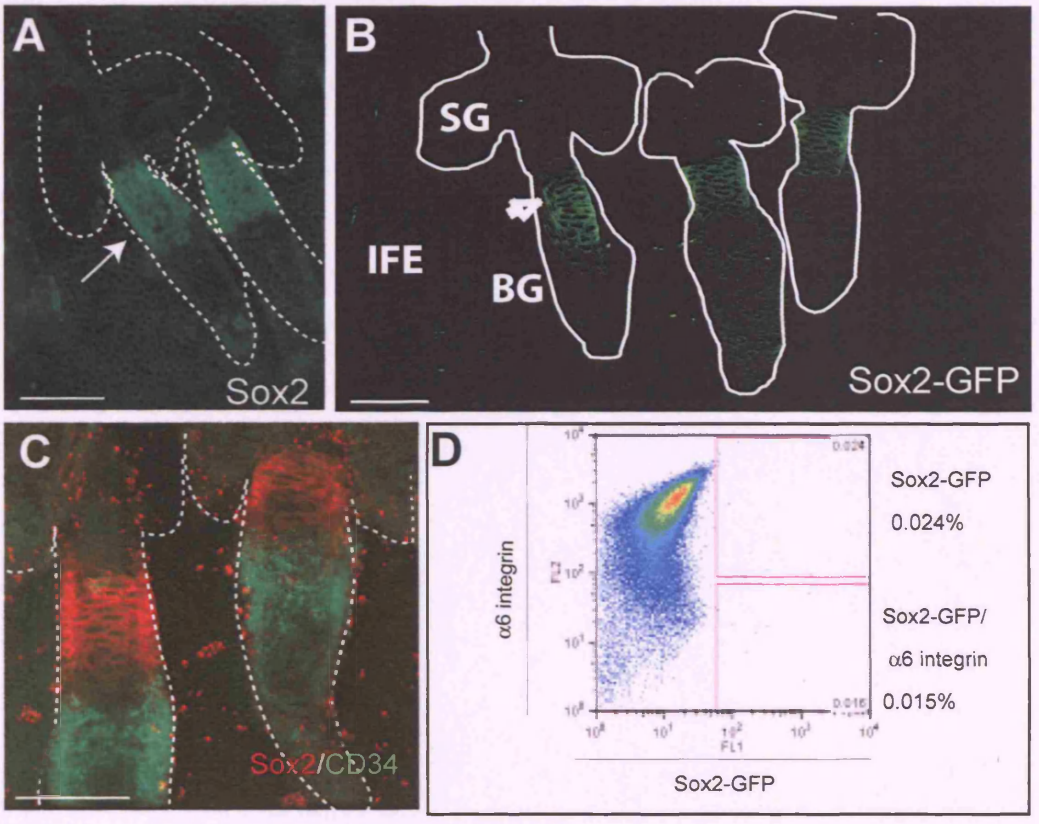

Figure 3.10- The Sox2-GFP reporter mice as a tool to study Sox2 positive cells (A) Immunolabelling of tail wholemount with an anti-Sox2 antibody. (B) GFP expression driven by the Sox2 promoter. In B locations of sebaceous glands (SG), bulge (BG) and interfollicular epidermis (IFE) are indicated. (C) Double labelling of Sox2 (red) and CD34 (green). (D) Tail keratinocytes were isolated from Sox2-GFP transgenic animals and immunolabelled with antibodies to α6 integrin and FACS sorted. The FACS profile shows the GFP and α6 integrin populations. Arrows in A and B show the Sox2 population. Scale bars: 100 μm.

3.8- Conclusions

The work presented in this introductory Chapter contributed to the development of the whole mount technique (Braun et al., 2003). I confirmed the location of LRC, Keratin 15 and CD34 positive cells and found new markers including Sox2, Nestin and pSMAD2. In addition, I also found markers of different regions of IFE and markers for different locations along the HF. I developed markers for non-keratinocyte cell populations in epidermis. Finally, I have showed that Sox2-GFP mice can be used to mark a new population of cells above the bulge in HF.

Chapter 4- β-catenin drives HF morphogenesis in tail epidermis

Aims

The first response of the skin to β-catenin activation is the entry of hair follicles into the anagen growth phase and subsequently ectopic hair follicles are formed. Sustained β-catenin activation leads to the formation of tumours of hair follicle origin, resembling trichofolliculomas (See Figure 1.9; Gat et al.1998, Van Mater, et al.2003, Lo Celso et al., 2004). These studies show that β-catenin activation determines lineage commitment in the epidermis; however, they also raise several questions that I wanted to address in this chapter.

The aim of my Thesis was to investigate how β-catenin activation leads to ectopic hair formation.

It is not known what is the effect of different levels of β-catenin activation and whether cells would exhibit a graded response to increasing β-catenin activation or HF induction would be a threshold response. The first issue I investigated was the effect of titrating β-catenin signalling.

It was previously shown that cells in all regions of the epidermis (HF, SG, IFE) are competent to respond to β-catenin, however, it is unclear whether responsiveness is restricted to the stem cell compartment or whether committed progenitors can also be reprogrammed to induce hair follicles even though they are lineage restricted. The second issue I analysed was the effect of β-catenin on the bulge stem cell LRC compartment and what was the contribution to hair follicle formation.

Thirdly, I wanted to study whether β-catenin induced HFs are capable of reconstructing a follicle niche including keratinocytes and non-epithelial cells that are normally resident in the hair follicle.

To explore these issues I used K14ΔNβ-cateninER mice that were previously generated in the laboratory (Lo Celso et al., 2004). For this, I collaborated with Cristina Lo Celso who helped me in the handling and the treatment of mice. I performed all the analysis of the experiments described unless stated. While

previous analysis was performed in dorsal skin, I mainly focused on the effect of β-catenin activation and on de novo hair follicle formation in tail skin, taking advantage of the whole-mount system described in Chapter 3.

4.1-Introduction to the K14ΔNβ-cateninER transgenic model

The K14ΔNβ-cateninER inducible transgenic mice were previously generated in the laboratory (Lo Celso et al., 2004). In this model, the keratin 14 promoter targets expression of an inducible β-catenin in the basal layer of the epidermis, the outer root sheath (ORS) of the hair follicle and the outer layers of the sebaceous glands (Figure 4.1 A and E). The N-terminus of mutant β-catenin has been removed and therefore the mutant cannot be degraded via GSK3β mediated phosphorylation The C-terminus is fused to a mutant estrogen receptor (ER) (see Figure 1.8 and 4.1 A). Without 4OHT treatment, the mutant protein is complexed with heat shock proteins and localised to the membrane complexed with E-cadherin, at adherens junctions (Lo Celso et al., 2004; Zhu and Watt, 1999). Upon 4OHT treatment, the transgenic protein is released from heat-shock proteins and it translocates to the nucleus (Figure 4.1 B-D) where it complexes with transcription factors, such as members of the Tcf/Lef family (Ciani and Salinas, 2005; Nelson and Nusse, 2004). With this model, β-catenin activity in normal adult mouse epidermis is induced by 4-OHT treatment and thus the onset and duration of β-catenin activation can be controlled (Lo Celso et al., 2004).

Two different transgenic lines were used in this study, a low copy number line called D2 and a high copy number called D4. These lines have different levels of ΔNβ-cateninER transgene, the D4 keratinocytes expressing twice as much when assessed by western blot of immortalised keratinocytes (Silva-Vargas et al., 2005). The level of transgenic β-catenin in D4 keratinocytes is similar to the level of endogenous β-catenin (Silva-Vargas et al., 2005). Although all basal cells (keratin 14 positive) express the transgene in tail epidermis, there is heterogeneity in the expression levels, with higher levels detected in the sebaceous glands, compared to IFE or ORS. In the IFE there are patches of higher

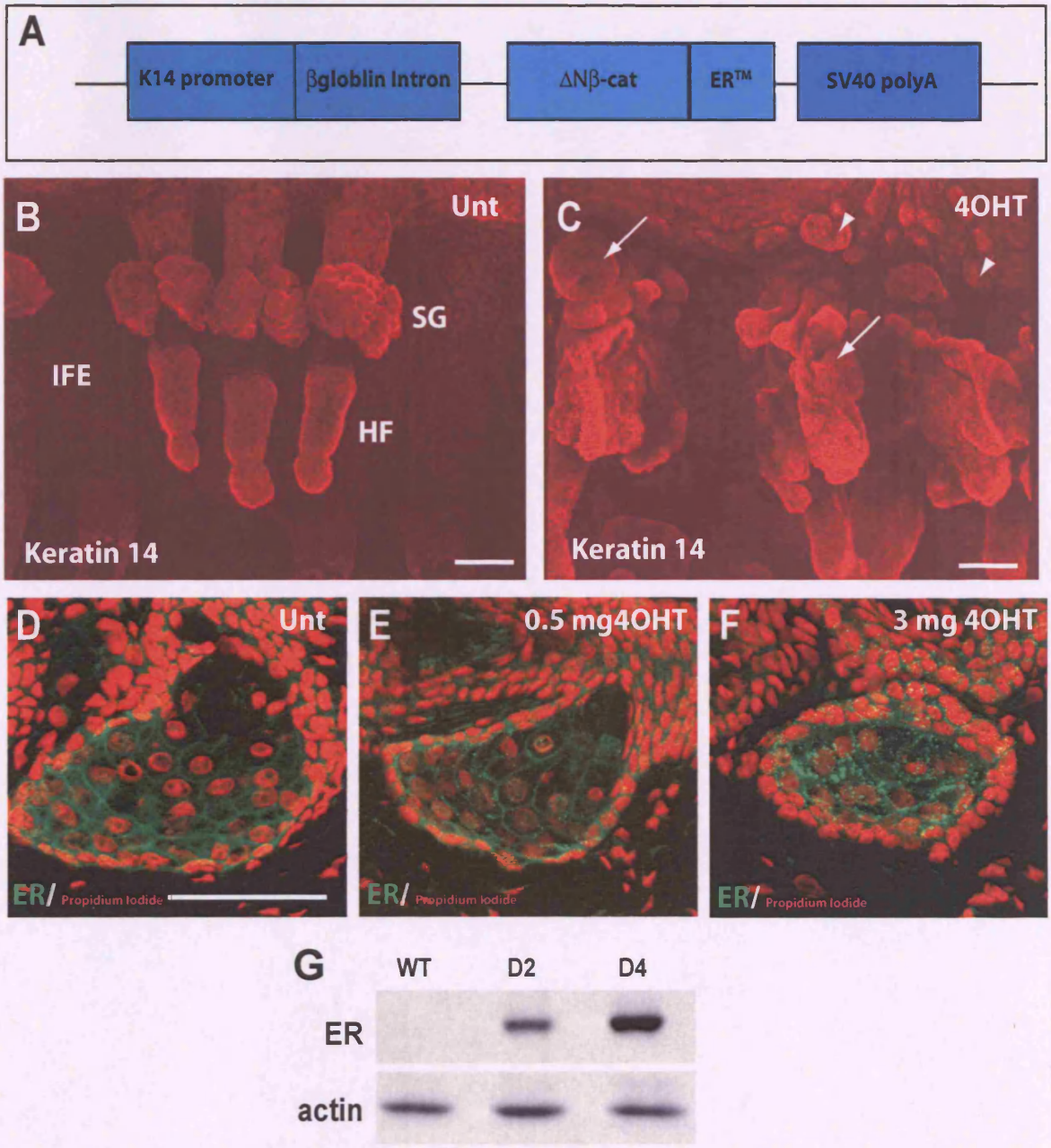

Figure 4.1- The ΔNβ–cateninER transgenic model. (A) Schematic diagram of the transgenic cassette.The trangene expression is driven by the keratin 14 (K14) promoter. The transgene is fused to a mutated form of the estrogen receptor (ER™). (B,C) Z-stack of 20x confocal images of tail epidermis whole-mounts immunostained with anti- Keratin 14. (B) Untreated (Unt) trangenic mouse or (C) treated for 21 days with 4OHT. Note that upon 4OHT treatment the hair re-growths and ectopic follicles are formed from IFE and SG. (D-F) ER immunofluorescence of skin, either untreated (Unt) (D) or treated (E,F) for 24 h with the 4OHT doses shown. (D) In untreated skin, the transgene is localised to cell-cell borders. Upon 4OHT treatment the transgene partially relocalised to the nucleus (E-F). (G) Comparison of relative levels on ΔNβ-cateninER by immunoblotting with anti-ER or, as a loading control, anti-actin antibody. Panels (D-G) were provided by Cristina Lo Celso. In (C) ectopic follicles originating from SG (arrows) and from IFE (arrowheads) are indicated. Scale bars: B and C 100 μm, D-F 50 μm.

expression (Silva-Vargas et al., 2005). This variation has not been commented on previously, although it appears to be a feature of all mice in which the K14 promoter is used to target transgene expression.

All mice used were 6 to 8 weeks old, so that the HF were in telogen and the skin looks pink. After 4OHT treatment, the wild-type skin would remain always pink without hair regrowth and the transgenic skin would gradually start getting dark and hairy. The changes in transgenic skin represented the entrance of hair follicles into anagen, when melanogenesis is activated (Hardy, 1992).

As previously mentioned in the Materials and Methods Chapter, in all the experiments presented in this Chapter for each condition there were three mice per group. The analysis of the harvested skin was performed as described in Chapter 3 (See Figure 3.3).

4.2- Titration of β-catenin activation *in vivo*: from HF morphogenesis to tumorigenesis

4.2.1-From morphogenesis to tumorigenesis

In order to exploit this inducible system and to achieve different levels of β-catenin activation I did not only used the two lines of K14ΔNβ-cateninER mice: D2, with 12 copies of the transgene, and D4, with 21 copies (Lo Celso et al., 2004), but also varied the doses of 4OHT applied to the skin.

In these studies I used three concentrations: 0.5 (low dose), 1.5 (medium dose) or 3 mg (high dose) per mouse, applying 4OHT every second day. I applied 4OHT to tail skin, so that I could use whole mount labelling to facilitate quantitative assessment of the induction of new hair follicles.

After several pilot experiments I could optimise the design of the time windows to analyse adequately the effect of titrating the signal in both transgenic lines (see Figure 4.2). Given that the phenotype in the D4 mice appeared early and I had to sacrifice the mice at two weeks, I designed experiments with small time windows in order to get a better insight of the development of the D4 phenotype. In case of the D2 line the phenotype developed more slowly and I designed experiments with one-week intervals between each time point and the mice were maintained

for up to 42 days (see Figure 4.2). I performed 4 different experiments. I first looked at the effects of titrating the β-catenin signal by examining Haematoxylin and Eosin stained tail skin sections (Figure 4.3). In the D2 line, sustained β-catenin induction with the medium dose of 4OHT leads to the formation of ectopic outgrowths by 3 weeks. The epithelial projections fully resemble rudimentary follicles and are capable of recruiting a dermal condensate (DP). If the signal is prolonged, the new follicles fuse and develop structures resembling trichofolliculomas (Figure 4.3 C), as previously described in back skin (Lo Celso et al., 2004). In the D4 line, sustained β-catenin activation with the medium 4OHT dose leads to an initial formation of outgrowths; although they increase greatly in size they fail to develop into a rudimentary follicle, instead forming hyperplastic structures resembling a tumour (Figure 4.3 F-H).

Interestingly, 4OHT treatment also affected the whisker follicles (Figure 4.3 I-L) and the eyelid follicles in both transgenic lines (Figure 4.3 M-O). At the high dose of 4OHT I could observe that in the whisker pad the ectopic follicles had fused (Figure 4.3 J-K) leading in some areas to really disorganised structures resembling tumours (Figure 4.3 K) with a strong dermal inflammatory infiltrates (Figure 4.3 L). In the eyelid follicles, the switch from a morphogenic event to tumour formation is particularly clear (See Figure 4.3 N-O).

4.2.2-Effects of β-catenin activation on lineage commitment in tail epidermis *in vivo*

In order to understand how ectopic hair follicles develop in tail epidermis, I assessed the changes in lineage commitment induced by activation of β-catenin. I monitored the 3 differentiation pathways in the epidermis and validated the tail epidermis as an adequate model to study hair follicle morphogenesis.

Hair differentiation was monitored by looking at 2 hair follicle differentiation markers: keratin 17, an early hair differentiation marker (McGowan and Coulombe, 1998), CAAT displacement protein (CDP), essential for normal formation of the hair follicle inner root sheath (Figure 4.4; Ellis et al., 2001). In wild type follicles, keratin 17 is confined to the outer root sheath cells, the IFE

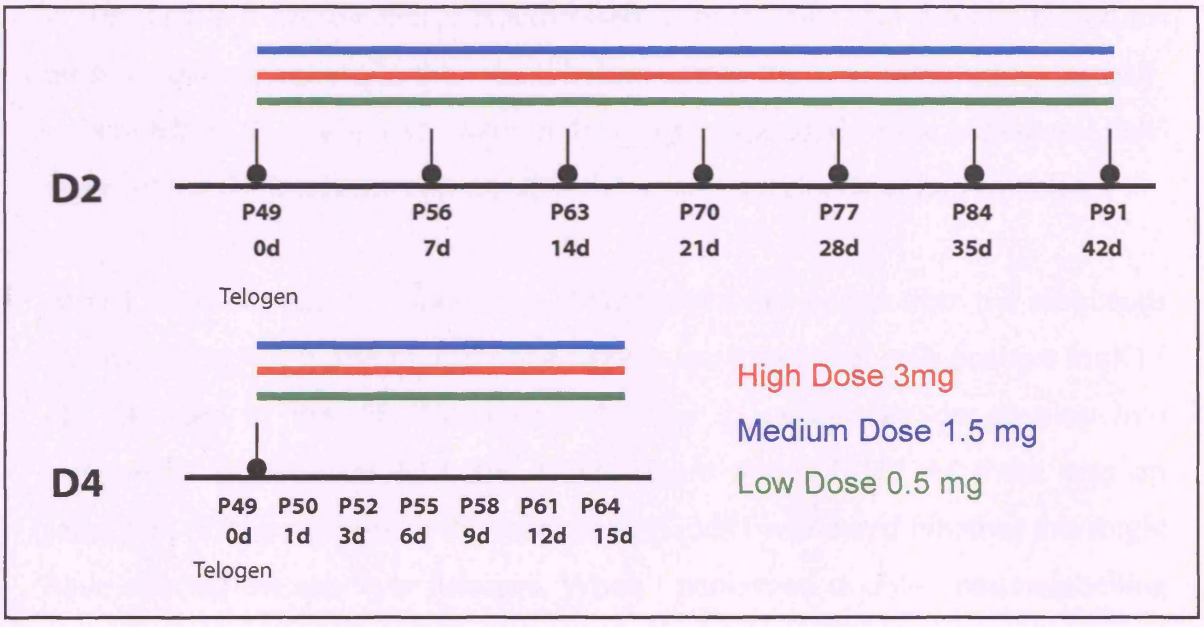

Figure 4.2- Titration of ΔNβ-catenin-ER activation in tail epidermis in vivo. Schematic diagram of the experimental design to look at the effects of titrating β-catenin activation in the D2 and D4 transgenic lines. **P** corresponds to postnatal day and **d** corresponds to the day of the experiment. Note that the experiments were started at P49 when mice where in telogen. Days indicate the timepoint when the skin was harvested and analysed. Mice were treated with the 3 doses of 4OHT, indicated by the coloured lines, every second day.

and the sebaceous glands are completely negative (Figure 4.4 A), CDP is expressed in hair keratinocytes that are terminally differentiating at the base of the hair follicle (Fig 4.4 B,E). It was previously shown that induction of CDP, together with Lef1 and keratin 17, is an early indicator of ectopic HF formation in dorsal skin (Lo Celso et al., 2004). In addition, I monitored sebaceous differentiation by using Nile Red, a lipid dye, that stains differentiated sebocytes (Figure 4.4 E) and early interfollicular differentiation by staining for Keratin 10 (K10). K10 is a marker that it is expressed in basal cells that are committed to terminal differentiation, in the infundibulum and in the area surrounding the hair follicle triplet (Figure 4.4 D). Keratin 10 is also expressed in the suprabasal cell layers of the IFE but is not expressed in the sebaceous glands or hair follicles.

After 1 week of treatment, formation of outgrowths first occurs from the sebaceous glands (Figure 4.4 B and F). After one week a few clusters of cells positive for K17 can be seen in the IFE. However only after 2 weeks they do develop into outgrowths positive for K17 and CDP (Figure 4.4 D,G,H). As there was an induction of hair markers in the sebaceous glands I wondered whether this might have affected the sebocyte lineages. When I performed double immunolabelling with the CDP marker and Nile Red, I could see clearly that the projections emanating from the sebaceous glands that were negative for Nile Red were positive for CDP (Figure 4.4 G). The induction of hair differentiation markers correlated with a decrease in the number of differentiated sebocytes in both lines. This indicates that sebaceous progenitors are driven to differentiate into hair keratinocytes and gradually the number of sebocytes is reduced, shown by the decreased areas stained with Nile Red (Figure 4.4 F and G).
As treatment progresses, the outgrowths adopt a follicle like structure and hair germs can be seen (Figure 4.4 G; see dotted line). After 4 weeks of treatment, the outgrowths and pre-existing follicles fused and formed benign tumours resembling trichofolliculomas (Figure 4.4 H; see dotted line), as previously reported (Gat et al., 1998; Lo Celso et al., 2004).

In the D4 line, after 1 day of treatment outgrowths were already apparent in the IFE (see Figure 4.4 I; see asterisks). After one week of treatment, the follicles were

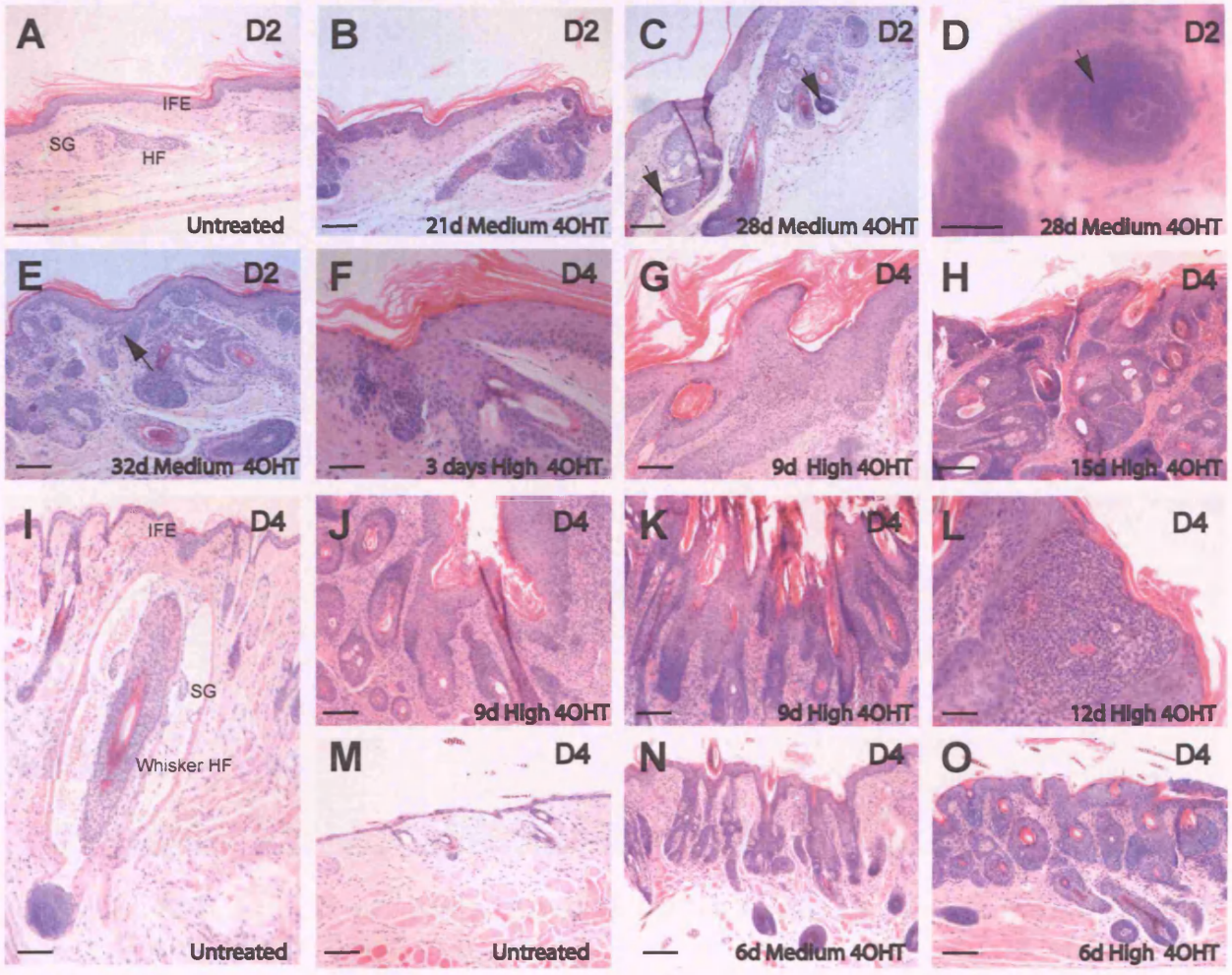

Figure 4.3- The levels of β-catenin activation determine whether a morphogenic or tumorigenic event is induced. (A-O) H & E stained sections of untreated (A, I and M) and D2 transgenic epidermis from tail (B-H), whisker pad (J-L) and eye lid (N and O) treated with 4OHT for the indicated time points. In A and I sebaceous glands (SG), hair follicles (HF) and interfollicular epidermis (IFE) are indicated. Arrows show ectopic dermal papillae (DP). Scale bars: 100 μm (A-C, E-O) and 50 μm (D).

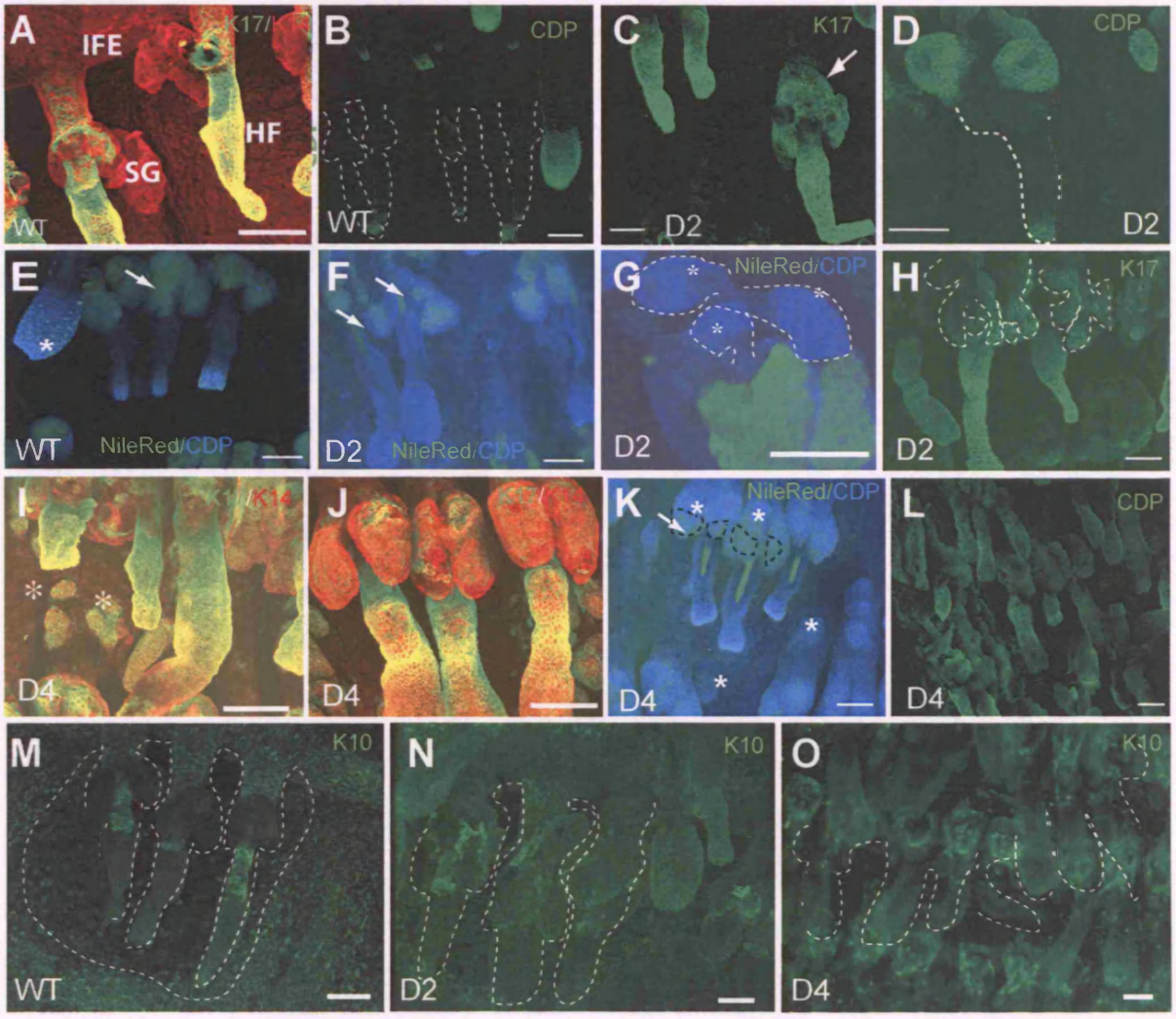

Figure 4.4- Effects of ΔNβ-cateninER activation on lineage commitment. Tail skin of untreated WT (A,B,E,M) or D2 transgenic treated for 7,14 and 21 days (C,D,E,F,G,H,N) and D4 transgenic treated for 1,3,6,9 days (I,J,K,L,O) treated with 1.5mg dose of 4OHT (medium, M) dose. In A, the location of sebaceous glands (SG), interfollicular epidermis (IFE) and hair follcile (HF) are indicated. (A,I,J) Double immunolabelling for keratin 17 (green) and keratin 14 (red); (B,D,L) Immunolabelling for CDP (HF differentiation); (C,H) Immunolabelling for K17; (F,G,K) Immunolabelling for CDP (hair differentiation) and staining with Nile Red (sebaceous differentiation). Note that in early stages of hair follicle morphogenesis (See F,G), SG are positive for hair differentiation and with some remnants of sebaceous differentiation. (M,N,O) Immunolabelling for K10 (IFE differentiation). Arrow in C indicate ectopic K17 expresion in SG. Arrow in I,F,K point to SG and asterisks in G,I,K indicate new outgrowths arising from IFE and SG. Dotted line in B demarcate HF and SG, and HF in D,N and O. In G, dotted lines demarcate newly arising ectopic HF; in K demarcate Nile Red positive areas and in M demarcate HF, SG and the parakeratotic scale negative for K10. Scale bars: 100 μm.

very thick, probably due to the massive proliferation (Figure 4.4 I, J). Although rudimentary follicles formed, they did not develop to the same extent as in the D2 line (Figure 4.4 L). The number of sebocytes was also markedly reduced (Figure 4.4 K; see dotted line). In addition, the new outgrowths induced by β-catenin in both transgenic lines (Figure 4.4 M-O) at the time points analysed were Keratin 10 negative.

My observations on the effects of β-catenin activation in tail epidermis confirmed what has been previously reported in back skin (Lo Celso et al., 2004). Hair marker staining in the transgenics reveals that ectopic hair follicle formation is not confined in the hair follicle, but also occurs in the sebaceous glands and IFE. The activation of β-catenin in adult skin leads not only to stimulation of hair differentiation at the expense of sebaceous and IFE lineages, but also, potentially, to reprogramming IFE keratinocytes and sebaceous keratinocytes to differentiate along the hair lineage.

4.2.3-HF formation is a threshold response to β-catenin activation

To get a better insight and define the threshold for global hair follicle formation in tail epidermis I evaluated the dynamics of ectopic hair follicle differentiation by monitoring the expression of CDP in the titration experiments described in the previous section. As previously mentioned, the expression of CDP precedes the formation of epithelial outgrowths that come to express markers of the different HF lineages. Examples of whole mounts taken from D2 and D4 tails treated with different 4OHT concentrations for different lengths of time are shown in Figure 4.5, and a summary of the results is represented in the diagram in Figure 4.6.
In the D2 line, the first site of ectopic follicle formation is in the SG (Figure 4.5 B). Next, as the dose and the length increase follicles are induced in the IFE (Figure 4.5 C) and finally, at high and prolonged 4 OHT doses, follicles are formed from pre-existing HF ORS (Figure 4.5 D) resulting in the formation of trichofolliculomas (Figure 4.5 E). Conversely, in the D4 line the first site for ectopic HF was the IFE (Figure 4.5 F), followed by the SG (Figure 4.5 H). HF did not arise from the pre-existing ORS. Instead, the ORS was thickened and positive for markers for hair follicle differentiation (Figure 4.5 I-M). I used the expression of keratin 17 as a

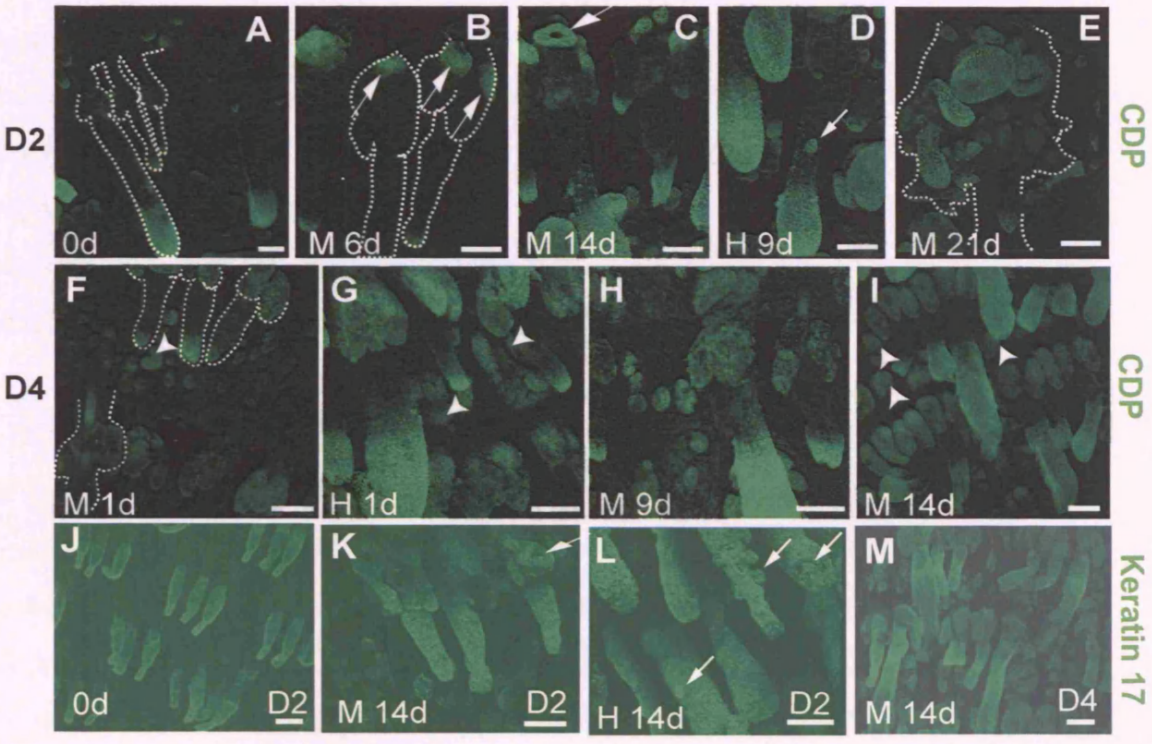

Figure 4.5. Effects on D2 and D4 transgenic epidermis of activating ΔNβ-cateninER with different concentrations of 4OHT for different lengths of time. 4OHT was applied at 0.5mg (low), 1.5mg (medium, M) and 3mg (high, H) doses. (A-M) Representative tail whole mounts immunolabelled for CDP (A-I) and Keratin 17 (J-M). Transgenic lines, 4OHT doses and time of treatments (days, d) are indicated. Dashed lines demarcate hair follicles and sebaceous glands in A,B,E and F. Arrows in B indicate CDP expression from SG, in C and K a dermal papilla and in D and L an outgrowth arising from ORS. Arrowheads in F, G and I indicate new outgrowths arising from IFE. Scale bars: 100 μm.

second marker of ectopic HF differentiation for these experiments and the results were the same (Figure 4.5 J-M).

I took advantage of the unique organisation of tail epidermis in order to obtain quantitative data on ectopic HF formation (Figure 4.6) as described in the Materials and Methods section. In wild-type and untreated K14ΔNβ-cateninER skin the hair follicles are arranged in rows and clustered in groups of three (triplets). As I showed in the previous Chapter one triplet and the adjacent interfollicular epidermis is defined as one epidermal unit, as illustrated schematically in Figure 4.7. First, I calculated the percentage of units in which ectopic expression of CDP occurred in the IFE (arrowheads in Figure 4.5 G), SG (arrows in Figure 4.5 B) and HF ORS (arrow in Figure 4.5 D) for each 4OHT concentration and on each transgenic line (Figure 7 B, C). In addition, I also calculated the number of CDP-positive patches per positive unit (Figure 4.7 D).

In D2 mice, the dose of 4OHT affected the proportion of units with ectopic CDP, the number of patches of ectopic CDP per unit and the time at which they appeared (Figure 4.7 B,D). I first observed ectopic CDP expression at day 6 with medium and high 4OHT concentrations and at day 9 with the low dose (Figure 4.5 A,B; Figure 4.7 B). CDP was most readily induced in the SG (Figure 4.5 B). For instance, after 6 days of treatment with the medium dose of 4OHT CDP-positive patches on SG were observed in 100% of units, whereas 47% had CDP-positive patches in the IFE, and only 17% in the pre-existing anagen HF outer root sheath (ORS). The HF was most refractory to induction of ectopic CDP: whereas CDP-positive regions of SG and IFE were achieved in 100% of units from day 9 onwards with medium and high dose 4OHT, the maximum % units with ectopic CDP expression in the ORS was 52% with the high dose and 34% with the medium dose (Figure 4.5 D). Medium dose 4OHT induced a higher number of CDP positive patches than low dose 4OHT and at all doses the number of positive patches per unit increased over time (Figure 4.7 D; compare Figure 4.5 D,F). However, at the high dose the number of CDP positive patches was lower than at the medium dose; this was because the high dose patches were larger (Figure 4.7 D).

second marker of ectopic HF differentiation for these experiments and the results were the same (Figure 4.5 J-M).

I took advantage of the unique organisation of tail epidermis in order to obtain quantitative data on ectopic HF formation (Figure 4.6) as described in the Materials and Methods section. In wild-type and untreated K14ΔNβ-cateninER skin the hair follicles are arranged in rows and clustered in groups of three (triplets). As I showed in the previous Chapter one triplet and the adjacent interfollicular epidermis is defined as one epidermal unit, as illustrated schematically in Figure 4.7. First, I calculated the percentage of units in which ectopic expression of CDP occurred in the IFE (arrowheads in Figure 4.5 G), SG (arrows in Figure 4.5 B) and HF ORS (arrow in Figure 4.5 D) for each 4OHT concentration and on each transgenic line (Figure 7 B, C). In addition, I also calculated the number of CDP-positive patches per positive unit (Figure 4.7 D).

In D2 mice, the dose of 4OHT affected the proportion of units with ectopic CDP, the number of patches of ectopic CDP per unit and the time at which they appeared (Figure 4.7 B,D). I first observed ectopic CDP expression at day 6 with medium and high 4OHT concentrations and at day 9 with the low dose (Figure 4.5 A,B; Figure 4.7 B). CDP was most readily induced in the SG (Figure 4.5 B). For instance, after 6 days of treatment with the medium dose of 4OHT CDP-positive patches on SG were observed in 100% of units, whereas 47% had CDP-positive patches in the IFE, and only 17% in the pre-existing anagen HF outer root sheath (ORS). The HF was most refractory to induction of ectopic CDP: whereas CDP-positive regions of SG and IFE were achieved in 100% of units from day 9 onwards with medium and high dose 4OHT, the maximum % units with ectopic CDP expression in the ORS was 52% with the high dose and 34% with the medium dose (Figure 4.5 D). Medium dose 4OHT induced a higher number of CDP positive patches than low dose 4OHT and at all doses the number of positive patches per unit increased over time (Figure 4.7 D; compare Figure 4.5 D,F). However, at the high dose the number of CDP positive patches was lower than at the medium dose; this was because the high dose patches were larger (Figure 4.7 D).

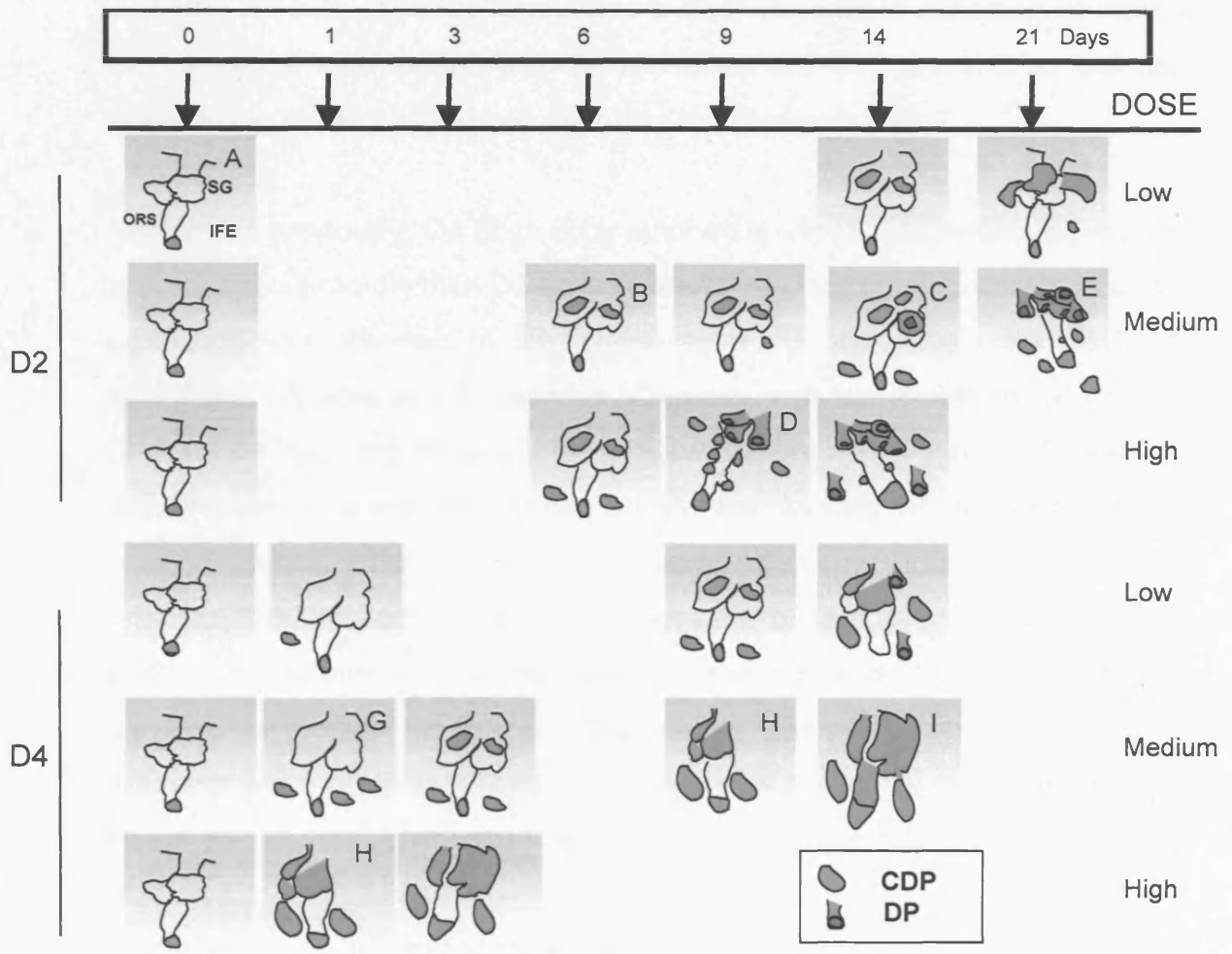

Figure 4.6- Effects on D2 and D4 transgenic epidermis of activating ΔNβ -cateninER with different concentrations of 4OHT for different lengths of time. 4OHT was applied at 0.5mg (low), 1.5mg (medium, M) and 3mg (high, H) doses. A) Schematic representation of the results, showing the outer root sheath (ORS) of a single HF with associated SG and IFE. CDP expression is represented in green and de novo dermal papillae (DP) are shown in red. Arrows represent time points at which skin was analysed. Individual letters correspond to whole mounts shown in Figure 4.5.

The follicular epithelium induced by β-catenin activation in K14ΔNβ-cateninER mice can induce the underlying mesenchyme to form a dermal papilla (Van Mater et al., 2003;Lo Celso et al., 2004). The epithelium at the base of the follicles forms a cup-like structure that encircles the dermal papilla (see, for example, Figure 4.9D, arrow). I also monitored the degree of 'maturity' of the ectopic hair follicles according whether they had recruited a DP. I could observe that the formation of dermal papillae occurs later than the induction of ectopic CDP (represented in red in Figure 4.6). In D2 mice there was a dose dependent induction of dermal papillae: none were formed with the low dose; and they appeared several days earlier in response to high dose rather than medium dose 4OHT.

As reported previously, D4 (high copy number) epidermis responded to β-catenin activation more rapidly than D2 epidermis and by 1 day of treatment ectopic CDP expression was observed in IFE (Figure 4.5 F, G and 4.7 C). As previously mentioned, whereas in D2 mice the SGs were most susceptible to induction of CDP, in D4 mice the IFE was most sensitive (Figure 4.5 G and 4.7 C). D4, like D2, HFs were most refractory to induction of new follicles. At 14 days of medium 4OHT treatment CDP expression was observed along most of the D4 ORS; however, I could hardly observe the formation of distinct projections of CDP-positive epithelium and dermal papillae and never in HF. The correlation between the number of CDP-positive patches and 4OHT dose and length of treatment was more pronounced in D2 than in D4 epidermis, largely because the size of the patches in D4 were larger due to individual patches merging with one another.

The results from the titration experiments show that by controlling the strength of β-catenin activation, through transgene copy number and 4OHT dose, it seems possible to control the number and location of new hair follicles. Different regions of the epidermis differed in their responsiveness to β-catenin activation. SGs were most responsive, because they were the sites where ectopic CDP expression was induced most rapidly and at lowest 4OHT concentrations in the lower copy number founder line, D2. Compared to IFE and SG, HF in both D2 and D4 mice were refractory to developing new follicles.

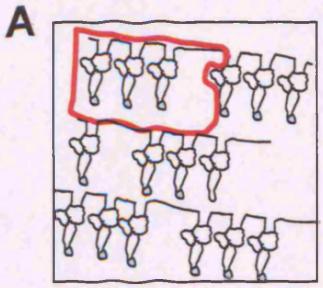

B

D2

Time	Dose	IFE	SG	HF
6 days	L	0 %	0 %	0 %
	M	47%	100 %	17 %
	H	100 %	100 %	27 %
9 days	L	25 %	38 %	0 %
	M	100 %	100 %	31 %
	H	100 %	100 %	52 %
14 days	L	42 %	53 %	0 %
	M	100 %	100 %	34 %
	H	100 %	100 %	43 %

C

D4

Time	Dose	IFE	SG	HF
1 days	L	70 %	3 %	0 %
	M	91 %	20 %	0 %
	H	100 %	63 %	0 %
3 days	L	100 %	20 %	0 %
	M	100 %	45 %	0 %
	H	87 %	60 %	0 %
6 days	L	100 %	40 %	0 %
	M	100 %	85 %	0 %
	H	100 %	100 %	0 %

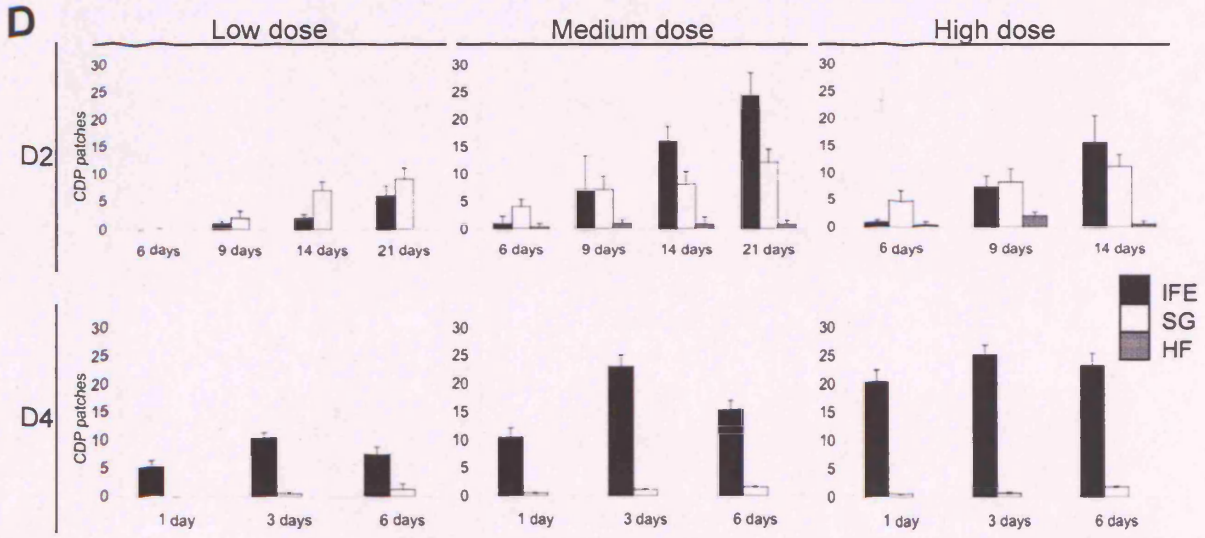

Figure 4.7- Quantitation of β-catenin signaling in vivo. (A) The unit of tail epidermis used for quantitation is shown outlined in red, corresponding to three HF with associated SG and IFE. (B, C) Percentage of units with ectopic CDP expression in IFE, SG and HF in D2 (B) and D4 (C) lines treated for the number of days shown with low (L), medium (M) and high (H) doses of 4OHT. (D) Average number of CDP positive patches per unit, broken down into IFE, SG and HF.

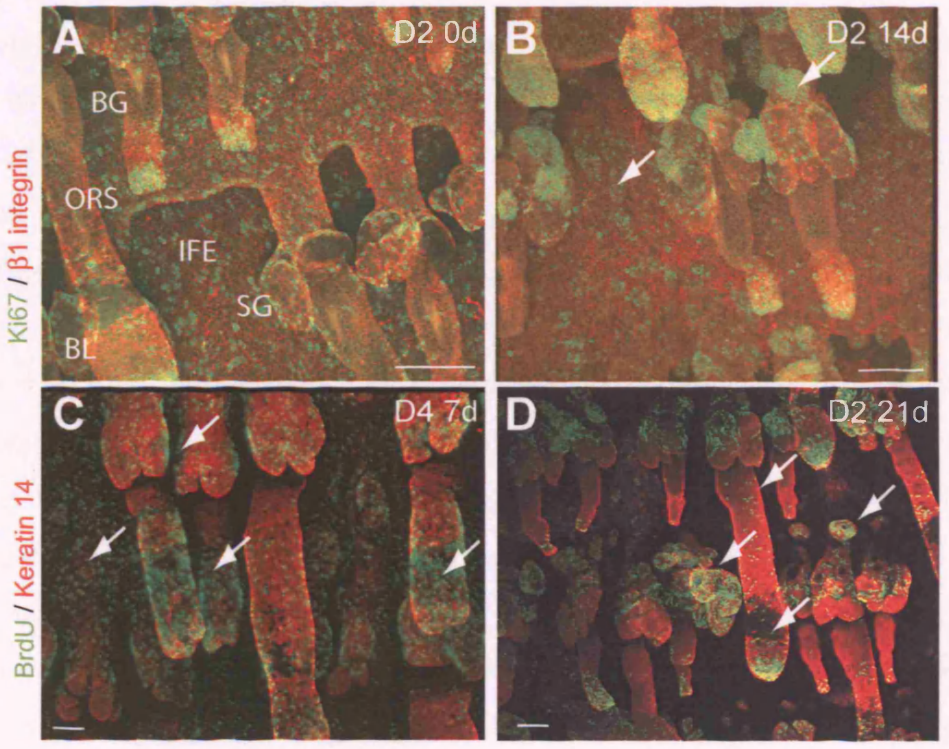

Figure 4.8-. Effects of ΔNβ-catenin-ER activation on proliferation. Transgenic line (D2 or D4) and days of 4OHT treatment (medium dose) are shown. In A locations of sebaceous glands (SG), hair follicle outer root sheath (ORS), bulge (BG) and bulb (BL) are indicated. (A and B) Double labelling for Ki67 (green) and β1integrin (red), (C and D) double labelling for BrdU (green) and keratin 14 (red). Arrows in B, C and D indicate clusters of proliferating cells in the sebaceous glands and IFE associated with ectopic HF formation. Scale bars: 100 μm.

4.3-Changes in proliferation during ectopic hair follicle formation

I next investigated the levels of proliferation in both transgenic lines, in order to see whether the differences in copy number reflected also differences in proliferation.

In wild-type epidermis, proliferation is confined to some cells in the IFE basal layer, the outer layer of the sebaceous glands and in the bottom part of the hair follicle known as the bulb (Figure 4.8 A and Braun et al., 2003). Proliferation can be monitored either by looking at the cell cycle marker Ki67 or by looking at BrdU incorporation during 1 hr-pulse prior to sacrifice (Figure 4.8 A and 3.7; Braun et al., 2003). Between 7 and 14 days of treatment, activation of β-catenin resulted in increased proliferation in clusters of cells at the sites of ectopic HF formation in the SG and IFE (Figure 4.8 B-D). As treatment continued these clusters developed into outgrowths (Figure 4.8 B-D). After one week of treatment of the D4 line, the follicles were very thick, probably due to the massive proliferation (Figure 4.8 C). In D4 epidermis the rudimentary follicles formed but did not develop to the same extent as in the D2 line. At three weeks in the D2 line epithelial projections with a dermal papilla could be observed (See arrows in figure 4.8 D), but not in the D4 line.

In addition, I looked at pathways that are known to be involved in proliferation and have previously been shown to be active at early stages of HF morphogenesis (Jamora et al., 2005). Sites that were positive for markers of proliferation were also positive for an antibody detecting active pMek1, a component of the Erk/MAPK pathway (Figure 4.9 A-D). In addition, it has been reported that TGFβ signalling is also active in the early stages of HF morphogenesis (Jamora et al., 2005). I could also detect increased pSMAD2/3 staining in ectopic HF from SG and IFE (Figure 4.9 E-F). It has been previously shown that proliferative epidermal cells, such as transit amplifying cells (TAC), can be detected by expression of Fatty acid binding protein (FABP), another marker for TAC (see Figure 3.6 H In Chapter 3 and Figure 4.9 G-I; O'Shaughnessy et al., 2000).

The results of this section show that in D2 epidermis lineage reprogramming is accompanied by only local increases in proliferation, whereas in D4 epidermis

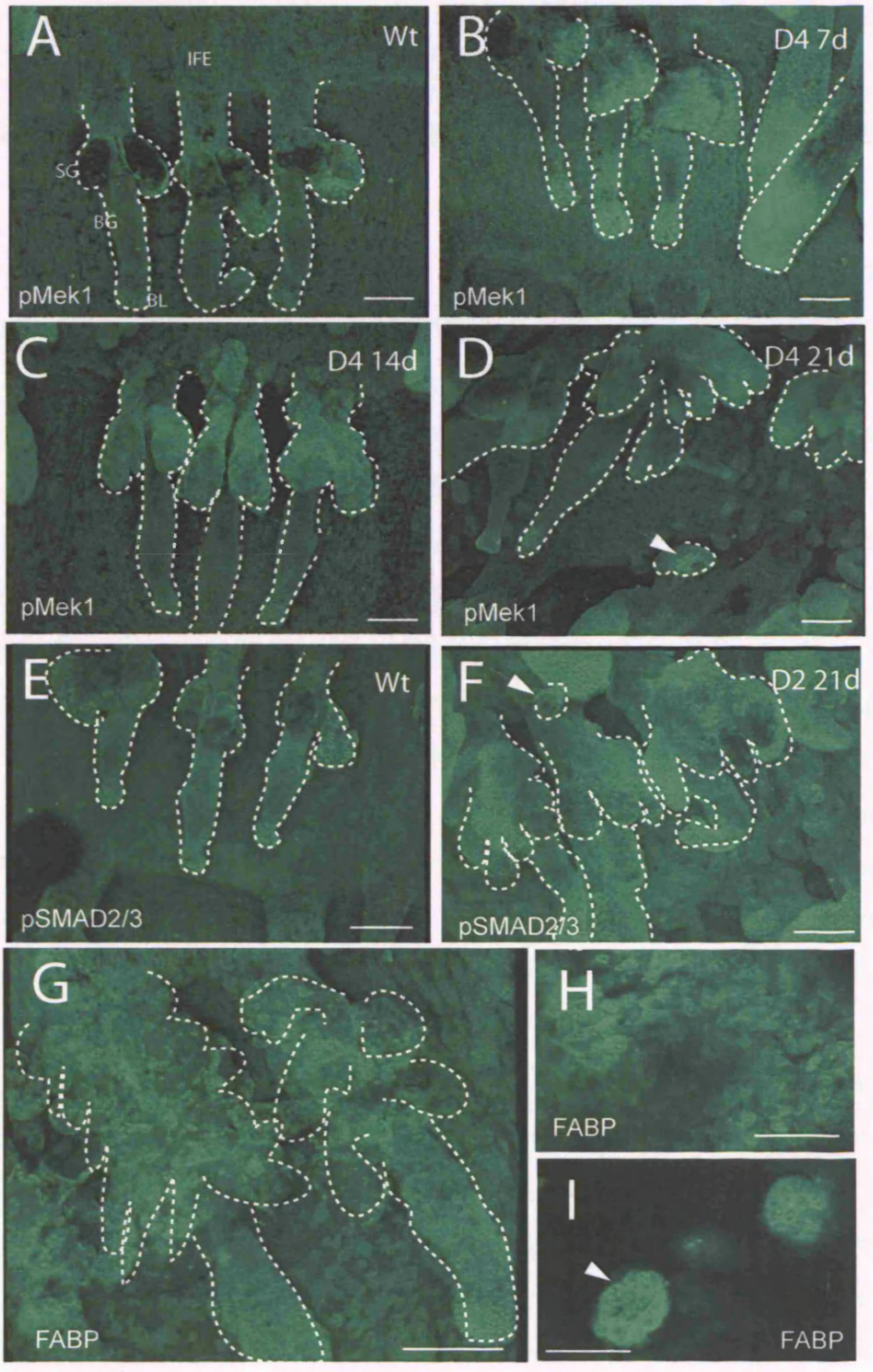

Figure 4.9- Effects of ΔNβ-catenin-ER activation on markers of proliferation signalling pathways. Transgenic mice (D2) were treated with 1.5 mg 4OHT (medium dose) for the dates shown. (A-D) Immunolabelling with a specific phospho-MEK1 antibody. In A locations of sebaceous glands (SG), hair follicle outer root sheath (ORS), bulge (BG) and bulb (BL) are indicated. (E and F) Labelling with pSMAD2/3 antibody. (G-I) Immunolabelling for Fatty Acid Binding Protein (FABP) to mark transit amplyfying cells (TACs). Arrows in D,F and I indicate clusters of proliferating cells associated with ectopic HF formation. Scale bars: 100 μm.

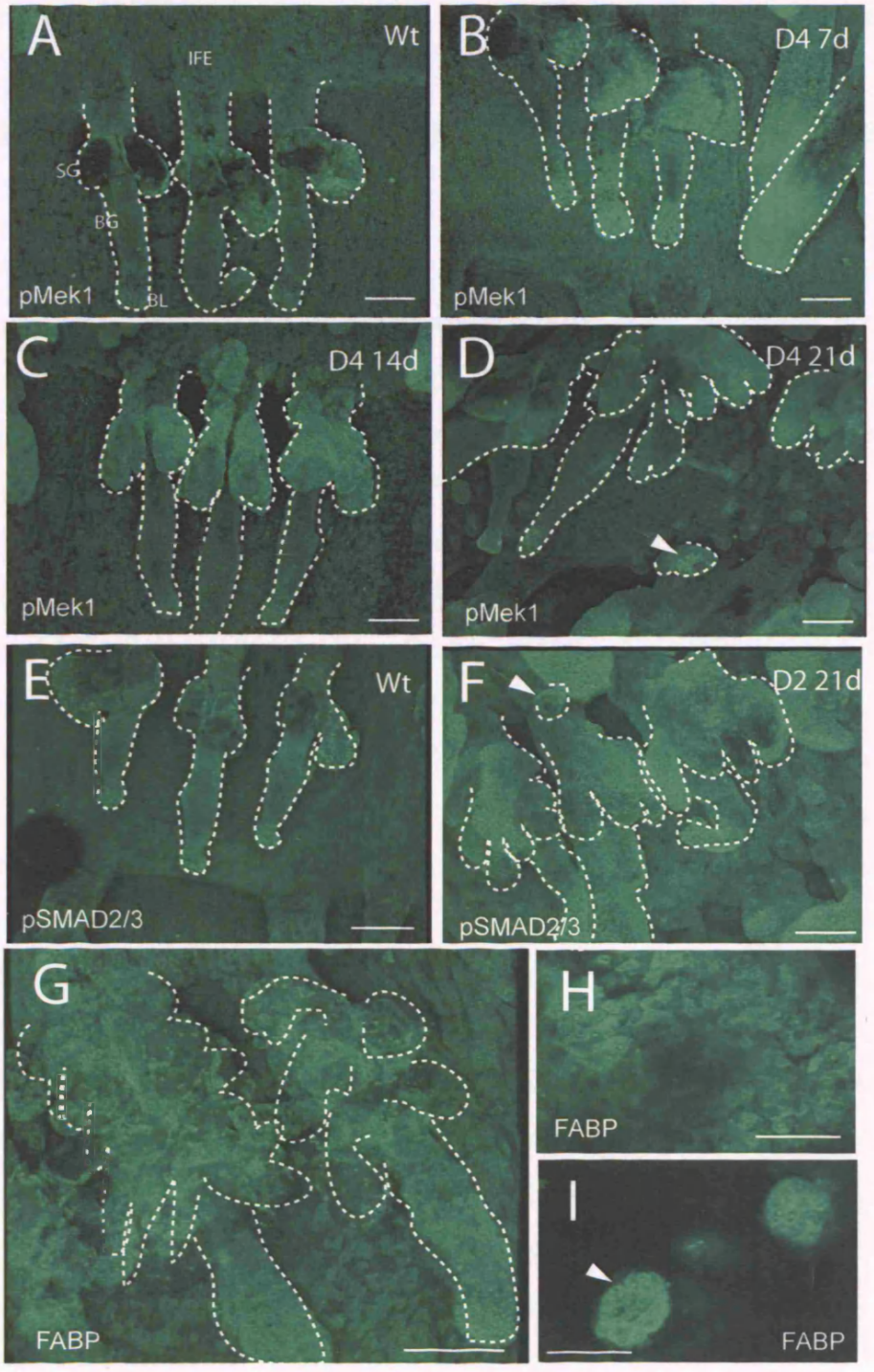

Figure 4.9- Effects of ΔNβ-catenin-ER activation on markers of proliferation signalling pathways. Transgenic mice (D2) were treated with 1.5 mg 4OHT (medium dose) for the dates shown. (A-D) Immunolabelling with a specific phospho-MEK1 antibody. In A locations of sebaceous glands (SG), hair follicle outer root sheath (ORS), bulge (BG) and bulb (BL) are indicated. (E and F) Labelling with pSMAD2/3 antibody. (G-I) Immunolabelling for Fatty Acid Binding Protein (FABP) to mark transit amplyfying cells (TACs). Arrows in D,F and I indicate clusters of proliferating cells associated with ectopic HF formation. Scale bars: 100 μm.

there is more extensive proliferation and the follicles become grossly thickened.

4.4-Effects of β-catenin activation in the LRC compartment *in vivo*

Cells in all regions of the epidermis (HF, SG, IFE) are competent to respond to β-catenin (Figure 4.6). Under steady-state conditions bulge stem cells give rise to hair follicle lineages (Levy et al., 2005; Ito et al., 2005) and a pulse of β-catenin induces bulge stem cells to proliferate, triggering the entry into the anagen phase of the hair growth cycle (Lowry et al., 2005). In this section I investigated the effects of β-catenin activation on the bulge stem cell compartment and whether new HF originated from this compartment or from cells in the IFE and SG.

To investigate the effect of β-catenin activation on the hair follicle stem cell compartment I used two of the stem cell markers described previously in Chapter 3: retention of BrdU label and expression of K15. Label retaining cells (LRC) were generated as described in the Materials and Methods section by giving neonatal mice repeated injections of BrdU and then examining the epidermis of adult animals after a minimum of 40 days chase-period. Mice from both lines were treated with the same doses as in the titration experiments. The design of the experiment is shown in Figure 4.10.

I monitored changes in LRC, by immunolabelling with antibodies against BrdU and visualising basal layer epidermal cells with an antibody against keratin 14. In wild-type mice and untreated transgenic mice LRC are concentrated in the permanent portion of the hair follicle, in the region known as the bulge, and there are scattered LRC in the sebaceous glands and IFE (Figure 4.11 A and G). In D2 hair follicles treated with 4OHT (medium dose) there was no evidence of LRC depletion in the bulge for up to 14 days when ectopic hair follicles were already formed (Figure 4.11 C). When I looked at D4 mice treated for up to 9 days I did not see any obvious change in numbers of BrdU positive cells (Figure 4.11 K). Thus at times when ectopic hair follicle formation was well advanced in IFE and SG (Figure 4.11) bulge LRC had not been lost and there was no evidence that they had moved. β-catenin activation did not trigger proliferation in the bulge (Figure 4.11 B,C,and H-

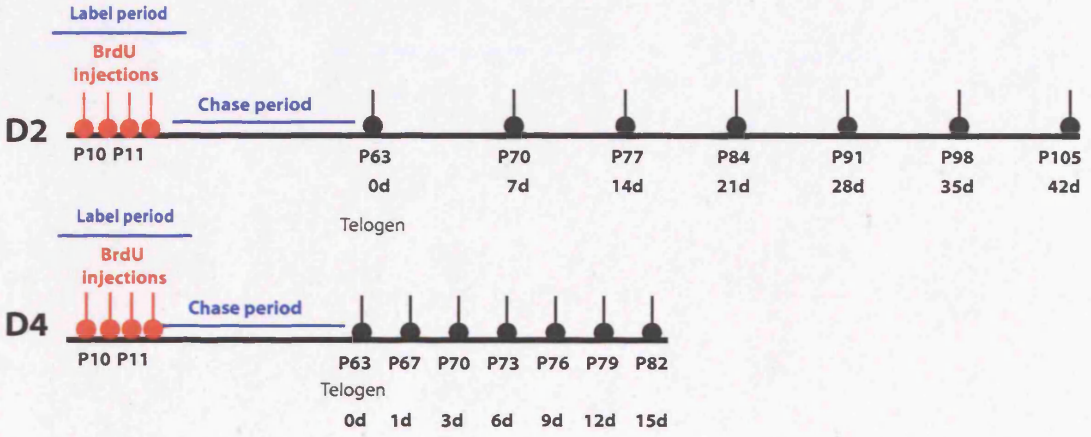

Figure 4.10- Effects of ΔNβ-catenin-ER activation on LRC of tail epidermis. Schematic diagram of the experimental design to look at the effects of β-catenin activation in the LRC compartment in the D2 and D4 transgenic lines. P corresponds to postnatal day and d corresponds to the day of the experiment. Note that the experiments were started at P63 when mice were in telogen. Days indicate the timepoint when the skin was harvested and analysed. Mice were treated with a medium dose of 4OHT every second day.

K) and it was only at 28 days of treatment of D2 mice (Figure 4.11 D) and 15 days of treatment of D4 mice (Figure 4.11 L) that the number of LRC in the bulge had declined significantly.

In order to find out how BrdU positive cells were lost at late time points, I first looked by TUNEL labelling at whether there was an increase in apoptosis between the different time points (example shown in Figure 4.12 B, L, D). I did not observe any obvious increase in the number of TUNEL positive cells in either of the time points analysed in this experiment and in either lines (Figure 4.12 C, D).

As shown previously, activation of β-catenin resulted in local increases in proliferation (Figure 4.8 and 4.9). I therefore looked at whether loss of bulge LRC correlated with stimulation of LRC to divide. I performed double immunolabelling with BrdU to detect LRC and Ki67 to detect cells that were in cycle (Figure 4.12 E-L). In wild-type epidermis LRC were confined to the bulge and scattered in IFE and SG, whereas proliferating cells were confined to the outer layers of the SG (see in red in Figure 4.12 E) and basal cells of the infundibulum and IFE (Figure 4.12 E in green). I could only detect double labelled cells in wild-type telogen follicles (Figure 4.12 H). During the first stages of ectopic follicle development in transgenics (between the first and second week of 4OHT treatment) I could not see an increase in double positive cells (Figure 4.12 F-G; see orange or yellow cells). As the phenotype developed (3 weeks) I could start detecting double labelled cells representing LRC cells that were entering into cycle (Figure 4.12 H,K). At later stages of the treatment (four to five weeks), when I observed the decrease in the number of LRC (Figure 4.12 I, J), I could detect Ki67 positive and non-labelled or lightly BrdU labelled cells appeared in the bulge (Figure 4.12 L). I conclude that on sustained activation of β-catenin LRC are lost through proliferation.

I next wondered whether LRC proliferation resulted in bulge compartment loss. I looked at Keratin 15, which is expressed in the bulge and corresponds to the zone of LRC (Figure 4.12 N; see Figure 3.4 in Chapter 3). Keratin 15 expression in the bulge was preserved in both transgenic lines, even at high 4OHT concentrations

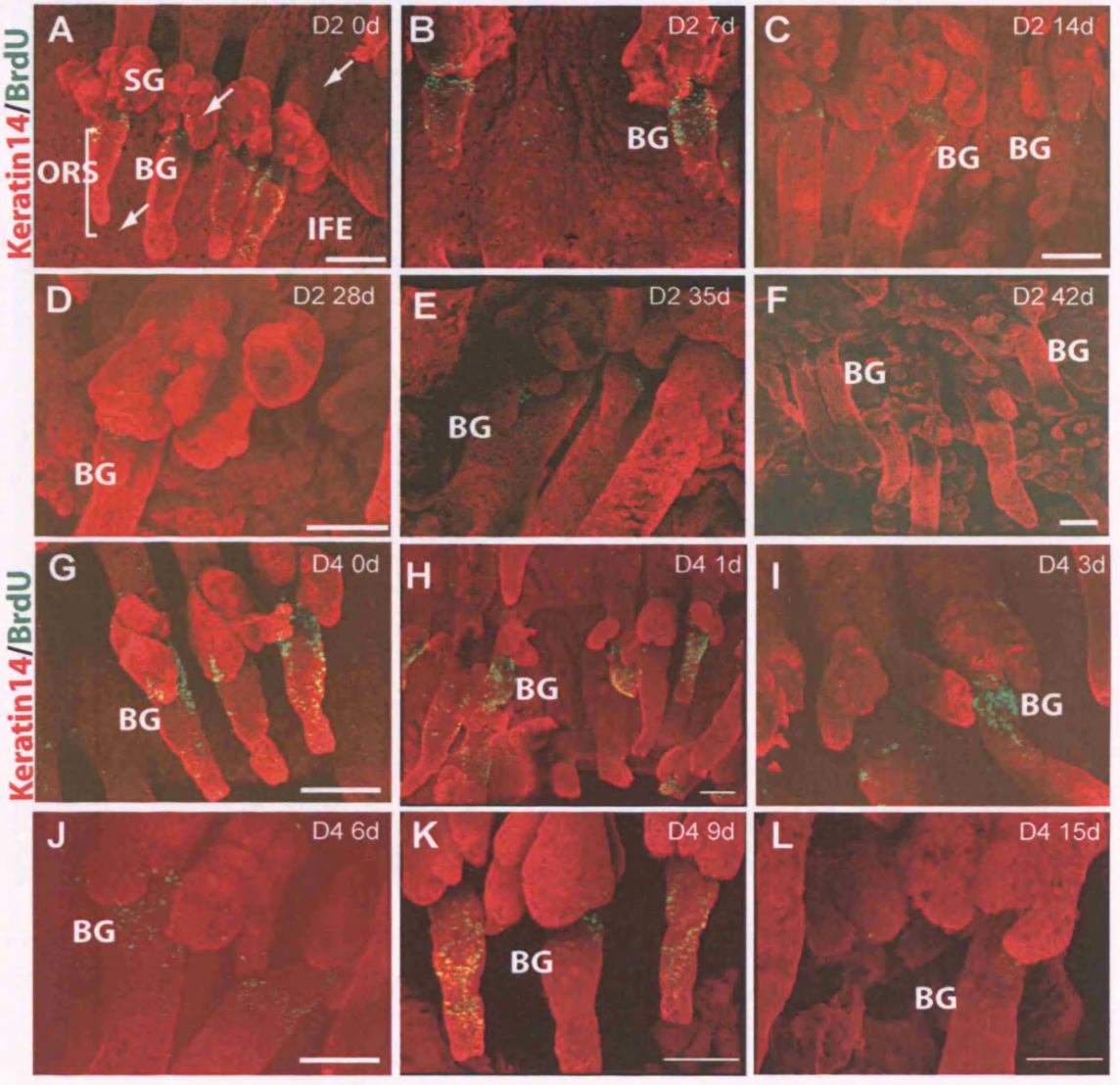

Figure 4.11- Effects of ΔNβ-catenin-ER activation on LRC of tail epidermis. Transgenic line (D2 or D4) were treated with 4OHT(medium dose) for the days shown. (A-L) green: BrdU; red: keratin 14. In A locations of sebaceous glands (SG), hair follicle outer root sheath (ORS), bulge (BG) and bulb (BL) are indicated and arrows show LRC. (B-L) Bulges are indicated (BG). Scale bars: 100 μm.

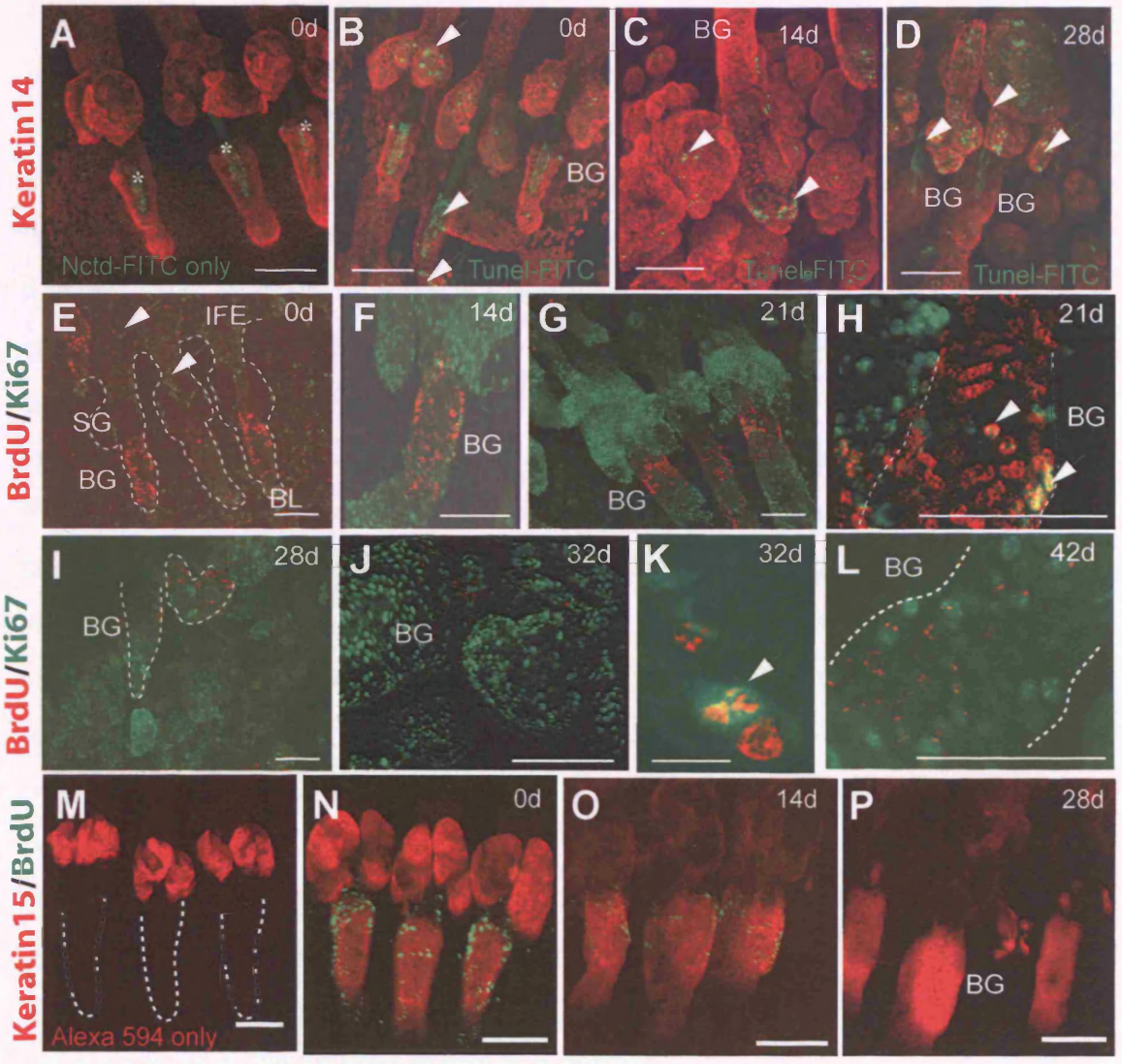

Figure 4.12- β-catenin activation induces LRC loss through proliferation and the bulge compartment is maintained. (A-P) Transgenic line D2 treated with 4OHT for the indicated days (d) (medium dose) are shown. A is untreated transgenic skin labelled with the nucleotide conjugated with FITC only as a negative control. (B-D) Apoptotic cells were analysed by Tunel immunolabelling. (E-L) Double labelling for Ki67 (green) and LRC (red). In E locations of sebaceous glands (SG), hair follicle outer root sheath (ORS), bulge (BG) and bulb (BL) are indicated and arrows show scattered LRC in SG and IFE. Dashed lines indicate the triplet (E) and the bulge in (G,H,I,L). M is wild type whole mount stained with secondary antibody alone, showing nonspecific SG labelling. N-P: double labelling for keratin 15 (red) and LRC (green). No SG remain in J, K. Note that at 28 days when LRC are lost there is no increase in apoptotic cells in the bulge. Scale bars: 100 μm (A-F and J-L), 10 μm (G).

and late time points (see examples in Figure 4.12 O,P). In D2 epidermis after 28 days of medium dose 4OHT treatment, when LRC had been completely lost from some bulges (Figure 4.12 P), the keratin 15 expression pattern was unchanged (Figure 4.12 P).

These results show that β-catenin induced HF formation could be initiated without involvement of bulge LRC and that even when LRC divided and lost their label the original bulge remained, as detected by keratin 15 expression.

Further evidence that ectopic hair follicles could originate in the IFE came from lineage trace analysis in triple transgenic mice (K14Cre-ERxRosa26/ K14ΔNβ-cateninER), in which IFE cell progeny can be followed by LacZ expression after β-catenin activation. These experiments were performed by Dr Adam Giangreco and Dr Kristin Braun (Silva-Vargas et al., 2005). The treatments were designed so that transgene activation would be homogenous but the LacZ expression would be patchy. After 4OHT treatment ectopic hair follicles originating from IFE that were positive for CDP, resembled the LacZ (either positive or negative) of the surrounding IFE (Silva-Vargas et al., 2005). These results strongly suggest that HF had originated from immediately adjacent epidermis rather than from neighbouring hair follicles and supports the notion that LRC from the bulge were not involved (Silva-Vargas et al., 2005).

I conclude that β-catenin activation can induce ectopic hair follicles without any obvious change in the number or location of bulge stem cells. After prolonged treatment bulge cells are induced to proliferate, however the compartment is maintained as bulge markers expression persists.

4.5-Characterisation of ectopic hair follicles

4.5.1-Recreation of a hair follicle niche in ectopic HF

Hair follicles constitute a very complex and dynamic niche in which several cell types reside and constantly go through cycles of growth and regression (Alonso and Fuchs, 2006). Ectopic hair follicles can recruit a dermal papilla (Figure 4.13 A; Van Mater, et al.2003 and (Lo Celso et al., 2004). I performed an array analysis of genes modulated by β-catenin at 7 days that is described in Chapter 5 and amongst the upregulated genes were several that play a role in melanin biosynthesis (Table 5.1). This led me to examine whether β-catenin induced

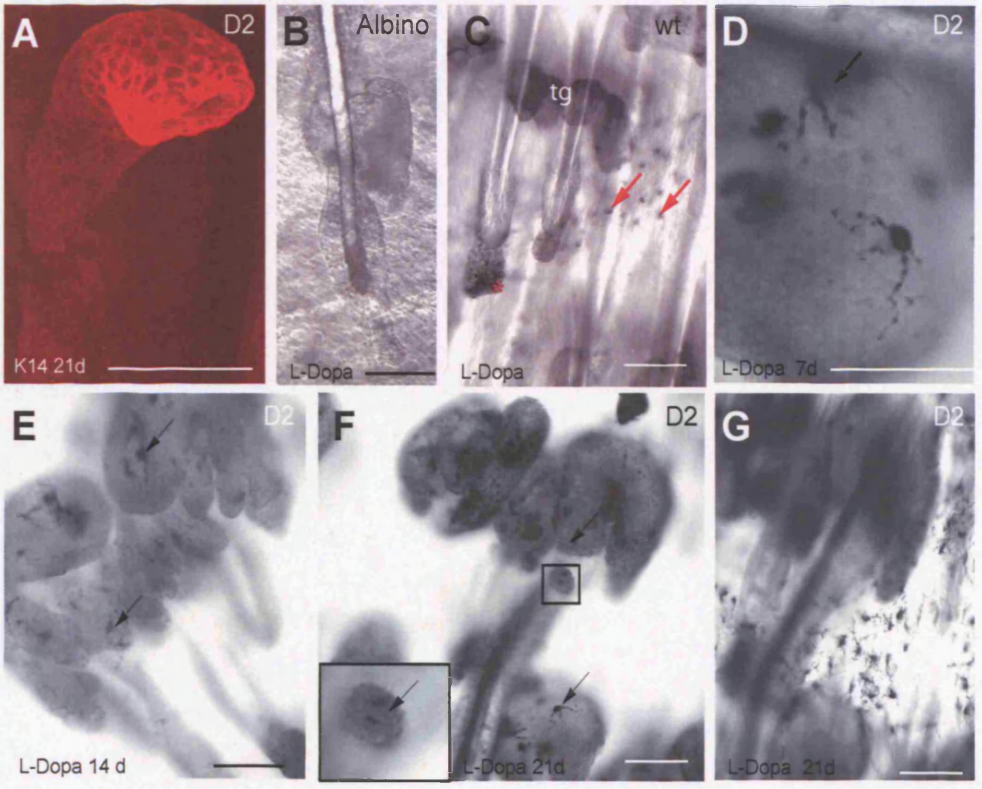

Figure 4.13- Ectopic hair follicles provide a niche for differentiated melanocytes. Whole mounts of wild-type (wt) and D2 transgenic (tg) tail skin. Tail skin was treated with a low (A) or medium (B-G) dose of 4OHT for the number of days shown. Epidermis was labelled with L-Dopa (B-G) or with an anti-keratin 14 antibody. (A) Cuff of keratinocytes at the base of the ectopic follicle into which dermal papilla cells insert. In B wild type mouse is Albino, serving as a negative control for L-Dopa staining. Melanocytes in follicle bulb (red asterisk) and IFE (red arrow) are indicated in C. In E and F melanocytes in HF induced from SG and ORS are shown with black arrows. Insert in F shows high magnification view of ectopic HF arising from ORS, with melanocyte indicated by arrow. Scale bars: 100 μm.

follicles were capable of providing a niche for neural crest derivatives such as melanocytes.

To visualise differentiated melanocytes I examined tyrosinase activity using L-Dopa as substrate (Nishimura et al., 2002). In order to ensure the specificity of this enzymatic reaction, skin from albino mice, devoid of melanocytes, was used as a negative control for the staining (Figure 4.13 B). In wild-type tail hair follicles melanocytes were concentrated at the base of the follicle (Figure 4.13 C, red asterisk). In adult dorsal epidermis, the differentiated melanocytes are confined to the hair follicles (Nishimura et al., 2002), but in the tail, small numbers of melanocytes were also found scattered in the IFE (Figure 4.13 C, arrows). Melanocytes were present in the ectopic follicles induced by β-catenin in SG (Figure 4.15 D, E), IFE (Figure 4.15 F) and HF (Figure 4.15 D).

In order to detect melanocyte precursors (melanoblasts), I used an antibody to c-Kit. In wild-type epidermis there are a few c-Kit positive cells, the putative melanocyte stem cells, in the bulge, as reported previously (Nishimura et al., 2002; Figure 4.14 A, lower arrow). In addition, in tail epidermis there are also some c-Kit positive melanoblasts in the HF infundibulum (Figure 4.14 A, upper arrow; Grichnik et al., 1996). In early stages of ectopic hair follicle development (9 days 4OHT treatment, D2 mice), c-Kit positive cells appeared in IFE immediately adjacent to the HF (Figure 4.14 B, arrowheads), and at later time points c-Kit positive cells were found in the base of the new follicles (Figure 4.16 C).

Interestingly, the c-Kit ligand is known to act as a homing cue for melanocytes (Grichnik et al., 1996). Thus, I looked at the changes in the c-Kit ligand expression in order to understand how migration of this melanocyte population might have taken place. In wild-type epidermis c-Kit ligands is highly expressed by keratinocytes of the hair follicle, infundibulum and parakeratotic scale area of the IFE (Figure 4.14 D). In the transgenic skin analysed at the same time points as for L-Dopa, c-Kit ligand expression was no longer restricted to those areas, but was widely expressed, including sites where differentiated melanocytes (L-Dopa positive) and melanoblasts (c-Kit positive) were recruited (Figure 4.14 E).

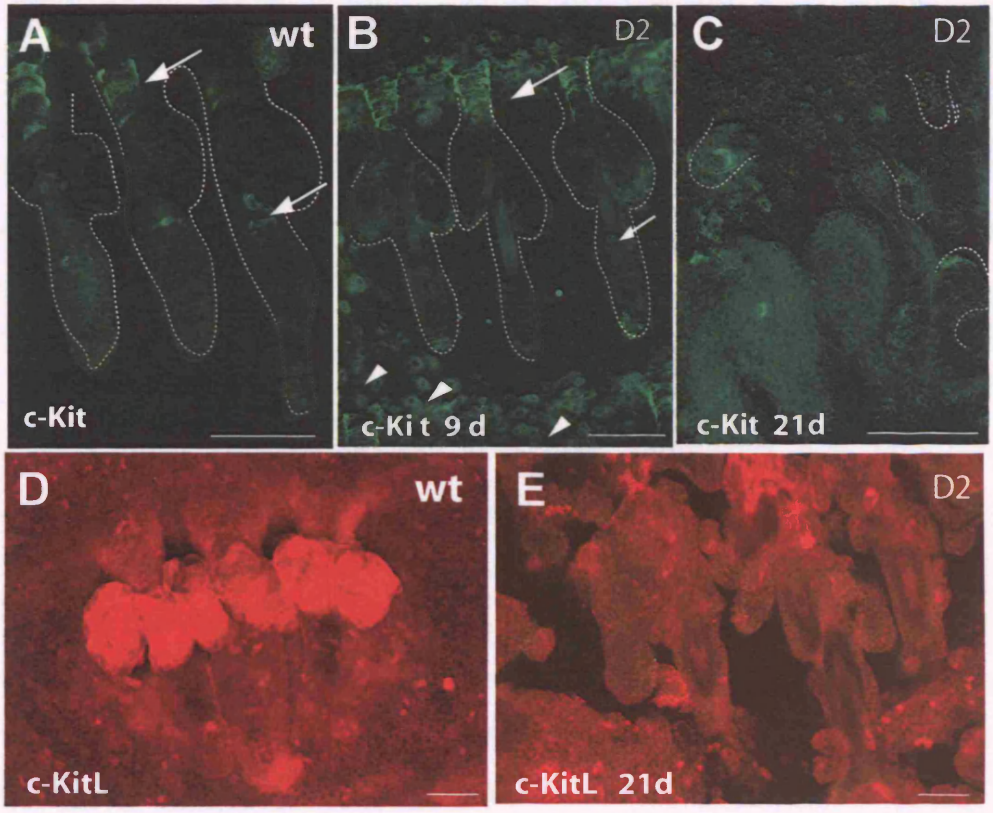

Figure 4.14- Ectopic hair follicles provide a niche for melanocyte progenitors. Whole mounts of wild-type (wt) and D2 transgenic (tg) tail skin. Tail skin was treated with a medium dose of 4OHT for the number of days shown. Epidermis was labelled with anti c-Kit antibody to mark melanocyte progenitors (A-C) or with an anti-c-Kit Ligand antibody (D and E). A and B c-Kit positive cells in infundibulum (top arrows), bulge (bottom arrow) and in the IFE (arrowheads) are shown. Dotted lines in A,B demarcate HF and SG. C: dotted lines demarcate new HF. Scale bars: 100 μm.

As previously mentioned, activation of β-catenin results in the formation of new dermal papillae, the specialised fibroblasts engulfed by the hair follicle bulb (Van Mater et al., 2003; Lo Celso et al., 2004). The cells encircled by the cuff of keratinocytes at the base of the follicle can be visualised with alkaline phosphatase (Lo Celso et al., 2004) and also with nestin, a marker expressed by neural crest derived stem cells in the dermal papilla (Toma et al., 2001); (Fernandes et al., 2004). In tail epidermis, nestin is also a marker of wild-type dermal papillae (Figure 4.15 D, arrow). In addition to the nestin positive cells in the DP (Figure 4.15 A), there are some nestin-positive cells with a dendritic morphology scattered along the length of wild-type follicles (see arrowhead in Figure 4.15 A). Their dendritic morphology suggested that they could be either differentiated melanocytes or Merkel cells, that together with sensory neurons, form cutaneous mechanoreceptors. Double labelling with keratin 18 indicated that the dendritic nestin positive cells are not Merkel cells (Figure 4.15 E,F). They are also L-Dopa negative (Figure 4.15 G-I), and I speculate that they are undifferentiated melanocyte precursors (Figure 4.15 G-I; Fernandes et al., 2004).
In conclusion, β-catenin induced follicles are capable of providing a niche for neural-crest derived cells such as differentiated melanocytes, melanoblasts and cells in the DP. These results show that even though the β-catenin transgene is activated in keratinocytes it has a great impact on other cell types that normally reside in close contact with keratinocytes. By simply activating β-catenin in basal layer keratinocytes, we can switch on a programme to develop a niche for other cell types.

4.5.2-Tail ectopic hair follicles can undergo cycles of growth and regression dependent of 4OHT

Hair follicles, in addition to providing a niche for other cell types, are very dynamic structures that undergo cycles of growth and regression (Alonso and Fuchs, 2006). Several pathways are involved in regulating the hair cycle, one being the Wnt pathway, which induces entry into the growth phase, anagen. The first response of K14ΔNβ-cateninER epidermis to 4OHT treatment is the entry into anagen and it was previously shown that withdrawal of 4OHT caused pre-existing follicles to regress and enter the resting phase (Lo Celso et al., 2004).

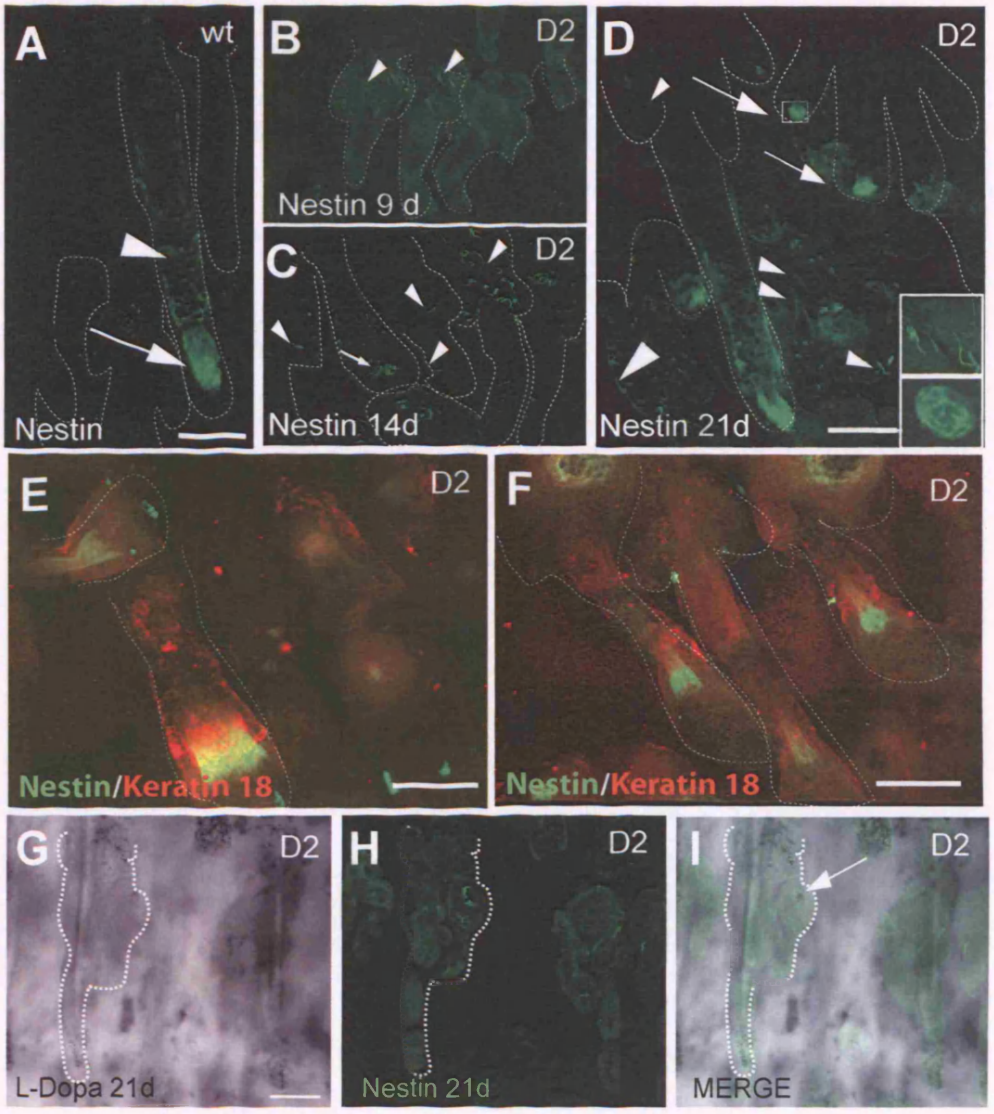

Figure 4.15- Ectopic hair follicles provide a niche for neural crest progenitors. Whole mounts of wild-type (wt) and D2 transgenic (tg) tail skin. Tail skin that was treated with a medium dose of 4OHT for the number of days shown. Epidermis was labelled with anti Nestin antibody to mark neural crest progenitors (A-D) or in combination with the Merkel cell marker keratin 18 (E,F) or with L-Dopa staining (G-I). Note that nestin positive cells are either clustered in the dermal papilla (white arrow) or scattered in ORS (A), SG (B and C) or IFE (D).Upper inset in D shows dendritic nestin positive cells and lower inset shows clustered nestin positive cells in dermal papilla of an ectopic HF. Dotted lines in A-I demarcate HF and SG. Scale bars: 100 μm

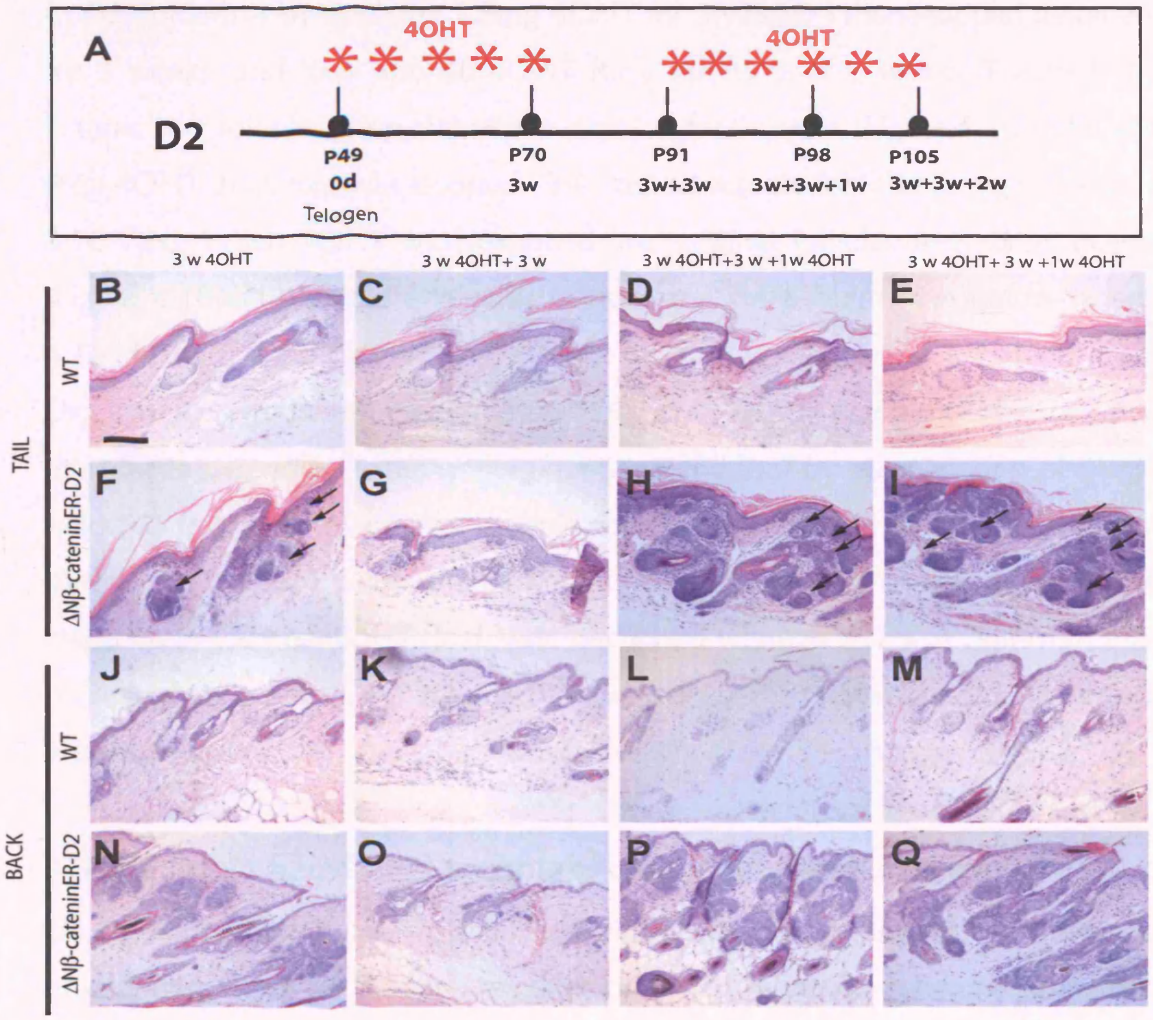

Figure 4.16. β-catenin induced hair follicles can undergo cycles of growth and regression. (A) Schematic diagram of the experimental design to look at the effects of titrating β-catenin activation on cycling of the ectopic follicles. P corresponds to postnatal day and w corresponds to the day of the experiment when tissue was harvested. Note that the experiments were started at P49 when mice where in telogen. Mice were treated with the 3 doses indicated of 4OHT every second day.(B-Q) H & E stained sections of WT (B-E and J-M) and D2 transgenic tail (F-I) and dorsal (N-Q) epidermis treated with 4OHT for 3 weeks and then harvested immediately (B, F, J, N) or left untreated for 3 weeks (+3w) and harvested (C,G,K,O) or treated with 4OHT for a further 1 (+1w) (D,H,L,P) or 2 (+2w) (E,I,M,Q) weeks.Arrows in F-I show examples of ectopic follicles. Scale bars: 100 μm

Therefore, it was intriguing to find out whether ΔNβ-cateninER induced follicles could also undergo cycles of growth and regression.

To investigate this, I designed an experiment in which I induced ectopic follicles in D2 epidermis by applying 1.5mg 4OHT for 3 weeks; I then stopped treatment for 3 weeks; and then applied 4OHT for a further 1 or 2 weeks (Figure 4.16). Ectopic hair follicles were allowed to develop for 3 weeks (Figure 4.16 E, M) and then 4OHT treatment was stopped. This caused ectopic follicles to regress (Figure 4.16 F,N). When 4OHT was reapplied, the original follicles re-entered anagen (Figure 4.16 G,O); ectopic follicles re-grew and were wider than before (Figure 4.16 H-I).

Dr Giangreco in the lab measured the number of sites of ectopic CDP expression in order to determine whether the phenotype induced by reapplication of 4OHT reflected re-growth of existing ectopic follicles or initiation of new ones (Silva-Vargas et al., 2005). Interestingly, the number of CDP positive sites increased in response to the first 4OHT treatment; decreased when 4OHT was removed; then on reapplication of 4OHT returned to the same level as after the first treatment. This suggests that the original ectopic follicles re-grew (Silva-Vargas et al., 2005).

4.5.3-Ectopic hair follicles contain clonogenic keratinocytes

Given that ectopic β-catenin induced hair follicles are capable of recruiting and providing a niche for neural-crest stem cells and more differentiated progeny, I wondered if they also expressed markers for bulge cells.

To evaluate this, I first stained whole mounts with antibodies to keratin 15 and CD34 (Figure 4.17 A-F). As previously shown, in wild-type follicles expression of both markers was confined to the permanent portion of the follicle (Figure 4.17 A; Trempus et al., 2003; Morris et al., 2004). Both markers were retained in the original bulge, even after prolonged β-catenin activation (Figure 4.12 N; Figure 4.17 E, F). However, the levels of CD34 were lower in the pre-existing bulges (Figure 4.17 E, F; see continuous line). This is consistent with the notion that these cells are cycling at this late stage of treatment (Figure 4.12 E-H) and therefore not quiescent. In addition, expression of both markers was observed in all sites of new HF development in D2 epidermis from 35 days of treatment (Figure 4.17 E and F).

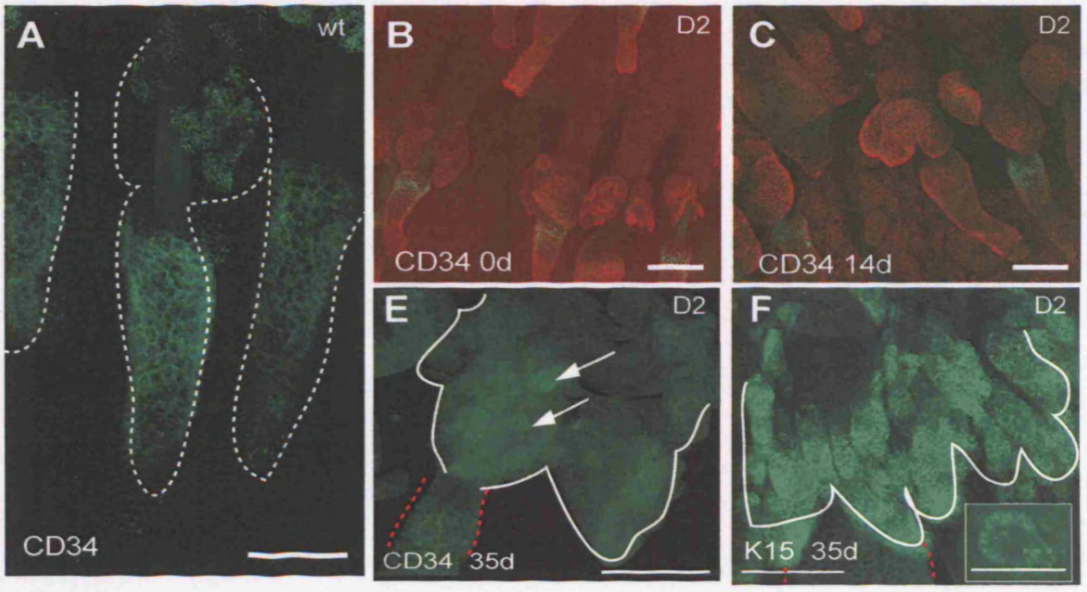

Figure 4.17- β-catenin activation induces formation of keratinocytes that have characteristics of bulge stem cells. Whole mounts from tail epidermis of Wt untreated (A) or D2 transgenic mice untreated (B) and treated with a medium dose of 4OHT (C-F) for the number of days shown. Whole mounts were immunolabelled with an anti-CD34 antibody (A-E) or with an anti-keratin 15 antibody (F). Ectopic follicles are demarcated with dotted lines in E and F. Inset in F shows a keratin 15 positive ectopic hair follicle. Continous line in E, F indicate ectopic hair follicles. Red dashed lines in E and F indicate pre-existing bulge. Scale bars: 100 μm

The same observations were made for back skin at these time points (Silva-Vargas et al., 2005).

An additional marker for assessing bulge cell characteristics is clonal proliferative capacity *in vitro*. Recently, it has been shown that cells expressing high levels of CD34 and α6 integrin constitute the epidermal population that has the highest clonal capacity *in vitro* (Morris et al., 2004; Blanpain et al., 2004; Tumbar et al., 2004; See also Chapter 3).

In order to obtain a quantitative assessment of the increase in CD34 positive cells and to evaluate whether or not they were capable of forming actively growing colonies I performed FACS analysis of disaggregated keratinocytes from back (Figure 4.18) and tail skin (Figure 4.19) in collaboration with Dr Adam Giangreco from the laboratory. CD34 is a widely expressed marker by other progenitor cells and not exclusively expressed on keratinocytes. In order to ensure enrichment of keratinocytes, we performed double labelling with antibodies to CD34 and to the α6 integrin subunit, which is expressed by undifferentiated keratinocytes of HF, SG and IFE. In addition, we further enriched for basal (small size) cells by gating out differentiated cells on the basis of high forward and side scatter (A, B in Figure 4.18 and Figure 4.19; Jones, et al.1995). Prior to analysis, the cell preparations were stained with a 7AAD dye to gate out dead cells. The majority of the gated cells (encircled in red in panels A and B) express the α6 integrin subunit, in both wild type and 4OHT treated transgenic epidermis and in both, tail or back skin (Figure 4.18 and Figure 4.19).

In 4OHT treated wild type epidermis approximately 4% of the α6 positive cells express high levels of both CD34 and α6 integrin and 2% are CD34 positive and have lower levels of α6 integrin. In D2 back epidermis the proportion that had high CD34/α6 integrin expression was similar (3.5%, compare C and D in Figure 4.18), but the proportion with a CD34 positive /α6 integrin low expression phenotype had increased to approximately 15% (Figure 4.18 D).

Interestingly, in tail epidermis the profile was different. In wild type epidermis, the proportion of α6 positive cells expressing high levels of both CD34 and α6 integrin was 3.22 %, while 0.49% are CD34 positive and have lower levels of α6

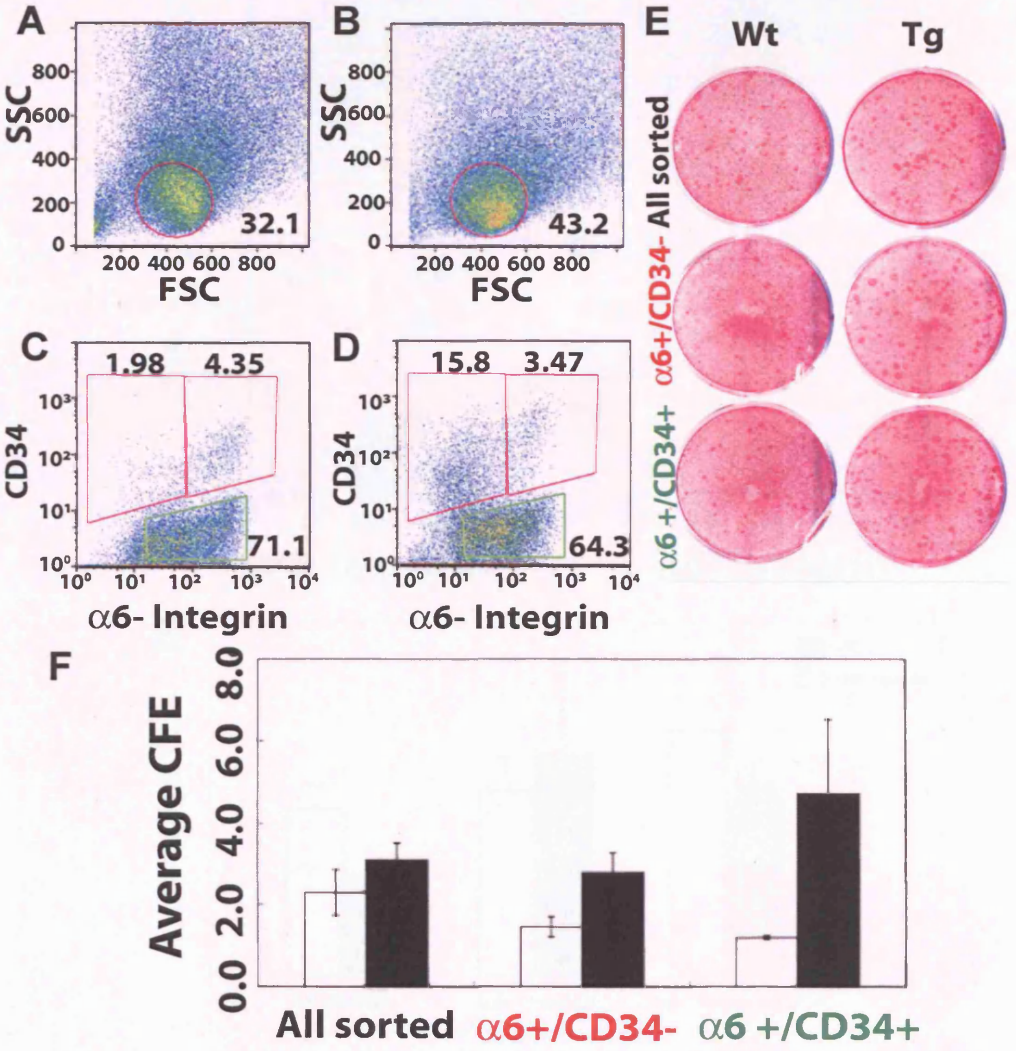

Figure 4.18- β-catenin activation induces formation of ectopic hair follicles with keratinocytes that have clonogenic capacity in vitro. FACS selection and culture of keratinocytes from dorsal epidermis of adult wild-type (A,C,E,F) and D2 transgenic (B,D,E,F) mice treated with a medium dose 4OHT for 3 weeks. Cells isolated from epidermis were double labelled for CD34 and α6 integrin. Cells with low forward and side scatter characteristics (circled in A,B) were either sorted directly onto culture dishes (all sorted (E,F) or further fractionated into α6 single positive (green boxes in C,D) or CD34/α6 double positive populations (red boxes in C,D). In C,D the left hand red boxes represent cells with lower surface α6 than the right hand red boxes. FACS sorted keratinocytes were cultured for 2 weeks at clonal density on a feeder layer, then stained with Rhodamine B to determine colony forming efficiency (E,F). The graph in (F) is representative of two separate experiments, in each of which cells from triplicates of wild-type or transgenic mice were pooled. White bars: wild-type; black bars: transgenic cells. Error bars represent values of standard deviation values. This experiment was performed in collaboration with Dr Adam Giangreco.

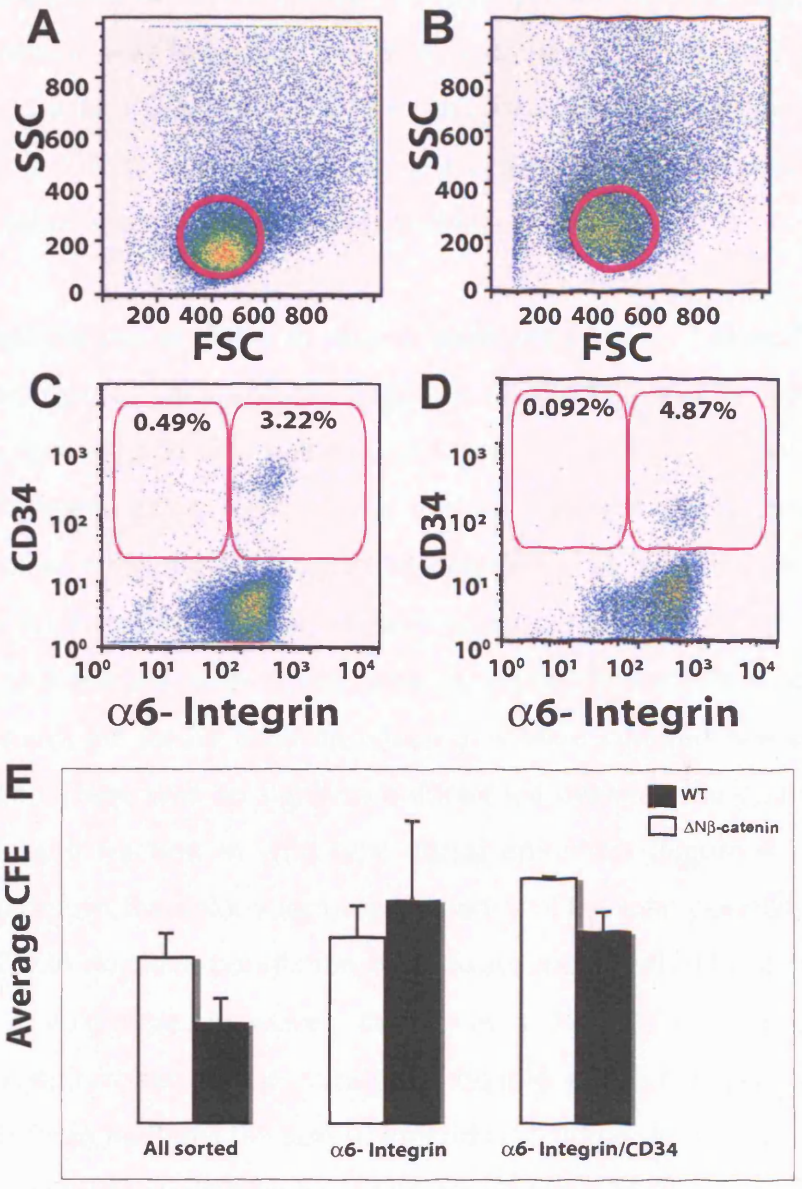

Figure 4.19- β-catenin activation induces formation of ectopic hair follicles with keratinocytes that have clonogenic capacity in vitro in tail epidermis. FACS selection and culture of keratinocytes from tail epidermis of adult wild-type (A,C,E) and D2 transgenic (B,D,E) mice treated with a medium dose 4OHT for 3 weeks. Cells isolated from epidermis were double labelled for CD34 and α6 integrin. Cells with low forward and side scatter characteristics (circled in A,B) were either sorted directly onto culture dishes (all sorted (E) or further fractionated into α6 single positive (green boxes in C,D) or CD34/α6 double positive populations (red boxes in C,D). In C,D the left hand red boxes represent cells with lower surface α6 than the right hand red boxes. FACS sorted keratinocytes were cultured for 2 weeks at clonal density on a feeder layer, then stained with Rhodamine B to determine colony forming efficiency (E). The graph in (E) is representative of three separate experiments, in each of which cells from triplicates of wild-type or transgenic mice were pooled. White bars: wild-type; black bars: transgenic cells. Error bars represent values of standard deviation values. This experiment was performed in collaboration with Dr Adam Giangreco.

integrin (Figure 4.19). In D2 tail epidermis the proportion that had high CD34/ α6 integrin expression was increased to 4.87%, (compare C and D in Figure 4.19). The proportion with a CD34 positive / α6 integrin low expression phenotype had decreased to 0.092 % (Figure 4.19 D). The changes in the proportions of the double population were different in back and tail.

In order to test the clonal ability *in vitro* of these populations, I selected by FACS three cell fractions for back and tail (Figure 4.18 and Figure 4.19, respectively): the total low forward and side scatter population ('all sorted'), α6 positive/CD34 negative cells (green gates, Figure 4.18), and all α6/CD34 double positive cells irrespective of whether the α6 integrin was expressed at high or low levels (red gates, Figure 4.18 and 4.19). After 14 days of culture without 4OHT, the dishes were fixed and stained with Rhodamine B, revealing individual colonies of keratinocytes and the feeder layer on which they were cultured (see an example in Figure 4.18). There was no significant difference between the colony forming efficiency of each fraction in wild type dorsal epidermis (Figure 4.18 E, F). In transgenic epidermis the colony forming efficiency of the total population and the α6 positive/CD34 negative population was always increased but not significantly different from wild type. However, there was a 2 fold higher proportion of clonogenic keratinocytes in the transgenic double positive population (Figure 4.18 F). In all three fractions the size of individual colonies tended to be larger in transgenic compared to wild type keratinocytes (Figure 4.18 F).
There were differences between the colony forming efficiency of each fraction in wild type tail epidermis (Figure 4.19 E). In transgenic epidermis the colony forming efficiency of the total population less than 1.5-fold compared to wild-type keratinocytes (Figure 4.19 E) and the α6 positive/CD34 negative population was slightly decreased in the transgenic compared to wild type. However, there was a slight increase (0.5-fold) in the proportion of clonogenic keratinocytes in the transgenic double positive population (Figure 4.19 E).

These results show that after prolonged β-catenin activation in dorsal adult epidermis, the induced HF contain cells with three characteristics of bulge stem cells: expression of keratin 15, expression of CD34, and clonal growth in culture.

In dorsal epidermis there is a 1.8-fold increase in the number of clones in 'All sorted'. However, in tail epidermis the increase is more moderate and enrichment for double positives wild-type keratinocytes does not enrich for clonogenic keratinocytes. In addition, the intensity of CD34 levels in the double positive populations was lower (See Figure 4.19 D, Right Box).

4.6- Discussion

The work described in this chapter validates the whole mount system of tail skin as an excellent system to assess *de novo* hair follicle formation in three dimensions and to obtain quantitative and spatial data on the dynamics of hair formation in tail skin. In addition, it is also very informative to evaluate changes in the epidermal stem cell compartment. A combination between this system and conventional histology provides an optimal system to analyse epidermal phenotypes.

Hair morphogenesis is a complex patterning 'puzzle'

During development, a complex array of pathways interacts to begin the process of hair follicle morphogenesis as explained in the Introduction. It is interesting to think of the process of de novo hair follicle morphogenesis described in this Chapter as a recapitulation in part of the processes that occur during development. So starting from a single monolayer epithelium (IFE) we can induce a morphogenetic switch to start the programme to develop an appendage, the hair, by activating β-catenin in all three epidermal compartments in adult epidermis.

HF induction is a threshold response: from morphogenesis to tumorigenesis

The response of adult epidermis to β-catenin activation is more complex than a simple switching on/off de novo HF formation. With increasing β-catenin activation we could alter the timing and location of ectopic HF formation. Titration of the signal was achieved by expression of different levels of ΔNβ-cateninER transgene in epidermal cells and by application of different concentrations of 4OHT. The concept that cells exhibit a graded response to a gradient of β-catenin regulatory activity was previously introduced from studies of

different APC mutations in a panel of ES cell lines (Kielman et al., 2002) which leads to differences in the level of activation. However, the ΔNβ-cateninER transgene has the important advantage that it allows to titrate transcriptional activity within individual cells, both *in vivo* and in culture.

As mentioned in the Introduction, there are several ways to activate β-catenin and they differ in the outcome. When non-degradable ΔNβ-catenin is constitutively activated since embryonic development (Gat et al., 1998) or when its activation is prolonged and sustained (Lo Celso et al., 2004) a tumour of hair follicle origin, known as a trichofolliculoma, is generated (Gat et al., 1998; Lo Celso et al., 2004; Chan et al., 1999). Interestingly, when β-catenin is activated either by the canonical Wnt3A ligand overexpression (Millar et al., 1999) or by Lithium, a GSK3β inhibitor treatment (Fathke et al., 2006) the effect is much milder. Only intermediate levels of β-catenin activation lead to the start of a programme to generate a hair follicle.

Epidermal compartments differ in their sensitivity to the β-catenin signal

This study confirms that β-catenin activation also promotes hair follicle differentiation in tail skin. Hair follicle lineages are promoted at the expenses of the other two lineages: sebaceous and interfollicular differentiation (Figure 4.4).

In addition, these compartments show different sensitivity to varying levels of β-catenin. Elucidation of additional markers for each compartment will allow their isolation and this will enable us to profile each of these compartments. This will give insights into how the β-catenin signal is processed and interpreted by each of these cell types.

In both transgenic lines the ORS of existing HFs was most refractory to induction of ectopic HF. Although there is heterogeneous expression of Wnts and their receptors in adult epidermis (Reddy et al., 2001; Reddy et al., 2004) and the secreted Wnt antagonist Dickkopf-3 is upregulated in the bulge (Tumbar et al., 2004; Morris et al., 2004), ΔNβ-catenin acts downstream, bypassing their effects. Even though we noticed different levels of transgene expression in HF, IFE and SG, a more likely explanation for the refractoriness of the ORS is that Tcf3 is expressed in the bulge and acts as a repressor of Wnt signalling (Merrill et al., 2001). This notion is re-inforced by the fact that the first site of ectopic hair

follicle formation in the D4 line is the IFE, rather than the SG where there is the highest expression of the transgene (Silva-Vargas et al., 2005).

Effects of β-catenin activation in the LRC compartment *in vivo*

Previous experiments had shown that cells in all regions of the epidermis are competent to respond to β-catenin (Figure 4.4). However, it was not clear if new HF were derived from bulge stem cells or whether committed IFE progenitors could be reprogrammed to induce hair follicles even though they are lineage restricted.

Bulge stem cells are multipotent, and under steady-state conditions they respond to the local signals from the niche and they replenish hair follicle lineages. However, in situations such as wounding they are capable of giving rise to all the differentiated lineages of the HF, IFE and SG (Watt, et al.2006). We did not observe any changes in number or evidence of bulge LRC migration at early stages of HF formation. Even when LRC eventually divided in response to prolonged β-catenin activation, thereby loosing the BrdU label, expression of two bulge stem cell markers, keratin 15 and CD34 (Trempus et al., 2003; Morris et al., 2004) was unchanged, indicating that the bulge stem cell compartment was maintained. Profiling analysis of the outcome of different levels of β-catenin signal in the bulge compartment and further elucidation of the effect in other bulge stem cell markers will also give insights on the phenotype.

Reconstructing a follicle niche including keratinocytes and non-epithelial cells that are normally resident in the hair follicle

β-catenin induced follicles were populated by melanocytes and Merkel cells and formed dermal papillae. The presence of Merkel cells and melanocytes is particularly striking since they are known to be associated with the bulge of wild type follicles (Nishimura et al., 2002; Szeder, 2003; Sieber-Blum, 2004). The expansion of these populations was correlated with a wider expression of the c-Kit ligand, including the keratinocytes of ectopic hair follicles. It has been shown that c-Kit Ligand is expressed in IFE, and by bulge LRC in the HF (Tumbar et al., 2004). Its expression in keratinocytes supports the presence of melanocytes in skin (Nishimura et al., 2002). It is also intriguing that these non-epithelial cell

types are neural crest derived and Wnt dependent. Wnt1 expression during embryogenesis is limited to neural crest cells; Wnt1 signalling is involved in the expansion and differentiation of melanocytes; and ablation of β-catenin in neural crest stem cells leads to lack of melanocytes (Dunn et al., 2004; Dunn et al., 2000; Hari et al., 2002; Le Douarin and Dupin, 2003). It will be interesting if this global recruitment of cells onto the ectopic follicles is recapitulated when β-catenin activation is performed in a more restricted compartment, for instance by driving the transgene with the keratin 15 promoter (targeting the bulge cells) or with the involucrin promoter (targeting the suprabasal cells). This latter will be interesting, as these cells will not be in direct contact with dermal cells.

In addition, it will be intriguing to activate the transgene in a dermal compartment, if the activation of β-catenin is a global and generic switch, it might lead to formation of ectopic hair follicles. In this case, β-catenin activation, the first signal in hair morphogenesis (Schmidt-Ullrich and Paus, 2005) will occur in the dermis instead of the epidermis.

Tail ectopic hair follicles can undergo cycles of growth and regression dependent of 4OHT and contain cells with bulge characteristics

As mentioned in the Introduction, normal follicles undergo cycles of growth and regression, requiring reciprocal signalling with dermal papilla cells (reviewed by Millar, 2002). The follicles induced by β-catenin activation can form a mature hair shaft (Figure 5E; Gat et al., 1998; Lo Celso et al., 2004) however they normally lack inner root sheath markers, such as trichohyalin (Lo Celso et al., 2004). In addition, the re-growth phenotype observed cannot be interpreted as a true hair growth cycle, since it was entirely 4OHT dependent. However, it is very interesting that although these are 'rudimentary' follicles, they are sensitive to the original signal, this is, β-catenin activation.

Furthermore, ectopic HF induced by β-catenin contained areas of keratin 15 and CD34 expression, raising the possibility that new bulge cells can be created from non-bulge epidermal cells with clonogenic capacity *in vitro*.

A role of Wnt signalling in increasing stem cell number has now been reported in a wide range of tissues, including the blood, mammary gland and nervous system (Reya et al., 2003; Megason and McMahon, 2002); Liu et al., 2004; Zhang et al.,

2003). Previous studies have shown that β-catenin activation in cultured human epidermal cells increases the number stem cells (Zhu and Watt, 1999). Whether the appearance of cells with bulge characteristics occurs through expansion of the pre-existing stem cell pool, as it was originally proposed, or through generation of new stem cells from committed progenitors remains to be further explored (Pearton et al., 2004; Silva-Vargas et al., 2005). LacZ expression analyses show that the new follicles are not obligatory clonal. Therefore, if IFE stem cells are not clustered these results suggest that HF originated from the TAC compartment (Silva-Vargas et al., 2005). Further lineage tracing experiments will throw light into these questions. However, it will first be very important to further assess the 'stemness' of these cells, for instance by looking at their reconstitutive capacity *in vivo*.

The results presented in this Chapter show that the epidermis exhibits a high degree of plasticity, as new hair follicles can be formed from SG and IFE, which normally provide sebocyte or interfollicular epidermis, respectively. Although β-catenin activation only occurs in basal keratinocytes, it causes the epidermis to induce a new dermal papilla and recruits melanocytes. This opens a new area in which the epidermal cells could provide a range of different cell types.

In this Chapter I wanted to analyse the process of hair follicle formation in tail epidermis. The results show that the levels of β-catenin activation determine the number and the location of ectopic hair follicles. As described in Chapter 3, wild-type tail skin is a highly patterned tissue. When β-catenin is activated these highly ordered pattern is disrupted as the different epidermal compartments become 'permissive' and ectopic follicles arise. The levels of β-catenin activation are critical in determining the number and location of ectopic follicle formation. It is interesting to look into what pathways are downstream of β-catenin, work that is described in Chapters 5 and 6.

Chapter 5- Identifying events downstream of the β-catenin signal during HF morphogenesis

Aims

β-catenin activation in adult epidermis results in ectopic hair follicle formation. The levels of activation determine the number and location of HF. Ectopic hair follicle formation is a threshold response: if the signal is too low hair formation does not occur and if it is too high tumours form. During hair follicle morphogenesis there are changes in proliferation, differentiation, cell-cell adhesion and patterning and at present it is unclear how the Wnt pathway exerts all the different effects. In order to find out, in this Chapter I have looked at what downstream pathways are modulated by β-catenin during hair follicle morphogenesis. I have also compared my microarray data with gene profiles of different cell populations in the skin that have recently been published by other labs.

5.1-Profiling of β-catenin activation *in vivo*

In collaboration with Cristina Lo Celso, I investigated what genes were activated in response to β-catenin. We designed an experiment in which we treated triplicates 6 week-old female K14ΔNβ-cateninER mice and transgene negative littermates daily with a dose of 1mg 4OHT for 0, 1 and 7 days. This age was chosen to ensure that the hair follicles were in the resting phase of the hair cycle at the beginning of the experiment.

As it can be seen from the H&E staining of sections, dorsal skin from wild-type mice at all three time points remained in telogen (Figure 5.1 A-C). In contrast, D2 mice had entered anagen phase after 7 days of treatment (Figure 5.1 F).

In order to evaluate changes in gene expression after β-catenin activation, we chose Affymetrix chip technology so that we could analyse more than18000 transcripts, representing over 14000 established mouse genes.

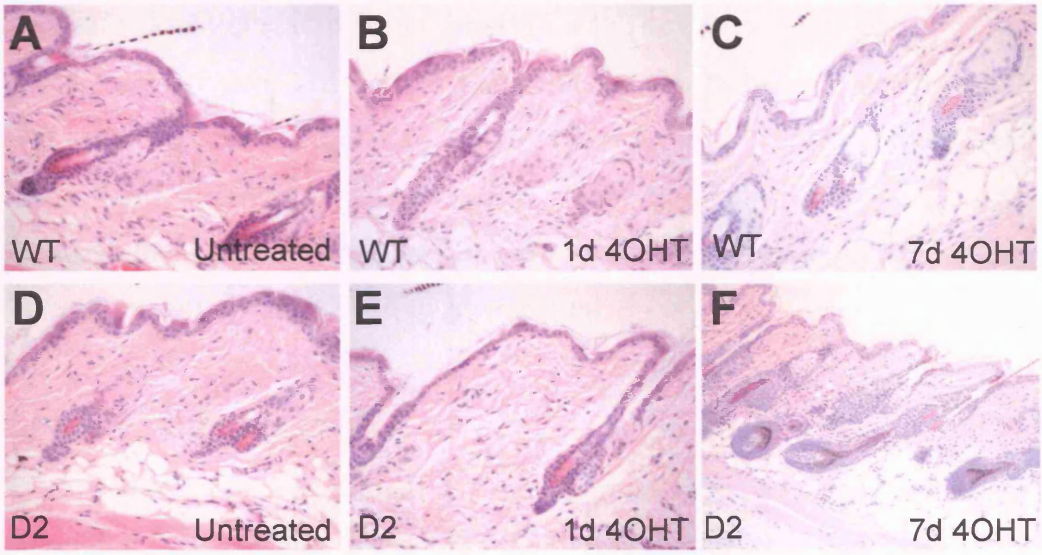

Figure 5.1- Profiling the response to β-catenin activation in dorsal skin in vivo. (A-F) Haematoxylin & Eosin stained sections of WT (A-C) and (D-F) D2 transgenic dorsal epidermis treated with 4OHT for 0, 1 or 7 days and then harvested immediately for RNA extraction.

5.2-Microarray analysis of the β-catenin signature

We isolated RNA from whole dorsal skin of the mice and the Gene Chip facility (Paterson Institute, Manchester, UK) performed the hybridisation of the microarrays.

The raw chip data were normalised and analysed with Genespring microarray analysis software. In our first analysis, 4OHT treated transgenics were compared with wild-type or untreated transgenic littermates. The graphs shown in Figure 5.2 A represent the total number of genes for transgenic (Tg) and wild-type (Wt) that were statistically called 'present'. In Figure 5.2 B are shown the genes that were upregulated and downregulated by at least 3-fold. The majority of genes were modulated at 7 days (Figure 5.1 C,F). A few genes appear to be modulated by 4-OHT in Wt samples, and we did not consider these genes in further. Obviously genes upregulated or downregulated only at 7 days may not be direct transcriptional targets. However, a lag in expression may also reflect time for 4OHT to penetrate and for activation to be maximal.

5.2.1- Genes 3-fold upregulated

We first normalised the data to identify changes in relative expression levels of at least 3 fold with a t-test p-value of less than 0.05. These parameters identified that after 7 days of 4OHT treatment, 150 probe sets were up regulated >3 fold and 13 probe sets down regulated 3 fold. Of these, 103 unique and established genes were up regulated and only 9 established genes downregulated after 7 days treatment. The full list is shown in the Appendix and a list of selected genes is shown in Table 5.1. The genes were classified into distinct functional groups (see pie chart in Figure 5.3).

29.1% of upregulated genes were involved in signalling or transcription, while 15 % were involved in cellular metabolism and 14% were keratins. The gene that was (2226 fold) most up-regulated was a Riken Clone (NM_133730) that corresponds to the Keratin 25 gene (K25irs1). Interestingly, K25irs1is expressed in the Henle layer, the Huxley layer, in the IRS cuticle and also present in the hair medulla. Its expression extends from the bulb region up to the points of terminal differentiation of the three layers (Langbein et al., 2006).

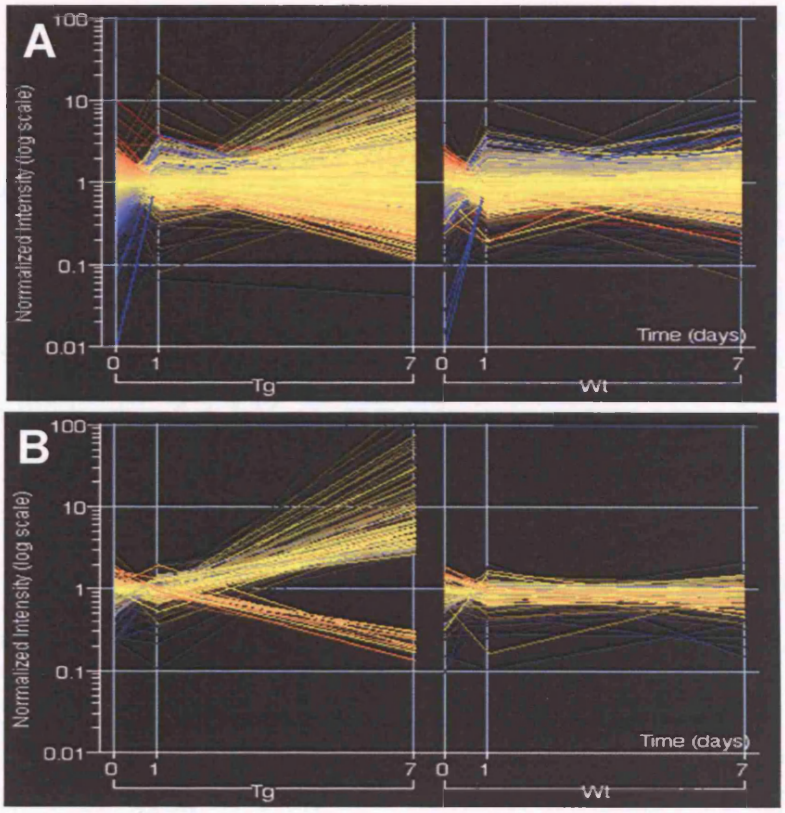

Figure 5.2.- Normalisation and filtering of the array data with the Genespring software. (A) The array data was quality controlled and normalised and the relative intensity of each probe statistically defined as 'present' are plotted in the graph. (B) Advanced filtering was applied to the data set by 3-fold upregulation. The relative intensity of genes falling in this category is plotted in the graph.

The list of upregulated genes included known targets of β-catenin or markers of hair follicle differentiation. Examples are Lef1 (upregulated 4 fold) and Cyclin D1 (upregulated 6.28) (Tetsu and McCormick, 1999; Shtutman et al., 1999). Keratin 17 was upregulated almost two fold and CDP 6.3 fold (see Figure 4.5 and 5.4 A-B). In addition to K25irs1, several other hair keratins were increased more than 20 fold at 7 days of activation (see Table 5.1). In the signalling category, several pathways were upregulated such as Wnt, Sox, Ephrin, Hedgehog, Bmp, (Figures 5.3 and 5.4 and Table 5.1).

Some of the genes showing the strongest induction were members of the Hedgehog signalling cascade, with Shh being induced. Increased expression of Shh and Ptc has already been observed when β-catenin is activated in the epidermis (Gat et al., 1998; Lo Celso et al., 2004). In wild-type tail epidermis Gli1 and Gli2 are mainly expressed in the cytoplasm of cells in the permanent portion of the HF and IFE (Figure 5.4 E,H). In response to β-catenin activation there was de novo expression in the SG, and relocalisation of Gli1 and Gli2 from the cytoplasm to the nucleus in the SG and IFE (Figure 5.4 F,G,I). Although c-Myc is reported to be a target of β-catenin in other tissues (He, 1998), c-Myc levels were not changed after 7 days of treatment, but only appeared to increase at 14 days (Figure 5.4 J-K). However, N-Myc, a target of Shh (Oliver et al., 2003; Kenney et al., 2004) was upregulated 8 fold at 7 days and continued to be highly expressed at 14 days (Table 5.1; Figure 5.4 L,M).

Amongst the transcription factors upregulated on the array were members of the SRY-related HMG box (Sox) family (Table 5.1), encoding transcription factors that can act both as activators and repressors (Wilson and Koopman, 2002). Sox 4 and 5 were upregulated more than 3 fold, while Sox 6, 8, 13, 18 and 21 were increased 1.5 to 3 fold. I confirmed the increased expression of Sox 4 using a specific antibody to label epidermal whole mounts (Figure 5.4 N,O). In wild-type epidermis Sox4 was detectable at low levels in the cytoplasm of hair matrix cells and ORS (Figure 5.4 N). Sox 4 was induced exclusively in the IRS and in de novo follicles in response to β-catenin (Figure 5.4 O).

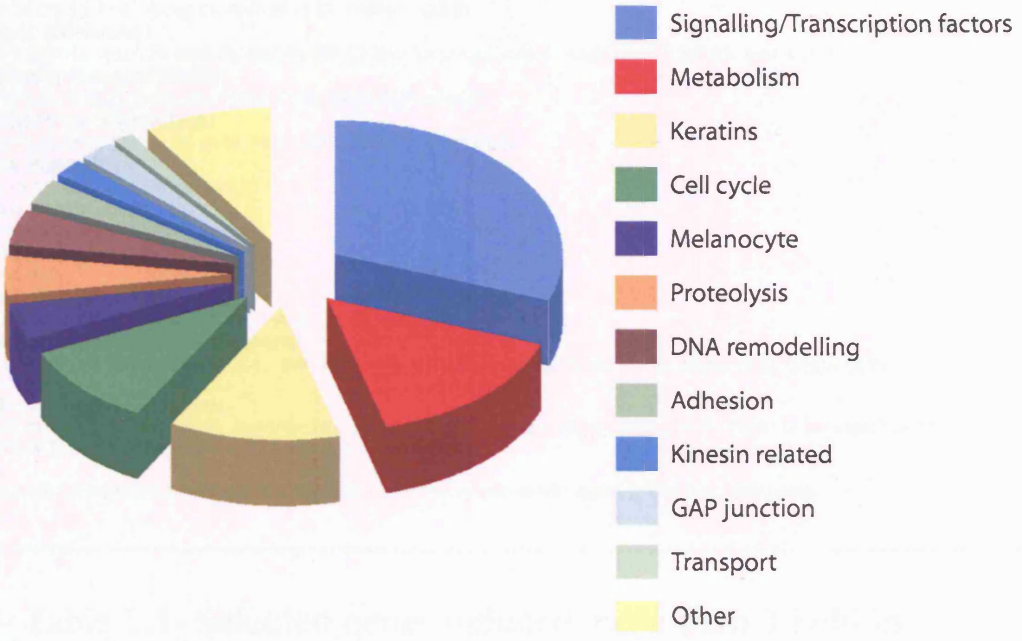

Figure 5.3.- Gene categories after normalisation and 3-fold filtering of the array data with the Gene Spring software. Array data was quality controlled and normalised. Advanced filtering was applied to the data set by 3-fold upregulation. The list of genes was divided into functional categories indicated by color coding.

Hair Keratins:
Krt1-24 (75.5), Krt2-10 (44.5), Krt2-19 (5.6), Krt2-ps1 (22.0)
Other Keratins:
Krt1-4 (237.4), Krt1-c29 (193.8), Krt2-6g (80.1), Krt2-18 (74.1), Krt1-1 (41.5), Krt1-3 (37.2), Krt1-5 (3.8)
Melanin Biosynthesis:
Tyr (16.5), Si (9.7), Dct (7.6), Tyrp1 (11.0), Edn3 (3.9), p (4.4)
Hedgehog Signaling:
Shh (70.6), Hhip (27.4), Gli (8.6), Ptch2 (6.6), Gli2 (3.8),Ptch (8.1)
Wnt Signaling:
Lef1 (5.8), Wif1 (5.4), Csnk1e (3.6)
Bmp Signaling:
Bambi (6.5), Bmp7 (3.8)
Ephrin Signaling:
Ephb1 (3.8)
Transcription Factors:
Dlx1 (27.1), Dlx2 (5.7), Dlx3 (4.8), Hoxc13 (4.1), Msx2 (8.5), Msx1 (3.7)
Other Transcription Factors:
Sox4 (41.2), Sox5 (9.0) Nmyc1 (8.4), CDP (6.3), Myb (3.7), Etv4 (11.6), Tcfe2a (12.8), Bach2 (3.3), Bcl11a (3.7), Sp6 (3.9)
Cell Cycle Regulators:
Cyclin B1 (8.6), Cyclin B2 (5.7), Cyclin D1 (5.0), Cyclin D2 (3.9), Cdc25c (22.4), Mllt1 (22.7), Gsg2 (14.2), Brca1 (10.1), Tubb3 (8.2), Np95 (8.0), Bub1b (6.8), Mns1 (5.2), Mki67 (4.9)

*Values in parenthesis are average fold induction relative to untreated transgenic or wild type littermates.

Table 5.1- Selected genes induced more than 3 Fold in ΔNβ-cateninER transgenic mice following 7 day 4OHT

5.2.2- Genes 2-fold upregulated

The analysis of genes regulated ± 3 fold was published (Silva-Vargas et al., 2005). However, we now know that changes of less than 3 fold can be highly significant biologically (i.e. Jones and Watt, 1993). Therefore, I decided to repeat my analysis by lowering the stringency of the filtering to 2 fold induction and lower p-value and additional genes were revealed (see Table 5.2). These included keratin and keratin-associated genes such as the hair specific keratins Keratin 19 (5.9 fold), mK6irs (90.5 fold). Additional Wnt family members to Lef 1 and Wif1 appeared: additional receptors like Ror2 (4.4) (Mikels and Nusse, 2006), inhibitors Dkk4 (2.9) Dkk1 (2), Sfrp1 (2.29) and canonical and non-canonical ligands Wnt5a (2.4), Wnt7b (2.3), Wnt10b (2.2), Fzd10 (2.1), Wnt6 (2.1), Wnt5b (3.2), Wnt7a (3.2). Dvl2, a pivotal downstream effector of the Wnt pathway was also up-regulated (3.8).

Members of genes involved in patterning during development such as the FGF, Bmp, Semaphorin, EGFR and Eph/ephrin family were also present in this list. Examples are Hgf (2.3), Ret (2.3), Fgf5 (2.4 Fgfr3 (3), Bmp8a (21.3), Edar (11.1), Eda (2.06), Hes5 (8.6), Hes2 (2.8), Jag1 (2.2), Sema7a (5), Nrp2 (3.3), Sema3a (2), Ephb1 (3.8), EphA1 (3), EphB3 (2.4), Efnb1 (2.3), EphA4 (2.7), EphA3 (2.3), Efnb2 (2.2) (See Table 5.2). A selected list of additional transcription factors, such as Pax6 (2.6), Barx2 (2.6), Olig3 (2.6), Gata5 (2.2), Runx2 (2) and Basonuclin (2.6) are also shown in the Table. Basonuclin is a zinc-finger protein, found in stratified squamous epithelia and hair follicles (Weiner and Green, 1998) that is involved in the transcription of ribosomal RNA genes (Tian et al., 2001). Basonuclin seems to regulate the maintenance of proliferative capacity and prevention of terminal differentiation in keratinocytes (Tseng and Green, 1994).

It is very important to note that two candidate genes involved in asymmetric division were present in the list: Msi2h, Musashi, (3.4), Piwil2 (2.4). Musashi protein is an RNA-binding protein associated with maintenance and/or asymmetric cell division of progenitor cells. Recent studies suggest that Musashi functions not only in the asymmetric division of early progenitor cells but also in the differentiation of IRS cells during HF development and hair cycle progression (Sugiyama-Nakagiri et al., 2006). Piwil2 is a member of the argonaute family. Family members are defined by conserved PAZ and Piwi domains and play

Cytoskeleton
Trio (9.94), Dvl2 (3.8), Grip1 (2.63), Rac3 (2.49), Wasf1 (2.45), Arhgap13 (2.75), Krt2-17 (2.8), Tiam2 (2.1), Rhpn2 (2.08), Racgap1 (3.37), Rhobtb3 (3.24)

BMP/TGFβ signalling
Bmp8a (21.3), Edar (11.1), Tgfb3 (2.6), Eda (2.06), Smad7 (2.48), Bmpr1b (2.15), Tgfb1i4 (2.08), Edaradd (2.1), Ect2 (3.49)

Notch signalling
Hes5 (8.614), Hes2 (2.823), Hey2 (2.54), Jag1 (2.163)

Semaphorin signalling
Sema7a (4.996), Nrp2 (3.24), Sema3a (2.002), Pxn (2.521)

Wnt signalling
Ror2 (4.365), Wnt5b (3.219), Wnt7a (3.176), Dkk4 (2.867), Wnt5a (2.376), Wnt7b (2.291), Wnt10b (2.2), Fzd10 (2.056), Wnt6 (2.057), Dkk1 (2.032), Sfrp1 (2.201)

Eph/ephrin signalling
Ephb1 (3.785), EphA1 (3.008), Ephb3 (2.402), Efnb1 (2.304), Epha4 (2.672), Epha3 (2.273), Efnb2 (2.158)

Transcription factors
Sox5 (5.237), Sox3 (5.222), Sox13 (2.436), Sox18 (2.549), Pax6 (2.57), Barx2 (2.552), Olig3 (2.529), Gata5 (2.119), Runx2 (2.019),
Runx3 (1.98), Slit2 (2.71), Foxm1 (3.209), Vdr (3.08), Foxn1 (2.11), Rxra (2.144), Nfkb1 (2.143), Lmyc1 (2.092), Lhx5 (2.754), Lhx2 (1.855), Tcf7l2 (1.6530, Irx2 (3.47), Irx4 (2.85)

RNA/DNA processing
Msi2h (3.371), Piwil2 (2.385), Bnc (2.516). Tert (2.712), Hmgb2 (2.509)

ECM/Adhesion remodeling
Itgb1 (4.325), Tnc (3.335), Lamr1 (3.232), Mmp14 (3.191), Adam15 (2.898), Adam34 (3.199), Itgb6 (2.59), Lamb1-1 (2.575), Tnn (2.385), Fn1 (2.309), Mmp19 (2.653), Cldn13 (3.16), Cldn9 (2.462), Cldn10 (2.334), P-cadherin (4.19), K-cadherin (2.9), Hmmr (3.1)

Other signalling
Casp9 (2.78), Spry4 (4.049), Madh6 (2.989), Bcl2 (2.07), Tle3 (3.197), Fgfr3 (2.982), Edil3 (2.998), Hgf (2.272), Ret (2.302), Fgf5 (2.418), Cckar (2.758), Ptgds (2.701), Dgkb (2.865), Diap3 (2.848), Areg (2.756), Plcz1(2.07), Drd4 (2.08)
Gpr2 (2.402), Gpr37 (2.563), Gpc3 (2.462), Dnm2 (2.466), Gsdm (2.005), En2 (2), Lrp8 (2.462), Ngfa (2.248), Egfr (2.167), Ctsb (2.042), IKK-beta (3.211)

*Values in parenthesis are average fold induction relative to untreated transgenic or wild type littermates.

Table 5.2- Selected genes induced more than 2 Fold in ΔNβ-cateninER transgenic mice following 7day 4OHT treatment.

important roles in stem-cell self-renewal, RNA silencing and translational regulation in various organisms (Lee et al., 2006b). Piwi has recently been shown to be a nuclear protein involved in gene silencing of retrotransposons and controlling their mobilization (Saito et al., 2006). In addition, Piwi proteins interact with small RNAs, constituting a new family of regulatory molecules with diverse functions in eukaryotes (Cheng et al., 2005).

Interestingly, in addition to activating expression of genes involved in proliferation and hair differentiation, β-catenin activation leads to changes in cell adhesion and ECM genes, leading to remodelling of the stem cell niche. For instance, the following genes are upregulated: Integrin β-1 (4.3), Tenascin C and N (3.3, 2.4), Lamininr1 (3.2), Mmp14 (3.2), Adam15 (2.9), Adam34 (3.2), Itgb6 (2.6), Lamb1-1 (2.6), Fn1 (2.3), Mmp19 (2.7) and Hmmr (3.1). β-catenin activation also leads to changes in expression of genes encoding cytoskeletal proteins, for example: Trio (10), Grip1 (2.7), Rac3 (2.5), Wasf1 (2.4), Arhgap13 (2.7), Krt2-17 (2.8), Tiam2 (2.1), Rhpn2 (2), Racgap1 (3.4) and Rhobtb3 (3.2).
From the genes that are upregulated at least two fold in the arrays it becomes clear that at early stages of hair follicle development changes in proliferation and early hair differentiation are accompanied by cytoskeletal rearrangements, changes in adhesion and ECM. This suggests that changes in the nature of the stem cell niche allow hair morphogenesis to take place in adult epidermis.

5.2.3-Dissecting the β-catenin program by looking at genes associated with distinct hair follicle cell populations

Although proliferation is one of the hallmarks of cells in the HF matrix (see Figure 1.4) they also express a number of signalling proteins and transcription factors that specify each of the six programs of differentiation in the IRS and HS. Recently, the molecular signature of several cell populations resident in the bulb has been elucidated. Rendl and colleagues have combined multicolour tagging with cell specific promoters and surface marker labelling to distinguish between ORS, matrix, dermal fibroblasts, dermal papilla and melanocytes. I reclassified our 3-fold gene list into categories representing these hair follicle populations (Table

3-Fold Analysis Hair Follicle Populations

Gene name	Matrix	ORS	DF	DP	Mc
Keratin associated Krtap8-1 (64.8), Krtap9-1 (16.7), Krtap12-1 (8.9), Krtap5-1 (4.6 **Hair keratins** Krt1-24 (76.2), Krt2-10 (64.9), Krt2-ps1 (25.0), Krt2-19 (6.4) **Other keratins** Krt1-4 (46.4), Krt1-3 (42.8), Krt1-5 (3.9)	Krt1-4, Krt1-c29, Krt1-3, Krt1-5, Krt1-24, Krt2-19	Krt1-4, Krt2-19	Krt2-19	Krt1-4	
Melanocyte biosynthesis Tyr (16.9), Tyrp1 (10.1), Si (9.5), Dct (7.4), P (4.4)			Tyrp1, Si , Dct	Tyr, Tyrp1, Si, Dct	Tyr , Tyrp1, Si , Dct
Hedgehog Gli (8.4), Hhip (6.8), Ptch2 (6.6), Shh (4.8), Gli2 (3.6) **Wnt** Wif1(5.4), Lef1 (4.0) **BMP** Bambi (6.4), Bmp7 (3.8) **Homeobox genes** Msx2 (8.5), Dlx2(5.4), Dlx3 (4.8), Hoxc13 (4.0), Msx1 (3.5)	Dlx2. Msx2, Dlx3, Hoxc13 Wif1 Bambi, Bmp7	Dlx2, Msx2, Dlx3, Hoxc13 Bmp7	Dlx2 Hhip Wif1	Msx2 Hhip Wif1 Bambi, Bmp7	
Transcription factors Sox4 (33.0), NMyc1 (8.3), Sox5 (7.2), CDP (6.3), Tcfeaa (7.9), Sp6 (3.9`), Bcl11a (3.8), Myb (3.7), Bach2 (3.3)	Sox4, NMyc1, Sox5, CDP, Tcfeaa, Sp6, Bcl11a, Myb, Bach2	Sox4, NMyc1, Sox5, CDP, Tcfeaa, Bcl11a,	Sox4, NMyc1, Tcfeaa	Tcfeaa, Bach2	Sox5, Bcl11a
Cell cycle regulation CyclinB1 (8.6), CyclinB2 (5.7), CyclinD1 (5.0), CyclinD2 (3.8), Tubb3 (8.6), Np95 (7.1), Mns1 (5.1), Mki67 (4.9)	CyclinB1, CyclinB2, CyclinD1, CyclinD2, Tubb3, Mns1, Mki67	CyclinB1, CyclinB2, CyclinD1, CyclinD2, Mns1 Mki67	CyclinD2, Mns1	Tubb3	Tubb3
Receptors Gprc5d (82.1), Cxcr4 (6.9), Cntfr (4.1)	Gprc5d	Gprc5d Cxcr4	Cxcr4	Gprc5d Cxcr4	
Kinase activity Melk (8.5)	Melk	Melk	Melk		
Other signalling Fbn2 (27.0) Racgap1 (4.7) Basp1 (3.8) Uhrf1	Racgap1 Uhrf1	Racgap1, Basp1 , Uhrf	Fbn2, Racgap1, Uhrf1	Fbn2, Basp1	Basp1
Kinesin-related Kif2c (7.7), Kif22-ps (7.4), Kif11 (5.0)	Kif2c , Kif11	Kif2c, Kif11	Kif11		
Adhesion Col11a1 (11.2), Hmmr (5.0), Alcam (3.6), Ncam1 (3.4)	Hmmr, Alcam	Ncam1, Hmmr, Alcam	Ncam1, Col11a1, Hmmr	Ncam1, Col11a1	Ncam1, Col11a11,Hmmr
Proteolysis Ctse 12.1, Lrp4 (5.8), Lap3 (4.5), Capn8 (3.2)	Ctse, Lrp4, Lap3	Ctse, Lap3	Ctse	Lrp4	
Vesicle transport Syt4 (44.8), Vti1b (7.5)	Vti1b		Syt4	Syt4	Syt4 , Vti1b
Gap junction Gjb2 (29.9), Gjb6 (23.9), Gja1 (4.3)					
DNA/Chromosome Xrcc1 (24.3), Hist1h2ae (17.7), Rad51ap1 (17.3), Hcapg (5.6), Smc4l1 (5.3), Top2a (4.8)	Rad51ap1, Xrcc1	Rad51ap1, Xrcc1	Rad51ap1		
Metabolic Gnmt (179.3), S100a3 (48.4), Padi3 (32.2), Fbp1 (18.6), Alp6v1b1 (17.6), Hsd11b2 (16.8), Padi1 (14.7), Upp (11.9), Ggl1 (8.6), Trpm1 (7.7), Has3 (6.3), Fads2 (4.9), Slc16a7 (4.8), Arg2 (4.7), Bdh (3.4), Alox15b (3.1)					Trpm1
Others Cryba4 (170.2), Crym (29.7), Ly6g6d (16.1), Spag5 (13.4), Edr (11.9), Rex3 (4.8), Pcg (4.5)	Pcg, Rex3	Pcg, Rex3	Pcg		Rex3
Downregulated Cyp2e1 (0.07), Cck (0.13), Mpz (0.13), Asb14 (0.13), Lep (0.17), Dscr1l1 (0.19), Mal (0.20), Tm4sf3 (0.20), Mbp (0.24)		Cyp2e1	Cyp2e1, Cck, Mpz, Asb14, Lep, Mal, Dscr1l1, Mbp	Cyp2e1, Mal, Dscr1l1,Mbp	Cck, Asb14, Lep

Table 5.3- Selected genes induced more than 3 Fold in ΔNβ-cateninER transgenic mice following 7day 4OHT treatment. These genes were re-classified into HF populations defined in Rendl, et al.2005. These genes are in red letters when their highest expression in the compartment or in black letters when they are simply expressed in wild-type skin.

5.3) to see what hair populations were expanded by β-catenin activation. It is striking that all the genes downregulated at 7 days lie into the dermal fibroblast category. Interestingly genes with highest expression in the DP such as Wif1, Hhip, Bambi, are inhibitors of Wnt, Shh and BMP. Apart from proliferation genes, most of the genes that lie in the matrix category are homeobox genes and keratins, together with Gpr5d, N-Myc, CDP and Bach2. The ORS signature is also highly upregulated, for instance Sox4, Bcl11a, Myb, CDP, Bach2, Melk and RacGap1 genes. Interestingly, most of the genes in my list fall into one of the categories defined by Rendl et al. This suggests that β-catenin activation promotes proliferation and differentiation of bulb cell lineages, where normally the pathway is active during the anagen phase.

5.2.4-Comparison between the profile of bulge cells after β-catenin activation and the profile of the hair germ during development

Some of the targets from our array matched genes isolated in a study profiling the bulge compartment after β-catenin activation. Sox4 is an intriguing example. Lowry and co-workers show that it is a protein that is specifically up-regulated in the SC niche during the follicle growth phase and also expressed in proliferating TA progeny (Lowry et al., 2005). In addition, Sox4 has been pinpointed as a putative marker of intestinal stem cells, although this has not yet been demonstrated. These findings further validate our array data and put Sox4 as a candidate for TA amplification and the transition to terminal differentiation. Further studies will give insights into the emerging roles of member of the HMG box superfamily of transcription factors in skin and hair biology.

It has been suggested that Wnt signalling has sequential roles temporally regulating the follicle SC lineage. Firstly, β-catenin stabilisation promotes SC maintenance (Zhu and Watt, 1999; Lowry et al., 2005). Then, it promotes activation and proliferation (Lowry et al., 2005). Lastly, a more sustained Wnt signal promotes the transition from proliferation to differentiation (Gat et al., 1998; DasGupta and Fuchs, 1999; Huelsken et al., 2001; Merrill et al., 2001; Millar, 2002; Braun et al., 2003).

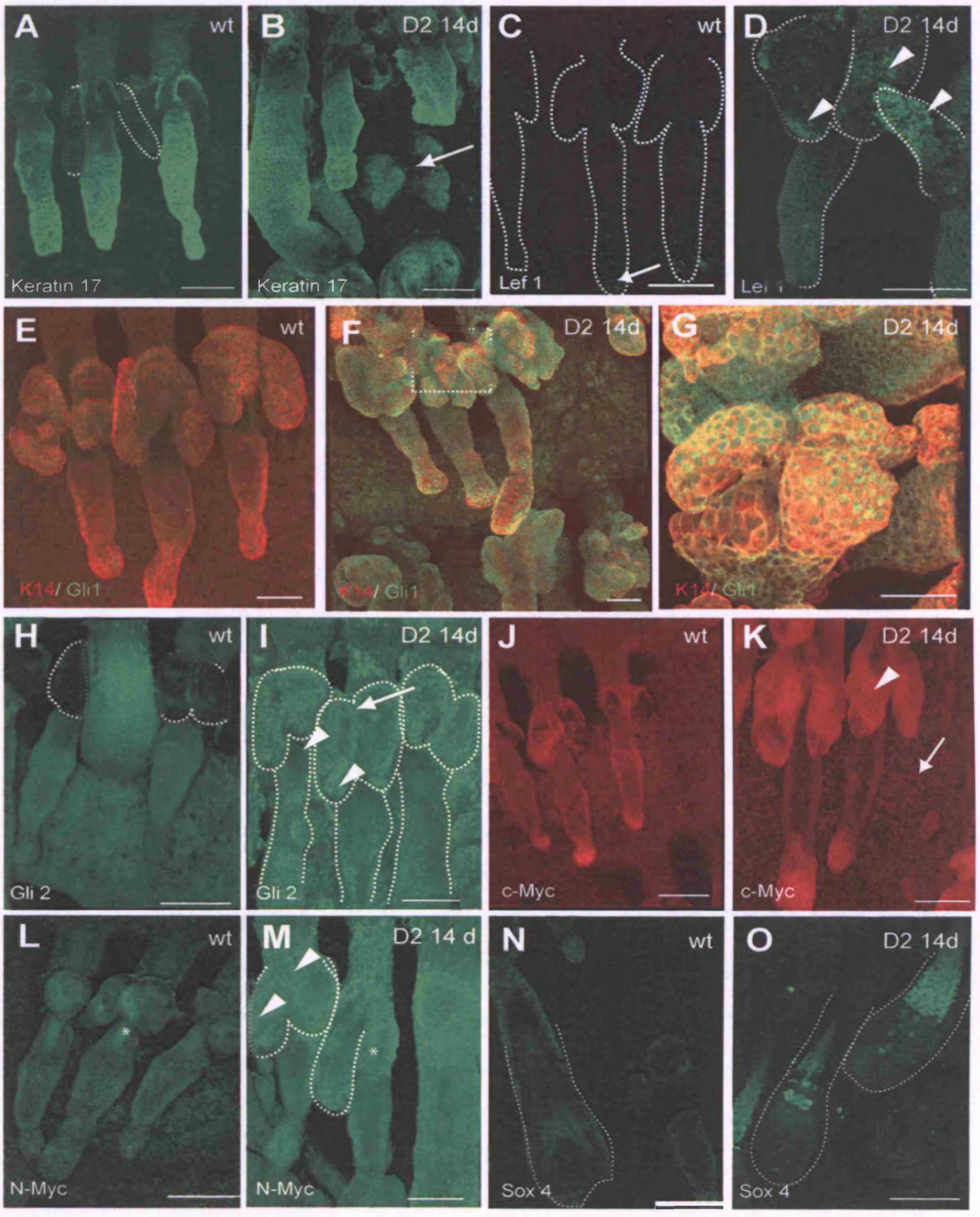

Figure 5.4- Validation of β-catenin target genes. Tail whole mounts from untreated wild-type (wt) or D2 transgenic mice were treated with a medium dose of 4OHT for the number of days shown and were labeled with antibodies to the proteins shown. Arrows and arrowheads indicate ectopic HF outgrowths in IFE and SG, respectively. G is an enlargement of the box in F. Dashed lines demarcate SG in A,H,M; HF with SG in C,D and I and ORS in N,O. Scale bars: 100 μm.

Recently a new approach to isolating and profiling hair germs during skin development has yield the signature of the hair germ population (Rhee et al., 2006). Interestingly, many of the genes highly upregulated in the hair germ are also highly upregulated in our array at 1 or 7 days. These include Wif1, Hhip1, Shh, Syt4, N-Myc, Eda, Bach2, Neuropilin2, Foxc1, Runx2, Runx1, Glypican3, Dkk4, Nfat, Sema3b, Basonuclin, Wnt5a, Fras1, VDR, Tcf7, Zfp365, RasGef13, Ltbp1 and Ncam. It will be of great interest to investigate some of these genes further as they are likely to be involved in the early stages of hair morphogenesis.

5.2.5-Genes upregulated more than 2-fold at 1 day

Whereas there were very few changes in 3-fold genes at day 1, when I looked at the profile of genes upregulated 2-fold at 1 day I could see that a whole of battery of transcription factors are upregulated (See Table 5.4). A few that were upregulated at 1 day also remained upregulated at 7 days including Bach2, Sox5, Runx1, Phox2b, Zfp346 3.277 and Foxp1. At 1 day, there also seems to be some rearrangements of ECM and adhesion with changes seen in several metalloproteinases, Adams, collagens, Fras1 and integrin β1. At 1 day there are also changes in cytoskeletal genes such as alpha-catenin, kaiso and Rock1. At this early time point changes are seen in Wnt ligands and receptors like Lrp6, Rorα2 and Wnt7b, Wnt9b, Wnt9a and intermediate members like Casein kinase-b and Apc. The Hedgehog pathway is also active at this stage with Shh, NMyc and Hhip upregulated. Members of the BMP and Semaphorin pathways and several Hes genes downstream of the Notch pathway are also upregulated (see Table 5.4). Interestingly, both RNA remodelling genes Piwi and Musashi are upregulated at day1 (see Table 5.4). It will be of great interest to investigate some of these genes further as they are likely to be very important in setting up the morphogenetic programme to make a hair.

The analyses I have presented in this Chapter are 'backwards', starting with the most stringent lists of genes modulated at 7 days by 3-fold and comparing it with a set of genes modulated by 2-fold. These filtering settings have allowed me to unveil a set of genes whose expression is modulated at 1day.

Transcription factors
Phox2b (10.650, Dlgh (8.831), Pou4f3 7.71, Foxa17.433, Zfp96 5.49, Mixl1 4.566, Nkx2-6 4.535, Nr2e14.028, Hoxa43.988, Barhl13.593, Pou6f13.503, Bach23.437, Hoxa103.419, Zfp346 3.277, Foxp1 2.7, Hoxd1 2.571, Runx1 2.424, Tbx5 2.38, Sox30 2.329, Pou2f2 2.249, Trim25 2.226, Hmx3 2.175, Myf5 2.132, Sox10 2.1, Sox5 2.027

ECM/Adhesion remodeling
Cldn 18 6.036, Timp2 5.306, Adam 7 5.19, Pcdhb4 4.827, Myo10 4.325, FGF22 4.14Col9a3 4.321, Col24a1 4.092, Col5a32.873, Hmmr2.85, Col19a1 2.637, Fras1 2.487, Adam26 2.486, Trygn16 2.367, Itgb1 2.231, Ncam2 2.143, Gpc6 2.121 Col9a3 2.119, Ela3b 2.103, Adam34 2.085, Timp2 2.045

Wnt Signalling
Lrp6 3.827, Rora2.717, Klf12 2.6, Csnb 2.471, Apc 2.404, Wnt7b 2.301, Wnt9b 2.283, Wnt9a 2.106

Notch Signalling
Hes 5 6.81, Hes3 2.393, Hes2 2.383, Hes7 2.105, Notch2 2.066

DNA/RNA remodeling
Hmgn1 5.779, Hdac10 4.846, Nup210 4.046, Mnt(max binding repressor) 3.07, Piwil1 2.629, Msi2h 2.382, Hist1h4h 2.334, Smarcb1 2.29

Semaphorin signaling
Sema6b3.587, Sema5a 3.49, Sema3b 2.501

BMP/TGFb signaling
Tgfb1i4 2.383, Tgfbr1 2.26, Bmpr1b 2.133, Bmp8a 2.039

Cytoskeleton
Alpha-catenin 1 3.101, Kaiso 3.015, Cdh82.719, Ctsf 2.524, Cdh3 2.263, Krt1-19 2.117, Rock1 2.077, Cldn7 2.044

Other signalling
Grpr 7.003, Srd 5a2 6.448, Fnbp2 6.181, Rassf1 6.076, edr 5.732, Tshb 5.49, Gpr22 5.416, Gys2 5.19, Syt4 4.848, Ccr3 4.191, Ifna13.988, Umod3.937, Nfatc2ip 3.816, Trpm5 3.745, Magea6 3.594, Usp15 3.461, Jak3 3.438, Nek13.431, Apom3.415, Tnfsf13b 3.398, Rdh7 3.347, Eps15-rs3.182, Spi113.138, Vil2.831, Lrp22.79, Lrp2bp-pending2.773, Ang42.765, Gfra12.734, Samhd12.733, Pdgfd2.722, Gpr63 2.646, Bcl7a 2.56, Ppp3r1 2.44, Il1r1 2.433, Bcl2l2 2.399, Fgf5 2.382, Ngfa 2.371, Camk2d 2.37, Pacsin1 2.346, Nr5a2 2.315, Trfr2 2.274, Rab27b 2.212 Tnfsf14 2.212, Ptch 2.196, Prkcn 2.194, Caspase-3, Igf2bp3 2.145, Pln 2.136, Cyp26a1 2.129, Igfbp5 2.125, Nrg3 2.091, Lrp4 2.08, Hhip 2.063, Igf2bp1 2.007

*Values in parenthesis are average fold induction relative to untreated transgenic or wild type littermates.

Table 5.4- Selected genes induced more than 2 Fold in ΔNβ-cateninER transgenic mice following 1 day 4OHT treatment.

Several profiling analysis of distinct HF cell populations have been published after I had analysed the array data. This prompted me to set out a further analysis of our array data and I went back to re-analyse my data and compare it with the signatures of several HF populations.

The arrays gave us important information about which pathways act downstream of β-catenin to promote ectopic HF formation. The laboratory has focused on three: Notch, Hedgehog and Eph/ephrin. Dr Estrach and Dr Ambler in the lab have focused on the Notch pathway while I have looked at the others.

5.3-Hedgehog drives proliferation during HF morphogenesis

It has been shown in previous studies that Shh is upregulated upon β-catenin activation (Gat et al., 1998; Van Mater et al., 2003 and Lo Celso et al., 2004). As shown in the previous section, in addition to Shh, several components of the Hedgehog signalling pathway were upregulated on β-catenin activation (See Table 5.1 and Figure 5.4). The activation of Hedgehog signalling was confirmed in tail skin by looking at Gli1 and Gli2 expression (Figure 5.4 E,H and 5.5 B-D). In order to monitor activation of the pathways we looked for nuclear localisation of Gli1 (Figure 5.5). Gli1 and 2 were nuclear at sites of ectopic hair follicles (Figure 5.4 G, I).

Given that β-catenin activation results in local increases in proliferation (see Figure 4.5 in Chapter 4) and that Shh drives proliferation during normal hair follicles anagen (Callahan and Oro, 2001) I investigated the role of the Hedgehog pathway downstream of β-catenin during ectopic hair follicle formation. For this, I designed an experiment in which I treated K14ΔNβ-catenin transgenic mice with the Hedgehog antagonist Cyclopamine at the same time as 1mg 4OHT (See experimental design in Figure 5.5). Cyclopamine is a pharmacological inhibitor that blocks Hedgehog signalling by binding to Smoothened (van den Brink et al., 2004). The dosage that we used in these experiments did not cause any phenotype in wild-type skin (Silva-Vargas et al., 2005). In order to validate that the drug was working, I used the whole-mount tail system to look at Gli1 localisation (Figure 5.5 B-D). As previously mentioned, in untreated epidermis Gli1 is mainly located in the cytoplasm of most cells and a

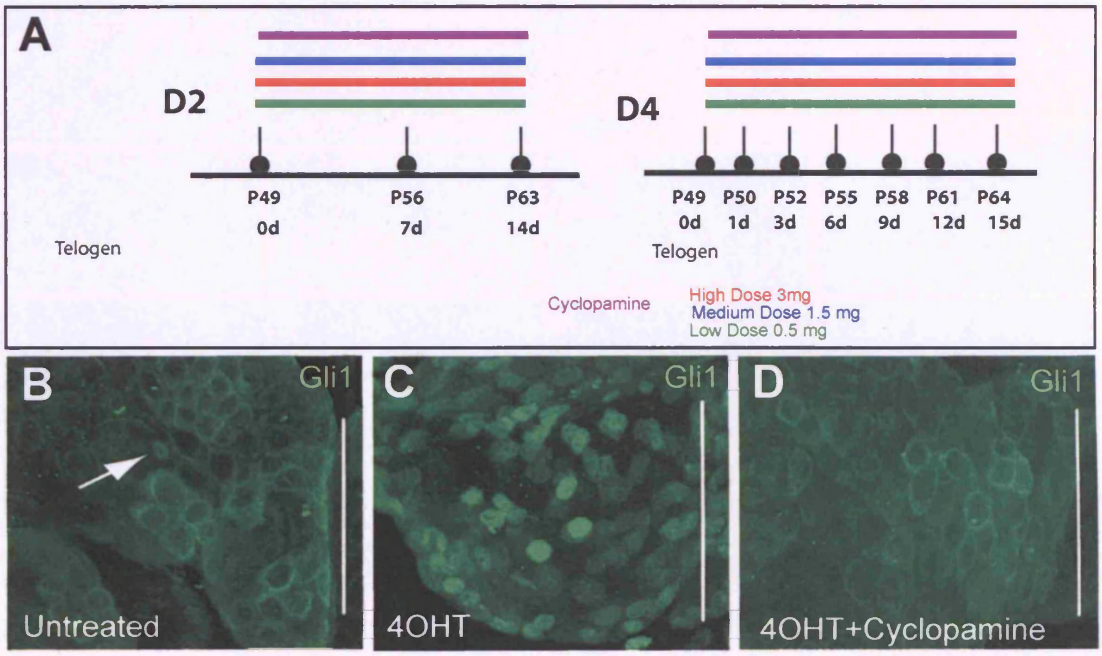

Figure 5.5- Cyclopamine blocks the Hedhehog pathway in tail epidermis. (A) Diagram shows the experimental design to look at the effects of blocking Shh pathway by Cyclopamine treatment in β-catenin induced ectopic hair follicle formation. **P** corresponds to postnatal day and **d** corresponds to the day of the experiment. D2 and D4 mice were either treated with 4OHT alone or with 4OHT and Cyclopamine for up to 2 weeks. (B-D) Tail whole mounts from D2 transgenic mouse were labelled with antibodies to Gli1. Arrow in B indicates Gli1 nuclear staining in untreated epidermis. The panels in B,C and D show a high magnification of SG. Scale bars: 50 μm.

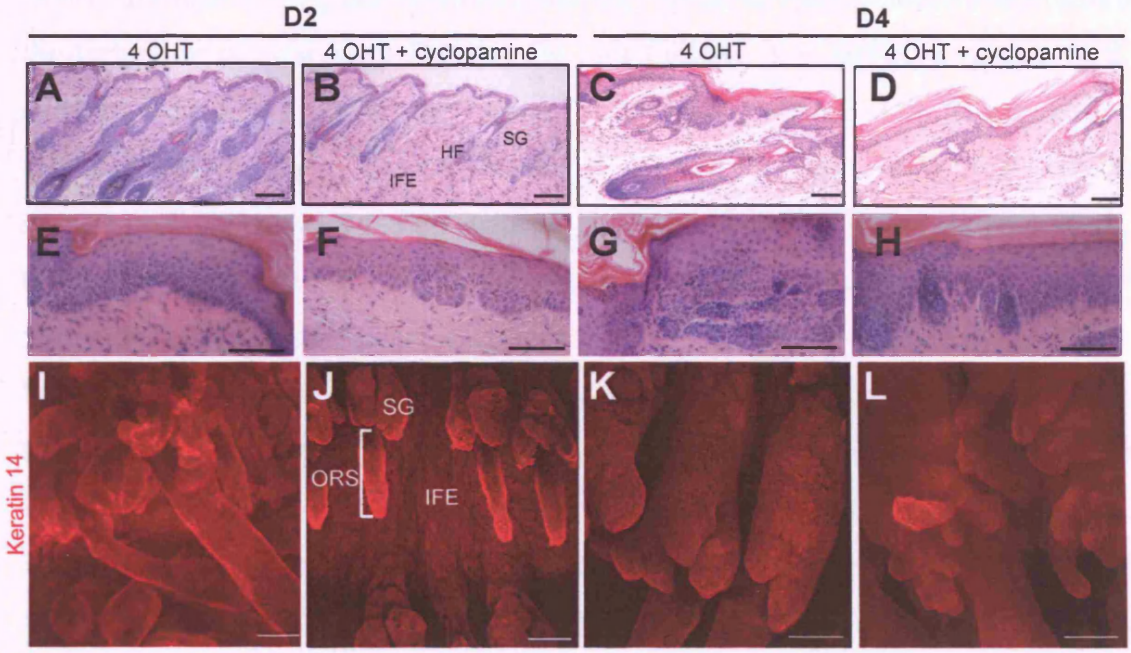

Figure 5.6- Hedgehog signalling is required for β-catenin-induced hair follicle formation. D2 and D4 mice were either treated with 4OHT alone or with 4OHT and cyclopamine for up to 2 weeks. Sections of dorsal (A,B) or tail (C-H) epidermis stained with hematoxylin and eosin. (I-L) Tail whole mounts were labelled with antibodies to keratin 14. Scale bars: 100 μm.

few cells in SG have nuclear Gli1(Figure 5.5 B), which it has been shown to be downstream of Ihh (Niemann et al., 2003). After 4OHT treatment there was a marked increase in the number of cells with Gli1 positive nuclei (Figure 5.5C), consistent with the location of Gli2 (Figure 5.4 I). However, when β-catenin was activated in the presence of Cyclopamine, Gli1 remained cytoplasmic (Figure 5.6 D), establishing that the conditions of Cyclopamine application were effective at inhibiting Hedgehog signalling.

Examination of skin by conventional histology showed that Cyclopamine blocked the induction of anagen in D2 and D4 hair follicles, the earliest response to β-catenin activation in K14ΔNβ-cateninER epidermis (Figure 5.6). Cyclopamine also reduced the appearance of ectopic HF (Figure 5.6 B,D). Interestingly, when we treated D2 and D4 skin with high levels of 4OHT for short periods, Cyclopamine reduced the thickness of hyperproliferative IFE in D2 and D4 and allowed the appearance of ectopic hair follicles (Figure 5.6 F-H).

I also analysed the effects of Cyclopamine by visualising whole mounts. The treatment with Cyclopamine could convert the D2 medium dose phenotype to wild type, blocking most new follicle formation in SG, HF and IFE (Figure 5.6 I-L). However, Cyclopamine did not revert completely the tumourigenic D4 phenotype, but instead it converted it to a morphogenic D2 phenotype (Figure 5.6 L). In Cyclopamine treated D4 epidermis the new follicles became more pronounced and dermal papilla formation was stimulated (Figure 5.6 H).

I confirmed the morphological observations by staining whole mounts with a range of antibodies. Keratin 17 expression induced by β-catenin in the IFE and SG (Figure 5.7 A) was largely inhibited and Keratin 17 expression was confined to the ORS (Figure 5.7 B), as in wild-type epidermis. Ectopic expression of CDP in D2 epidermis (Figure 5.7 E) was also inhibited by Cyclopamine (Figure 5.7 F). In D4 epidermis the size of the ectopic CDP patches was reduced (Figure 5.8 D).

I also looked at whether the effects of Cyclopamine correlated with a reduction of proliferation. When I evaluated Ki67 staining I could confirm that proliferation was decreased in Cyclopamine treated skin (Figure 5.7 C, D and 5.8 A,B).

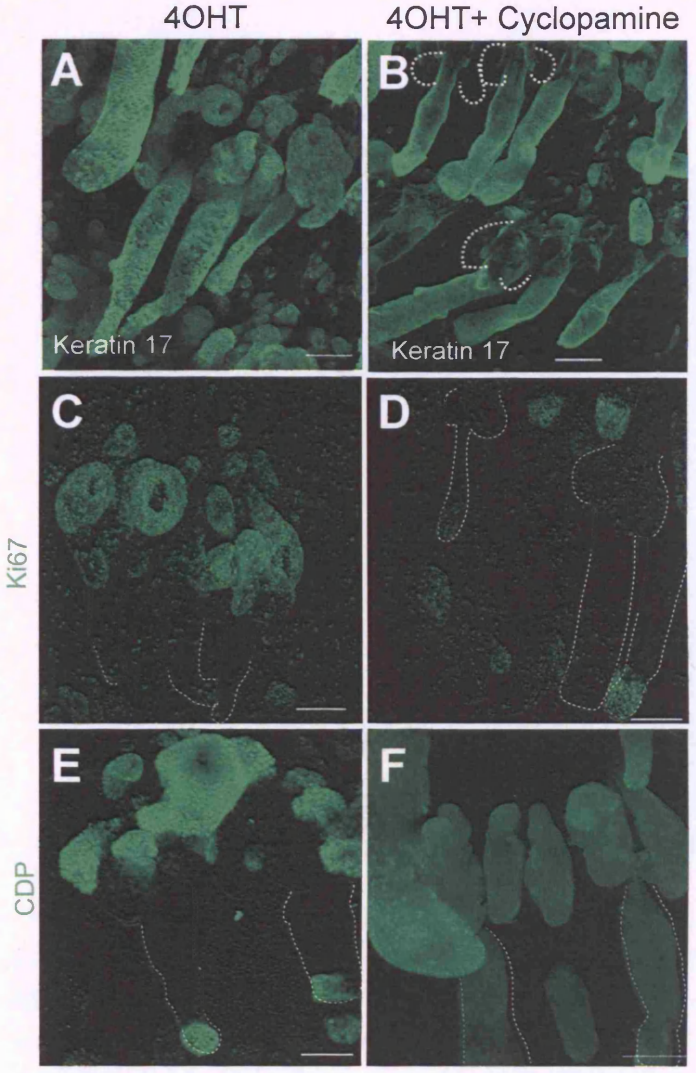

Figure 5.7- Hedgehog signalling is required for β-catenin induced hair follicle formation in the D2 line. D2 mice were either treated with 4OHT alone or with 4OHT and cyclopamine for up to 2 weeks. Tail whole mounts were labelled with antibodies to keratin 17 (A,B), Ki67 (C,D) or CDP (E,F). Dashed lines outline SG (B), ORS (C,E,F) or HF with SG (D). Scale bars: 100 μm.

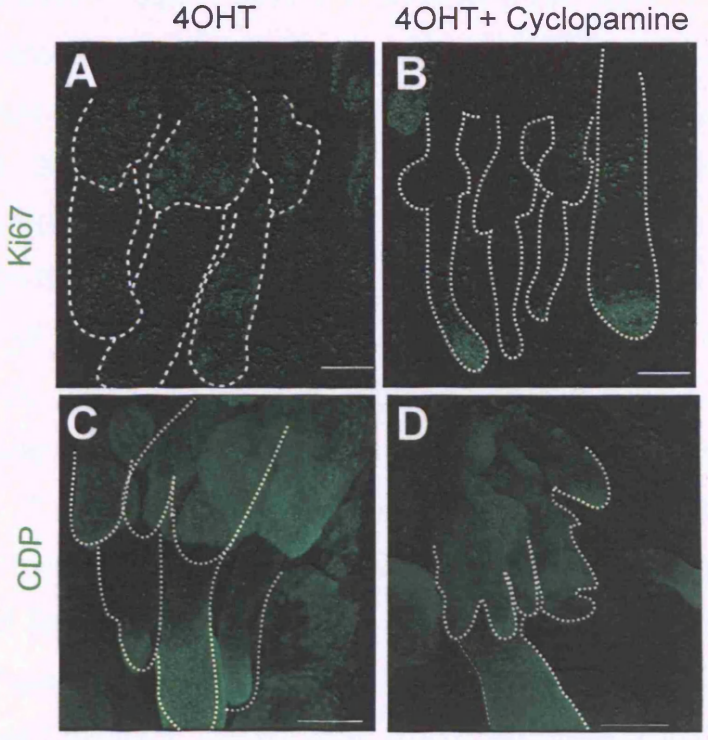

Figure 5.8- Blocking Hedgehog signalling reduces β–catenin induced proliferation and promotes hair follicle morphogenesis in the D4 line. D4 mice were either treated with 4OHT alone (A,C) or with 4OHT and cyclopamine for up to 2 weeks (B,D). Tail whole mounts were labelled with antibodies to Ki67 (A,B) or CDP (C,D). Dashed lines outline HF with SG (A-D). Scale bars: 100μm.

5.4- Eph/ephrin superfamily, candidates for positioning signals of ectopic hair follicles

Additional analysis of the β-catenin profile revealed that members of the family of Ephrin receptors (Ephs) and their membrane-bound ligands (Ephrins) are upregulated by β-catenin in skin. This family has been shown to act downstream of β-catenin in controlling stem cell maintenance, proliferation and niche architecture in several tissues including the intestinal epithelium (Batlle et al., 2002; Sancho et al., 2003). Several Ephs and Ephrins were upregulated between 1.5 and 3 fold on activation of β-catenin in the epidermis: EphB1 (3.8), EphA1 (3), ephrin-B2 (2), ephrin-B1 (2), EphA4 (2), EphB3 (2), EphA3 (2) and EphA7 (3).

I validated several of these genes by immunofluorescence staining of tail skin (Figure 5.9 A-F). The ligand ephrin-B1 is expressed predominantly in the hair matrix and the lower portion of the ORS in early and late anagen wild-type follicles (Figure 5.9 C). In response to β-catenin activation EphrinB1 was induced in the IFE and SG (Figure 5.9 D), coinciding with CDP expression (Figure 5.9 F). The upregulation of EphrinB1 correlated with increased expression of one of its receptors, EphB3 (Figure 5.9 B). In addition, EphA4, which is normally expressed in the bulge area (See Chapter 3; Tumbar et al., 2004), was upregulated in ectopic hair follicles (Figure 5.9 E). This is of interest because it has been shown that EphA4 is expressed in the feather placode together with Bmp7 and 8 and Follistatin (McKinnell et al., 2004a). In the next Chapter, I will discuss the role of Eph/ephrin signalling in patterning the mammalian epidermis.

5.5- Discussion

In this chapter I have described the β-catenin signature in whole skin. The signature list includes established and expected Wnt target genes, and it is characterised with proliferation-associated genes, signalling molecules and transcription factors involved in ORS, matrix and DP lineage determination. An important aspect is that components of signalling pathways include activators and

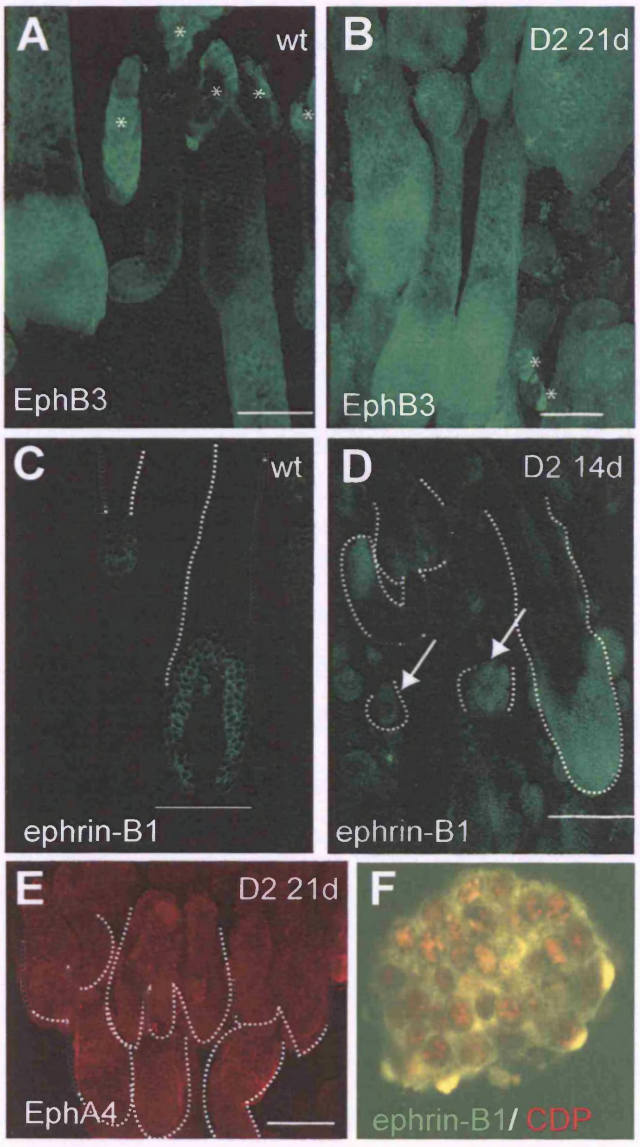

Figure 5.9- Eph/ephrin family is induced during ectopic hair follicle formation. Tail whole mounts from untreated wild-type (wt) or D2 transgenic mice treated with a medium dose of 4OHT for the number of days shown were labeled with antibodies to EphB3, ephrin-B1 and EphA4. Arrows in D indicate ectopic HF outgrowths in IFE . Asterisks in A indicate nonspecific staining of SG. Dashed lines demarcate ORS in C, HF with SG in D,E. Note that the ectopic follicle arising from the IFE shown in F is ephrin-B1 and CDP positive. Scale bars: 100 μm.

inhibitors providing a tight and controlled activation that allows the formation of ectopic HF to be formed. β-catenin signature also leads to changes in adhesion and ECM reflecting remodelling of the stem cell niche during this process. Finally, the array data have allowed me to identify what pathways are downstream of β-catenin during early phases of HF morphogenesis.

β-catenin activation leads to the induction of proliferation and hair differentiation

Our array data set was validated by the presence of known targets of β-catenin or markers of hair follicle differentiation in the list of upregulated genes. Examples are Lef1, Cyclin D1, Shh and several hair keratins previously reported in skin.

β-catenin activation selectively up-regulated the expression of a large proportion of genes encoding for proteins involved in proliferation and cell cycle progression and hair differentiation. The induction of these genes allows hair follicle morphogenesis to start, promoting the amplification of TA and in the transition of the TA cell to a committed hair lineage (see Figure 5.10).

A big surprise from the array is the lack of overlap between β-catenin and Myc regulated epidermal genes (Frye et al., 2003). In intestinal epithelium Myc is a β-catenin target gene (He et al., 1998) and c-Myc plays a central role in progenitor maintenance downstream of the β-catenin/Tcf4 complex (van de Wetering et al., 2002).

However, the picture is quite different in skin. Myc induces exit from the stem cell compartment by inducing cell adhesion and ECM remodelling related genes, promoting sebocyte rather than hair follicle differentiation (Arnold and Watt, 2001; Waikel et al., 2001; Frye et al., 2003) and in the epidermis, β-catenin activation causes localised increases in proliferation and hair differentiation and does not upregulate c-Myc at the time points analysed. Nevertheless, N-Myc is upregulated. It has been shown that N-Myc is downstream of Shh and that N-Myc modulates GSK3β (Mill et al., 2005), adding an additional level of regulation by β-catenin activation. It is tempting to suggest that perhaps in skin N-Myc is the Myc member that is downstream of β-catenin. Further analysis will be important in determining whether it is a direct target and its role of in skin.

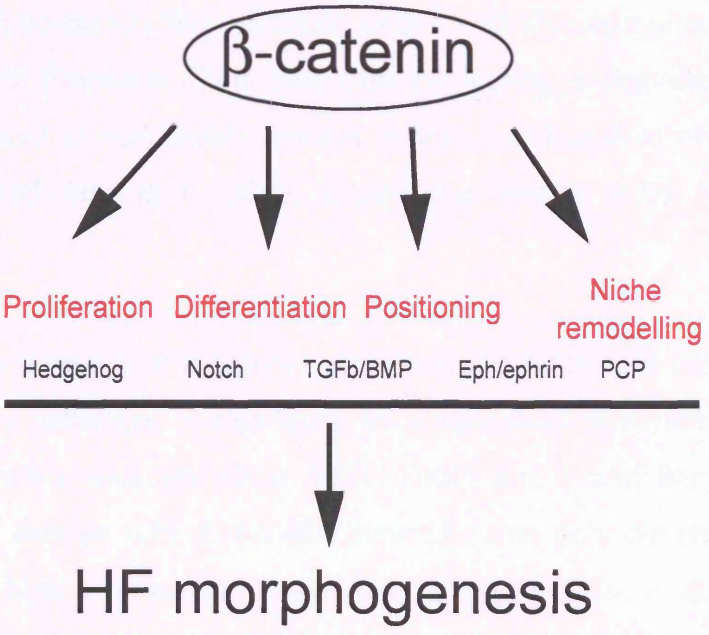

Figure 5.10 - Intersection of signalling events downtream of β–catenin during HF formation. Diagram representing the main signalling pathways activated by β-catenin. For simplification, only selected pathways are indicated in this diagram. The relationship between them and how they feedback to β-catenin is a main focus on analysis.

Negative feedback versus signal amplification of the β-catenin signal

Hedgehog and Wnt signalling interact during embryonic development (Reya et al., 2003 and Taipale and Beachy, 2001) and inappropriate activation of Wnt or Hedgehog signalling is associated with a range of epidermal cancers in humans and mice (Gat et al., 1998;Chan et al., 1999; Callahan and Oro, 2001;Niemann et al., 2003; Lo Celso et al., 2004; Takeda et al., 2006). This study shows that Shh and other members are upregulated in response to β-catenin activation in K14ΔNβ-cateninER epidermis and inhibition of Shh with Cyclopamine reduces β-catenin induced HF formation. This data puts Hedgehog antagonists as useful tools in the treatment of epidermal tumours in which either Wnt or Hedgehog signalling is activated (Reya et al., 2003; Taipale and Beachy, 2001; Niemann et al., 2003).

It is interesting the notion that β-catenin activation in addition of activating the Bmp, Shh and Wnt pathways, it also leads to upregulation of several Shh, Wnt and Bmp inhibitors (for example Hhip, Wif1, DKK1 and 4 and Bambi) (Figure 8.11). This might explain why K14ΔNβ-cateninER mice only develop tumours after prolonged or high level activation (see Figure 1.9; Lo Celso et al., 2004). In order to trigger a morphogenetic event, in D2 epidermis, lineage reprogramming is accompanied by only local increases in proliferation, whereas in D4 epidermis there is greater proliferation and the follicles become grossly thickened triggering a tumorigenic-like event. Therefore, the fact that Cyclopamine lowers the proliferation induced by β-catenin activation converting the D4 to the D2 phenotype shows that in order to de novo follicle formation to occur there must be an appropriate signal strength leading to a balance between Wnt and Shh signalling activation and inhibition (Figure 8.1).

Wnt pathway and niche remodelling

Several Wnts are induced upon β-catenin induction. These ligands are normally expressed in discrete domains in the bulb area of the follicle (Millar, 2002) and are known to activate the canonical Wnt pathway via β-catenin (Wnt7a, Wnt6, Wnt10b) and non-canonical pathway via the Planar Cell Polarity (PCP) pathway

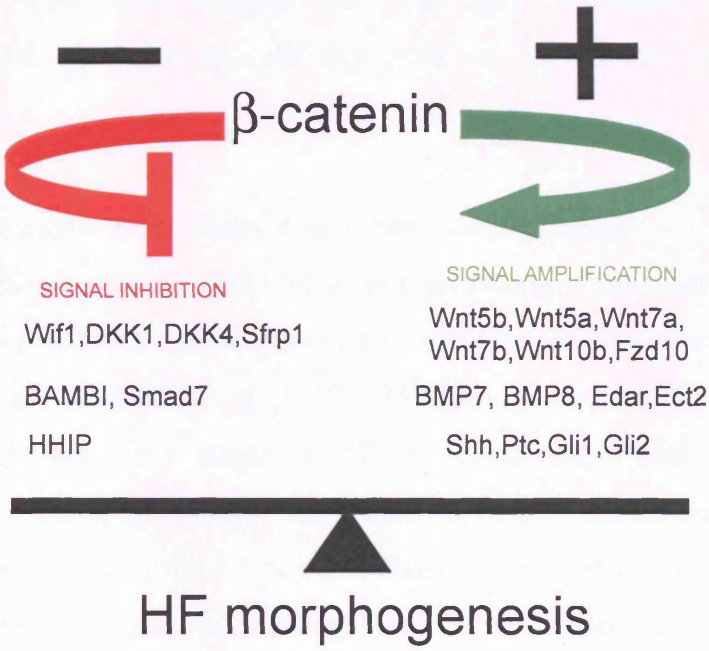

Figure 5.11 - Negative feedback versus amplification of the β–catenin signal . Diagram representing genes of the Wnt, BMP and Hedgehog pathways that are activated by b-catenin that either promote or inhibit the activation of the pathway. Note that a balance between the two must be acheived in order for HF to be formed.

and (Wnt5a, Wnt11, Wnt5b). This is of importance as the two pathways have different downstream effectors leading to different outcomes and are active during hair follicle differentiation. For instance, Wnt11 functions in gastrulation by controlling cell cohesion through Rab5c and E-cadherin. (Ulrich et al., 2005) Intriguingly, the Wnt11 receptor Frizzled-7 (Fz-7) (Djiane et al., 2000) is required for tissue separation during *Xenopus* gastrulation (Winklbauer et al., 2001), suggesting that non-canonical Wnt signalling controls cell migration by modulating cell adhesion. Several cytoskeletal proteins and activators of GTPases are upregulated upon β-catenin activation, further suggesting that the PCP is active also (Figure 5.10). It is not well understood how they cross-talk in epidermis and during hair follicle morphogenesis and it will be very important to pursue this question.

It is striking that all the genes down-regulated at 7 days, lie into the dermal fibroblast category (Rendl et al,. 2005). It will be worth following these findings as it might give new insights into the early crosstalk between epidermal keratinocytes and dermal cells that goes on after initial Wnt activation in the epidermis.

Novel pathways interactions downstream of β-catenin

These studies have revealed that several pathways are activated downstream of β-catenin activation to promote ectopic HF formation. As previously mentioned, members of the Hedhehog, BMP, TGFβ and Notch pathways are upregulated already at very early stages of HF morphogenesis, after 1 day of β-catenin activation. These pathways have been reported active during embryonic HF morphogenesis (Schmidt-Ullrich and Paus, 2005). However, how they are related to β-catenin and how these are regulated is the focus of current investigation.

In addition, new pathways, such as Eph signalling and Sox, not previously described in skin are also up-regulated.

Sox genes were amongst the transcription factors upregulated in response to β-catenin activation in the epidermis. Recent studies have put Sox9 in the list for new markers of the bulge stem cell population (Vidal et al., 2005). It is intriguing that Sox9 is induced by β-catenin in intestine (Blache et al., 2004) and in

embryonic lung (Okubo and Hogan, 2004). In the lung β-catenin activation results in stimulation of proliferation and a switch in lineage commitment from lung to intestinal cell types (Okubo and Hogan, 2004). Interestingly, some of the targets from our array matched genes isolated in a study profiling the bulge compartment after β-catenin activation. Sox4 is an intriguing example. Lowry and co-workers show that is a protein specifically up-regulated in the SC niche during the follicle growth phase and also expressed in proliferating TA progeny (Lowry et al., 2005). In addition, Sox4 has been pinpointed as a putative marker of intestinal stem cells. These findings further validate our array data and put Sox4 as a candidate for the TA amplification and transition into committed differentiation. It will be interesting to investigate epidermal Sox function further, given the physical interaction of β-catenin with certain Sox proteins (Zorn et al., 1999). This will give insights into the emerging roles of member of the HMG box superfamily of transcription factors in skin and hair biology.

In intestinal epithelium β-catenin/Tcf regulates the expression of EphB2, EphB3 and EphrinB1 and thereby controls cell positioning (Batlle et al., 2002). Our screen of genes regulated by β-catenin revealed a modest increase in expression of several members of the Eph/ephrin family. Components of this family (ephrin-B1, EphA4, ephrin-B2) are also upregulated in bulge LRC (Tumbar et al., 2004). In addition, EphA4 is expressed in the feather placode (McKinnell et al., 2004a). It is therefore tempting to speculate that in the epidermis, as in the intestinal epithelium, Eph/ephrin expression may couple stem cell self-renewal and differentiation to cell position. Analysis presented in Chapter 6 will attempt to unravel how Eph/ephrins pattern mammalian epidermis and might contribute to determining ectopic hair follicle positioning in part by modulating β-catenin signalling.

It is of particular interest the appearance of two genes, Musashi and Piwil2 involved in RNA remodelling and gene silencing during asymmetric stem cell division. It is very important to follow up these two proteins during hair follicle morphogenesis and in other processes regulated by β-catenin. It will be important to unveil the mechanism of action of how β-catenin regulates small RNAs, known as regulatory molecules that provide a new mechanism of

regulation (Kim, 2006), also in the skin (Yi et al., 2006). A very recent study has shown that sRNAs are crucial for ORS identity and maintenance (Andl et al., 2006).

Chapter 6- EphB/ephrin-B signalling determines hair follicle patterning

Aims

As discussed in previous Chapters, β-catenin activation controls hair follicle formation in adult and embryonic skin (Silva-Vargas et al., 2005; Lowry et al., 2005). Little is known about how pattern is controlled in mammalian skin: the placing of individual follicles within the epidermis, and the distribution of undifferentiated and differentiated cells along the hair follicle outer root sheath. I found that several Eph receptors and ephrin ligands are upregulated in response to β-catenin activation in adult epidermis (see Chapter 5). These findings prompted me investigate whether Eph/ephrin signalling plays a role in epidermal patterning.

6.1- Analysis of expression of EphB/EphrinB expression in wild-type skin

To address the question as to where ephrin-B and EphB receptors might interact to control patterning in the epidermis, I first looked at their expression patterns.

I analysed where ephrin-B and EphB receptors are expressed in adult epidermis by labelling tail whole-mounts and conventional back skin sections with specific antibodies (Figures 6.1, 6.2 and 6.3). As negative controls I used skin from ephrin-B1, EphB2 and EphB3 null mice or omitted primary antibodies during staining (See Figure 6.1 and 6.2). It was not possible to reach any conclusions about expression of ephrin-B and EphB proteins in the sebaceous glands of tail epidermal whole mounts because of high levels of non-specific staining (asterisks, Figure 6.1 A, C, D).

Three B-type ligands were expressed. Ephrin-B1 expression was highest in the bulb (base) of growing anagen hair follicles (Figure 6.1A, B, F; Figure 6.2 C,G and 6.3; Tumbar et al., 2004). Ephrin-B2 was highly expressed in the zone where the hair follicle becomes continuous with the IFE, called the infundibulum, and also in the neighbouring IFE, which in tail skin is known as the parakeratotic scale

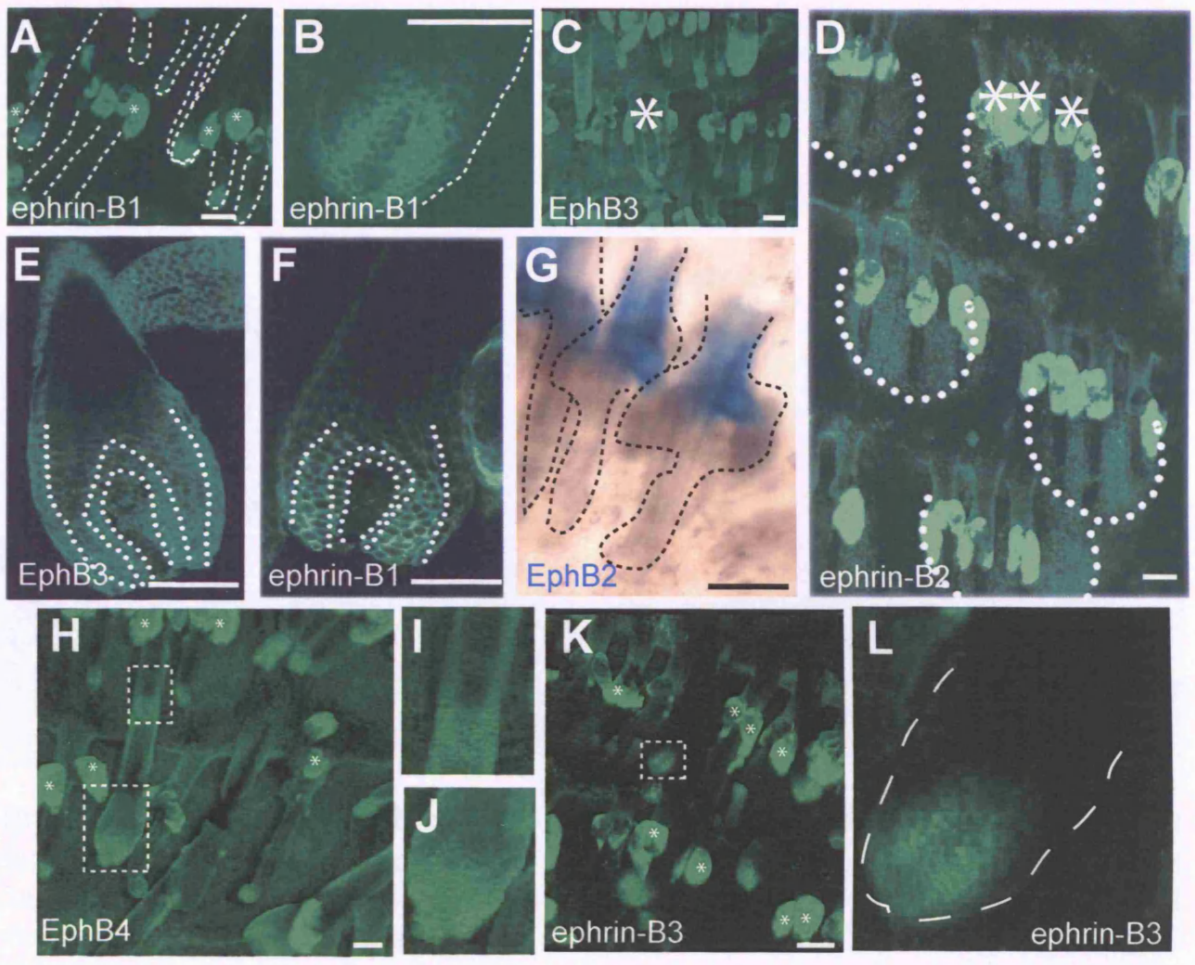

Figure 6.1- Expression pattern of EphB receptors and ephrin-B ligands in adult wild type tail epidermis. (A-L) Immunolabelling of tail skin whole mounts of wild type epidermis with antibodies to the proteins indicated. I and J are enlargements of the boxes in H. L is an enlargement of K. As a negative control either omission of primary antibody or tissue from ephrin-B1 null (*Efnb1*KO), EphB2 null (*Ephb2*KO) and EphB3 null (*Ephb3*KO) was used. Asterisks indicate SG non-specific staining. Scale bars: 100 μm.

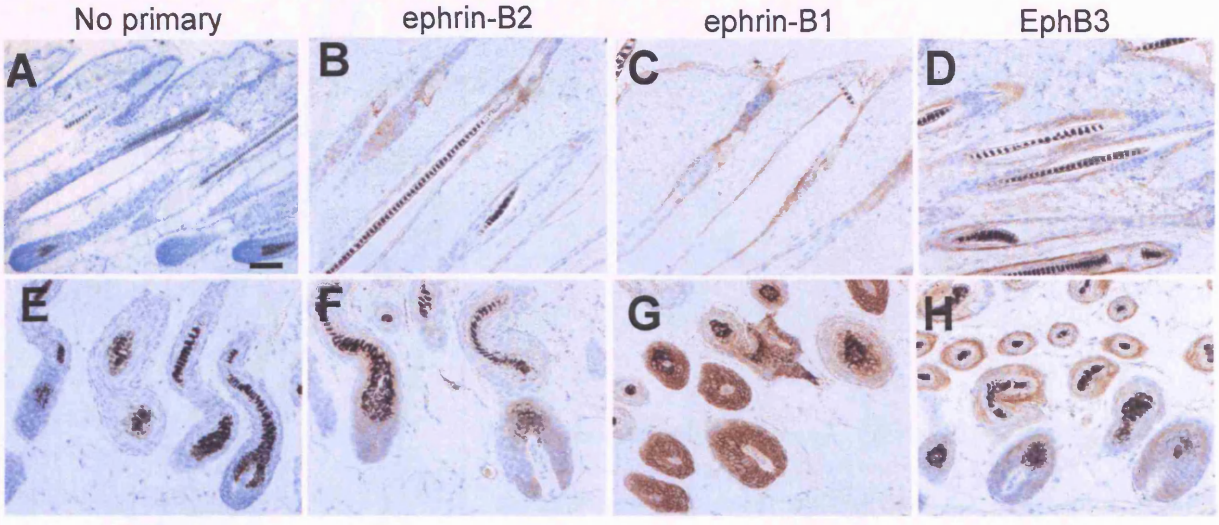

Figure 6.2- Expression pattern of EphB receptors and ephrin-B ligands in adult wild type dorsal epidermis. (A-H) Immunolabelling of dorsal skin sections of wild type epidermis with with antibodies to the proteins indicated. As a negative control either omission of primary antibody or tissue from ephrin-B1null (*Efnb1*KO), EphB2 null (*Ephb2*KO) and EphB3 null (*Ephb3*KO) were used. Asterisks indicate SG non-specific staining. Scale bars: 100 μm.

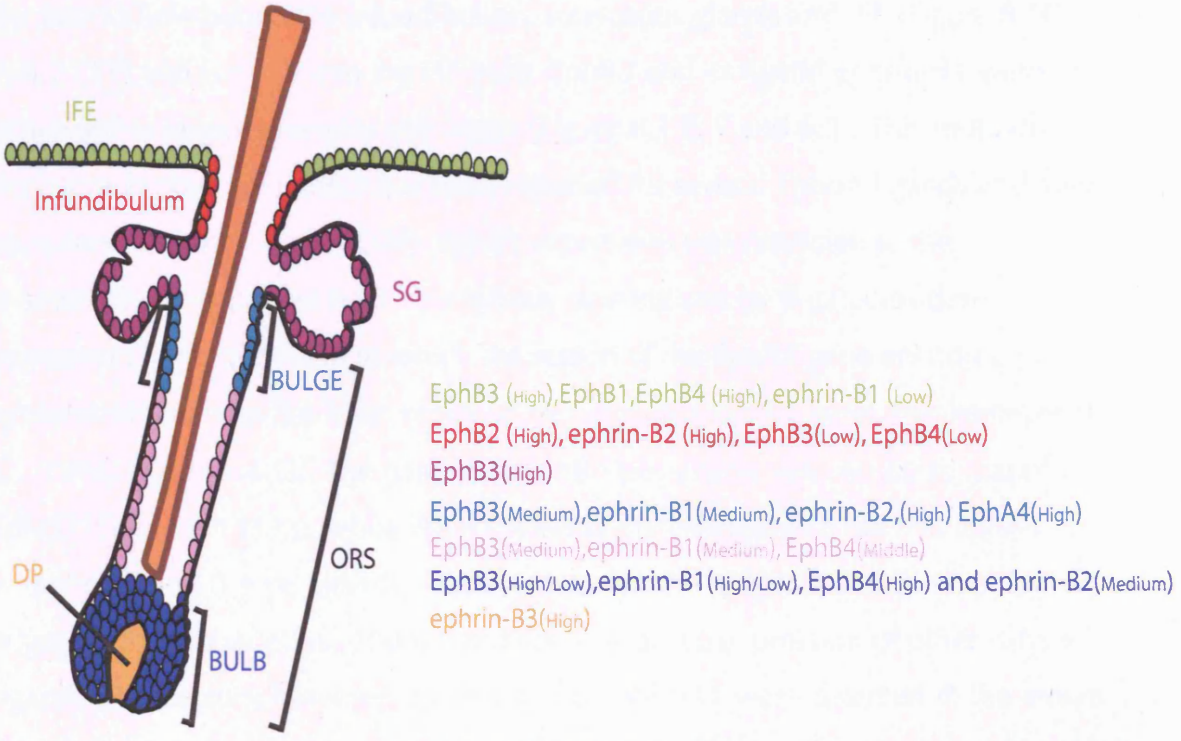

Figure 6.3- Expression pattern of EphB receptors and ephrin-B ligands in wild type epidermis. Schematic summary of high expression of ephrin-B ligands and EphB receptors in different epidermal regions. DP: dermal papilla. ORS: outer rooth sheath, IFE: Interfollicular epidermis and SG: sebaceous glands.The relative levels of expression are indicated by High,Medium and Low.

(Schweizer and Marks, 1977;Lopez-Rovira et al., 2005). In addition, it is expressed at lower levels in the HF bulge and the bulb (Figure 6.1 D, 6.2 B, F and 6.3). Ephrin-B3 was mainly detected in the dermal papilla, the specialised mesenchymal cells at the base of the hair follicles (Figure 6.1 and 6.3;Rendl et al., 2005).

I also examined the expression of the B-type Eph receptors. EphB3 was most highly expressed in the bulb of anagen hair follicles, but could also be detected in the hair follicle bulge, the infundibulum, sebaceous glands and IFE (Figure 6 1C, E, 6.2 D,H and 6.3). Within the HF bulb, EphB3 and its ligand ephrin-B1 were expressed in complementary cell layers (Figure 6.1 E, F and 6.3). This mutually exclusive expression pattern has been reported for several Ephrin ligands and their receptors (Poliakov et al., 2004). EphB2 expression was restricted to the infundibulum, as judged both by antibody staining and by β-galactosidase expression in mutant mice in which the region of the EphB2 gene encoding the cytoplasmic domain has been replaced by a β-galactosidase gene (Henkemeyer et al., 1996; Figure 6.1 G). The pattern of EphB4 expression was similar to that of EphB3 (Figure 6.1 H,I,J), while EphB1 was mainly expressed in the IFE. EphA4, which can bind B-type ligands, was expressed in the bulge area of the hair follicle (Figure 6.3; Tumbar et al., 2004). I did not look at the expression of other A-type ligands or receptors; however, EphA7, 4 and EphrinA1 were detected in the arrays thus they might be also expressed (See Table 5.1 in Chapter 5).

6.2-Macroscopic and Histological analysis of Eph null gross phenotype

In order to study the *in vivo* function of ephrin-B1 and its cognate receptors, EphB3 and EphB2, in epidermal patterning, I analysed the skin of mice in which the ephrin-B1 (Compagni et al., 2003), EphB2 (Orioli et al., 1996) and EphB3 (Orioli et al., 1996) genes had been deleted by homologous recombination. None of the mice exhibited obvious hair loss. Ephrin-B1 null mice had no macroscopic skin phenotype. EphB3 null mice had greasy skin and ruffled fur that was associated with abnormal clumping of the follicles. The same phenotype was

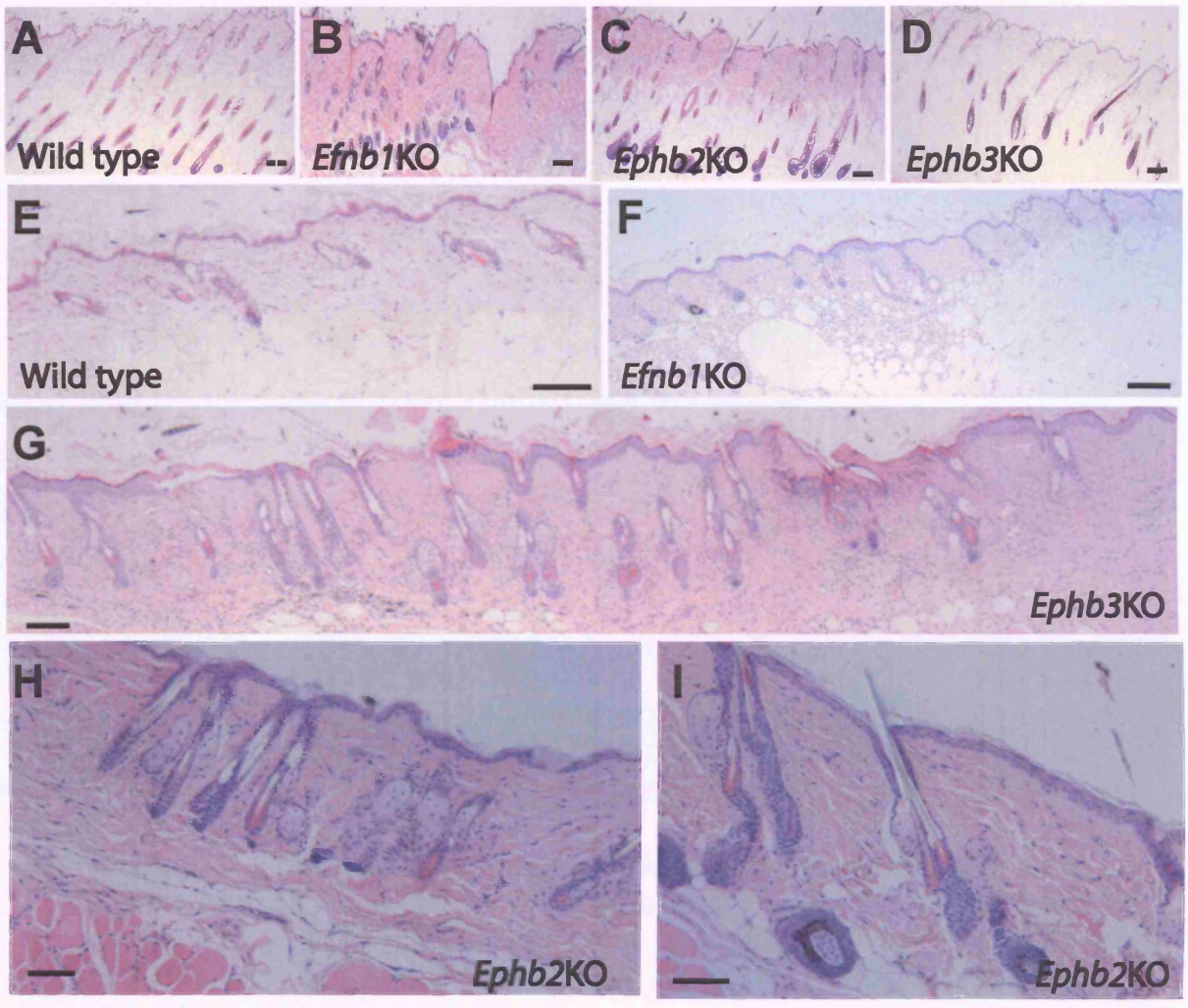

Figure 6.4- Histological changes in ephrin-B/EphB mutant skin (A-I) Hematoxylin and Eosin stained sections of dorsal skin of wild type, ephrin-B1 (*Efnb1*KO), EphB2 (*Ephb2*KO) and EphB3 (*Ephb3*KO) null epidermis. Mice analysed were from 6 months old to 1 year old (See Table 6.1 for details). Scale bars: 100 μm.

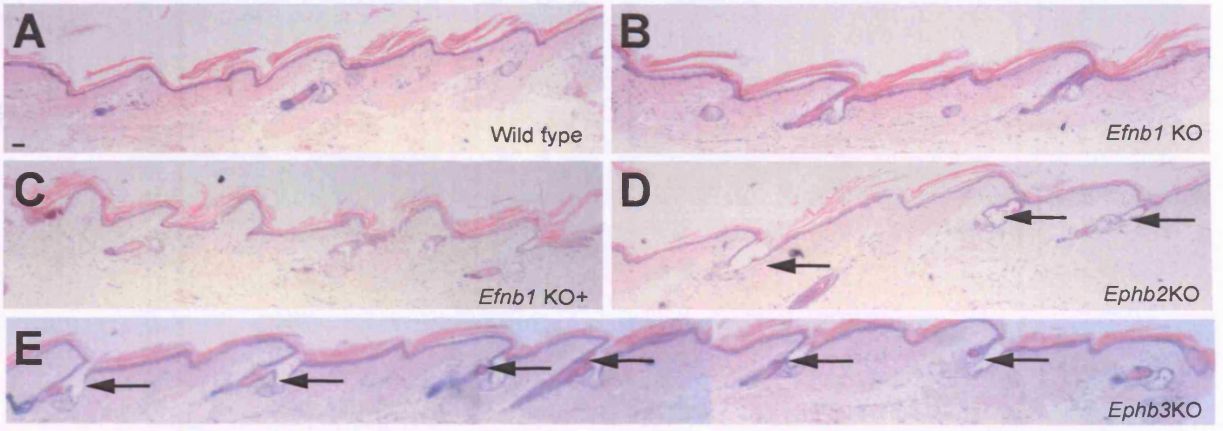

Figure 6.5- Histological changes in Eph/ephrin mutant tail skin
(A-G) Hematoxylin and Eosin stained sections of dorsal skin of Wild type, ephrin-B1null (*Efnb1*KO), EphB2 null (*Ephb2*KO) and EphB3 null (*Ephb3*KO) epidermis. Mice analysed were from 6 months old to 1 year old (See Table 6.1 for details). Scale bars: 50 μm.

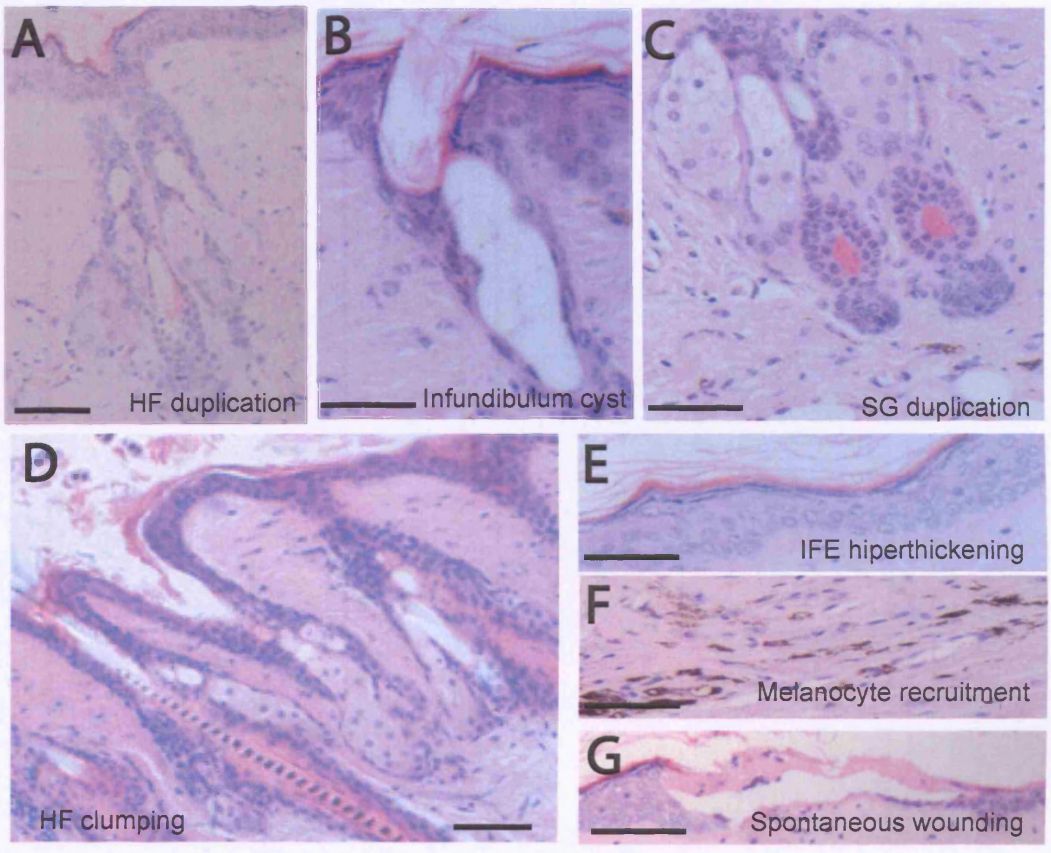

Figure 6.6- Histological changes in EphB3 mutant skin (A-G) Hematoxylin and Eosin stained sections of dorsal skin of EphB3 (*Ephb3*KO) epidermis. Mice analysed were from 6 months old to 1 year old (See Table 6.1 for details). Scale bars: 50 μm.

occasionally seen, in milder form, in EphB2 null mice. A summary of the defects in adult epidermis and the details of the mice analysed are shown in Table 6.1.
In order to monitor if hair re-grew over time we shaved by hair clipping the dorsal skin. In both, wild type and mutant back skin follicles entered anagen, indicating that the hair growth cycle was not inhibited (Figure 6.4 A-D). In all three mutants the IFE was thicker than in wild type mice (Figure 6.4 E-H, N); this was the only abnormality detected in ephrin-B1 null skin (Figure 6.4 F). By looking at the histology in the tail I could observe the appearance of infundibulum cysts (see Arrows, Figure 6.5; Table 6.1). In dorsal skin, EphB3 null animals showed the most pronounced phenotype. Spontaneous wounds developed in the IFE (Figure 6.6 G) and melanocytes accumulated in the dermis (Figure 6.6 F). Enlargement and duplication of sebaceous glands occurred (Figure 6.4 G, C; table 6.1). In some cases, two or three hair follicles shared a common infundibulum (Figure 6.6 A). Another characteristic lesion in dorsal skin was also the expansion of the infundibulum and the formation of infundibulum cysts (Figure 6.4 G, 6.5 E and 6.6 B; Table 6.1). We also observed sebocytes intermingled with infundibulum keratinocytes (Figure 6.6 B; Table 6.1). All of the changes observed in EphB3 null skin were also seen in EphB2 null skin, albeit with lower frequency and severity (Figure 6.4 H, I and 6.5 D).
When I looked at skin of double mutants (EphB3/EphB2KO homozygous) the severity of the phenotype was more severe (Figure 6.7). There were patches of hyperthickened epidermis (Figure 6.7 A), and cells in the basal layer were more invasive, and less polarised (Figure 6.7). Intermingling of sebocytes and keratinocytes was more frequent (Figure 6.7 G, H). Hair clumping, SG duplication and enlargement were also observed (Figure 6.7 I-L). One of the four mice analysed had a small papilloma (Figure 6.7 E-F).

6.3- Changes in patterning of hair follicle and interfollicular epidermis

In order to dissect in more detail the patterning defects observed by conventional histology of back skin (Figures 6.4, 6.5, 6.6 and 6.7), I used the tail skin whole

Genotype	Phenotypes			
	HF Triplets	**IFE**	**HF**	**SG**
*Ephb3*KO ♀♂ (n= 20) (6 months -1.5 year)	NO (18)	Very thick (12)	Duplicated **(14)** Infundibulum cyst Ruffled hair (11)	Enlarged **(15)** duplicated Greasy skin
*Ephb2*KO ♀♂ (n= 11) (6 months -1.5 year)	YES (11)	Thick (5)	Infundibulum **(7)** cyst Ruffled hair (5)	Enlarged **(5)** duplicated Greasy skin
*Efnb1*KO ♂ (n= 11) (6 months -1.5 year)	YES (11)	Normal/Thick (5)	HF thickness **(6)**	Enlarged **(4)** duplicated
*Ephb2/3*KO ♀♂ (n= 4) (1 year)	NO (4)	Very thick Invasive patches **(4)**	Hair duplication **(4)** Ruffled hair (3)	Enlarged **(4)** duplicated Greasy skin

Table 6.1- Summary of the defects in adult mutant epidermis. The number of affected mutants for each phenotype is given together with the total number of animals analysed (in parentheses).

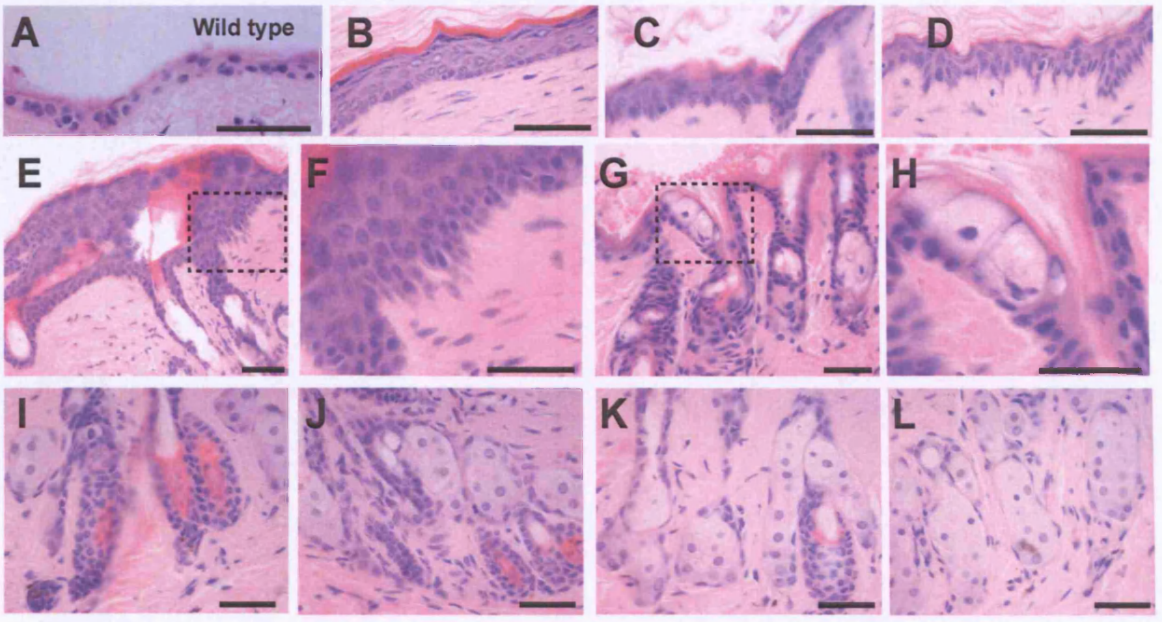

Figure 6.7- Histological changes in EphB3/EphB2 double mutant skin (A-L) Hematoxylin and Eosin stained sections of dorsal skin of wild type (A) and *Ephb3/Ephb2* KO epidermis (B-L). (A-D) Close-ups of IFE (3 mice). (E) One of the mice developed a papilloma in the upper side of the back. (F) High magnification of the window in (E). (G) Sebocyte intermingled in the infundibulum. (H) Magnification of the window in (G). Total of three 6 months old animals were analysed (See Table 6.1 for details). Scale bars: 50 μm.

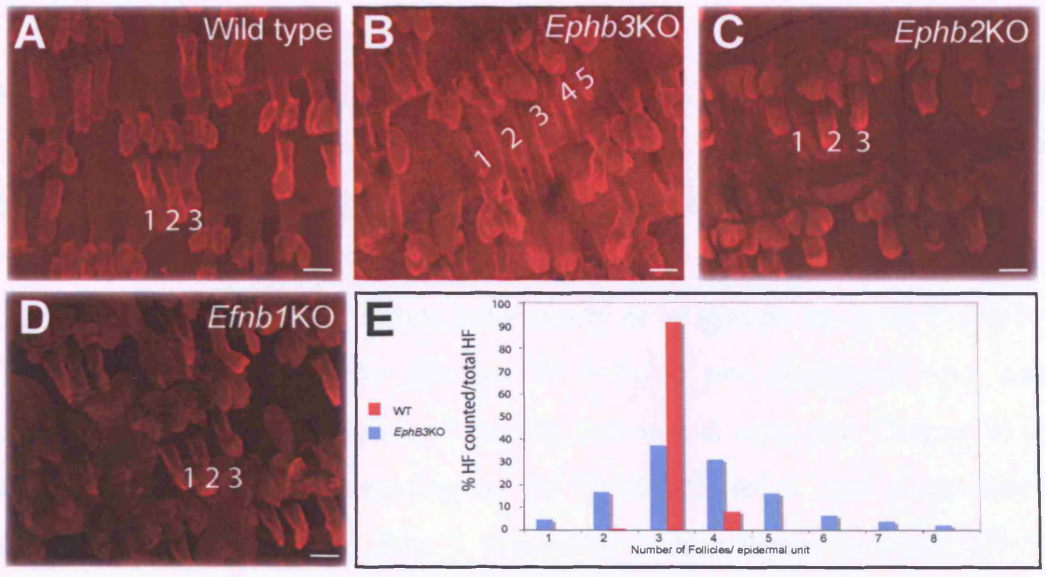

Figure 6.8- Loss of ephrin-B/EphB leads to abnormal triplet patterning within the epidermis. (A-D) Tail epidermal whole mounts of wild type (A), EphB3 (B), EphB2 (C) and ephrin-B1null mice were immunolabelled with a keratin 14 antibody. Individual hair follicles arranged in triplets are numbered 1,2,3 (A,C,D). (B) Shows a row of 5 follicles. (E) Follicle number was counted per epidermal unit of a total of 24 different pieces of WT or Ephb3 null epidermis (n= 25 units per piece) and the distribution was plotted as percentage values of counted follicles per unit over the total number of units per piece analysed. Scale bars: 100 μm.

mount system, which allows a three-dimensional assessment of changes occurring in large areas of skin. The epidermis of the tail is highly patterned, as can be appreciated in whole-mount preparations (Schweizer and Marks, 1977; Braun et al., 2003 and see Chapter 3). As discussed in previous Chapters, in wild type skin, hair follicles are arranged groups of three (triplets) and are organised in rows, such that the hair follicle triplets in one row are staggered relative to those in the rows on either side (Figure 6.8 A, E, see Chapter 2).

In ephrin-B1, EphB2 and EphB3 null tail skin the follicles were arranged in rows and the spacing between rows was maintained (Figure 6.8 B-D). In ephrin-B1 or EphB2 null epidermis the follicles were generally grouped in triplets (Figure 6.8 C, D). However, in EphB3 mutants the triplet organisation was completely disrupted, such that follicles were found either individually or in groups of up to 7 (Figure 6.8 E). The distribution of the number of follicles per epidermal unit was calculated by counting the number of follicles/ epidermal units (see Chapter 5) of a total of 24 pieces corresponding to 18 *EphB3*KO mice and each piece containing about 25 epidermal units. 5 % of units contain groups of 1 hair follicle (HF), 15 % of units contain 2 HF, in 35% of units the triplets are maintained, in 30 % of units groups of 4 HF are present, 15 % of units contain groups of 5 HF, 5 % had groups of 6 HF, 2.5 % had groups of 7 HF and 2% had groups of 8 HF (See Figure 6.8 E). In wild-type epidermis the 95 % of units contained HF in triplets (Figure 6.8 E). Quadruplets also are present in epidermal units but at much lower frequency (4%) and 1% of units contain very rare sextuplets or duplets (See Figure 6.8 E).

Within tail IFE, two types of differentiation can be distinguished (see Chapter 2; López-Rovira et al., 2005). I have found that the IFE that encircles each hair follicle triplet, known as the parakeratotic scale, does not express keratin 10 (Figure 3.5 E, Q) but does express caspase 14 (Figure 3.5 B,C,D,E). The remainder of the tail IFE is keratin 10 positive and caspase 14 negative (Figure 3E, I, Q).

In all three mutants IFE differentiation was disturbed (Figure 6.9). In EphB3 null epidermis expression of caspase 14 was normal (Figure 6.9 E), but keratin 10 was

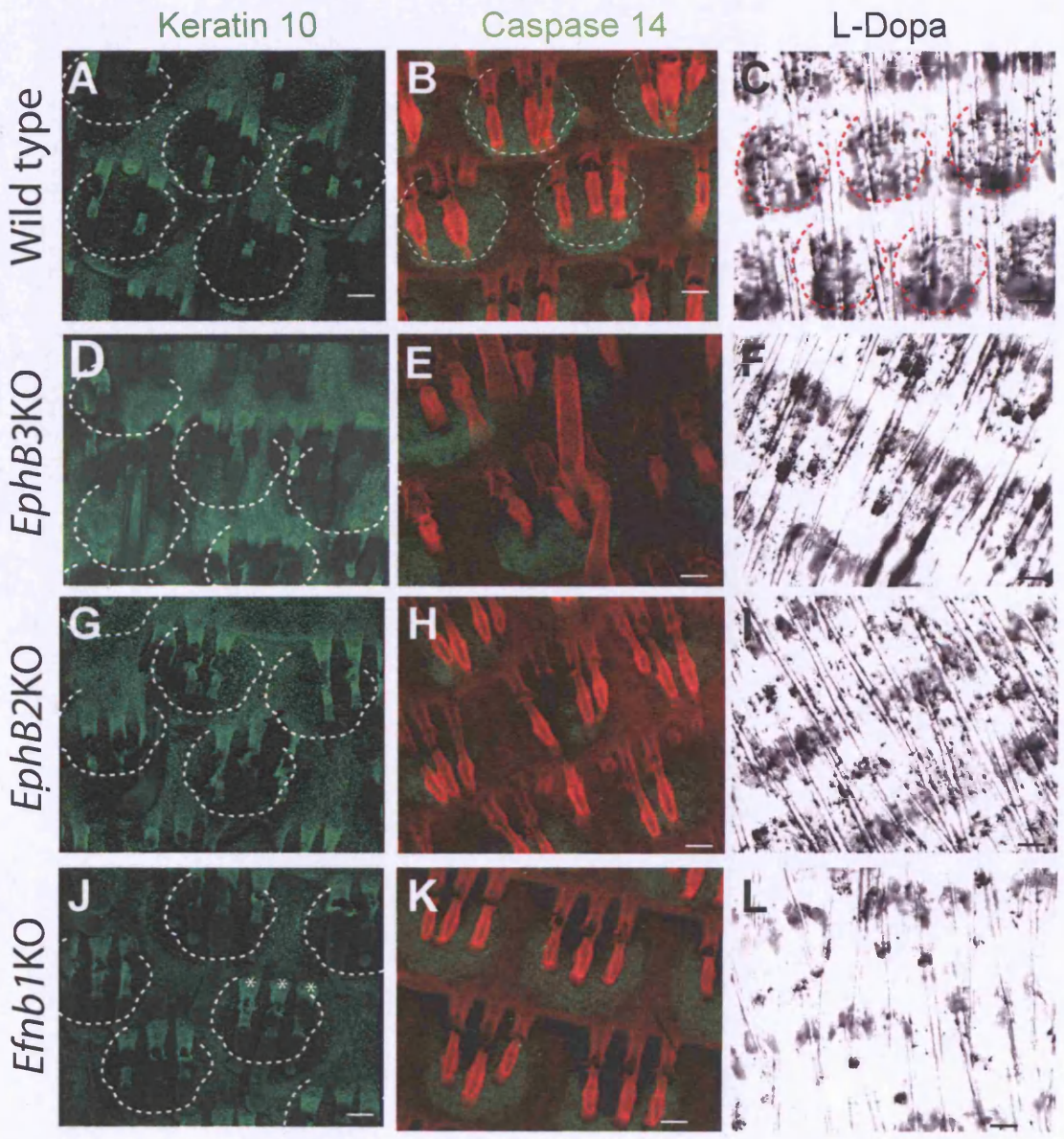

Figure 6.9- Loss of ephrin-B/EphB leads to abnormal patterning within the epidermis (A-L) Tail epidermal whole mounts of wild type (A-C), EphB3 (D-F), EphB2 (G-I) and ephrin-B1 (J-L) null mice were immunolabelled with the antibodies shown or stained for L-Dopa. Dashed lines demarcate parakeratotic scales (A,B,C,D,G,J). Scale bars: 100 μm.

expressed throughout the IFE (Figure 6.9 D). Keratin 10 was also expressed throughout EphB2 null tail epidermis (Figure 6.11 G), and caspase 14 expression was reduced or absent (Figure 6.9 H). Conversely, in ephrin-B1 null epidermis, the IFE was keratin 10 negative, expression being confined to the hair follicle infundibulum (Figure 6.9 J). In ephrin-B1 null epidermis, caspase 14 expression was normal (Figure 6.9 K).

The loss of boundaries within the IFE observed with K10 and caspase 14, correlated with a loss of boundaries in the distribution of differentiated melanocytes (Figure 6.9 C, F, I, L). In wild type tail IFE, differentiated melanocytes are confined to the parakeratotic scales and can be visualised by L-Dopa reactivity in whole mounts (Figure 6.9 C; Figure 3.8) In EphB2 null epidermis, L-Dopa positive melanocytes were no longer confined to the parakeratotic scales, but were more widely scattered throughout the IFE (Figure 6.9 I). This effect was less pronounced in EphB3 null epidermis (Figure 6.9 F). Conversely, there was a marked decrease in the number of melanocytes in ephrin-B1 null epidermis (Figure 6.9 L). The changes in the distribution of melanocyte population correlated with changes in expression of the c-kit ligand known to act as a cue for melanocyte homing (Figure 6.13; Tumbar et al., 2004).

I conclude that EphB3 loss disrupts the normal triplet pattern of hair follicles in tail epidermis, and that loss of EphB2, EphB3 or ephrin-B1 disturbs the pattern of IFE differentiation and the localisation of melanocytes within the IFE.

6.4- Changes in patterning along the hair follicle axis

Having established that disruption of ephrin-B/EphB signalling led to changes in hair follicle position and patterning of the IFE, I examined whether it also affected patterning along the length (proximo-distal axis) of the hair follicles, including the sebaceous glands (Figure 6.10, 6.11, 6.12). I thought it is likely that patterning was disturbed because H&E staining revealed intermingling of sebocytes with infundibulum keratinocytes, as well as hair follicles with abnormal morphology (Figures 6.4, 6.6.).

In wild type epidermis, keratin 17 is expressed along the length of the outer root sheath but not in the infundibulum (Figure 6.10 A, D, G, J). CDP is highly

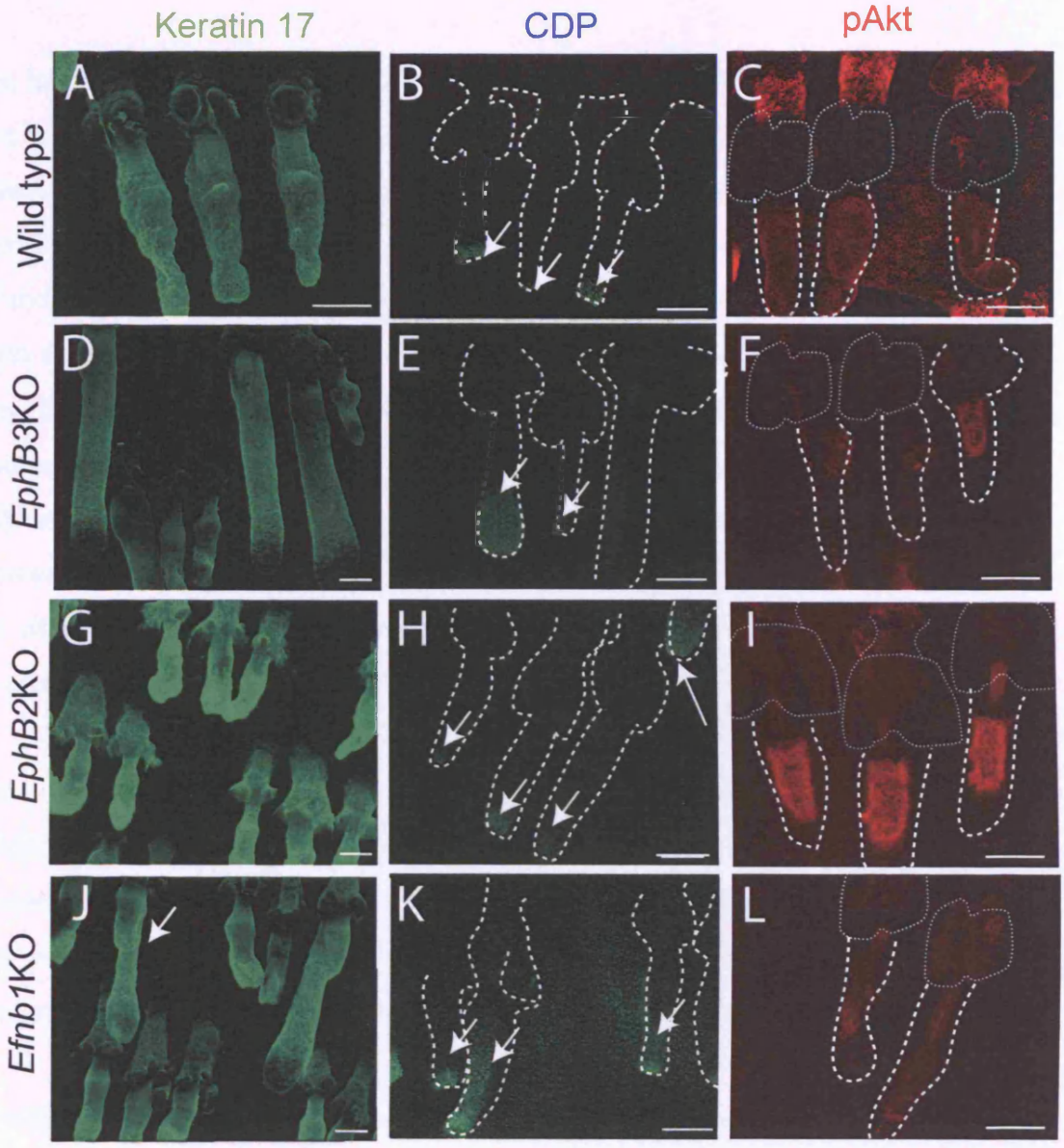

Figure 6.10- Loss of ephrin-B/EphB leads to abnormal patterning along the hair follicle. Tail epidermal whole mounts of wild type (A-C), EphB3 (D-F), EphB2 (G-I) and ephrin-B1 (J-L) null mice were immunolabelled with the antibodies shown . Dotted lines demarcate HF and SG (B,E,H,K) and SG and infundibulum (C,F,I,L). Arrow in J shows thickened bulge. Scale bars: 100 μm.

expressed in the bulb of anagen follicles (Figure 6.10 B). The infundibulum is specifically labelled with antibodies to phosphorylated Akt in telogen follicles (pAkt; Figure 6.12 C; Alonso et al., 2005).

The hair follicle outer root sheath in ephrin-B1, EphB2 and EphB3 null epidermis was keratin 17 positive (Figure 6.10 A, D, G, J). Keratin 17 staining did, however, reveal abnormalities in follicle morphology that were consistent with the changes seen in back skin (Figure 6.4). In addition, keratin 17 expression extended into the infundibulum in EphB3 and EphB2 null epidermis (Figure 6.10 D and G). It has been shown that Keratin 17 is upregulated in proliferative skin, and the increase may be due to increased proliferation or Bmp and TGFβ upregulation. For instance, Tenascin expression is a marker of the ORS that could be used instead. CDP expression was normal in EphB3 and EphB2 null tail follicles (Figure 6.10). However, in ephrin-B1 follicles CDP positive cells were not confined to the bulb, but were also present in the inner root sheath (Figure 6.10 B,K), correlating with an increase in proliferating, Ki67 positive cells (See Figure 6.14 J-L).

The location of phosphoAkt positive cells was not normal in ephrin-B1 null epidermis (Figure 6.10 L). In EphB2 null, and to a lesser extent in EphB3 null, epidermis phosphoAkt was no longer detected in the infundibulum, but instead was present in the outer root sheath below the sebaceous glands, in the region corresponding to the bulge (Figure 6.10 I, F).

In wild type tail follicles, the differentiated, L-Dopa positive, melanocytes are confined to the bulb (Figure 6.11 A). This was also the case in ephrin-B1 null follicles (Figure 6.11 D). However, in EphB3 null follicles L-Dopa positive melanocytes were also found in the bulge (see red asterisks in figure 6.11 B). In EphB2 follicles L-Dopa positive melanocytes were absent from the bulb and present in the infundibulum (see red line in Figure 6.11 C). The changes in the distribution of melanocytes correlated with changes in expression of the c-Kit ligand (Figure 6.11 E-H; (Tumbar et al., 2004; Nishimura et al., 2002). In *EphB3*KO and *EphB2*KO skin c-Kit ligand was widely localised in the epidermis.

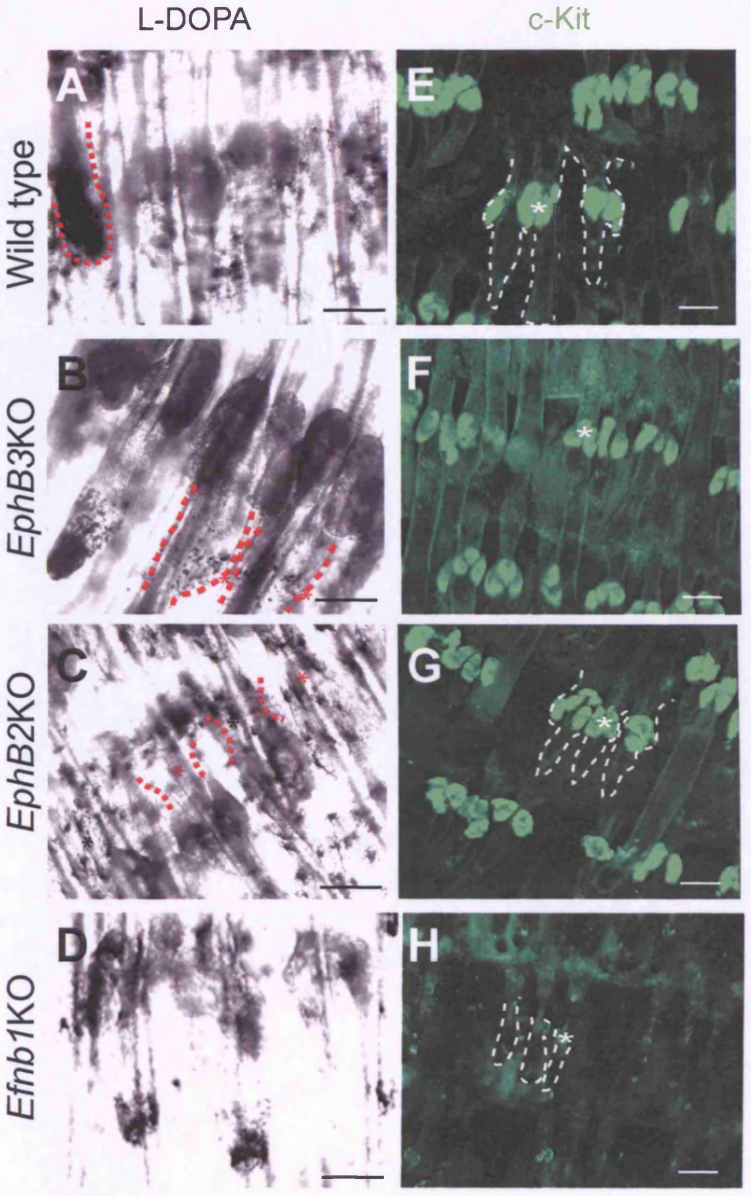

Figure 6.11- Loss of ephrin-B/EphB leads to abnormal patterning of melanocytes along the hair follicle. Tail epidermal whole mounts of wild type (A, E), EphB3 (B, F), EphB2 (C, G) and ephrin-B1 (D, H) null mice were stained for L-Dopa (A-D). Dotted lines demarcate HF and SG (E,G). Asterisks in B indicate the bulge and in C indicate the infundibulum. White asterisks in E-H indicates non-specific staining of the SG. Scale bars: 100 μm (A-H).

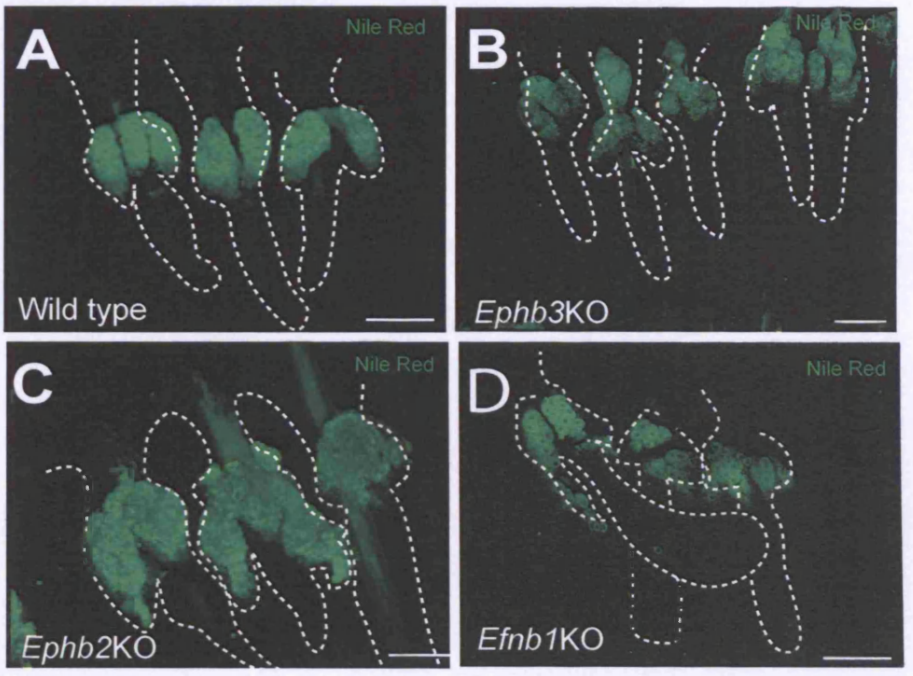

Figure 6.12- Loss of ephrin-B/EphB leads to abnormal patterning of the SG. Tail epidermal whole mounts of wild type (A), Ephb3 (B), Ephb2 (C) and ephrin-B1(D) null mice were stained with Nile Red . Dotted lines demarcate HF and SG (A-D). Scale bars: 100 μm.

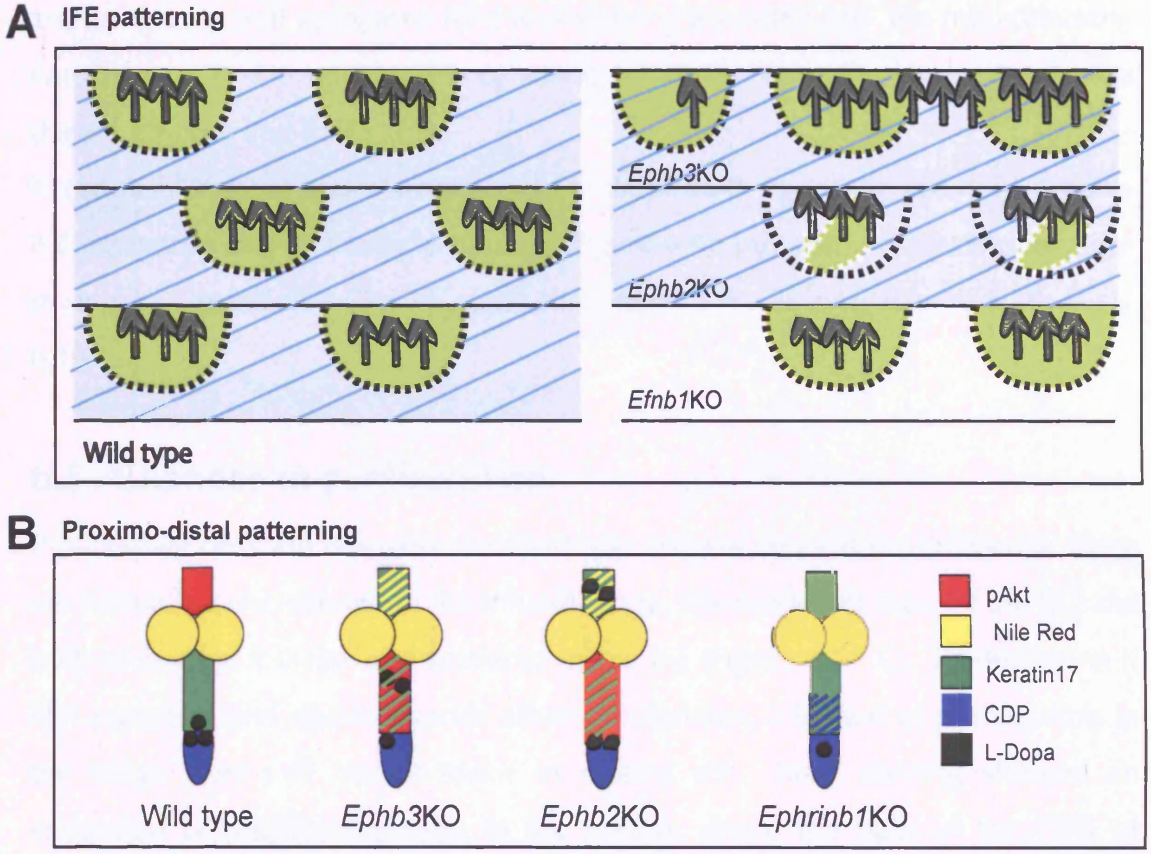

Figure 6.13- Eph/ephrin signalling control patterning in tail skin. (A) Summarises schematically the data presented in Figure 6.9. In A grey arrows are hair follicles; parakeratotic scales are demarcated by dotted lines. Green: caspase 14; Blue stripes: keratin 10. (B) Summarises schematically the data presented in Figure 6.10 and 6.11; In A and B stripes indicate co-expression.

In *Efnb1*KO skin there was a decrease consistent with a reduction of melanocytes (Figure 6.11 H).

The lipophilic dye Nile Red provides a specific marker of sebocytes (Figure 6.12). Sebaceous glands were normal in ephrin-B1 null epidermis (Figure 6.12 D), but were enlarged in EphB3 null tail epidermis (Figure 6.12 B). In both EphB3, EphB2 and in double null epidermis Nile Red staining extended into the infundibulum, consistent with the appearance of sebocytes in the infundibulum of back skin (Figure 6.4, 6.6 and 6.7).

These results show that disruption of EphB/ephrin-B signalling not only disturbs IFE patterning and hair follicle spacing (Figure 6.9), but also changes the location of marker expression in the SG along the length of the follicles (Figure 6.10, 6.11, 6.13).

6.5- Changes in proliferation

Proliferative cells are normally confined into discrete areas of the epidermis. They are normally concentrated in the infundibulum, the outermost layer of the SG, the bulb of anagen follicles and scattered in the IFE (Figure 6.14 C). To determine if Eph receptors and ephrin ligands affect proliferation, I looked at proliferation in the bulge stem cell compartment in mutant skin. Ki67 staining showed an expansion of proliferating cells in the portion above the bulb in the ORS of *EphB3*KO and *Efnb1*KO skin (Figure 6.14 H, I, K, L). There was also an increase in proliferating cells in the IFE of *EphB3*KO and *EphB2*KO (Figure 6.14 F, I). The same changes were observed in dorsal epidermis (Figure 6.14 A,D,G,J).

6.6- Changes in the bulge stem cell compartment

To investigate whether the changes in epidermal patterning correlated with changes in the bulge stem cell compartment, I analysed two markers of bulge stem cells, keratin 15 and CD34 (Lyle et al., 1998; Trempus et al., 2003). In whole mounts of wild type tail epidermis keratin 15 expression is restricted to the bulge, the sebaceous glands staining non-specifically (Figure 6.15 A, see Figure 4.12 in Chapter 4). In the three mutants, keratin 15 was co-expressed with CD34,

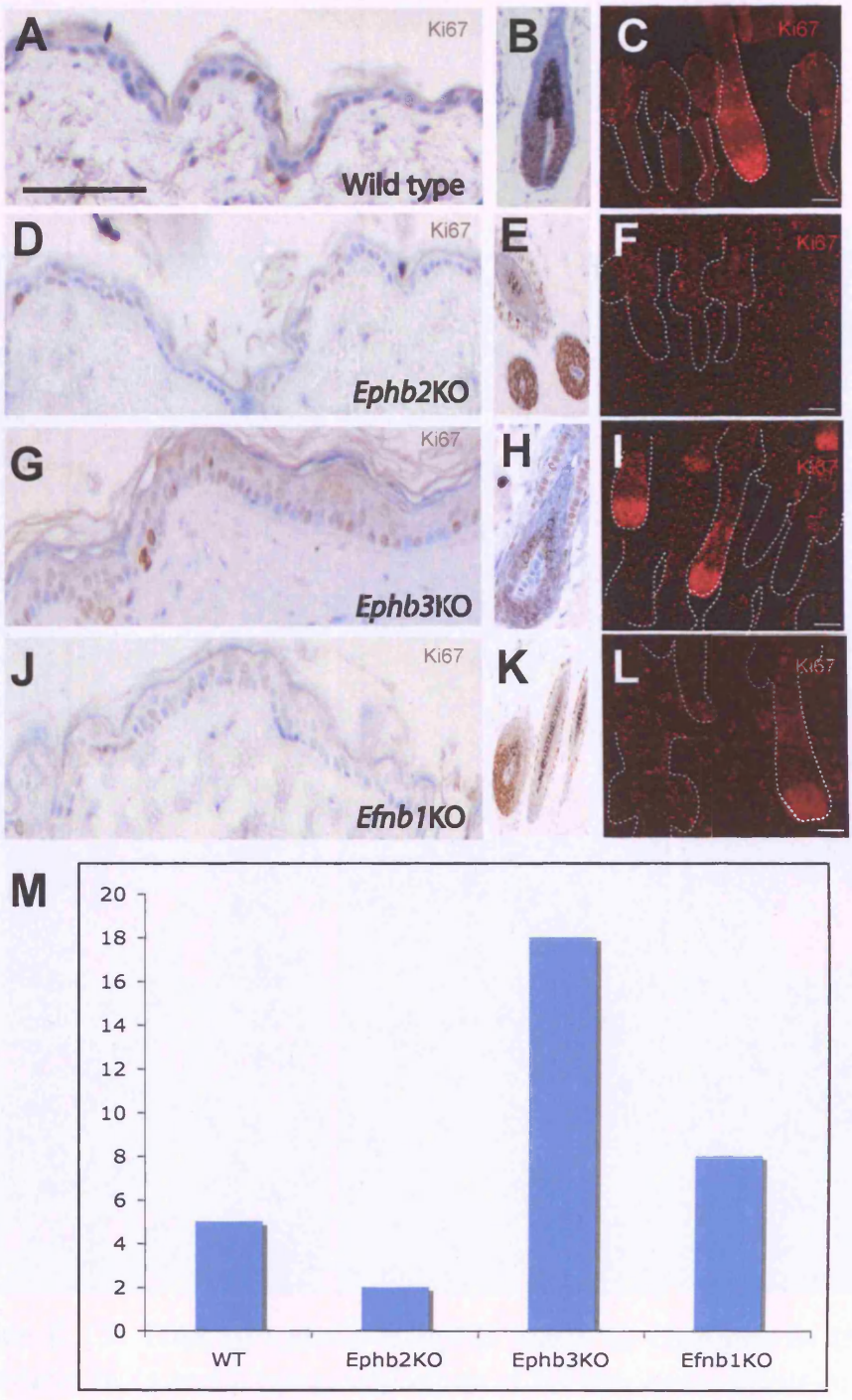

Figure 6.14- Changes in proliferation in ephrin-B/EphB mutant skin (A-L) Immunolabelling of sections of dorsal skin (A,B,D,E,G,H,J,K) or tail skin whole mounts (C,F,I,L) of wild type, ephrin-B1 (*Efnb1*KO), EphB2 (*Ephb2*KO) and EphB3 (*Ephb3*KO) epidermis with an anti-Ki67. (M) Graph shows Ki67 positive cells that were counted from conventional back sections. Scale bars: 100 μm.

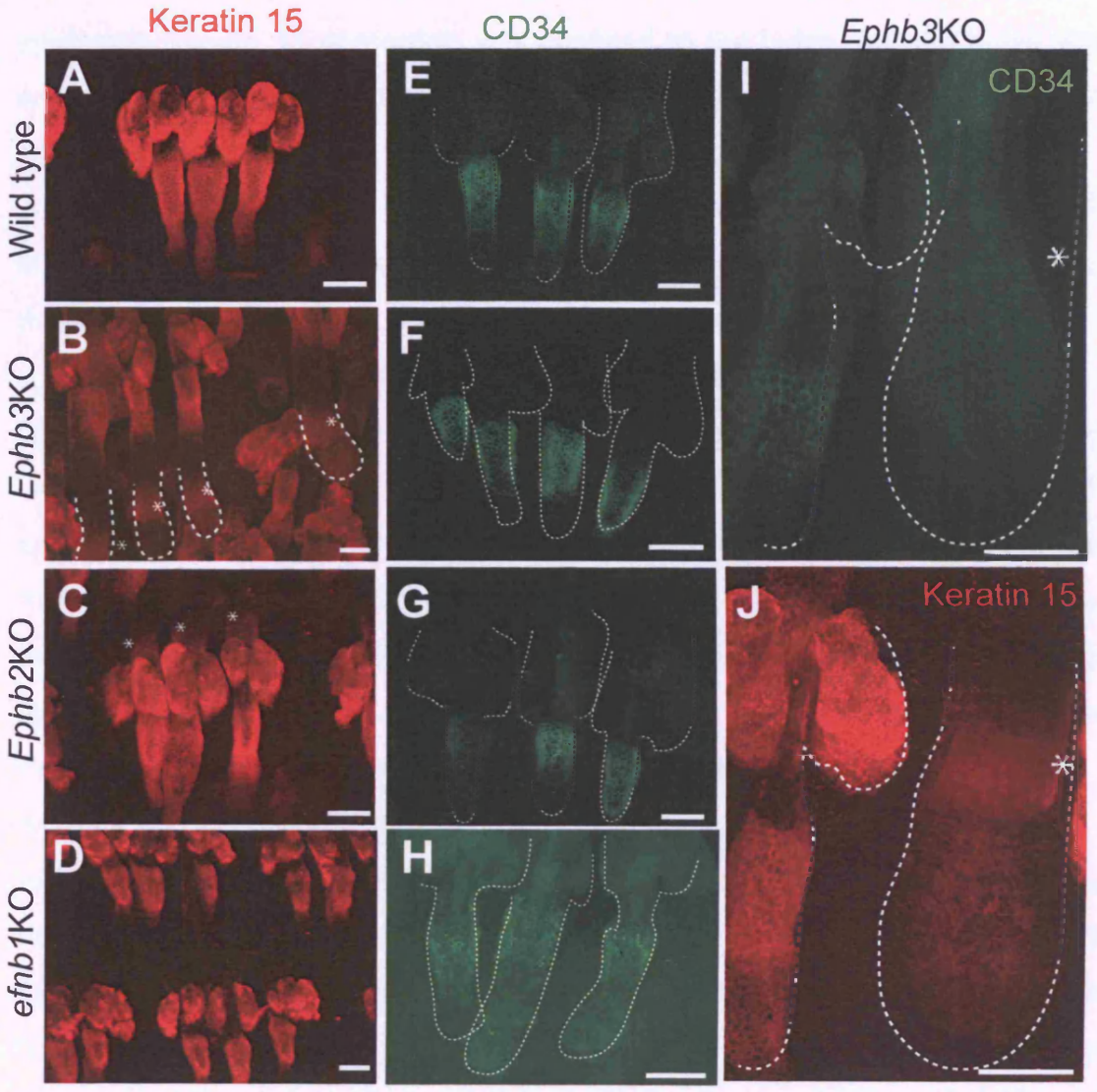

Figure 6.15- Loss of ephrin-B/EphB leads to changes in the bulge compartment (A-D and J) Immunolabelling of tail epidermal whole mounts with anti-keratin 15. (E-H and I) Immunolabelling of tail epidermal whole mounts with anti-CD34. In (B,I,J) dotted lines indicate the bulb of the HF and asterisks show the domain positive for keratin 15. Dotted lines in (E-H) demarcate the SG and HF. Scale bars: 100

another bulge marker (Figure 6.15 E-H). In EphB3 null epidermis there was an additional population of keratin 15 positive cells, lying just above the bulb (Figure 6.15 B, asterisks); these cells did not, however, express CD34 (Figure 6.15 I-J). In EphB2 null epidermis, there was a second keratin 15 positive population, but it was located in the infundibulum (Figure 6.15 C, asterisks). In ephrin-B1 null epidermis, keratin 15 expression was confined to the bulge, but the bulge was enlarged and it contained more keratin 15 positive cells than in wild type epidermis (Figure 6.15 D).

To obtain a quantitative measure of changes in the second bulge stem cell marker, CD34, I isolated cells from back skin and double labelled for CD34 and the α6 integrin subunit, a marker of undifferentiated basal keratinocytes in all epidermal regions (Figure 6.16 A-D; Blanpain et al., 2004). In EphB3 null and EphB2 null epidermis there was a decrease in the proportion of cells expressing the highest levels of CD34 (R4; Figure 6.16 B, C). In contrast, in ephrin-B1 null epidermis the proportion of cells with the highest levels of CD34 (R4) was markedly higher than in wild type epidermis (Figure 6.16 D). In all three mutants, there was an increase in α6 integrin levels, which was most striking in the case of ephrin-B1 (Figure 6.16 A-D). This experiment is representative of three independent experiments in which at least 2 mice were pooled.

As a further means of evaluating the stem cell compartment (see Chapter 5), I isolated keratinocytes from normal and mutant dorsal skin and plated equal numbers in culture at clonal density on a J2-3T3 feeder layer (Figure 6.17). Ephrin-B1 null keratinocytes had three times the colony forming efficiency of wild type keratinocytes (Figure 6.17 A, E). EphB3 null keratinocytes also showed increased colony formation (Figure 6.17 B, E). In contrast, EphB2 null keratinocytes had less than half the colony forming efficiency of wild type keratinocytes (Figure 6.17 C, E). The high colony forming efficiency of ephrin-B1 null keratinocytes correlated with thickening of the hair follicle bulge (Figure 6.16 D).

I conclude that disruption of EphB/ephrin-B signalling changes the size of the stem cell compartment and disturbs expression of stem cell markers. It is particularly striking that in EphB3 null follicles there were cells that were keratin

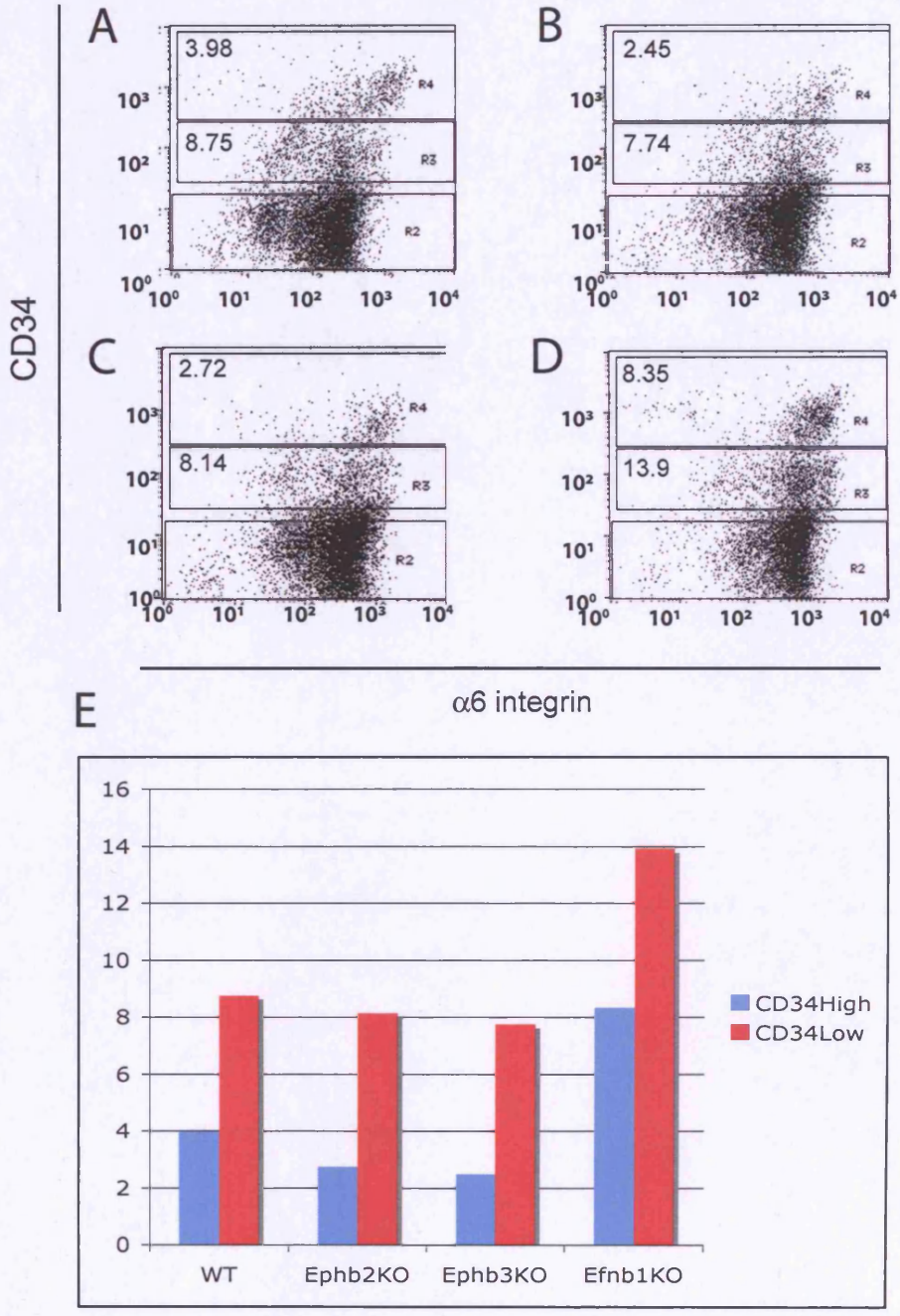

Figure 6.16- Loss of ephrin-B/EphB leads to changes in the bulge populations. Flow cytometry of basal keratinocytes (gated on basis of FSC and SSC) labelled with antibodies to CD34 and α6 integrin. (A) Wild type; (B) EphB3 null; (C) EphB2 null; (D) ephrin-B1 null.(E) The values for the CD34 High and Low populations were plotted from 3 experiments and are shown in the graph. This is representative of three separate experiments, in each of which cells from at least two wild-type or mutant mice were pooled.

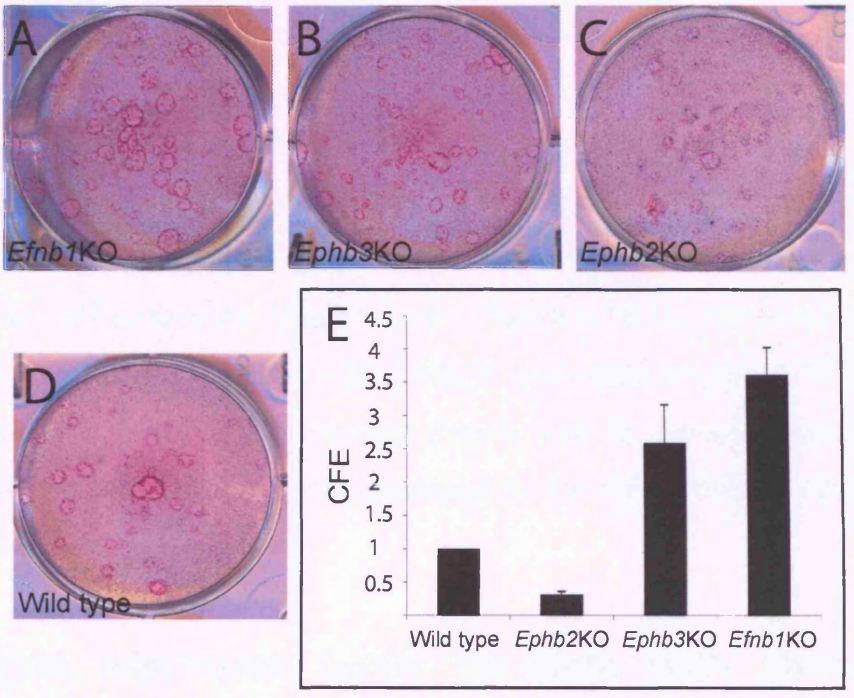

Figure 6.17- Loss of ephrin-B/EphB leads to changes in colony forming capacity in vitro. Colony forming efficiency of FACS sorted CD34/α6 double positive keratinocytes on J2-3T3 feeder layer. A-D: individual dishes stained with Rhodamine B. (E) Quantitation of data (mean ± S.D.) from three separate experiments, in each of which cells from triplicate wild-type or mutant mice were pooled. Values are standardised relative to a wild type value of 1.

15 positive and CD34 negative, and that whereas EphB2 and EphB3 null epidermal cells had similar CD34 expression there were marked differences in the colony forming efficiency. Thus, three well-established epidermal stem cell markers are not obligatorily co-expressed.

6.7- Eph/ephrin signalling modulates keratinocyte integrin levels *in vivo*

To investigate possible mechanisms by which EphB/ephrin-B signalling could alter epidermal patterning, I initially looked at integrin expression *in vivo*.

Analysis by whole mount labelling showed that the levels of the two main integrins expressed in basal keratinocytes, α6 integrin and β1 integrin, are increased in all three mutants (Figure 6.18). Loss of ephrin-B1 did not have a major effect on cell surface β1 integrin levels (Figure 6.18 L). However, loss of EphB3 led to a massive increase in β1 integrin expression (Figure 6.19 J) and EphB2 loss led to a more modest increase (Figure 6.18 K). Double labelling for Ki67 confirmed that proliferation was increased in the IFE of mutant epidermis (Figure 6.18 I-L).

6.8- Integrin expression levels correlate with abnormal localisation of pSMAD2/3 in mutant skin

It has been previously shown that missexpresion of α6β4 leads to impaired localisation of pSMAD2/3 (Owens et al., 2003). This prompted me to look at downstream effectors of TGFβ, pSMAD2 and 3, which are also known to be involved in skin homeostasis and development (Jamora et al., 2005). The pSMAD2 and 3 are effectors of non-canonical TGFβ, and in mouse skin are expressed throughout all the compartments in the basal layer (Figure 6.19). However, in the SG and bulb their localisation is cytoplasmic, whereas in the bulge and IFE it is nuclear (Figure 6.19 A, E). Interestingly, in EphB3 and EphB2 mutants all the pSMAD2/3 is localised in the cytoplasm, and the levels are increased in EphB2 mutants (see Figure 6.19 B, C, F-H). This does not occur in the ephrin-B1 mutant, which shows normal localisation (Figure 6.19 D, I). In addition, the pSMAD2/3 positive SG population is misslocalised and appears

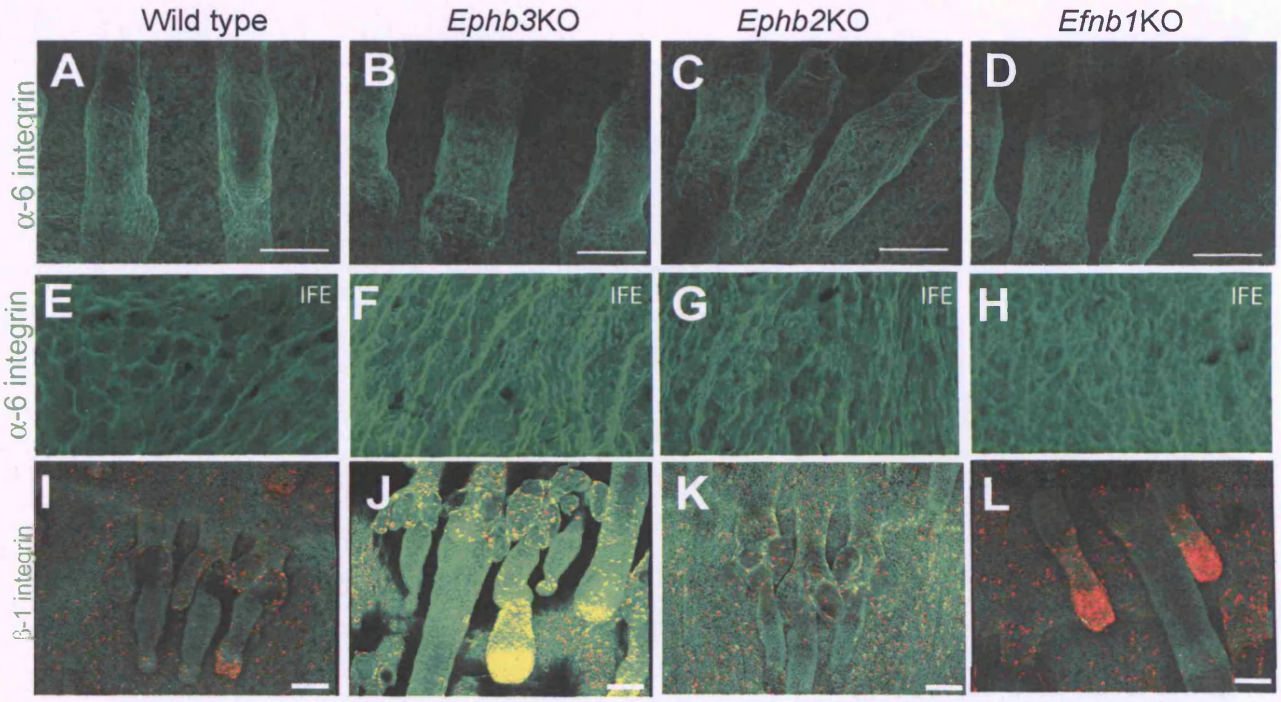

Figure 6.18- EphB/ephrin-B signalling modulates keratinocyte integrin levels *in vivo*. Tail epidermal whole mounts labelled with anti-α6 integrin (A-H) or anti-β1 integrin (green) and Ki67 (red) (I-L). Scale bars: 100 μm (A-D,I-L), 50 μm (E-H).

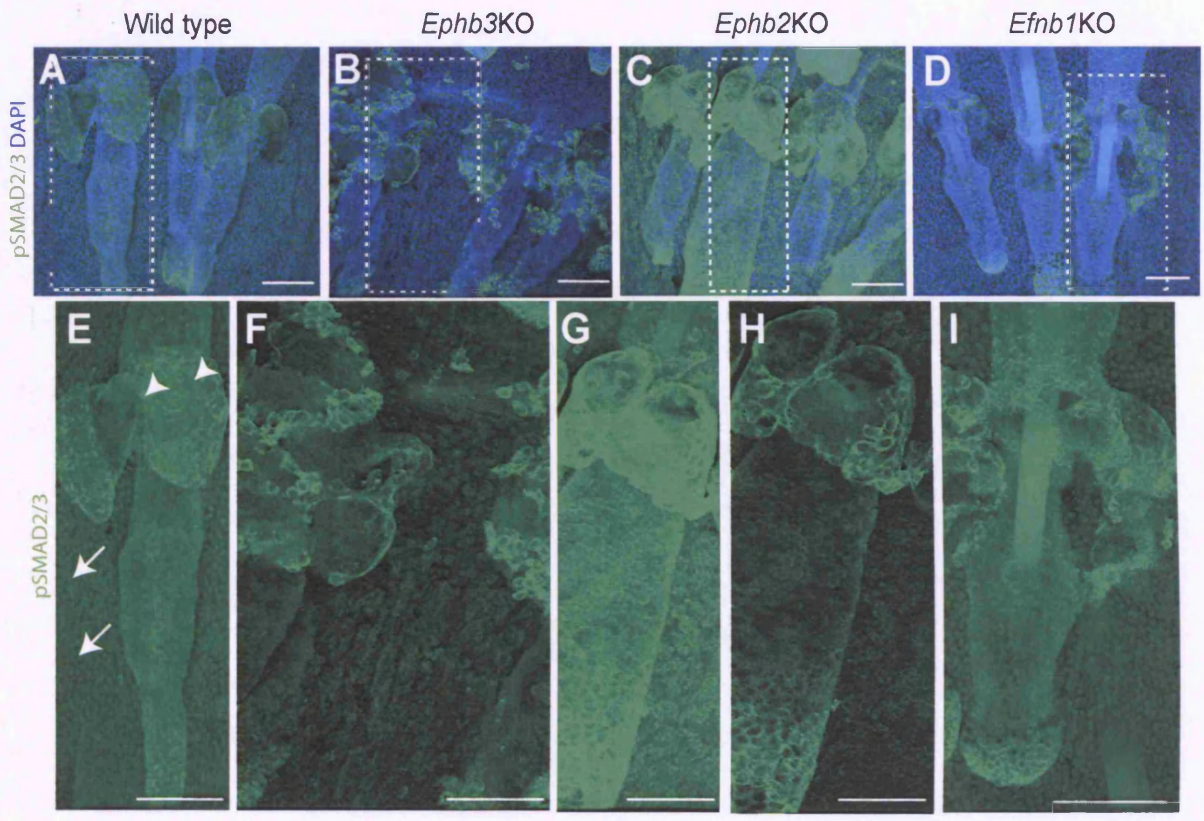

Figure 6.19- Loss of ephrin-B/EphB leads to abnormal pSMAD 2/3 expression. Tail epidermal whole mounts of wild type (A,E), EphB3 (B,F), EphB2 (C,G,H) and ephrin-B1 (D,I) null mice were immunolabelled with a pSMAD2/3 antibody . Note in (E) that pSMAD2/3 in WT is localised to the nucleus (arrow) in most IFE basal keratinocytes, whereas, in the SG it is localised in the cytoplasm (arrowhead).(G) Enlargement of the box in (C). (E) Enlargement of the box in (A), (F) Enlargement of the box in (B). (G,H) Enlargement of the box in (C) and (I) enlargement of the box in (D). Note that in H the original settings shown in G are lowered. Scale bars: 100 μm.

intermingled with IFE keratinocytes (Figure 6.19 B, F), coinciding with changes observed in sebocytes that are miss-localised (See Figure 6.6, 6.12). Further experiments are required to determine whether or not the changes in pSMAD2/3 are a direct consequence of altered integrin expression in this model.

6.9- Discussion

EphB receptors and ephrin-B ligands are expressed in distinct domains in skin

I have shown that EphB receptors and ephrin-B ligands are expressed in distinct domains in IFE and along the HF. As discussed earlier, the first step of HF morphogenesis after β-catenin activation is to "disturb" the existing boundaries, altering therefore the "balance" between proliferation and differentiation, and then the boundaries need to be re-established after the new hairs have been developed. In addition, the hair cycle progression also requires that patterning along the HF axis to be very dynamic. So in these two programmes, Eph/Ephrin signalling needs to be dynamically modulated. One or two cells are expressed at the most distal tip of the hair placode (E15.5) during development (Amelia Compagni, personal communication). It will be important to study further the pattern of expression of Eph and ephrin during embryonic hair formation to understand further how the pattern is set during early stages and look in the mutants to understand when the phenotypic defects arise.

EphB/ephrin-B signalling controls patterning in tail skin

The experiments described in this chapter show that EphB/ephrin-B signalling controls three types of patterning in mouse tail epidermis: hair follicle spacing, cell position along the proximo-distal follicle axis, and the location of cells undergoing different programmes of IFE differentiation. These phenotypes not only occurred in tail skin, but also in back skin. Disruption of EphB/ephrin-B signalling alters the localisation of melanocytes, both within the epidermis and the dermis, causes the appearance of sebocytes within the infundibulum and increases epidermal proliferation.

Loss of Eph/ephrin signalling: are changes cell-autonomous or niche related?

These changes may either be a direct consequence of disturbed signalling, or a response of cells to being placed in an abnormal environment. It is quite remarkable that when Eph/ephrin signalling was disrupted the tissue was still functional, the hair cycle continuing normally, even though patterning along the follicles was disturbed and the size and location of the stem cell compartment were altered. As the expression of these molecules is redundant, single deletions have a milder effect than when more than one gene is deleted. When I analysed the double mutant (*EphB3/EphB2*KO) I could clearly see that the phenotype was much more severe as it has been previously reported in the intestine (Batlle et al., 2002). Further studies addressing if there is compensation will be needed to clarify this issue.

There were different effects on deleting the ligand (ephrin-B1) or the receptors (EphB2 or 3, EphB3 deletion being more severe). In ephrin-B1 null tissue, the increase in proliferation is correlated with expansion of the bulge and of the CDP positive bulb population, possibly reflecting a failure of cells to migrate from these locations. In EphB3 null epidermis the increase in proliferation is correlated with a decrease in bulge cells, at evidenced by reduced numbers of CD34 positive cells, possibly reflecting increased departure from the niche.

The differential effects on CD34, keratin 15 and clonogenicity demonstrate that these three bulge stem cell markers do not co-segregate obligatorily, and that the epidermis can be maintained with greater or fewer stem cells. This calls into question whether the bulge stem cells have inherent stem cell characteristics or whether they are responding to their unique niche (Rendl et al., 2005). I can speculate that ephrin-B1 promotes differentiation while EphB3 preserves the stem cell compartment.

The changes in proliferation observed in the EphB3 and in the ephrin-B1 null skin are in agreement with data from the nervous system that Eph/ephrin signalling regulates proliferation (Holmberg et al., 2005; Conover et al., 2000). There are a number of possible mechanisms for increased proliferation, including the upregulation of integrins that occurs when EphB/ephrin-B signalling is disrupted.

In human IFE high β1 integrin expression is a marker of stem cells (Jones et al., 1995) and high levels of β1 integrins are required to maintain the human epidermal stem cell compartment *in vitro* (Zhu et al., 1999). Nevertheless, overexpression of β1 integrins does not result in increased proliferation in mouse epidermis (Gebhardt et al., 2006).

The parallel between integrin overexpression and pSMAD2/3 localisation is intriguing. It was previously shown that suprabasal expression of α6β4 leads to increased sensitivity to chemical carcinogenesis and the mechanism involving inhibition of pSMAD2/3 translocation to the nucleus (Owens et al., 2003). The Eph/ephrin mutant mice provide an important new approach to analysing the mechanisms linking α6β4 to impaired TGFβ sensitivity.

My results have close parallels with studies of intestinal epithelium. In the epidermis disruption of EphB/ephrin-B signalling affects the position of large groups of cells (entire hair follicles and parakeratotic scales), whereas in the intestine the effects are at the level of single cells (Batlle et al., 2002). The changes in proliferation and differentiation could be, in part, a secondary consequence of placing cells in different niches. However, it is clear that this is not the only mechanism as there are also cell autonomous consequences of altering Eph/ ephrin signalling. In the next chapter I will describe experiments with cultured keratinocytes in which I investigate the mechanism of action of Eph/ephrin signalling in controlling epidermal patterning.

Chapter 7- Mechanisms of Eph/ephrin signalling

Aims

In this Chapter I investigate possible mechanisms by which EphB/ephrin-B signalling could alter epidermal patterning, including effects on integrin expression and cell-cell adhesion. I also demonstrate that Eph/ephrin signalling modulates canonical Wnt signalling.

7.1- EphB/ephrin-B signalling modulate integrin expression

Analysis by whole mount labelling showed that the levels of the two main integrins expressed in basal keratinocytes, α6 integrin and β1 integrin are increased in all three mutants (Figure 6.18 in Chapter 6). In order to get quantitative data of these changes I performed flow cytometry analysis that confirmed that α6 integrin expression was increased in mutant epidermis (Figure 7.1), the effect being most dramatic in ephrin-B1 null keratinocytes (Figure 7.1 C). The loss of ephrin-B1 did not have a major effect on cell surface β1 integrin levels, whether judged by flow cytometry (Figure 7.1 F) or whole mount labelling (Figure 6.18 L). However, loss of EphB3 led to a massive increase in β1 integrin expression (Figure 6.18 J) and EphB2 loss led to a more modest increase (Figure 6.18 K). Double labelling for Ki67 confirmed that proliferation was increased in the IFE of mutant epidermis (Figure 6.18 I-L). It is interesting to note that in addition to the increase in the membrane levels of integrins (Figure 7.1), there were increased cytoplasmic levels, as revealed by immunofluorescence (Figure 6.18).

7.2- EphB/ephrin-B mutants have abnormal morphology

In order to investigate how EphB/ephrin-B signalling affected keratinocyte adhesion, I generated spontaneously immortalised keratinocyte lines from ephrin-B1, EphB3 and EphB2 null mice. Mutant keratinocytes displayed abnormal morphology, being very elongated with several lamellopodial protrusions

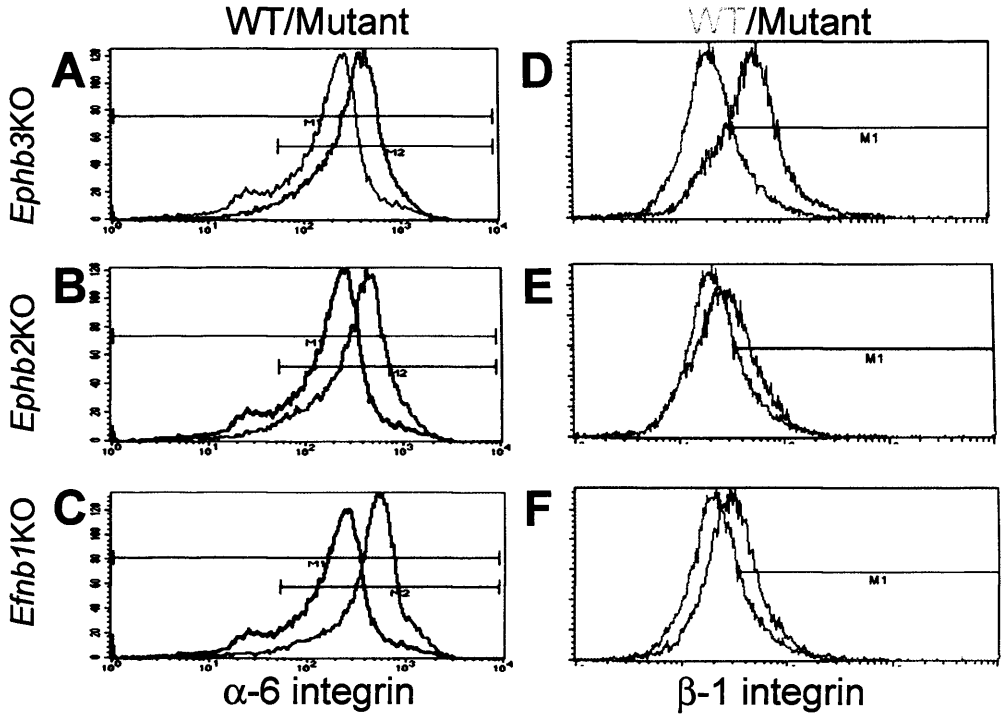

Figure 7.1- EphB/ephrin-B signalling modulates keratinocyte integrin levels. (A-F) Flow cytometry of basal keratinocytes (low forward side scatter (FSC) and small side scatter (SSC) were labelled with antibodies to α6 (A-C) or β1 (D-F) integrins. Wild type keratinocytes are shown in black (A-C) or green (D-F); mutant keratinocytes are shown in red (A-C) or black (D-F).

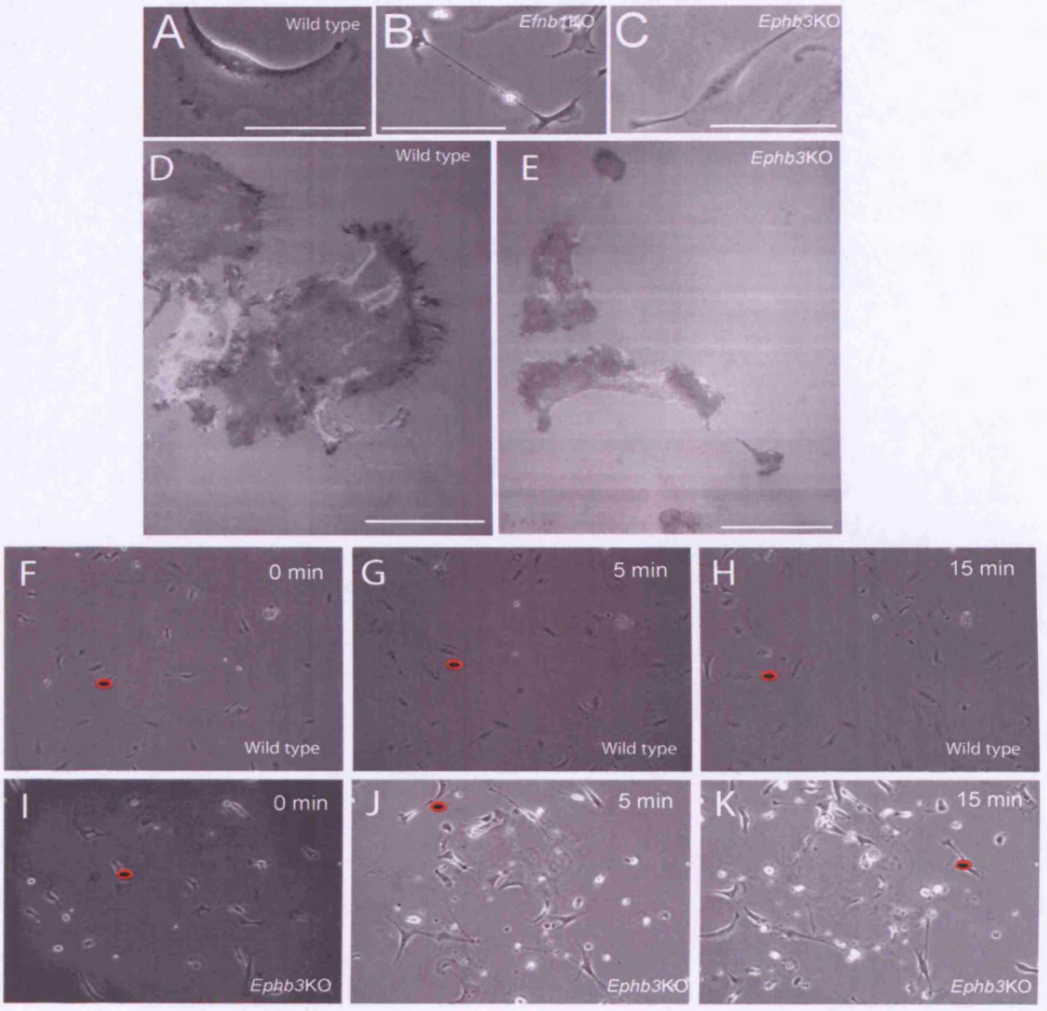

Figure 7.2 - EphB/ephrin-B mutants have abnormal morphology and motility. (A-C) Phase contrast micrographs of adherent cultured keratinocytes from wild-type (WT), EphB3 null (*Ephb3*KO) and ephrin-B1 null (*Efnb1*KO) mice. (D,E) Interference reflection microscopy (IRM) micrographs of adherent cultured keratinocytes from WT and *Ephb3*KO mice. (F-K) These pictures are stills of movies that recorded the motility of WT and *Ephb3*KO keratinocytes seeded at low density on collagen coated dishes for several hours. In order to compare between the motility of WT and *Ephb3*KO keratinocytes, and example is shown, in which the position of a cell of each type is indicated with a red dot and tracked in the time points at 0 min, 5 min and 15 min indicated. Scale bars: (A-C) 100μm, (D-E) 50μm

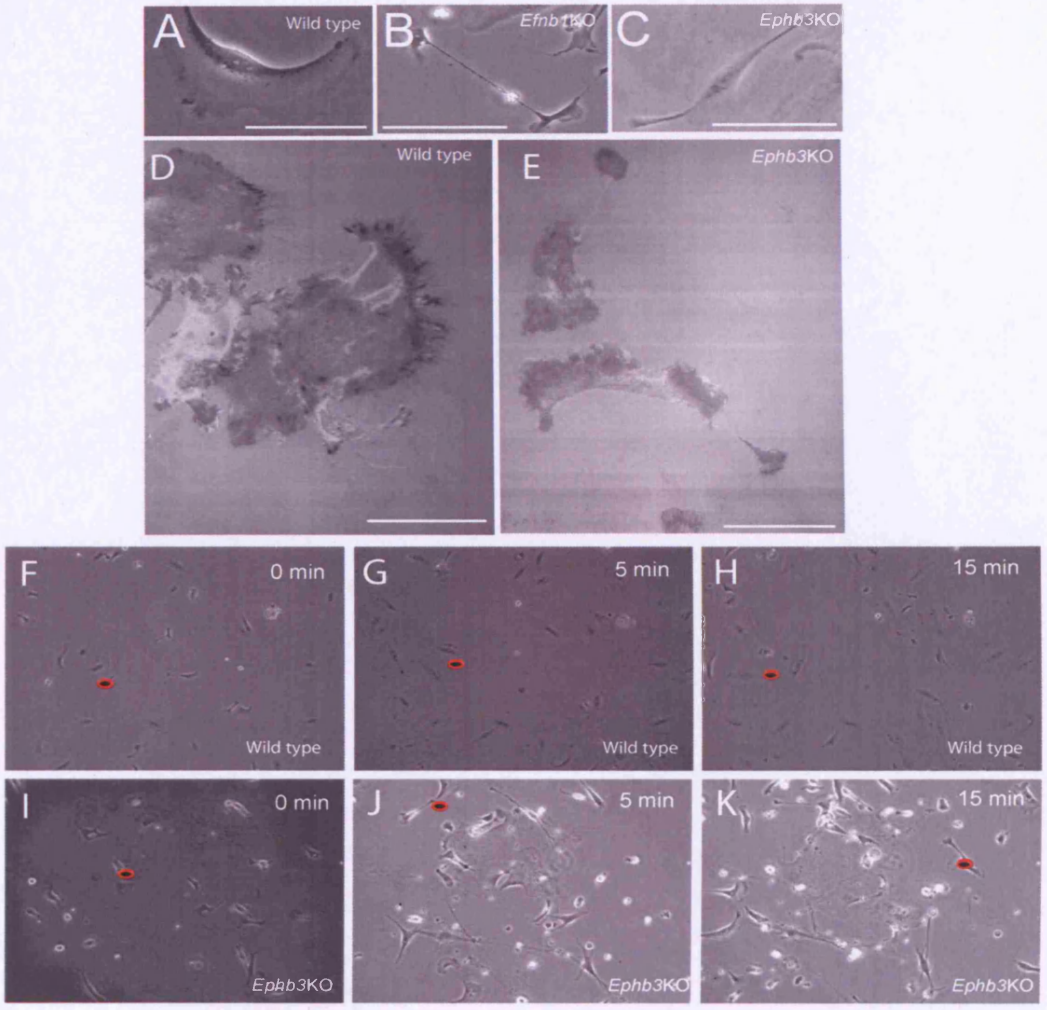

Figure 7.2 - EphB/ephrin-B mutants have abnormal morphology and motility. (A-C) Phase contrast micrographs of adherent cultured keratinocytes from wild-type (WT), EphB3 null (*Ephb3*KO) and ephrin-B1 null (*Efnb1*KO) mice. (D,E) Interference reflection microscopy (IRM) micrographs of adherent cultured keratinocytes from WT and *Ephb3*KO mice. (F-K) These pictures are stills of movies that recorded the motility of WT and *Ephb3*KO keratinocytes seeded at low density on collagen coated dishes for several hours. In order to compare between the motility of WT and *Ephb3*KO keratinocytes, and example is shown, in which the position of a cell of each type is indicated with a red dot and tracked in the time points at 0 min, 5 min and 15 min indicated. Scale bars: (A-C) 100μm, (D-E) 50μm

compared to wild-type keratinocytes (see Figure 7.2 A-E). They did not spread to the same extent as wild type keratinocytes; they formed elongated membrane protrusions (Figure 7.2), they had fewer contacts with the plate as indicated by the IRM micrographs (Figure 7.2). In addition, they exhibited increased motility. An example is shown in the stills of movies shown in Figure 7.2.

7.3- EphB/ephrin-B activation in keratinocytes *in vitro*

In order to look at the effects of the forward and reverse signalling, I set up an assay to activate Eph signalling in keratinocytes (Figure 7.3). Treatment of wild-type keratinocytes with recombinant ephrin-B1Fc and EphB3Fc proteins showed that activation of either forward or reverse signalling led to F-actin reorganisation, as described for intestinal cells (Figure 7.3; Batlle et al., 2002). Treatment with Fc only did not induce any changes in morphology and F-actin, which remained mainly cortical (Figure 7.3 A-C).

Stimulation of reverse signalling via treatment with EphB3Fc promoted cell detachment, with lamellopodia and fillopodia formation in wild-type cells (Figure 7.3 D-F). This was similar when forward signalling was stimulated with ephrin-B2Fc (Figure 7.3 J-L). In contrast, when forward signalling was activated with ephrin-B1Fc, cells formed lamellopodia in the first 10 min, but after 30 min they appeared to cluster (Figure 7.3 G-I).

To validate this assay I monitored receptor or ligand clustering upon stimulation. Two examples are shown in Figure 7.4 and 7.5. Cells were either treated with the ligand or the receptor and were then immunolabelled for either the receptor or the ligand that was being activated (see Figures 7.4 and 7.5). No clustering was observed when cells were stimulated alone with Fc or non-clustered ligand or receptor (see Figure 7.4 A and 7.5 A). Small clusters were observed when cells were stimulated (Figure 7.4 B, F and C and 7.5 C, D). Interestingly, when I activated β-catenin either via Wnt3A or activating ΔNβ-cateninER with 4OHT the degree of clustering seemed much increased, and some internalisation was observed (see Figure 7.4 C, D, E and 7.5 E-G).

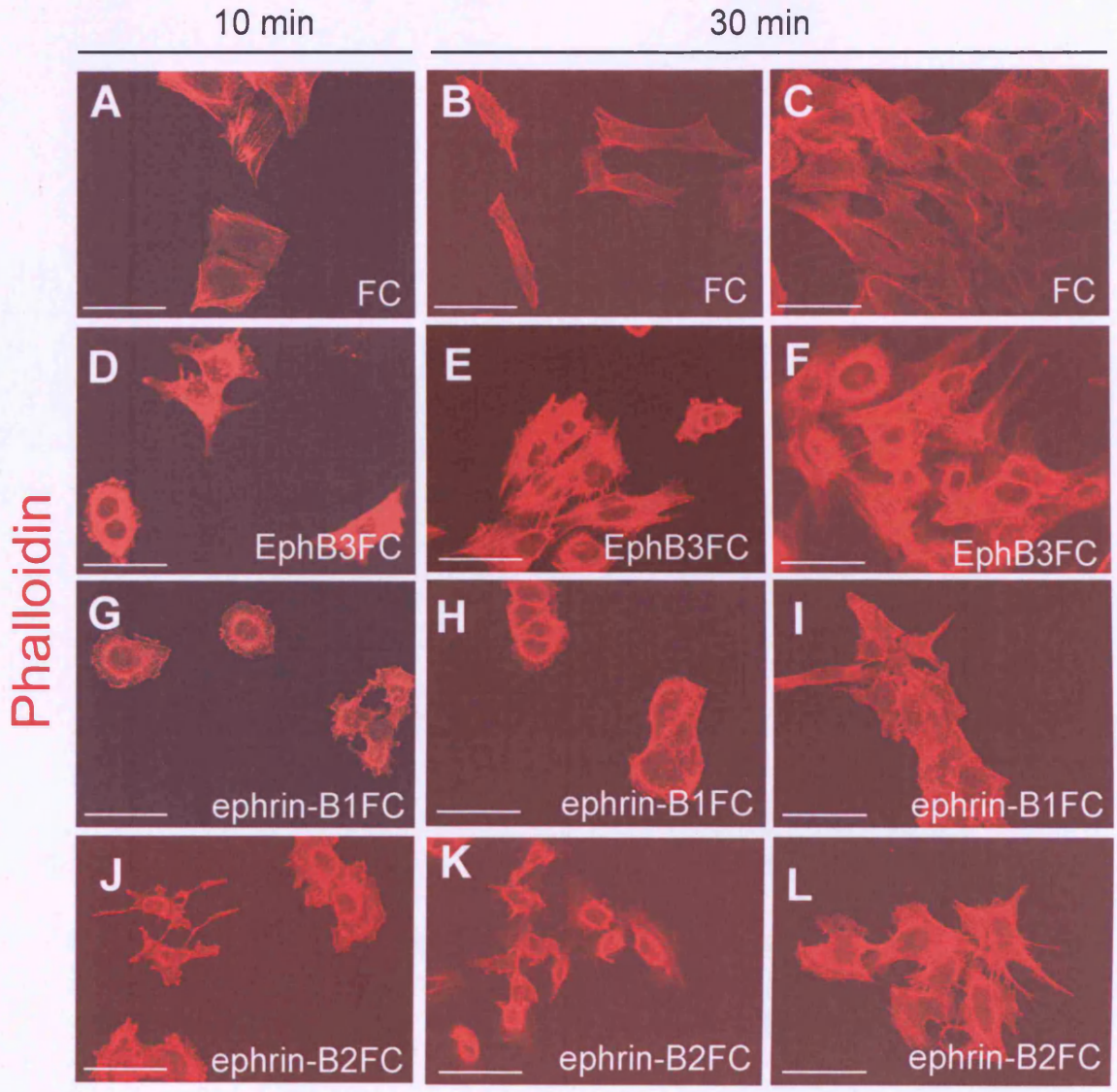

Figure 7.3- EphB/ephrin-B signalling induces keratinocyte F-actin remodelling and changes in cell shape. (A-L) Wild type keratinocytes plated at low density on Collagen I coated tissue culture dishes and left to attach overnight. Cells were stimulated with either FC alone (A-C), pre-clustered recombinant EphB3Fc (D-F), pre-clustered recombinant ephrin-B1FC (G-I) or recombinant ephrin-B2FC (J-L) for 10 min (A,D,E,G,J) or 30 min (B,C,E,F,H,I,K,L). Cells were fixed and then stained with Phalloidin-TRITC. Scale bars: 100 μm.

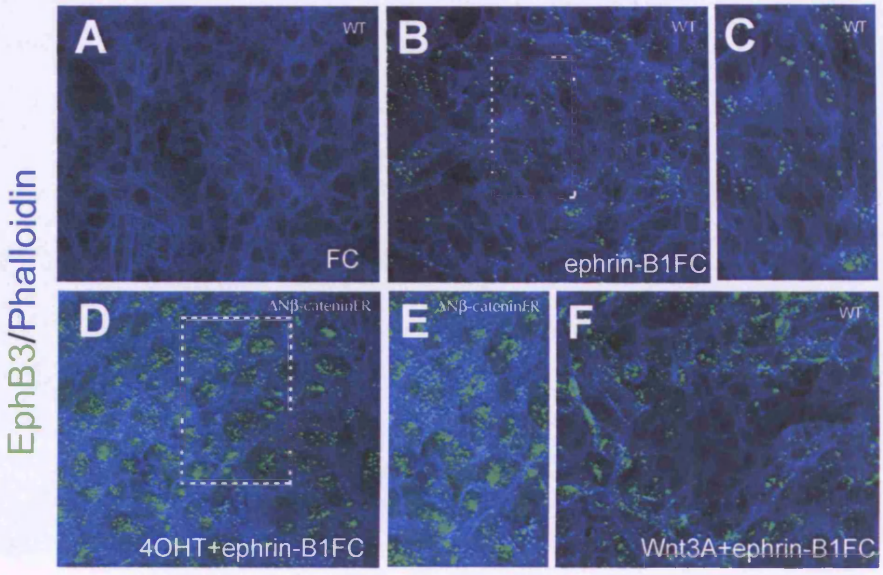

Figure 7.4- Stimulation with ephrin-B1Fc induces EphB3 clustering in keratinocytes. Wild type (A-C,F) or ΔNβ-cateninER (D,E) keratinocytes were stimulated with either FC alone (A), pre-clustered recombinant ephrin-b1Fc alone (B,C), or in combination with 4OHT (D,E) or in combination with Wnt3A (F) for 2 days. Cells were fixed and then immunolabelled with anti-EphB3 antibody (Green) and Phalloidin-633 (blue).

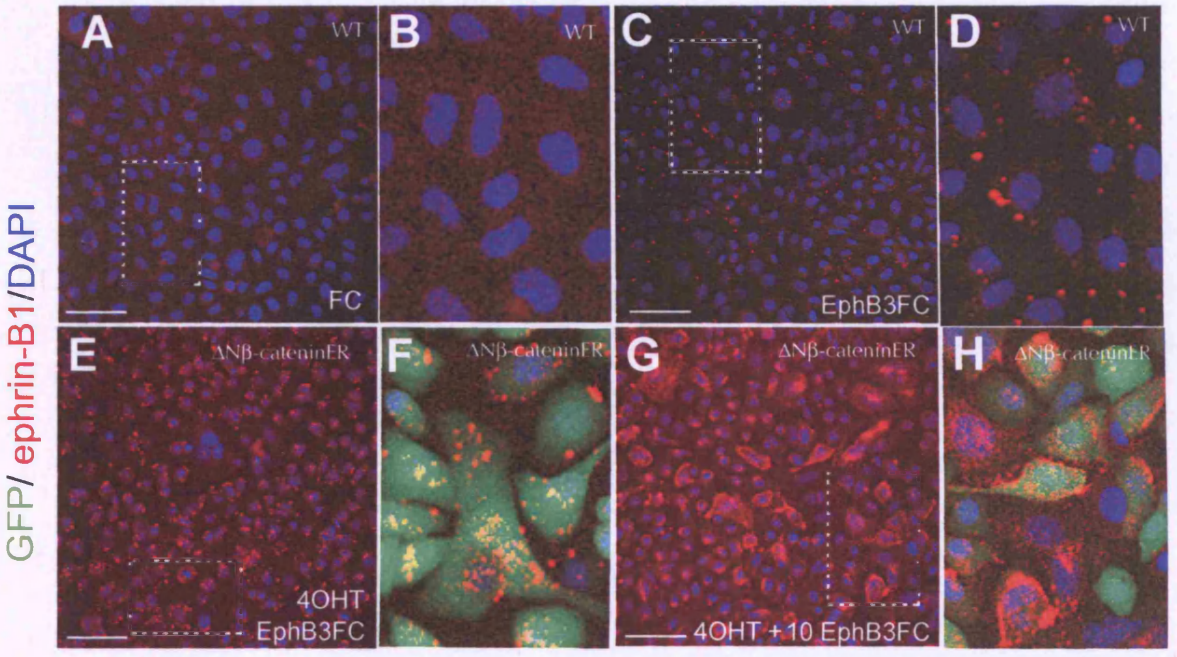

Figure 7.5- Stimulation with EphB3Fc induces ephrin-B1 clustering in keratinocytes. Wild type keratinocytes (A-D) or ΔNβ-cateninER keratinocytes (E-H) were stimulated with either FC alone (A,B), pre-clustered recombinant EphB3Fc alone (C,D), or in combination with 4OHT (E-H) or 10x more concentrated EphB3Fc with 4OHT (G,H) for 2 days. Cells were fixed and then immunolabelled with anti-ephrin-B1 antibody. Red corresponds to ephrin-B1 expression, blue correspond to the nuclear counterstain DAPI and green show EGFP expression. Scale bars; 50μm.

7.4- β-catenin drives expression of EphB 3 and ephrin-B1

In Chapter 5, the array analysis of β-catenin activation signature genes showed that ephrin-B1 was up-regulated 2.3 fold, and EphB3 was 1.6 fold. I was intrigued by the notion that β-catenin might control cell positioning in the epidermis by controlling the expression of Eph receptors and Ephrin ligands. To test whether β-catenin does indeed upregulate Eph/ephrin, I looked at the expression of ephrin-B1 and EphB3 in β-catenin driven hair formation *in vivo*. The first response of β-catenin is to drive proliferation. I could observe clusters of proliferative cells at early stages of β-catenin activation (see Figure 4.8 and 4.9 in Chapter 4). When I looked at the expression of ephrin-B1 and EphB3 with conventional sections or whole-mount immunolabelling, I could see that at initial stages of β-catenin activation, there was increased expression of ephrin-B1 and EphB3. As treatment progressed, I could observed that the initial bumps, or clusters, of proliferating cells contained cells with high expression of ephrin-B1 (Figure 7.6 B, D) and EphB3 (Figure 7.6 A, C). As I had observed previously (Figure 5.9), as hair formation continues, the expression of both the receptor and the ligand are expanded along the new follicles (Fig 7.6 E, F).

7.5- Loss of ephrin-B/EphB signalling leads to abnormal β-catenin levels

I next wondered whether Eph signalling modulates Wnt responsiveness. I first looked at the localisation of β-catenin in mutant epidermis. In wild-type skin, β-catenin is localised mainly to cell-cell borders (Figure 7.7 A,B) and nuclear β-catenin is only detectable in a subpopulation of keratinocytes in the matrix at the base of the hair follicles (Figure 7.8 A; DasGupta and Fuchs, 1999; Niemann et al., 2002). Interestingly, I observed that the levels of membrane-associated β-catenin were higher in both the *Efnb1*KO and *EphB3*KO follicles than wild-type follicles (Figure 7.7 D and H). In *Efnb1*KO keratinocytes the increased levels of β-catenin were largely cytoplasmic or in the nucleus (Figure 7.7 C, D, 7.8 D, 7.9 D, E). In the case of *EphB3*KO follicles, I could observe high levels at the membrane

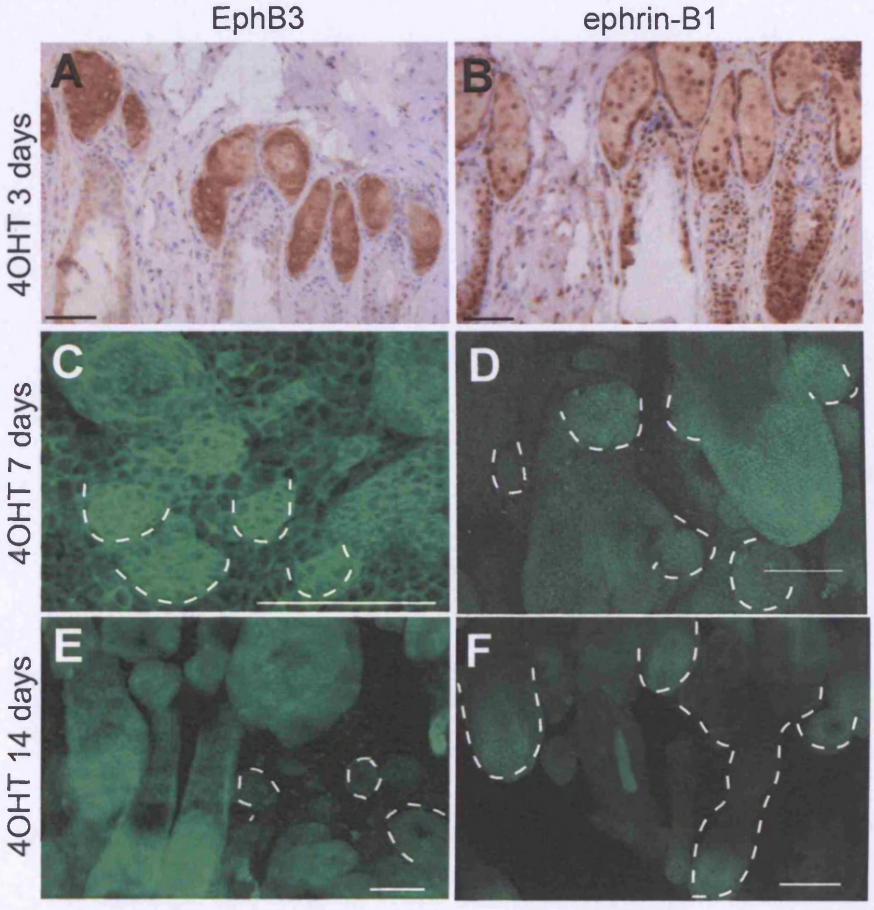

Figure 7.6- β-catenin stimulation induces ephrin-B1 and EphB3 expression in sites of ectopic hair follcile formation. Sections of dorsal skin (A-B) or tail whole-mounts (C-F) of K14ΔNβ-cateninER mice were treated for the indicated days with a 1.5 mg dose of 4OHT. Immunolabelling with anti-EphB3 (A,C,E) or anti-ephrin-B1 (B,D,F) antibodies. Scale bars: 100μm

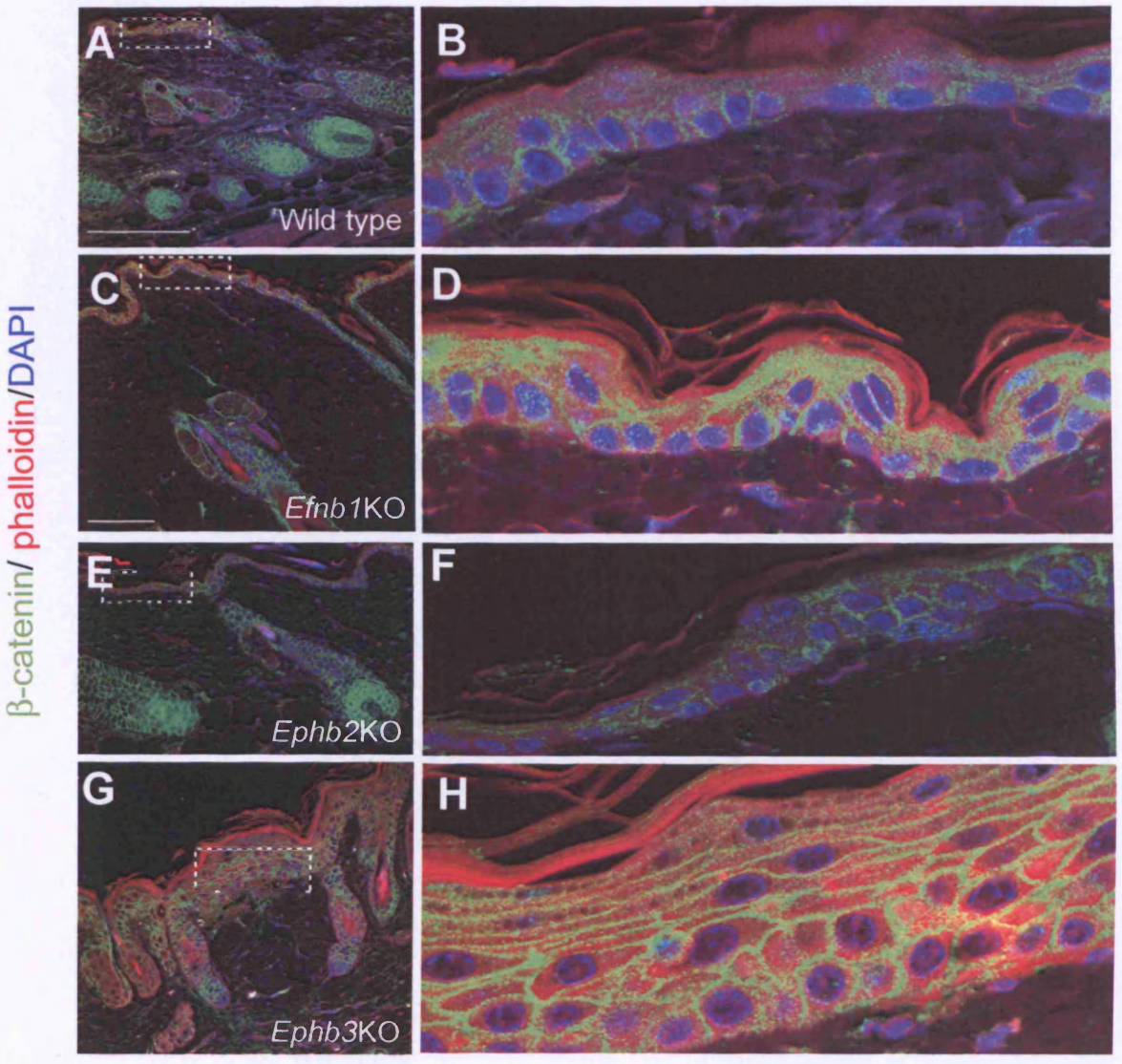

Figure 7.7- Loss of ephrin-B/EphB leads to abnormal β-catenin levels in IFE. Sections of dorsal skin of wild type (A,B), ephrin-B1 null (*Efnb1*KO) (C,D), EphB2 null (*Ephb2*KO) (E,F) and EphB3 null (*Ephb3*KO) (G,H) mice were immunolabelled with a β-catenin antibody. Blue corresponds to DAPI positive nuclei, green corresponds to β-catenin and red corresponds to F-actin stained with Phalloidin TRITC. (B,D,F,H) Enlargements of boxes in A,C,E,G respectively showing a high magnification of the IFE. Scale bars: 100 μm.

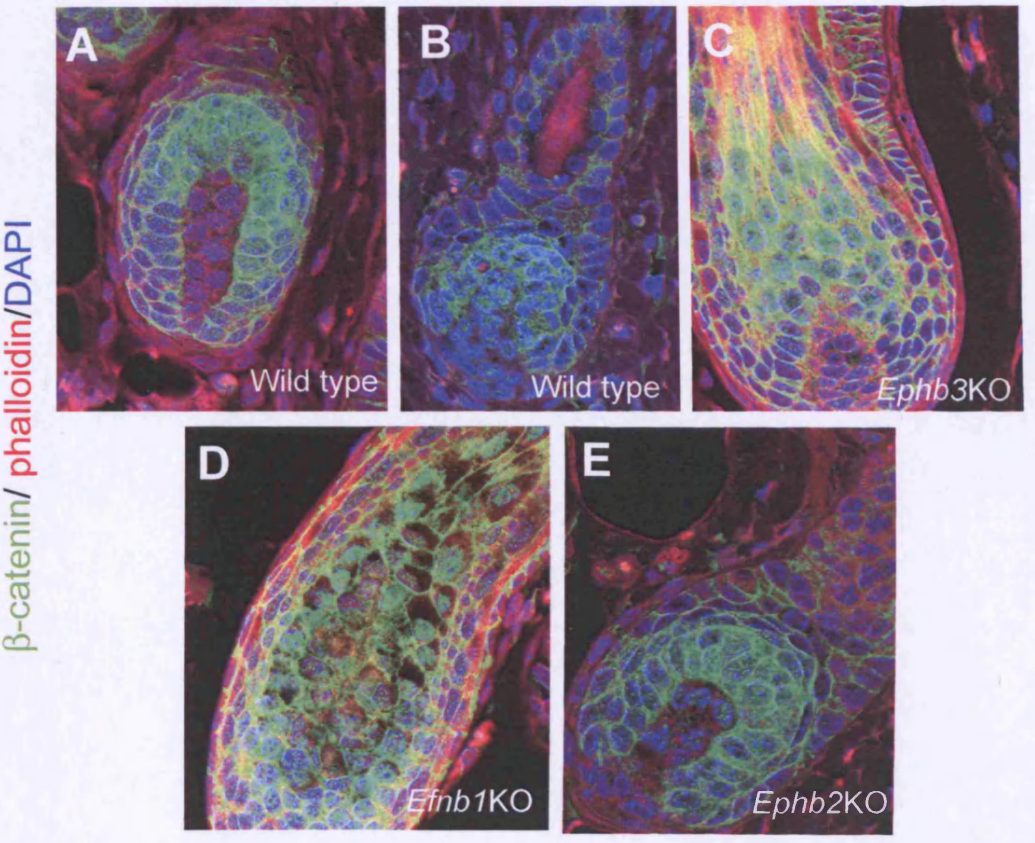

Figure 7.8 - Loss of ephrin-B/EphB leads to increased β-catenin levels in the hair follicle bulb. Sections of dorsal skin of wild type (A,B), ephrin-B1 null (*Efnb1*KO) (D), EphB2 null (*Ephb2*KO (E) and EphB3 null (*Ephb3*KO) (C) mice were immunolabelled with a β-catenin antibody. Blue corresponds to DAPI positive nuclei, green corresponds to β-catenin and red corresponds to F-actin stained with Phalloidin TRITC.Scale bars: 100 μm.

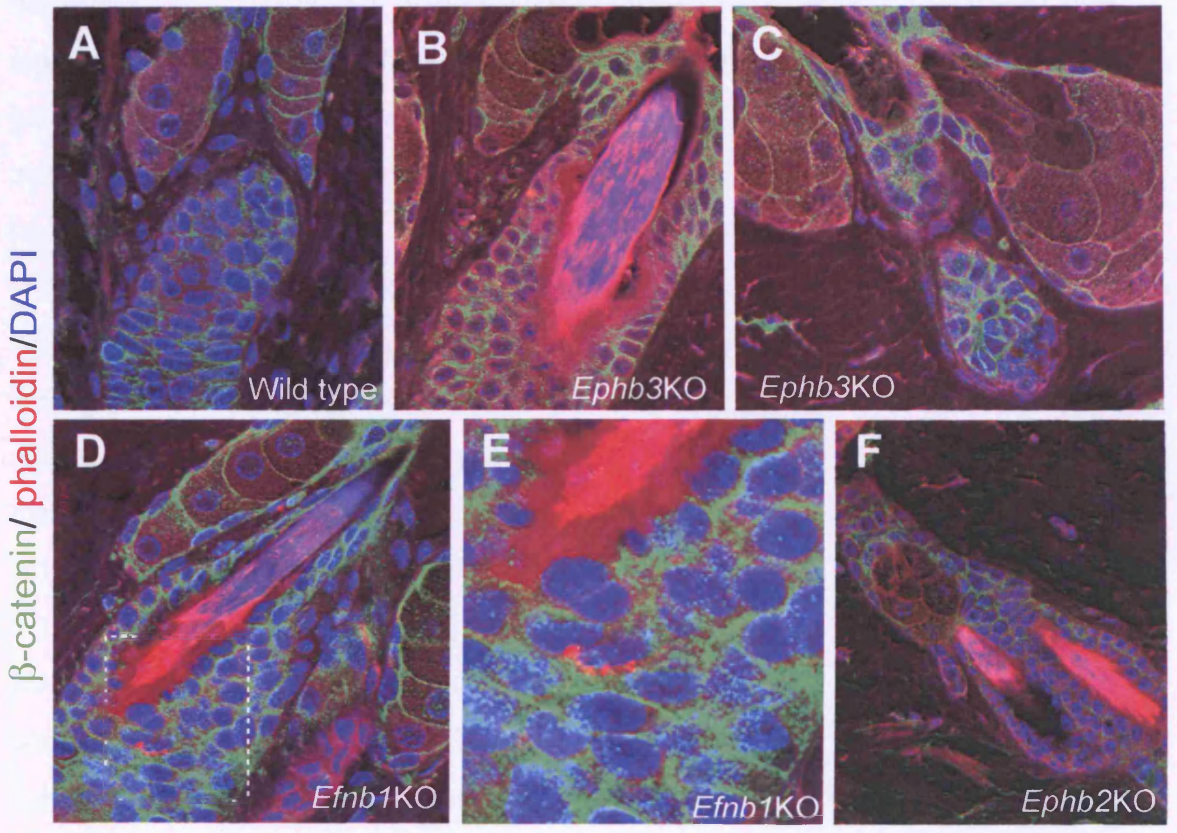

Figure 7.9 - Loss of ephrin-B/EphB leads to increased β-catenin levels in the hair follicle bulge. Sections of dorsal skin of wild type (A), ephrin-B1 null (*Efnb1*KO) (D,E), EphB2 null (*Ephb2*KO) (F) and EphB3 null (*Ephb3*KO) (B,C) mice were immunolabelled with a β-catenin antibody.Blue corresponds to DAPI positive nuclei, green corresponds to β-catenin and red corresponds to F-actin stained with Phalloidin TRITC. (E) is an enlargement of the box in D. Scale bars: 100 μm.

(Figure 7.7 G, H; 7.8 C and 7.9 B,C). The same effects were seen in immortalised cells cultured from mutant epidermis (see Figure 7.10).

7.6- EphB/ephrin-B signalling modulate β-catenin transcriptional activity

To investigate whether loss of Eph/ephrin resulted in increased β-catenin dependent transcriptional activity, I transfected keratinocytes with the TOPFLASH reporter, in which an enhancer with multiple Lef1/Tcf binding sites drives luciferase expression (van de Wetering et al., 1997). I activated β-catenin by treating the cells with recombinant Wnt3A. Since the cells had not been transfected with exogenous Lef/Tcf or activated β-catenin (Zhu and Watt, 1999; Niemann et al., 2002), there was only a small increase in luciferase activity in wild type keratinocytes treated with Wnt3A, as reported previously (Lowry et al., 2005). However, in both ephrin-B1 and EphB3 null keratinocytes transcriptional activation by Wnt3A was significantly increased (Figure 7.10 A).

Interestingly, when I stimulated either reverse (EphB3-Fc) or forward (ephrin-B1 Fc) signalling in the mutant keratinocytes there was a super induction of TOPFLASH activity (See Figure 7.11).

These results show that the increased levels of β-catenin in mutant keratinocytes correlate with an increase of the β-catenin transcriptional activity. In addition, Eph/ephrin signalling can modulate β-catenin transcriptional responsiveness.

7.7- Effects of EphB/ephrin-B signalling on β-catenin induced proliferation

In order to start dissecting what part of the β-catenin response was modulated by Eph signalling, I first analysed proliferation of stimulated cells, for a period of 7 days. As expected, Wnt3A-treated wild-type cells show increased proliferation (Figure 7.12). Interestingly, proliferation was reduced in cells co-stimulated with Wnt3A and EphrinB1-FC and EphB3-Fc. This may explain why β-catenin can either drive proliferation or differentiation. In this case, it appears that Eph/ephrin signalling reduces the β-catenin induced proliferation in wild-type.

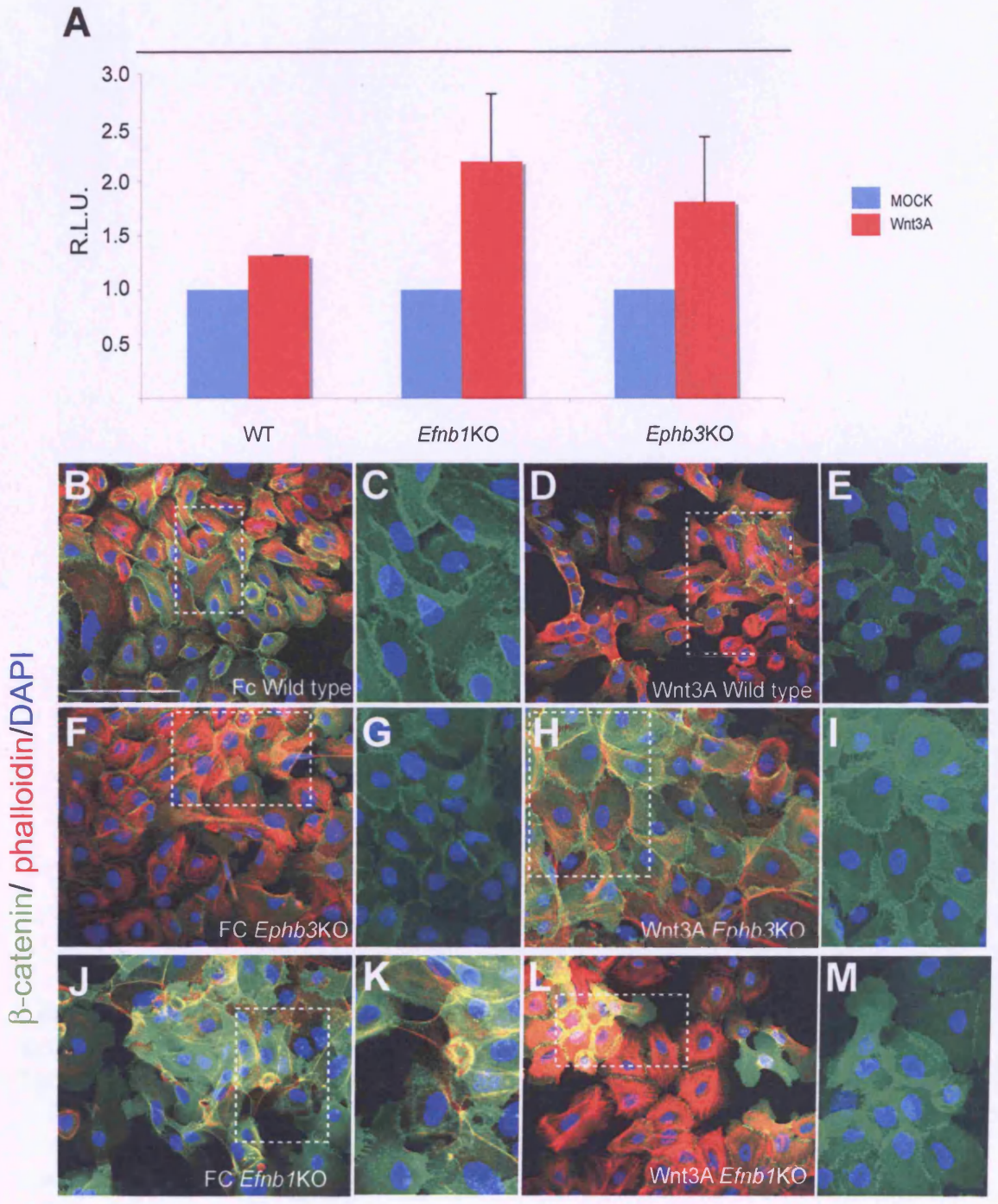

Figure 7.10- Abnormal levels of β-catenin in mutant keratinocytes lead to increased transcriptional activity. (A) Cultured keratinocytes from wild-type (WT), EphB3 null (*Ephb3*KO) and ephrin-B1 null (*Efnb1*KO) mice were transiently transfected with TOPFLASH in the presence or absence (Mock) of Wnt3A. Relative light units (RLU) are shown. Bars represent means of at least 3 replicate samples in up to 4 experiments ± S.D. (B-M) Wild type (B-E), *Ephb3*KO (F-I) or *EfnB1*KO (J-M) keratinocytes were stimulated with either FC alone (B,C,F,G,J,K), or with Wnt3A (D,E,H,I,L,M) for 2 days. Cells were fixed and then immunolabelled with an anti-β-catenin antibody (green), DAPI (blue) and phalloidin (red). C,G,K,E,I,M Enlargements of boxes in B,F,J,D,L, respectively. Scale bars: 50μm

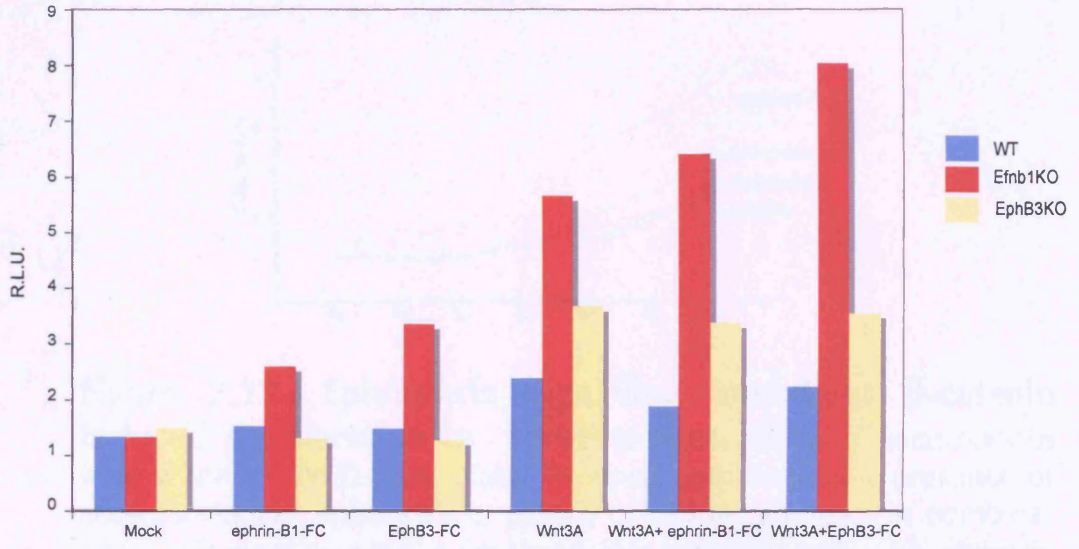

Figure 7.11 - Eph/ephrin signalling modulates β-catenin transcriptional activity in keratinocytes. Cultured keratinocytes from wild-type (WT) (blue), EphB3 null (yellow) and ephrin-B1 null mice (red) were transiently transfected with TOPFLASH in the presence of (Mock of CHAPS buffer), ephrin-B1Fc, EphB3Fc, Wnt3A (diluted in CHAPS buffer) alone or in combination. Relative light units (RLU) mean values are shown. This experiment was performed twice.

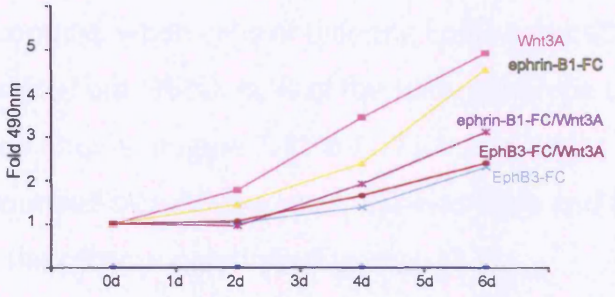

Figure 7.12- Eph/ephrin signalling modulates β-catenin induced proliferation in keratinocytes. Cultured keratinocytes from wild-type (WT) were plated in equal numbers in the presence or absence (Mock), ephrin-B1Fc, EphB3Fc, Wnt3A, alone or in combination. Cells were counted at the timepoints indicated with a colorimetric assay at 490 nm. This experiment was performed twice and the data shown in this figure is from one experiment

7.8- EphB/ephrin-B signalling modulates keratinocyte mixing

To see whether the changes in cell-cell interaction and adhesion and β-catenin levels would affect cell patterning *in vitro*, I introduced a retroviral vector encoding GFP into wild type and mutant cells and then performed mixing experiments with GFP positive and negative populations, as described in the Materials and Methods section (Figure 7.13). When wild type GFP positive cells were mixed with wild type GFP negative cells, the two populations were completely intermingled (Figure 7.13 A). I consistently observed 75 % of the cells intermingled and 25% of the rest were next to one or two GFP positive cells (see Figure 7.4 13,F). In contrast, when cells of differing EphB/ephrin-B1 status were mixed, they always sorted out (96%), cells of the same genotype clustering preferentially with one another (Figure 7.13 B-D, F). Interestingly, when a single mutant cell was surrounded by wild-type cells this was large and flattened and tend to repulse from the other populations (Figure 7.13 E).

These results show that disruption of EphB/ephrin-B signalling changes the adhesive properties of the cells, such that populations that differ in EphB/ephrin-B expression (Figure 7.13) will tend to segregate from one another. This in turn could explain the effects of EphB/ephrin-B1 ablation on epidermal patterning.

7.9- Effects of Eph/ephrin signalling on β-catenin induced cell mixing

If Eph/ ephrin signalling plays a role in determining the sites of β-catenin induced HF formation, I would expect to see effects in mixing experiments in culture. I therefore mixed cell lines previously generated from the ΔNβ-catenin ER mice and wild-type keratinocytes. I observed that when activated β-catenin with 4OHT the responding cells clustered more with each-other in a dose-dependent fashion (Figure 7.14 A-D).

I next combined β-catenin activation (via 4OHT treatment or Wnt3A treatment) and activation of reverse (with EphB3Fc) or forward (with ephrin-B1Fc) signalling. Activation of reverse signalling led to an enhanced β-catenin response (cell clustering) (Figure 7.14 C, D) that coincided with enhanced EphrinB1 clustering

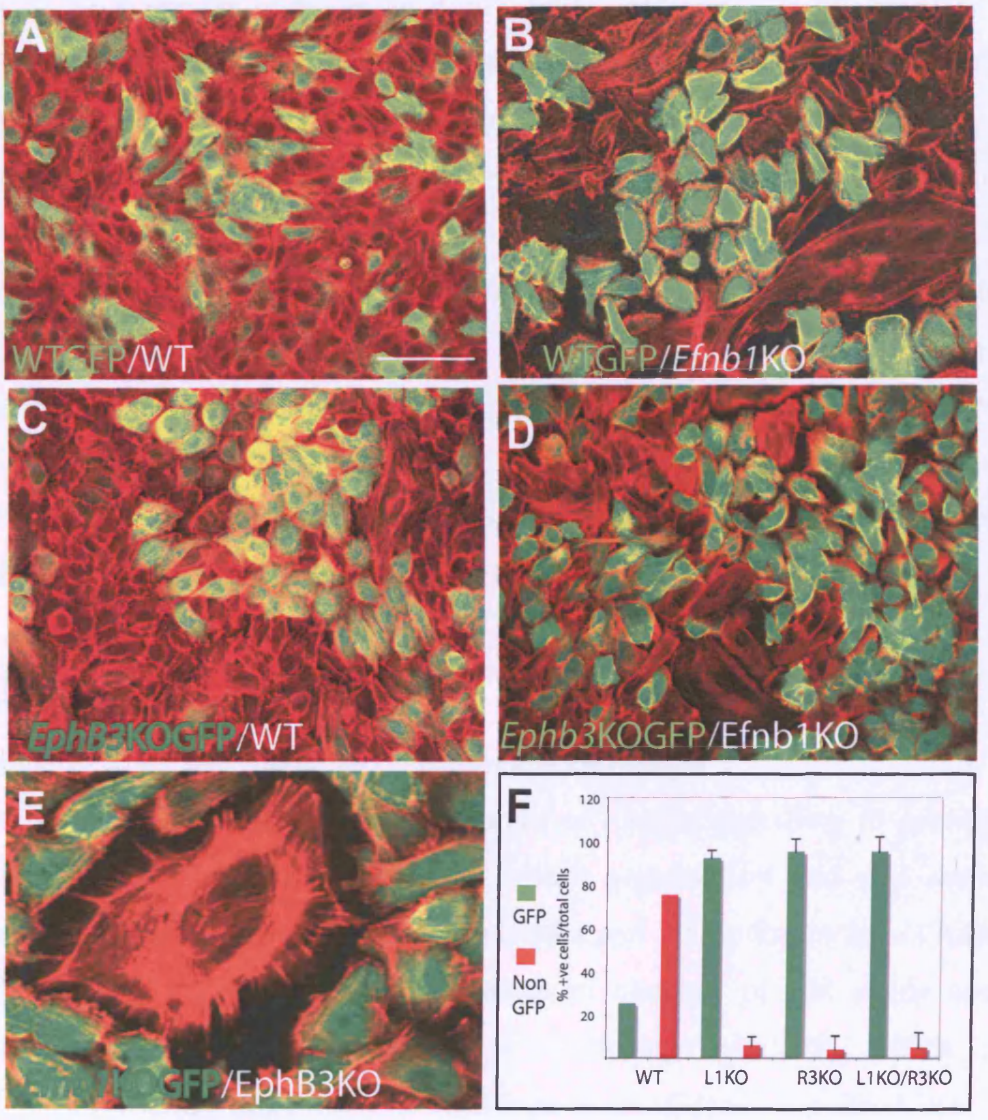

Figure 7.13- EphB/ephrin-B signalling modulates keratinocyte mixing. Cell sorting was examined by mixing GFP transduced and unlabelled keratinocytes of the genotypes shown. Polymerised actin was detected with Phalloidin-Alexa 594 (red). (F) Cell grouping was calculated by scoring 500 cells per condition as either being next to a GFP cell (green) or not (red). These results represent four independent experiment in triplicate are shown. Error bar indicates the SD values per condition. Scale bars: 100 μm (A-E).

on the cell membrane (see Figure 7.5). The same response was also observed when cells were treated with Wnt3A (Figure 7.4).

In order to validate these observations, I performed the same experiment with *Efnb1*KO and *EphB3*KO cells and wild-type or ΔNβ-cateninER cells (Figure 7.14 and look at the summary of the experiments shown in Table 7.1). As previously observed, cells with different 'ephrin status' segregated from one another, with either *Efnb1*KO or *EphB3*KO cells tending to segregate from WT cells (see Figure 7.14 E and G; Table 7.1). When I treated a mixture of *EphB3*KO and WT cells with Wnt3A, WT cells clustered as previously described (Figure 7.13). However, the *EphB3*KO cells did not clustered and were generally found as single cells with enlarged morphology (Figure 7.14 F and J; Table 7.1). The same phenomenon was observed when reverse signalling was activated with EphB3Fc (see figure 7.14 J; Table 7.1). When I performed the same experiment with *Efnb1*KO cells, I could still observe cell clustering, but the clusters were larger and less compacted compared to wild-type cells (Figure 7.14 G, H, I; Table 7.1).

7.10- Discussion

EphB/ephrin-B signalling modulate adhesion and cell shape

I have shown that activation of either forward or reverse signalling in primary mouse keratinocytes leads to changes in F-actin organisation and cell shape changes, predominantly formation of lamellopodia and fillopodia. In turn, I have found that loss of Eph/ephrin signalling leads to changes of cell shape and spreading. These changes are reminiscent of situations in which the activity of Rho GTPases is being modulated, in particular Rac1, Cdc42 and RhoA (**Hall, 2000**). These results in keratinocytes are in agreement with previous reports showing a role of Eph/ephrin in cystoskeletal remodelling and GTPase activation (Batlle et al., 2002; Noren and Pasquale, 2004). Further analyses of changes in Rho GTPases activity are required to elucidate the molecular mechanism of these changes.

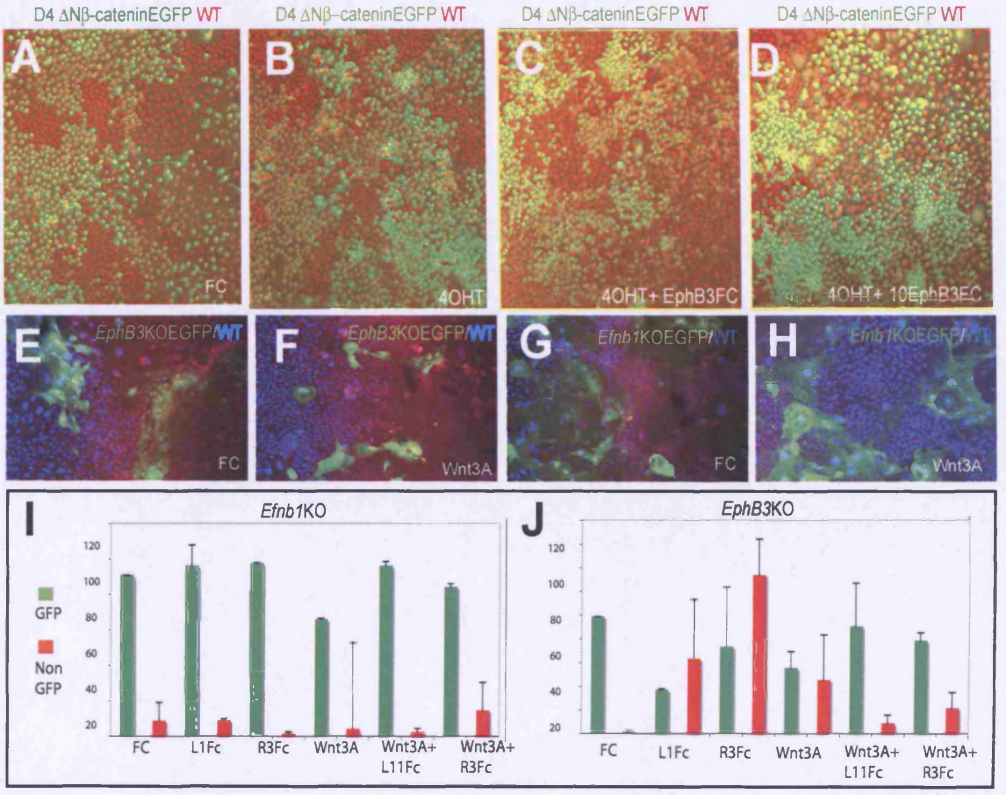

Figure 7.14- β-catenin modulates keratinocyte mixing in vitro. Cultured keratinocytes infected with EGFP from wild-type (WT), ΔNβ–cateninER (D4), EphB3 null and ephrin-B1 null mice were mixed and plated with equal numbers with non-GFP infected cells. Cells were either treated with FC alone, or with Wnt3A for 2 days. Cells were fixed and then stained with DAPI (blue) and phalloidin (red). Cell grouping was calculated by scoring an average of 500 cells per condition as either being next to a GFP cell (green) or not (red). These results represent 2 independent experiments that were counted.

Genotypes: / Treatments:	FC only	ephrin-B1-Fc	EphB3-Fc	+ β-catenin activation: FC only	ephrin-B1-Fc	EphB3-Fc
WT/β-catenin	YES (95%)	YES (85%)	YES (85%)	YES (85%)	YES (85%)	YES (85%)
WT/WT	NO (85%)	NO (85%)	NO (85%)	NO (85%)	NO (85%)	NO (85%)
Ephb3KO/WT	YES (80%)	YES (40%)	YES (60%)	YES (50%)	YES (70%)	YES (70%)
Efnb1KO/WT	YES (90%)	YES (90%)	YES (90%)	YES (75%)	YES (90%)	YES (90%)

Phenotypes

Table 7.1- Summary of the keratinocyte mixing experiments. This table summarises the results of mixing experiments shown in Figures 7.13 and 7.14. The phenotype indicated is the ability of two cell populations that are initially mixed to segragate from one another. YES indicates that the two populations do not intermingle and NO that cells remained intermingled in a mixed population. The percentages values are also shown.

EphB/ephrin-B signalling is important for cell-cell interaction and boundary formation

As mentioned in the introduction, Eph/ephrin signalling is bidirectional. This is the expression of ephrin-B ligand on one cell population leads to activation of forward signalling on neighbouring EphB expressing cells, and also to activation of reverse signalling on ephrin-B expressing cells. This allows the formation of a boundary separating cells of different identities, the boundary being maintained because cells on either side differ in their adhesive properties and sort from one another (Watt, 1984; Cooke et al., 2005). This notion is supported by the mixing studies, in which I have shown that the 'Eph/ephrin status' of a cell population determines whether or not cells will intermingle or segregate from one another. This provides a dramatic demonstration of the power of Eph receptors and ephrins as patterning molecules (Pasquale, 2005). The fact that loss of Eph/ephrin signalling *in vivo* leads to changes in two critical basal integrins important for anchorage to the BM, further supports the role of Eph/ephrin molecules in determining the adhesion status of a cell and thus its fate. In Chapter 6, I have shown that ephrin-B1 and EphB3 are expressed in distinct "domains". I speculate that the formation of these boundaries might be coupling the processes of migration, differentiation and proliferation. The specific expression of ephrin-B ligands or Eph receptors of a cell population also correlate with the differentiation and proliferation status and also allow or not intermingling with other populations by modulating cell adhesion, migration, etc.

EphB/ephrin-B signalling modulates Wnt responsiveness

I have shown that β-catenin activation drives the expression of EphB3 and ephrin-B1 during ectopic HF formation. As mentioned in the Introduction, hair follicle and feather formation have an absolute requirement for reciprocal Wnt signalling between the ectoderm and the underlying mesenchyme (Millar, 2002; Chang et al., 2004; Yu et al., 2004). It is intriguing that EphA4 is expressed during early feather placode formation and that modulation of its levels in a chicken culture system showed that EphA4 signalling is required for proper induction and maintenance of the feather bud and this occurs in part via RhoB (McKinnell et al.,

2004a). This suggests that Eph/ephrin signalling downstream of the Wnt pathway might be evolutionary conserved in skin appendage formation.

I have shown that keratinocytes in IFE and HF of mutant skin have increased levels of β-catenin and that loss of EphB3 or ephrin-B1 resulted in increased β-catenin levels and transcriptional activity. The mechanism by which loss of EphB/ephrin-B upregulates β-catenin could be via increased expression of Cdc42, as it has been shown that Cdc42 protects β-catenin from degradation (Wu et al., 2006; Miao et al., 2005). In addition, I have shown in Chapter 6 that pSMAD 2/3 is misslocalised in mutant skin. Altered TGFβ sensitivity could also be contributing to altered β-catenin levels, as it has been recently shown that SMAD7 directly interacts and regulates the levels of β-catenin by targeting it to proteosomal degradation. This having a big impact on the β-catenin levels and β-catenin directed lineage commitment (Han et al., 2006). β-catenin increased levels observed in mutant skin are likely to impact on the increased proliferation observed, as β-catenin activation can stimulate proliferation of epidermal cells (Zhu and Watt, 1999; Silva-Vargas et al., 2005 and Lowry et al., 2005).

While I propose that EphB/ephrin-B signalling influences proliferation via its effects on β-catenin, the effects on integrin expression, cell shape and motility are also likely to control epidermal pattern. These functions have been well described *in vitro* (Miao et al., 2005), but my results are the first to document dramatic effects on integrin expression *in vivo*.

Eph/ephrins not only modulate Cdc42 activity, but also the activity of the Rho GTPases, Rac1 and RhoA (Noren and Pasquale, 2004; Tanaka et al., 2003; Miao et al., 2005) and this will impact on the adhesive properties of epidermal cells and also affect the size of stem cell compartment (Benitah et al., 2005; Wu et al., 2006). These are not only pleiotropic effectors of Eph/ephrin, integrin and growth factors signalling but they are also key regulators of the non-canonical Wnt also known as planar cell polarity (PCP) pathway.

In addition, I have shown that Eph/ephrin signalling modulates the effects of β-catenin on transcriptional activity, proliferation and cell mixing.

It is intriguing, that Ephrin-B1 and EphB2 can bind to Dishevelled (Tanaka et al., 2003; Lee et al., 2006a) and could therefore alter the balance between canonical and non-canonical (PCP) Wnt signalling (Poliakov and Wilkinson, 2006). It will be very important to test this hypothesis *in vitro* and *in vivo*, as it will open a new avenue of understanding the interaction between canonical and non-canonical Wnt pathway in epidermis. The effects observed in the IFE of the mutants also suggest that this mechanism might be at place and β-catenin may play a role in IFE, perhaps in the process in which basal cells detach from the BM and start the programme of differentiation, in which CDC42 and the PAR complex has recently been shown to be involved (Lechler and Fuchs, 2005).

The *in vitro* assay for activating Eph/ephrin signalling in wild-type keratinocytes and the mutant keratinocytes described in this Chapter will provide a very good tool to elucidate which of these downstream effectors are modulated in order to start dissecting further the mechanism at the molecular level. It will also give an insight to dissect further whether activation of Eph/ephrin in keratinocytes leads to repulsive and/or adhesive signals contributing to the formation or not of a boundary.

EphB/ephrin-B signalling and tumorigenesis

In both intestine and epidermis inappropriate activation of Wnt pathway is associated with tumour formation (Radtke et al., 2006; Gat et al., 1998; Chan et al., 1999; Lo Celso et al., 2004). Recent studies suggest a role of Eph/ephrin signalling as a tumour supressors (Batlle et al., 2005; Noren et al., 2006; Guo et al., 2006). This would be consistent with the observation that Eph/Ephrin may negatively regulate β-catenin responsiveness. A good way to test this hypothesis in skin *in vivo* would be to cross the mutants with the K14ΔNβ-cateninER mice. I could then examine whether β-catenin activation would lead to increased tumour formation in an EphB/ ephrin-B null background.

Model of ephrin-B/EphB signalling in epidermis

I propose that ephrin-B1 acts as a ligand of the EphB3 receptor expressed in neighbouring cells. The expression of ephrin-B1 in one cell population leads to

activation of forward signalling on neighbouring EphB3 expressing cells, and also to activation of reverse signalling on ephrin-B1 expressing cells. This leads to: 1- activation of forward signalling on EphB3 expressing cells, leading to the modification of β-catenin (proliferation/cohesiveness) and 2- activation of reverse signalling on ephrin-B1 expressing cell that tells the cell to (differentiate, migrate, so determining the fate of the cell), and these together 3- leading to the formation of a boundary on one side cells that are committed to differentiate and on the other the progenitors. It is tempting to speculate that EphB/ephrin-B signalling might regulate the abundance of progenitor and differentiated cells, and perhaps restrict undifferentiated cells to regions where Eph signalling is kept to a specific level (Pasquale, 2005). This notion will be important to keep in mind in further analyses to conclude that this is the case in the skin.

In the absence of EphB3, the ligand does not activate EphB3 receptor; therefore β-catenin response is not modulated and there is a massive increase of β1 integrin and α6 integrin. In this case, the pathway activated downstream of ephrin-B1 (reverse) is favoured leading to increased proliferation/differentiation. So leading to an enhancement of the β-catenin response. In the absence of ephrin-B1, again the receptor is not activated so β-catenin response is not modulated with a large increase in α6 integrin and a moderate increase in β1. In addition ephrin-B1 downstream signalling upon EphB3 ligation is not activated, so no differentiation/migration occurs.

I propose that EphB/ ephrin-B signalling acts primarily to determine boundary formation. The changes in proliferation and differentiation could be, in part, a secondary consequence of placing cells in different niches or reflecting an increase of a population that 'got stuck' at some point of their development or migratory pathway. However, it is clear that there are also cell autonomous consequences of altering Eph/ ephrin signalling (Foo et al., 2006) in particular the changes in integrin and β-catenin levels that could have a direct role in tumour development.

Chapter 8- Final Discussion

8.1-HF morphogenesis is a threshold event

In this thesis I have analysed the effects of titrating the levels of β-catenin activity in adult epidermis by using a drug inducible model, N-terminally truncated β-catenin fused to a mutant estrogen receptor (K14ΔNβ-cateninER transgenic mice) that allowed me to control the levels of activation.

The results presented in Chapter 4 show that levels of β-catenin activation induces de novo hair follicle formation from sebaceous glands and IFE, while only sustained, high-level activation induces hair follicles in pre-existing hair follicles. Even though the expression of the K14ΔNβ-cateninER transgene is homogenous not all the cells generate follicles. The three different compartments have different sensitivity to β-catenin activation. It will be important to elucidate the molecular basis of the differences in interpreting the β-catenin signal.

My results show that β-catenin activation in adult tail epidermis is enough to be 'the first signal' to trigger a morphogenetic process to generate a hair. However, this has to be within a fine threshold of β-catenin activation: very low levels promote bulge stem cell maintenance, medium levels activate the stem cells without any changes in the compartment (Lowry et al., 2005) and induce the entry into anagen already reported (Gat et al., 1998; Van Mater et al., 2003; Lo Celso et al., 2004, Silva-Vargas et al.,2005). My results also show that within this threshold of signal a HF niche will form or not (see Figure 8.1; Silva-Vargas et al., 2005). When the levels are too high, a tumour is formed instead (Figure 8.1; Lo Celso et al., 2004; Gat et al., 1998). This raises the question as to whether it is important or not in which skin compartment the first signal 'to make a hair' is made. If β-catenin activation is a 'global switch' to make an appendage then if we use a dermal specific promoter we should obtain similar results. This will be intriguing to find out.

8.2- Adult epidermis is a very plastic tissue

The experiments discussed in Chapter 4 show that the ectopic hair follicles that arise from the IFE originate from this compartment, and not by migration or division of bulge stem cells (Silva-Vargas et al., 2005). The results place adult epidermis with a remarkable flexibility when it comes to generating new appendages. This suggests that given the right stimulus, any epidermal cell might contribute to the formation of a hair.

Next, it will be very important to characterise and to unveil how IFE stem cells are arranged and establish whether transit-amplifying cells are a discrete cell population. If indeed stem cells are not clustered in the interfollicular epidermis, these observations raise the intriguing possibility that interfollicular epidermal transit-amplifying cells have the potential to become hair follicle stem cells. Although it is generally believed that the progression from stem cells to transit-amplifying cells is irreversible and unidirectional, there are precedents in *Drosophila* for suggesting that transit-amplifying cells can convert into stem cells in some circumstances (Kai and Spradling, 2004). This will be a concept worth pursuing.

De novo hair follicles induced from the interfollicular epidermis provide a niche for neural crest cell populations and contain cells with characteristics of bulge stem cells: K15 and CD34 expression, and clonal growth in culture.
It will be important to test the 'stemness' of these new populations. Several groups are using as an *in vivo* assay the capacity of a cell population to generate HF when transplanted together with dermal fibroblasts onto nude mice. The use of these *in vivo* assays is already very informative but raises the issue of using mixed populations. In the future, as new markers are revealed, it will be important to improve these assays and to clarify the epidermal stem cell hierarchy. Studies of new populations in skin might reveal new populations with perhaps the capacity to make up for the two compartments needed to generate a hair, keratinocytes and dermal fibroblasts, thus allowing to perform an *in vivo* assay of hair regeneration with a single population.

8.3- Modelling β-catenin activation in skin

The study presented in this Thesis clearly shows that the timing, location and strength of the Wnt signal is critical, and this opens the question on how the pathway exerts all the different responses. From the analyses presented in Chapter 5 it becomes clear that at early stages of hair follicle development changes in proliferation and early hair differentiation are also accompanied by cytoskeletal rearrangements, changes in adhesion and ECM remodelling. This change in the nature of the 'adult niche' thus allows for hair morphogenesis to take place in adult epidermis. Some of the genes are the same as those active during embryonic development, however the adult niche is different than the dynamic changes that undergo during embryonic hair development. This might account with some differences observed.

My array analysis provides with new data to help the discovery of new β-catenin target genes and regulatory pathways. It will be of great interest to investigate further some of the candidate genes elucidated in this study, as they are likely to be very important in setting up the morphogenetic programme to make a hair. In addition, it will be important to profile the β-catenin signal at the single cell level. Using an *in vivo* reporter for β-catenin activity would allow us to follow the dynamics of β-catenin activation during ectopic HF formation in real time. This will allow single cell isolation and we will be able to profile at the single cell level what the β-catenin signal means.

8.4- Intersection of the β-catenin/Wnt pathway with other signalling families

Another important aspect will be to elucidate alternative transcriptional partners of β-catenin in skin and to study the intersection between Wnt and other pathways. We can think of the Wnt pathway as part of a spider's web, in which different pathways intersect in many different ways: touching the web at any point will impact on multiple threads (Watt et al., 2006).

For example, two of the pathways that intersect with the Wnt pathway in epidermis are the Notch and vitamin D pathways. It has been shown that both

pathways are essential for postnatal hair follicle development and homeostasis, since the Notch deletion in epidermis results in almost complete hair loss followed by cyst formation (Vauclair et al., 2005) and loss or mutations of the vitamin D receptor (VDR) are associated with hair loss in mice and humans (Watt et al., 2006). In the case of the VDR, the molecular basis of the binding of β-catenin to ligand-activated VDR has recently been elucidated (Shah et al., 2006) and although, the physiological relevance has not yet been described, it seems likely that Tcf/Lef-independent transcriptional activation by β-catenin is important in regulating hair follicle growth and differentiation (Watt et al., 2006). In the case of the Notch pathway, *in vitro* studies highlighted this intersection with the Wnt pathway. Devgan et al. have shown that Wnt4 is negatively regulated by p21, a direct transcriptional target of Notch activation (Devgan et al., 2005). The *in vivo* consequences of the intersection of the two pathways have recently been elucidated. Estrach et al, have shown that the Jagged1 ligand is a direct target of β-catenin in skin (Estrach et al., 2006). The Notch pathway is required for maintenance of HF cycling and ectopic HF formation (Estrach et al., 2006). This is of interest as Notch pathway has been shown to regulate Eph/ephrin signalling in the vascular system (Hainaud et al., 2006) and it will be very important to test if this is also occurring in skin, in particular during HF morphogenesis.

8.5-Wnt and tumorigenesis

Mutations in members of the Wnt pathway have been usually associated with stabilisation of β-catenin and transcriptional activation of Lef/Tcf transcription factors leading to inappropriate activation and formation of epidermal tumours (Chan et al., 1999). These benign tumours have a high degree of hair differentiation and in humans have been associated with activating mutations of β-catenin (Chan et al., 1999). In addition, prolonged activation of β-catenin in adult epidermis leads to the formation of trichofolliculomas, although these can regress when β-catenin activation returns to normal levels (Lo Celso et al., 2004). A big surprise was a recent report showing for the first time a human-associated sebaceous gland tumour harbouring a mutation in the Lef1 gene that inactivates the Wnt pathway (Takeda et al., 2006). The Lef 1 gene's mutation impairs the binding of Lef1 protein to β-catenin and its transcriptional activity and determines

the sebaceous nature of the tumours, as assessed by an increased sebaceous differentiation programme (Takeda et al., 2006). This brings an interesting notion that Lef1 can contribute to tumour formation via a β-catenin independent mechanism (Watt et al., 2006).

Interestingly, the array analysis revealed that for each set of activators of a given pathway, the expression of a number of inhibitors is also induced (Figure 8.1). The balance of these opposing signals allows for HF to occur. Therefore, if the balance were lost it would lead to abnormal morphogenesis giving rise to tumour formation. In this line, one of the pathways upregulated by β-catenin activation in the epidermis is Sonic hedgehog (Shh) signalling. It has been shown very recently that Wnt inhibitors directly regulate the activity of Shh during neural tube formation (Lei et al., 2006), indicating that this model also applies for members of different pathways. Furthermore, in addition to the Wnt signalling, Shh signalling is also inappropriately activated in epidermal tumours.

Another pathway that I have described downstream of β-catenin is the family of Eph/ephrin and in Chapter 7 I show that Eph/ephrin signalling modulates the Wnt responsiveness in keratinocytes. I propose that this mechanism might be important for understanding the development of skin tumours. This hypothesis has been already tested in breast and colon tumour development (Clevers and Batlle, 2006; Batlle et al., 2005; Noren et al., 2006). And a very recent report supports the idea and shows that EphA2 may be involved in the susceptibility to develop skin tumours (Guo et al., 2006). It will be important to test this hypothesis.

8.6- Tail skin whole mount is a good system to solve 'patterning problems'.

The results shown in this Thesis validate the whole mount system of tail skin to assess *de novo* hair follicle formation in three dimensions and to obtain quantitative and spatial data on the dynamics of hair formation in tail skin. It is also very informative to characterise markers of LRC and their committed progeny and evaluate changes in the epidermal stem cell compartment.

I have shown three types of patterning in mouse tail epidermis: hair follicle spacing, cell position along the proximo-distal follicle axis, and the location of

cells undergoing different programmes of IFE differentiation in parakeratotic scales. The whole mount system will allow to test new markers in the future and help unveil for example how IFE stem cells are distributed whether they are clustered or scattered randomly.

The expression pattern domains and their boundaries that I have described are reminiscent of the Drosophila imaginal disks, one of the classical examples to study planar cell polarity (Saburi and McNeill, 2005). HF formation is a complex process and it is intriguing that the downward growth of the follicular cells is carried out at a precise angle relative to the plane of the epidermis, which also dictates the angle of the outgrowth. Frizzled 6, expressed in the adjacent epidermis seems to be in charge for the parallel orientation of HF. It will be interesting to investigate if the rules of PCP can be applied to HF morphogenesis (Barrow, 2006).

I have established that EphB/ephrin-B signalling controls three types of patterning in mouse tail epidermis: hair follicle spacing, cell position along the proximo-distal follicle axis, and the location of cells undergoing different programmes of IFE differentiation. In addition, it also controls localisation of melanocytes, both within the epidermis and the dermis, causes the appearance of sebocytes within the infundibulum, and increases epidermal proliferation. The *in vitro* model that I present in Chapter 7 will be important to further dissect the proposed mechanism of action of Eph/ephrin signalling *in vitro*.

We can use the whole mount system for understanding patterning and given that we can quantify events it will be important to apply the biological data into mathematical models to further understand and predict new patterns (Reeves et al., 2006).

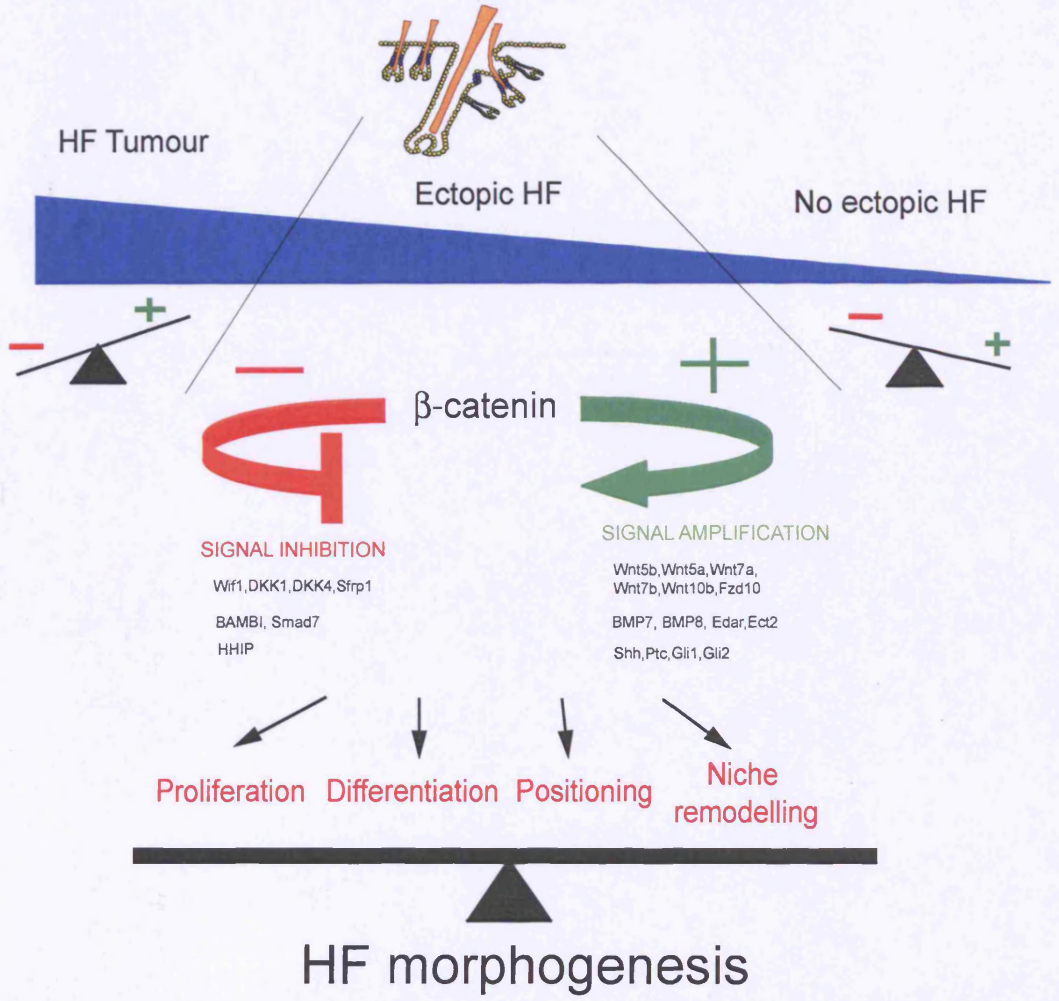

Figure 8.1 - A model for β-catenin action during hair follicle formation. Hair follicle formation is a threshold response to β-catenin activation and results from a balance between negative feedback versus amplification of the β–catenin signal. This leads to a balanced modulation of proliferation, differentaition, positionning and niche remodelling, which are all required for HF formation.This diagram indicates that genes of the Wnt, BMP and Hedgehog pathways are activated by β-catenin that either promote or inhibit the activation of the pathway. Note that a balance between the two must be achieved in order for HF to be formed. If there are more activators than inhibitors it could lead to tumour development, instead if there are more inhibitors than activators no HF will be formed. For simplification, only selected pathways are indicated in this diagram. The relationship between them and how they feedback to β-catenin is a main focus on analysis.

8.7- Concluding remarks and future prospects

Future analyses to understand how β-catenin signal is interpreted will be very important and will shed on how β-catenin intersects with other pathways and how these are integrated to generate a message to make a hair. It is of particular interest the relationship between the canonical Wnt and the PCP pathways and to test if Eph/ephrin signalling is at their intersection.

The Wnt pathway and function is highly conserved through evolution. It is intriguing that the Cnidarians genomes encode a diversity of 11 of the 12 Wnt genes described in man. How the Wnt gradients are arranged in the HF and the process of HF morphogenesis highly resembles the process of head formation in the Hydra model (Galliot et al., 2006), hyperactivation of β-catenin leads to ectopic head formation. In addition, the process of inducing ectopic HF in the multilayered adult epidermis is a problem similar to adult epithelial regeneration in which Wnt inductive signals are reactivated and have to overcome the inhibitory signals from multilayered epitheliums, for example the chick limb (He and Axelrod, 2006). It will be important to compare these situations in the future. Perhaps when looking at complex patterning programmes we should always keep an eye open on how ancient ancestors give rise to their appendages (He and Axelrod, 2006).

Publications

The results presented in this Thesis have contributed to the following publications:

Silva-Vargas,V., Adams,R., and Watt,F.M. Eph/ephrin-B signalling patterns mammalian epidermis". In Review in Developmental Cell.

Watt,F.M., Lo Celso,C., and **Silva-Vargas,V.**(2006). Epidermal stem cells: an update. Curr Opin Cell Biol.16,518-24. Epub 2006 Aug 17.

López-Rovira,T., **Silva-Vargas,V.,** and Watt,F.M. (2005). Different consequences of beta1 integrin deletion in neonatal and adult mouse epidermis reveal a context-dependent role of integrins in regulating proliferation, differentiation and intercellular communication. J Invest Dermatol. 125,1215-27.

Silva-Vargas, V., Lo Celso, C., Giangreco, A., Ofstad, T., Prowse, D.M., Braun, K.M., and Watt, F.M. (2005). β–catenin and Hedgehog signal strength specify number and location of hair follicles in adult epidermis without recruitment of bulge stem cells. DevCell. 9:121-131.

Hobbs, R.M., **Silva-Vargas, V.**, Groves, R., and Watt, F.M. (2004).Expression of activated MEK1 in differentiating epidermal cells is sufficient to generate hyperproliferative and inflammatory skin lesions.J Invest Dermatol.123,503-15.

Braun, K.M., Niemann,C., Jensen,U.B., Sundberg, J.P., **Silva-Vargas, V.**, and Watt, F.M. (2003). Manipulation of stem cell proliferation and lineage commitment: visualisation of label-retaining cells in whole mounts of mouse epidermis". Development.130,5241-55

References

Alonso, L., and Fuchs, E. (2006). The hair cycle. J Cell Sci *119*, 391-393.

Alonso, L., Okada, H., Pasolli, H.A., Wakeham, A., You-Ten, A.I., Mak, T.W., and Fuchs, E. (2005). Sgk3 links growth factor signalling to maintenance of progenitor cells in the hair follicle. J Cell Biol *170*, 559-570.

Andl, T., Murchison, E.P., Liu, F., Zhang, Y., Yunta-Gonzalez, M., Tobias, J.W., Andl, C.D., Seykora, J.T., Hannon, G.J., and Millar, S.E. (2006). The miRNA-processing enzyme dicer is essential for the morphogenesis and maintenance of hair follicles. Curr Biol *16*, 1041-1049.

Andl, T., Reddy, S.T., Gaddapara, T., and Millar, S.E. (2002). WNT signals are required for the initiation of hair follicle development. Dev Cell *2*, 643-653.

Arck, P.C., Slominski, A., Theoharides, T.C., Peters, E.M., and Paus, R. (2006). Neuroimmunology of stress: skin takes center stage. J Invest Dermatol *126*, 1697-1704.

Arnold, I., and Watt, F.M. (2001). c-Myc activation in transgenic mouse epidermis results in mobilization of stem cells and differentiation of their progeny. Curr Biol *11*, 558-568.

Barrandon, Y., and Green, H. (1985). Cell size as a determinant of the clone-forming ability of human keratinocytes. Proc Natl Acad Sci U S A *82*, 5390-5394.

Barrow, J.R. (2006). Wnt/PCP signaling: a veritable polar star in establishing patterns of polarity in embryonic tissues. Semin Cell Dev Biol *17*, 185-193.

Batlle, E., Bacani, J., Begthel, H., Jonkheer, S., Gregorieff, A., van de Born, M., Malats, N., Sancho, E., Boon, E., Pawson, T., *et al.* (2005). EphB receptor activity suppresses colorectal cancer progression. Nature *435*, 1126-1130.

Batlle, E., Henderson, J.T., Beghtel, H., van den Born, M.M., Sancho, E., Huls, G., Meeldijk, J., Robertson, J., van de Wetering, M., Pawson, T., *et al.* (2002). Beta-catenin and TCF mediate cell positioning in the intestinal epithelium by controlling the expression of EphB/ephrinB. Cell *111*, 251-263.

Benitah, S.A., Frye, M., Glogauer, M., and Watt, F.M. (2005). Stem cell depletion through epidermal deletion of Rac1. Science *309*, 933-935.

Bickenbach, J.R. (1981). Identification and behavior of label-retaining cells in oral mucosa and skin. J Dent Res *60 Spec No C*, 1611-1620.

Blache, P., van de Wetering, M., Duluc, I., Domon, C., Berta, P., Freund, J.N., Clevers, H., and Jay, P. (2004). SOX9 is an intestine crypt transcription factor, is regulated by the Wnt pathway, and represses the CDX2 and MUC2 genes. J Cell Biol *166*, 37-47.

Blanpain, C., and Fuchs, E. (2005). Epidermal Stem Cells of the Skin. Annu Rev Cell Dev Biol.
Blanpain, C., Lowry, W.E., Geoghegan, A., Polak, L., and Fuchs, E. (2004). Self-renewal, multipotency, and the existence of two cell populations within an epithelial stem cell niche. Cell *118*, 635-648.

Braun, K.M., Niemann, C., Jensen, U.B., Sundberg, J.P., Silva-Vargas, V., and Watt, F.M. (2003). Manipulation of stem cell proliferation and lineage commitment: visualisation of label-retaining cells in wholemounts of mouse epidermis. Development *130*, 5241-5255.

Brembeck, F.H., Rosario, M., and Birchmeier, W. (2006). Balancing cell adhesion and Wnt signaling, the key role of beta-catenin. Curr Opin Genet Dev *16*, 51-59.

Callahan, C.A., and Oro, A.E. (2001). Monstrous attempts at adnexogenesis: regulating hair follicle progenitors through Sonic hedgehog signaling. Curr Opin Genet Dev *11*, 541-546.

Capdevila, J., and Izpisua Belmonte, J.C. (2001). Patterning mechanisms controlling vertebrate limb development. Annu Rev Cell Dev Biol *17*, 87-132.

Chan, E.F., Gat, U., McNiff, J.M., and Fuchs, E. (1999). A common human skin tumour is caused by activating mutations in beta- catenin. Nat Genet *21*, 410-413.

Chang, C.H., Jiang, T.X., Lin, C.M., Burrus, L.W., Chuong, C.M., and Widelitz, R. (2004). Distinct Wnt members regulate the hierarchical morphogenesis of skin regions (spinal tract) and individual feathers. Mech Dev *121*, 157-171.

Cheng, L.C., Tavazoie, M., and Doetsch, F. (2005). Stem cells: from epigenetics to microRNAs. Neuron *46*, 363-367.

Ciani, L., and Salinas, P.C. (2005). WNTs in the vertebrate nervous system: from patterning to neuronal connectivity. Nat Rev Neurosci *6*, 351-362.

Claudinot, S., Nicolas, M., Oshima, H., Rochat, A., and Barrandon, Y. (2005). Long-term renewal of hair follicles from clonogenic multipotent stem cells. Proc Natl Acad Sci U S A *102*, 14677-14682.

Clevers, H., and Batlle, E. (2006). EphB/EphrinB receptors and Wnt signaling in colorectal cancer. Cancer Res *66*, 2-5.

Compagni, A., Logan, M., Klein, R., and Adams, R.H. (2003). Control of skeletal patterning by ephrinB1-EphB interactions. Dev Cell *5*, 217-230.

Conover, J.C., Doetsch, F., Garcia-Verdugo, J.M., Gale, N.W., Yancopoulos, G.D., and Alvarez-Buylla, A. (2000). Disruption of Eph/ephrin signaling affects migration and proliferation in the adult subventricular zone. Nat Neurosci *3*, 1091-1097.

Cooke, J.E., Kemp, H.A., and Moens, C.B. (2005). EphA4 is required for cell adhesion and rhombomere-boundary formation in the zebrafish. Curr Biol *15*, 536-542.

Cotsarelis, G. (2006). Gene expression profiling gets to the root of human hair follicle stem cells. J Clin Invest *116*, 19-22.

D'Amour, K.A., and Gage, F.H. (2003). Genetic and functional differences between multipotent neural and pluripotent embryonic stem cells. Proc Natl Acad Sci U S A *100 Suppl 1*, 11866-11872.

DasGupta, R., and Fuchs, E. (1999). Multiple roles for activated LEF/TCF transcription complexes during hair follicle development and differentiation. Development *126*, 4557-4568.

DasGupta, R., Rhee, H., and Fuchs, E. (2002). A developmental conundrum: a stabilized form of beta-catenin lacking the transcriptional activation domain triggers features of hair cell fate in epidermal cells and epidermal cell fate in hair follicle cells. J Cell Biol *158*, 331-344.

Devgan, V., Mammucari, C., Millar, S.E., Brisken, C., and Dotto, G.P. (2005). p21WAF1/Cip1 is a negative transcriptional regulator of Wnt4 expression downstream of Notch1 activation. Genes Dev *19*, 1485-1495.

Djiane, A., Riou, J., Umbhauer, M., Boucaut, J., and Shi, D. (2000). Role of frizzled 7 in the regulation of convergent extension movements during gastrulation in Xenopus laevis. Development *127*, 3091-3100.

Dunn, K.J., Brady, M., Ochsenbauer, C., Snyder, S., Incao, A., and Pavan, W.J. (2004). WNT1 and WNT3A promote expansion of Melanocytes through distinct modes of action. Pigment Cell Res *17*, 431-432.

Dunn, K.J., Williams, B.O., Li, Y., and Pavan, W.J. (2000). Neural crest-directed gene transfer demonstrates Wnt1 role in melanocyte expansion and differentiation during mouse development. Proc Natl Acad Sci U S A *97*, 10050-10055.

Ellis, T., Gambardella, L., Horcher, M., Tschanz, S., Capol, J., Bertram, P., Jochum, W., Barrandon, Y., and Busslinger, M. (2001). The transcriptional repressor CDP (Cutl1) is essential for epithelial cell differentiation of the lung and the hair follicle. Genes Dev *15*, 2307-2319.

Estrach, S., Ambler, C.A., Lo Celso, C., Hozumi, K., and Watt, F.M. (2006). Jagged 1 is a beta-catenin target gene required for ectopic hair follicle formation in adult epidermis. Development *133*, 4427-4438.

Fernandes, K.J., McKenzie, I.A., Mill, P., Smith, K.M., Akhavan, M., Barnabe-Heider, F., Biernaskie, J., Junek, A., Kobayashi, N.R., Toma, J.G., *et al.* (2004). A dermal niche for multipotent adult skin-derived precursor cells. Nat Cell Biol *6*, 1082-1093.

Flake, A. (2000). Fate Mapping of Stem Cells (Cold Spring Harbour Press).

Flores, I., Cayuela, M.L., and Blasco, M.A. (2005). Effects of telomerase and telomere length on epidermal stem cell behavior. Science *309*, 1253-1256.

Foo, S.S., Turner, C.J., Adams, S., Compagni, A., Aubyn, D., Kogata, N., Lindblom, P., Shani, M., Zicha, D., and Adams, R.H. (2006). Ephrin-B2 controls cell motility and adhesion during blood-vessel-wall assembly. Cell *124*, 161-173.

Frye, M., Gardner, C., Li, E.R., Arnold, I., and Watt, F.M. (2003). Evidence that Myc activation depletes the epidermal stem cell compartment by modulating adhesive interactions with the local microenvironment. Development *130*, 2793-2808.

Fuchs, E., Tumbar, T., and Guasch, G. (2004). Socializing with the neighbors: stem cells and their niche. Cell *116*, 769-778.

Galliot, B., Miljkovic-Licina, M., de Rosa, R., and Chera, S. (2006). Hydra, a niche for cell and developmental plasticity. Semin Cell Dev Biol *17*, 492-502.

Gat, U., DasGupta, R., Degenstein, L., and Fuchs, E. (1998). De Novo hair follicle morphogenesis and hair tumors in mice expressing a truncated beta-catenin in skin. Cell *95*, 605-614.

Gebhardt, A., Frye, M., Herold, S., Benitah, S.A., Braun, K., Samans, B., Watt, F.M., Elsasser, H.P., and Eilers, M. (2006). Myc regulates keratinocyte adhesion and differentiation via complex formation with Miz1. J Cell Biol *172*, 139-149.

Ghazizadeh, S., and Taichman, L.B. (2001). Multiple classes of stem cells in cutaneous epithelium: a lineage analysis of adult mouse skin. Embo J *20*, 1215-1222.

Giancotti, F.G., and Ruoslahti, E. (1999). Integrin signaling. Science *285*, 1028-1032.
Gniadecki, R., and Bang, B. (2003). Flotillas of lipid rafts in transit amplifying cell-like keratinocytes. J Invest Dermatol *121*, 522-528.

Grichnik, J.M., Ali, W.N., Burch, J.A., Byers, J.D., Garcia, C.A., Clark, R.E., and Shea, C.R. (1996). KIT expression reveals a population of precursor melanocytes in human skin. J Invest Dermatol *106*, 967-971.

Grossi, M., Hiou-Feige, A., Tommasi Di Vignano, A., Calautti, E., Ostano, P., Lee, S., Chiorino, G., and Dotto, G.P. (2005). Negative control of keratinocyte differentiation by Rho/CRIK signaling coupled with up-regulation of KyoT1/2 (FHL1) expression. Proc Natl Acad Sci U S A *102*, 11313-11318.

Guo, H., Miao, H., Gerber, L., Singh, J., Denning, M.F., Gilliam, A.C., and Wang, B. (2006). Disruption of EphA2 receptor tyrosine kinase leads to increased susceptibility to carcinogenesis in mouse skin. Cancer Res *66*, 7050-7058.

Hainaud, P., Contreres, J.O., Villemain, A., Liu, L.X., Plouet, J., Tobelem, G., and Dupuy, E. (2006). The Role of the Vascular Endothelial Growth Factor-Delta-like 4 Ligand/Notch4-Ephrin B2 Cascade in Tumor Vessel Remodeling and Endothelial Cell Functions. Cancer Res *66*, 8501-8510.
Hall, A. (2000). GTPases (Oxford University Press).

Han, G., Li, A.G., Liang, Y.Y., Owens, P., He, W., Lu, S., Yoshimatsu, Y., Wang, D., Ten Dijke, P., Lin, X., *et al.* (2006). Smad7-induced beta-catenin degradation alters epidermal appendage development. Dev Cell *11*, 301-312.

Hardy, M.H. (1992). The secret life of the hair follicle. Trends Genet *8*, 55-61.

Hari, L., Brault, V., Kleber, M., Lee, H.Y., Ille, F., Leimeroth, R., Paratore, C., Suter, U., Kemler, R., and Sommer, L. (2002). Lineage-specific requirements of beta-catenin in neural crest development. J Cell Biol *159*, 867-880.

He, T.C., Sparks, A.B., Rago, C., Hermeking, H., Zawel, L., da Costa, L.T., Morin, P.J., Vogelstein, B., and Kinzler, K.W. (1998). Identification of c-MYC as a target of the APC pathway. Science *281*, 1509-1512.

He, X., and Axelrod, J.D. (2006). A WNTer wonderland in Snowbird. Development *133*, 2597-2603.

Henkemeyer, M., Orioli, D., Henderson, J.T., Saxton, T.M., Roder, J., Pawson, T., and Klein, R. (1996). Nuk controls pathfinding of commissural axons in the mammalian central nervous system. Cell *86*, 35-46.

Holmberg, J., Armulik, A., Senti, K.A., Edoff, K., Spalding, K., Momma, S., Cassidy, R., Flanagan, J.G., and Frisen, J. (2005). Ephrin-A2 reverse signaling negatively regulates neural progenitor proliferation and neurogenesis. Genes Dev *19*, 462-471.

Horsley, V., O'Carroll, D., Tooze, R., Ohinata, Y., Saitou, M., Obukhanych, T., Nussenzweig, M., Tarakhovsky, A., and Fuchs, E. (2006). Blimp1 defines a progenitor population that governs cellular input to the sebaceous gland. Cell *126*, 597-609.

Huelsken, J., Vogel, R., Erdmann, B., Cotsarelis, G., and Birchmeier, W. (2001). beta-Catenin controls hair follicle morphogenesis and stem cell differentiation in the skin. Cell *105*, 533-545.

Iso, T., Kedes, L., and Hamamori, Y. (2003). HES and HERP families: multiple effectors of the Notch signaling pathway. J Cell Physiol *194*, 237-255.

Ito, M., Liu, Y., Yang, Z., Nguyen, J., Liang, F., Morris, R.J., and Cotsarelis, G. (2005). Stem cells in the hair follicle bulge contribute to wound repair but not to homeostasis of the epidermis. Nat Med *11*, 1351-1354.

Jamora, C., DasGupta, R., Kocieniewski, P., and Fuchs, E. (2003). Links between signal transduction, transcription and adhesion in epithelial bud development. Nature *422*, 317-322.

Jamora, C., Lee, P., Kocieniewski, P., Azhar, M., Hosokawa, R., Chai, Y., and Fuchs, E. (2005). A signaling pathway involving TGF-beta2 and snail in hair follicle morphogenesis. PLoS Biol *3*, e11.

Jensen, K.B., and Watt, F.M. (2006). Single-cell expression profiling of human epidermal stem and transit-amplifying cells: Lrig1 is a regulator of stem cell quiescence. Proc Natl Acad Sci U S A *103*, 11958-11963.

Jensen, U.B., Lowell, S., and Watt, F.M. (1999). The spatial relationship between stem cells and their progeny in the basal layer of human epidermis: a new view based on whole-mount labelling and lineage analysis. Development *126*, 2409-2418.

Jones, P.H., Harper, S., and Watt, F.M. (1995). Stem cell patterning and fate in human epidermis. Cell *80*, 83-93.

Jones, P.H., and Watt, F.M. (1993). Separation of human epidermal stem cells from transit amplifying cells on the basis of differences in integrin function and expression. Cell *73*, 713-724.

Jung, H.S., Francis-West, P.H., Widelitz, R.B., Jiang, T.X., Ting-Berreth, S., Tickle, C., Wolpert, L., and Chuong, C.M. (1998). Local inhibitory action of BMPs and their relationships with activators in feather formation: implications for periodic patterning. Dev Biol *196*, 11-23.

Kai, T., and Spradling, A. (2004). Differentiating germ cells can revert into functional stem cells in Drosophila melanogaster ovaries. Nature *428*, 564-569.

Kenney, A.M., Widlund, H.R., and Rowitch, D.H. (2004). Hedgehog and PI-3 kinase signaling converge on Nmyc1 to promote cell cycle progression in cerebellar neuronal precursors. Development *131*, 217-228.

Kielman, M.F., Rindapaa, M., Gaspar, C., van Poppel, N., Breukel, C., van Leeuwen, S., Taketo, M.M., Roberts, S., Smits, R., and Fodde, R. (2002). Apc modulates embryonic stem-cell differentiation by controlling the dosage of beta-catenin signaling. Nat Genet *32*, 594-605.

Kim, V.N. (2006). Small RNAs just got bigger: Piwi-interacting RNAs (piRNAs) in mammalian testes. Genes Dev *20*, 1993-1997.

Koster, M.I., Kim, S., Mills, A.A., DeMayo, F.J., and Roop, D.R. (2004). p63 is the molecular switch for initiation of an epithelial stratification program. Genes Dev *18*, 126-131.

Koster, M.I., Kim, S., and Roop, D.R. (2005). P63 deficiency: a failure of lineage commitment or stem cell maintenance? J Investig Dermatol Symp Proc *10*, 118-123.

Koster, M.I., Lu, S.L., White, L.D., Wang, X.J., and Roop, D.R. (2006). Reactivation of developmentally expressed p63 isoforms predisposes to tumor development and progression. Cancer Res *66*, 3981-3986.

Kullander, K., and Klein, R. (2002). Mechanisms and functions of Eph and ephrin signalling. Nat Rev Mol Cell Biol *3*, 475-486.

Laemmli, U.K. (1970). Cleavage of structural proteins during the assembly of the head of bacteriophage T4. Nature *227*, 680-685.

Langbein, L., Rogers, M.A., Praetzel-Wunder, S., Helmke, B., Schirmacher, P., and Schweizer, J. (2006). K25 (K25irs1), K26 (K25irs2), K27 (K25irs3), and K28 (K25irs4) Represent the Type I Inner Root Sheath Keratins of the Human Hair Follicle. J Invest Dermatol.

Le Douarin, N.M., and Dupin, E. (2003). Multipotentiality of the neural crest. Curr Opin Genet Dev *13*, 529-536.

Lechler, T., and Fuchs, E. (2005). Asymmetric cell divisions promote stratification and differentiation of mammalian skin. Nature *437*, 275-280.

Lee, H.S., Bong, Y.S., Moore, K.B., Soria, K., Moody, S.A., and Daar, I.O. (2006a). Dishevelled mediates ephrinB1 signalling in the eye field through the planar cell polarity pathway. Nat Cell Biol *8*, 55-63.

Lee, J.H., Schutte, D., Wulf, G., Fuzesi, L., Radzun, H.J., Schweyer, S., Engel, W., and Nayernia, K. (2006b). Stem-cell protein Piwil2 is widely expressed in tumors and inhibits apoptosis through activation of Stat3/Bcl-XL pathway. Hum Mol Genet *15*, 201-211.

Legg, J., Jensen, U.B., Broad, S., Leigh, I., and Watt, F.M. (2003). Role of melanoma chondroitin sulphate proteoglycan in patterning stem cells in human interfollicular epidermis. Development *130*, 6049-6063.

Legue, E., and Nicolas, J.F. (2005). Hair follicle renewal: organization of stem cells in the matrix and the role of stereotyped lineages and behaviors. Development *132*, 4143-4154.

Lei, Q., Jeong, Y., Misra, K., Li, S., Zelman, A.K., Epstein, D.J., and Matise, M.P. (2006). Wnt signaling inhibitors regulate the transcriptional response to morphogenetic Shh-Gli signaling in the neural tube. Dev Cell *11*, 325-337.

Levy, V., Lindon, C., Harfe, B.D., and Morgan, B.A. (2005). Distinct stem cell populations regenerate the follicle and interfollicular epidermis. Dev Cell *9*, 855-861.

Li, L., Mignone, J., Yang, M., Matic, M., Penman, S., Enikolopov, G., and Hoffman, R.M. (2003). Nestin expression in hair follicle sheath progenitor cells. Proc Natl Acad Sci U S A *100*, 9958-9961.

Li, L., and Xie, T. (2005). Stem cell niche: structure and function. Annu Rev Cell Dev Biol *21*, 605-631.

Liu, B.Y., McDermott, S.P., Khwaja, S.S., and Alexander, C.M. (2004). The transforming activity of Wnt effectors correlates with their ability to induce the accumulation of mammary progenitor cells. Proc Natl Acad Sci U S A *101*, 4158-4163.

Lo Celso, C., Prowse, D.M., and Watt, F.M. (2004). Transient activation of beta-catenin signalling in adult mouse epidermis is sufficient to induce new hair follicles but continuous activation is required to maintain hair follicle tumours. Development *131*, 1787-1799.

Lopez-Rovira, T., Silva-Vargas, V., and Watt, F.M. (2005). Different consequences of beta1 integrin deletion in neonatal and adult mouse epidermis reveal a context-dependent role of integrins in regulating proliferation, differentiation, and intercellular communication. J Invest Dermatol *125*, 1215-1227.

Lowell, S., Jones, P., Le Roux, I., Dunne, J., and Watt, F.M. (2000). Stimulation of human epidermal differentiation by delta-notch signalling at the boundaries of stem-cell clusters. Curr Biol *10*, 491-500.

Lowry, W.E., Blanpain, C., Nowak, J.A., Guasch, G., Lewis, L., and Fuchs, E. (2005). Defining the impact of beta-catenin/Tcf transactivation on epithelial stem cells. Genes Dev *19*, 1596-1611.

Lyle, S., Christofidou-Solomidou, M., Liu, Y., Elder, D.E., Albelda, S., and Cotsarelis, G. (1998). The C8/144B monoclonal antibody recognizes cytokeratin 15 and defines the location of human hair follicle stem cells. J Cell Sci *111 (Pt 21)*, 3179-3188.

Marvin, M.J., Dahlstrand, J., Lendahl, U., and McKay, R.D. (1998). A rod end deletion in the intermediate filament protein nestin alters its subcellular localization in neuroepithelial cells of transgenic mice. J Cell Sci *111 (Pt 14)*, 1951-1961.

McGowan, K.M., and Coulombe, P.A. (1998). Onset of keratin 17 expression coincides with the definition of major epithelial lineages during skin development. J Cell Biol *143*, 469-486.

McKinnell, I.W., Makarenkova, H., de Curtis, I., Turmaine, M., and Patel, K. (2004a). EphA4, RhoB and the molecular development of feather buds are maintained by the integrity of the actin cytoskeleton. Dev Biol *270*, 94-105.

McKinnell, I.W., Turmaine, M., and Patel, K. (2004b). Sonic Hedgehog functions by localizing the region of proliferation in early developing feather buds. Dev Biol *272*, 76-88.

Megason, S.G., and McMahon, A.P. (2002). A mitogen gradient of dorsal midline Wnts organizes growth in the CNS. Development *129*, 2087-2098.

Mellitzer, G., Xu, Q., and Wilkinson, D.G. (1999). Eph receptors and ephrins restrict cell intermingling and communication. Nature *400*, 77-81.

Merrill, B.J., Gat, U., DasGupta, R., and Fuchs, E. (2001). Tcf3 and Lef1 regulate lineage differentiation of multipotent stem cells in skin. Genes Dev *15*, 1688-1705.

Miao, H., Strebhardt, K., Pasquale, E.B., Shen, T.L., Guan, J.L., and Wang, B. (2005). Inhibition of integrin-mediated cell adhesion but not directional cell migration requires catalytic activity of EphB3 receptor tyrosine kinase. Role of Rho family small GTPases. J Biol Chem *280*, 923-932.

Michno, K., Boras-Granic, K., Mill, P., Hui, C.C., and Hamel, P.A. (2003). Shh expression is required for embryonic hair follicle but not mammary gland development. Dev Biol *264*, 153-165.

Mikels, A.J., and Nusse, R. (2006). Purified Wnt5a protein activates or inhibits beta-catenin-TCF signaling depending on receptor context. PLoS Biol *4*, e115.

Mill, P., Mo, R., Hu, M.C., Dagnino, L., Rosenblum, N.D., and Hui, C.C. (2005). Shh controls epithelial proliferation via independent pathways that converge on N-Myc. Dev Cell *9*, 293-303.

Millar, S.E. (2002). Molecular mechanisms regulating hair follicle development. J Invest Dermatol *118*, 216-225.

Millar, S.E. (2003). WNTs: multiple genes, multiple functions. J Invest Dermatol *120*, 7-8.

Millar, S.E. (2005). An ideal society? Neighbors of diverse origins interact to create and maintain complex mini-organs in the skin. PLoS Biol *3*, e372.

Millar, S.E., Willert, K., Salinas, P.C., Roelink, H., Nusse, R., Sussman, D.J., and Barsh, G.S. (1999). WNT signaling in the control of hair growth and structure. Dev Biol *207*, 133-149.

Moon, R.T., Bowerman, B., Boutros, M., and Perrimon, N. (2002). The promise and perils of Wnt signaling through beta-catenin. Science *296*, 1644-1646.

Morris, R.J., Liu, Y., Marles, L., Yang, Z., Trempus, C., Li, S., Lin, J.S., Sawicki, J.A., and Cotsarelis, G. (2004). Capturing and profiling adult hair follicle stem cells. Nat Biotechnol *22*, 411-417.

Mou, C., Jackson, B., Schneider, P., Overbeek, P.A., and Headon, D.J. (2006). Generation of the primary hair follicle pattern. Proc Natl Acad Sci U S A *103*, 9075-9080.

Nelson, W.J., and Nusse, R. (2004). Convergence of Wnt, beta-catenin, and cadherin pathways. Science *303*, 1483-1487.

Nicolas, M., Wolfer, A., Raj, K., Kummer, J.A., Mill, P., van Noort, M., Hui, C.C., Clevers, H., Dotto, G.P., and Radtke, F. (2003). Notch1 functions as a tumor suppressor in mouse skin. Nat Genet *33*, 416-421.

Niemann, C., Owens, D.M., Hulsken, J., Birchmeier, W., and Watt, F.M. (2002). Expression of DeltaNLef1 in mouse epidermis results in differentiation of hair follicles into squamous epidermal cysts and formation of skin tumours. Development *129*, 95-109.

Niemann, C., Unden, A.B., Lyle, S., Zouboulis Ch, C., Toftgard, R., and Watt, F.M. (2003b). Indian hedgehog and beta-catenin signaling: role in the sebaceous lineage of normal and neoplastic mammalian epidermis. Proc Natl Acad Sci U S A *100 Suppl 1*, 11873-11880.

Niemann, C., and Watt, F.M. (2002). Designer skin: lineage commitment in postnatal epidermis. Trends Cell Biol *12*, 185-192.

Nijhof, J.G., Braun, K.M., Giangreco, A., van Pelt, C., Kawamoto, H., Boyd, R.L., Willemze, R., Mullenders, L.H., Watt, F.M., de Gruijl, F.R., *et al.* (2006). The cell-surface marker MTS24 identifies a novel population of follicular keratinocytes with characteristics of progenitor cells. Development *133*, 3027-3037.

Nishimura, E.K., Jordan, S.A., Oshima, H., Yoshida, H., Osawa, M., Moriyama, M., Jackson, I.J., Barrandon, Y., Miyachi, Y., and Nishikawa, S. (2002). Dominant role of the niche in melanocyte stem-cell fate determination. Nature *416*, 854-860.

Noren, N.K., Foos, G., Hauser, C.A., and Pasquale, E.B. (2006). The EphB4 receptor suppresses breast cancer cell tumorigenicity through an Abl-Crk pathway. Nat Cell Biol *8*, 815-825.

Noren, N.K., and Pasquale, E.B. (2004). Eph receptor-ephrin bidirectional signals that target Ras and Rho proteins. Cell Signal *16*, 655-666.

Nystul, T.G., and Spradling, A.C. (2006). Breaking out of the mold: diversity within adult stem cells and their niches. Curr Opin Genet Dev *16*, 463-468.

O'Shaughnessy, R.F., Seery, J.P., Celis, J.E., Frischauf, A., and Watt, F.M. (2000). PA-FABP, a novel marker of human epidermal transit amplifying cells revealed by 2D protein gel electrophoresis and cDNA array hybridisation. FEBS Lett *486*, 149-154.

Ohyama, M., Terunuma, A., Tock, C.L., Radonovich, M.F., Pise-Masison, C.A., Hopping, S.B., Brady, J.N., Udey, M.C., and Vogel, J.C. (2006). Characterization and isolation of stem cell-enriched human hair follicle bulge cells. J Clin Invest *116*, 249-260.

Okubo, T., and Hogan, B.L. (2004). Hyperactive Wnt signaling changes the developmental potential of embryonic lung endoderm. J Biol *3*, 11.

Oliver, T.G., Grasfeder, L.L., Carroll, A.L., Kaiser, C., Gillingham, C.L., Lin, S.M., Wickramasinghe, R., Scott, M.P., and Wechsler-Reya, R.J. (2003). Transcriptional profiling of the Sonic hedgehog response: a critical role for N-myc in proliferation of neuronal precursors. Proc Natl Acad Sci U S A *100*, 7331-7336.

Orioli, D., Henkemeyer, M., Lemke, G., Klein, R., and Pawson, T. (1996). Sek4 and Nuk receptors cooperate in guidance of commissural axons and in palate formation. Embo J *15*, 6035-6049.

Oshima, H., Rochat, A., Kedzia, C., Kobayashi, K., and Barrandon, Y. (2001). Morphogenesis and renewal of hair follicles from adult multipotent stem cells. Cell *104*, 233-245.

Owens, D.M., Romero, M.R., Gardner, C., and Watt, F.M. (2003). Suprabasal alpha6beta4 integrin expression in epidermis results in enhanced tumourigenesis and disruption of TGFbeta signalling. J Cell Sci *116*, 3783-3791.

Owens, D.M., and Watt, F.M. (2003). Contribution of stem cells and differentiated cells to epidermal tumours. Nat Rev Cancer *3*, 444-451.

Pasquale, E.B. (2005). Eph receptor signalling casts a wide net on cell behaviour. Nat Rev Mol Cell Biol *6*, 462-475.

Paus, R., Nickoloff, B.J., and Ito, T. (2005). A 'hairy' privilege. Trends Immunol *26*, 32-40.

Paus, R., Theoharides, T.C., and Arck, P.C. (2006). Neuroimmunoendocrine circuitry of the 'brain-skin connection'. Trends Immunol *27*, 32-39.

Pearton, D.J., Ferraris, C., and Dhouailly, D. (2004). Transdifferentiation of corneal epithelium: evidence for a linkage between the segregation of epidermal stem cells and the induction of hair follicles during embryogenesis. Int J Dev Biol *48*, 197-201.

Poliakov, A., Cotrina, M., and Wilkinson, D.G. (2004). Diverse roles of eph receptors and ephrins in the regulation of cell migration and tissue assembly. Dev Cell *7*, 465-480.

Poliakov, A., and Wilkinson, D.G. (2006). Ephrins make eyes with planar cell polarity. Nat Cell Biol *8*, 7-8.

Potten, C. (1997). Stem Cells (Academic Press).

Radtke, F., Clevers, H., and Riccio, O. (2006). From gut homeostasis to cancer. Curr Mol Med *6*, 275-289.

Reddy, S., Andl, T., Bagasra, A., Lu, M.M., Epstein, D.J., Morrisey, E.E., and Millar, S.E. (2001). Characterization of Wnt gene expression in developing and postnatal hair follicles and identification of Wnt5a as a target of Sonic hedgehog in hair follicle morphogenesis. Mech Dev *107*, 69-82.

Reddy, S.T., Andl, T., Lu, M.M., Morrisey, E.E., and Millar, S.E. (2004). Expression of Frizzled genes in developing and postnatal hair follicles. J Invest Dermatol *123*, 275-282.

Reeves, G.T., Muratov, C.B., Schupbach, T., and Shvartsman, S.Y. (2006). Quantitative models of developmental pattern formation. Dev Cell *11*, 289-300.

Rendl, M., Lewis, L., and Fuchs, E. (2005). Molecular dissection of mesenchymal-epithelial interactions in the hair follicle. PLoS Biol *3*, e331.

Reya, T., Duncan, A.W., Ailles, L., Domen, J., Scherer, D.C., Willert, K., Hintz, L., Nusse, R., and Weissman, I.L. (2003). A role for Wnt signalling in self-renewal of haematopoietic stem cells. Nature *423*, 409-414.

Rhee, H., Polak, L., and Fuchs, E. (2006). Lhx2 maintains stem cell character in hair follicles. Science *312*, 1946-1949.

Rheinwald, J.G., and Green, H. (1975). Serial cultivation of strains of human epidermal keratinocytes: the formation of keratinizing colonies from single cells. Cell *6*, 331-343.

Romero, M.R., Carroll, J.M., and Watt, F.M. (1999). Analysis of cultured keratinocytes from a transgenic mouse model of psoriasis: effects of suprabasal integrin expression on keratinocyte adhesion, proliferation and terminal differentiation. Exp Dermatol *8*, 53-67.

Saburi, S., and McNeill, H. (2005). Organising cells into tissues: new roles for cell adhesion molecules in planar cell polarity. Curr Opin Cell Biol *17*, 482-488.

Saito, K., Nishida, K.M., Mori, T., Kawamura, Y., Miyoshi, K., Nagami, T., Siomi, H., and Siomi, M.C. (2006). Specific association of Piwi with rasiRNAs derived from retrotransposon and heterochromatic regions in the Drosophila genome. Genes Dev *20*, 2214-2222.

Sambrook, J., Frischt, E.F., and Maniatis,T. (1989). Molecular cloning. A laboratory manual. (Cold Spring Harbor Laboratory Press).

Sancho, E., Batlle, E., and Clevers, H. (2003). Live and let die in the intestinal epithelium. Curr Opin Cell Biol *15*, 763-770.

Schmidt-Ullrich, R., and Paus, R. (2005). Molecular principles of hair follicle induction and morphogenesis. Bioessays *27*, 247-261.

Schmidt-Ullrich, R., Tobin, D.J., Lenhard, D., Schneider, P., Paus, R., and Scheidereit, C. (2006). NF-kappaB transmits Eda A1/EdaR signalling to activate Shh and cyclin D1 expression, and controls post-initiation hair placode down growth. Development *133*, 1045-1057.

Schofield, R. (1978). The relationship between the spleen colony-forming cell and the haemopoietic stem cell. Blood Cells *4*, 7-25.

Schweizer, J., and Marks, F. (1977). A developmental study of the distribution and frequency of Langerhans cells in relation to formation of patterning in mouse tail epidermis. J Invest Dermatol *69*, 198-204.

Seery, J.P., and Watt, F.M. (2000). Asymmetric stem-cell divisions define the architecture of human oesophageal epithelium. Curr Biol *10*, 1447-1450.

Sela-Donenfeld, D., and Wilkinson, D.G. (2005). Eph receptors: two ways to sharpen boundaries. Curr Biol *15*, R210-212.

Shah, S., Islam, M.N., Dakshanamurthy, S., Rizvi, I., Rao, M., Herrell, R., Zinser, G., Valrance, M., Aranda, A., Moras, D., *et al.* (2006). The molecular basis of vitamin D receptor and beta-catenin crossregulation. Mol Cell *21*, 799-809.

Shtutman, M., Zhurinsky, J., Simcha, I., Albanese, C., D'Amico, M., Pestell, R., and Ben-Ze'ev, A. (1999). The cyclin D1 gene is a target of the beta-catenin/LEF-1 pathway. Proc Natl Acad Sci U S A *96*, 5522-5527.

Silva-Vargas, V., Lo Celso, C., Giangreco, A., Ofstad, T., Prowse, D.M., Braun, K.M., and Watt, F.M. (2005). Beta-catenin and Hedgehog signal strength can specify number and location of hair follicles in adult epidermis without recruitment of bulge stem cells. Dev Cell *9*, 121-131.

Smith, A. (2006). A glossary for stem-cell biology. Nature *441*, 1060.

St-Jacques, B., Dassule, H.R., Karavanova, I., Botchkarev, V.A., Li, J., Danielian, P.S., McMahon, J.A., Lewis, P.M., Paus, R., and McMahon, A.P. (1998). Sonic hedgehog signaling is essential for hair development. Curr Biol *8*, 1058-1068.

Steingrimsson, E., Copeland, N.G., and Jenkins, N.A. (2005). Melanocyte stem cell maintenance and hair graying. Cell *121*, 9-12.

Stenn, K.S., and Paus, R. (2001). Controls of hair follicle cycling. Physiol Rev *81*, 449-494.

Sugiyama-Nakagiri, Y., Akiyama, M., Shibata, S., Okano, H., and Shimizu, H. (2006). Expression of RNA-binding protein Musashi in hair follicle development and hair cycle progression. Am J Pathol *168*, 80-92.

Taipale, J., and Beachy, P.A. (2001). The Hedgehog and Wnt signalling pathways in cancer. Nature *411*, 349-354.

Takeda, H., Lyle, S., Lazar, A.J., Zouboulis, C.C., Smyth, I., and Watt, F.M. (2006). Human sebaceous tumors harbor inactivating mutations in LEF1. Nat Med *12*, 395-397.

Tanaka, M., Kamo, T., Ota, S., and Sugimura, H. (2003). Association of Dishevelled with Eph tyrosine kinase receptor and ephrin mediates cell repulsion. Embo J *22*, 847-858.

Taylor, G., Lehrer, M.S., Jensen, P.J., Sun, T.T., and Lavker, R.M. (2000). Involvement of follicular stem cells in forming not only the follicle but also the epidermis. Cell *102*, 451-461.

Tetsu, O., and McCormick, F. (1999). Beta-catenin regulates expression of cyclin D1 in colon carcinoma cells. Nature *398*, 422-426.

Tian, Q., Kopf, G.S., Brown, R.S., and Tseng, H. (2001). Function of basonuclin in increasing transcription of the ribosomal RNA genes during mouse oogenesis. Development *128*, 407-416.

Toma, J.G., Akhavan, M., Fernandes, K.J., Barnabe-Heider, F., Sadikot, A., Kaplan, D.R., and Miller, F.D. (2001). Isolation of multipotent adult stem cells from the dermis of mammalian skin. Nat Cell Biol *3*, 778-784.

Trempus, C.S., Morris, R.J., Bortner, C.D., Cotsarelis, G., Faircloth, R.S., Reece, J.M., and Tennant, R.W. (2003). Enrichment for living murine keratinocytes from the hair follicle bulge with the cell surface marker CD34. J Invest Dermatol *120*, 501-511.

Tseng, H., and Green, H. (1994). Association of basonuclin with ability of keratinocytes to multiply and with absence of terminal differentiation. J Cell Biol *126*, 495-506.

Tumbar, T., Guasch, G., Greco, V., Blanpain, C., Lowry, W.E., Rendl, M., and Fuchs, E. (2004). Defining the epithelial stem cell niche in skin. Science *303*, 359-363.

Ulrich, F., Krieg, M., Schotz, E.M., Link, V., Castanon, I., Schnabel, V., Taubenberger, A., Mueller, D., Puech, P.H., and Heisenberg, C.P. (2005). Wnt11 functions in gastrulation by controlling cell cohesion through Rab5c and E-cadherin. Dev Cell *9*, 555-564.

van de Wetering, M., Cavallo, R., Dooijes, D., van Beest, M., van Es, J., Loureiro, J., Ypma, A., Hursh, D., Jones, T., Bejsovec, A., *et al.* (1997). Armadillo coactivates transcription driven by the product of the Drosophila segment polarity gene dTCF. Cell *88*, 789-799.

van de Wetering, M., Sancho, E., Verweij, C., de Lau, W., Oving, I., Hurlstone, A., van der Horn, K., Batlle, E., Coudreuse, D., Haramis, A.P., *et al.* (2002). The beta-catenin/TCF-4 complex imposes a crypt progenitor phenotype on colorectal cancer cells. Cell *111*, 241-250.

van den Brink, G.R., Bleuming, S.A., Hardwick, J.C., Schepman, B.L., Offerhaus, G.J., Keller, J.J., Nielsen, C., Gaffield, W., van Deventer, S.J., Roberts, D.J., *et al.* (2004). Indian Hedgehog is an antagonist of Wnt signaling in colonic epithelial cell differentiation. Nat Genet *36*, 277-282.

Van Mater, D., Kolligs, F.T., Dlugosz, A.A., and Fearon, E.R. (2003). Transient activation of beta - catenin signaling in cutaneous keratinocytes is sufficient to trigger the active growth phase of the hair cycle in mice. Genes Dev *17*, 1219-1224.

Vauclair, S., Nicolas, M., Barrandon, Y., and Radtke, F. (2005). Notch1 is essential for postnatal hair follicle development and homeostasis. Dev Biol *284*, 184-193.

Vidal, V.P., Chaboissier, M.C., Lutzkendorf, S., Cotsarelis, G., Mill, P., Hui, C.C., Ortonne, N., Ortonne, J.P., and Schedl, A. (2005). Sox9 is essential for outer root sheath differentiation and the formation of the hair stem cell compartment. Curr Biol *15*, 1340-1351.

Wagers, A.J., and Weissman, I.L. (2004). Plasticity of adult stem cells. Cell *116*, 639-648.

Waikel, R.L., Kawachi, Y., Waikel, P.A., Wang, X.J., and Roop, D.R. (2001). Deregulated expression of c-Myc depletes epidermal stem cells. Nat Genet *28*, 165-168.

Watt, F.M. (1984). Selective migration of terminally differentiating cells from the basal layer of cultured human epidermis. J Cell Biol *98*, 16-21.

Watt, F.M. (2002). Role of integrins in regulating epidermal adhesion, growth and differentiation. Embo J *21*, 3919-3926.

Watt, F.M., Celso, C.L., and Silva-Vargas, V. (2006). Epidermal stem cells: an update. Curr Opin Genet Dev *16*, 518-524.

Watt, F.M., and Green, H. (1982). Stratification and terminal differentiation of cultured epidermal cells. Nature *295*, 434-436.

Watt, F.M., and Hogan, B.L. (2000a). Out of Eden: stem cells and their niches. Science *287*, 1427-1430.

Watt, F.M., and Hogan, B.L. (2000b). Out of Eden: stem cells and their niches. Science *287*, 1427-1430.

Weiner, L., and Green, H. (1998). Basonuclin as a cell marker in the formation and cycling of the murine hair follicle. Differentiation *63*, 263-272.

Willert, K., Brown, J.D., Danenberg, E., Duncan, A.W., Weissman, I.L., Reya, T., Yates, J.R., 3rd, and Nusse, R. (2003). Wnt proteins are lipid-modified and can act as stem cell growth factors. Nature *423*, 448-452.

Wilson, M., and Koopman, P. (2002). Matching SOX: partner proteins and co-factors of the SOX family of transcriptional regulators. Curr Opin Genet Dev *12*, 441-446.

Winklbauer, R., Medina, A., Swain, R.K., and Steinbeisser, H. (2001). Frizzled-7 signalling controls tissue separation during Xenopus gastrulation. Nature *413*, 856-860.

Wolpert, L. (1998). Pattern formation in epithelial development: the vertebrate limb and feather bud spacing. Philos Trans R Soc Lond B Biol Sci *353*, 871-875.

Wolpert L; Beddington R, B.J., Jessell T, Lawrence P, Meyerowitz E (1998). Principles of Development (Current Biology Ltd. Oxford University Press).

Wu, X., Quondamatteo, F., Lefever, T., Czuchra, A., Meyer, H., Chrostek, A., Paus, R., Langbein, L., and Brakebusch, C. (2006). Cdc42 controls progenitor cell differentiation and beta-catenin turnover in skin. Genes Dev *20*, 571-585.

Xu, Q., Mellitzer, G., Robinson, V., and Wilkinson, D.G. (1999). In vivo cell sorting in complementary segmental domains mediated by Eph receptors and ephrins. Nature *399*, 267-271.

Yi, R., O'Carroll, D., Pasolli, H.A., Zhang, Z., Dietrich, F.S., Tarakhovsky, A., and Fuchs, E. (2006). Morphogenesis in skin is governed by discrete sets of differentially expressed microRNAs. Nat Genet *38*, 356-362.

Yu, H., Fang, D., Kumar, S.M., Li, L., Nguyen, T.K., Acs, G., Herlyn, M., and Xu, X. (2006). Isolation of a novel population of multipotent adult stem cells from human hair follicles. Am J Pathol *168*, 1879-1888.

Yu, M., Yue, Z., Wu, P., Wu, D.Y., Mayer, J.A., Medina, M., Widelitz, R.B., Jiang, T.X., and Chuong, C.M. (2004). The biology of feather follicles. Int J Dev Biol *48*, 181-191.

Yue, Z., Jiang, T.X., Widelitz, R.B., and Chuong, C.M. (2006). Wnt3a gradient converts radial to bilateral feather symmetry via topological arrangement of epithelia. Proc Natl Acad Sci U S A *103*, 951-955.

Yuhki, M., Yamada, M., Kawano, M., Iwasato, T., Itohara, S., Yoshida, H., Ogawa, M., and Mishina, Y. (2004). BMPR1A signaling is necessary for hair follicle cycling and hair shaft differentiation in mice. Development *131*, 1825-1833.

Zanet, J., Pibre, S., Jacquet, C., Ramirez, A., de Alboran, I.M., and Gandarillas, A. (2005). Endogenous Myc controls mammalian epidermal cell size, hyperproliferation, endoreplication and stem cell amplification. J Cell Sci *118*, 1693-1704.

Vauclair, S., Nicolas, M., Barrandon, Y., and Radtke, F. (2005). Notch1 is essential for postnatal hair follicle development and homeostasis. Dev Biol *284*, 184-193.

Vidal, V.P., Chaboissier, M.C., Lutzkendorf, S., Cotsarelis, G., Mill, P., Hui, C.C., Ortonne, N., Ortonne, J.P., and Schedl, A. (2005). Sox9 is essential for outer root sheath differentiation and the formation of the hair stem cell compartment. Curr Biol *15*, 1340-1351.

Wagers, A.J., and Weissman, I.L. (2004). Plasticity of adult stem cells. Cell *116*, 639-648.

Waikel, R.L., Kawachi, Y., Waikel, P.A., Wang, X.J., and Roop, D.R. (2001). Deregulated expression of c-Myc depletes epidermal stem cells. Nat Genet *28*, 165-168.

Watt, F.M. (1984). Selective migration of terminally differentiating cells from the basal layer of cultured human epidermis. J Cell Biol *98*, 16-21.

Watt, F.M. (2002). Role of integrins in regulating epidermal adhesion, growth and differentiation. Embo J *21*, 3919-3926.

Watt, F.M., Celso, C.L., and Silva-Vargas, V. (2006). Epidermal stem cells: an update. Curr Opin Genet Dev *16*, 518-524.

Watt, F.M., and Green, H. (1982). Stratification and terminal differentiation of cultured epidermal cells. Nature *295*, 434-436.

Watt, F.M., and Hogan, B.L. (2000a). Out of Eden: stem cells and their niches. Science *287*, 1427-1430.

Watt, F.M., and Hogan, B.L. (2000b). Out of Eden: stem cells and their niches. Science *287*, 1427-1430.

Weiner, L., and Green, H. (1998). Basonuclin as a cell marker in the formation and cycling of the murine hair follicle. Differentiation *63*, 263-272.

Willert, K., Brown, J.D., Danenberg, E., Duncan, A.W., Weissman, I.L., Reya, T., Yates, J.R., 3rd, and Nusse, R. (2003). Wnt proteins are lipid-modified and can act as stem cell growth factors. Nature *423*, 448-452.

Wilson, M., and Koopman, P. (2002). Matching SOX: partner proteins and co-factors of the SOX family of transcriptional regulators. Curr Opin Genet Dev *12*, 441-446.

Zhang, J., Niu, C., Ye, L., Huang, H., He, X., Tong, W.G., Ross, J., Haug, J., Johnson, T., Feng, J.Q., *et al.* (2003). Identification of the haematopoietic stem cell niche and control of the niche size. Nature *425*, 836-841.

Zhu, A.J., Haase, I., and Watt, F.M. (1999). Signaling via beta1 integrins and mitogen-activated protein kinase determines human epidermal stem cell fate in vitro. Proc Natl Acad Sci U S A *96*, 6728-6733.

Zhu, A.J., and Watt, F.M. (1999). beta-catenin signalling modulates proliferative potential of human epidermal keratinocytes independently of intercellular adhesion. Development *126*, 2285-2298.

Zorn, A.M., Barish, G.D., Williams, B.O., Lavender, P., Klymkowsky, M.W., and Varmus, H.E. (1999). Regulation of Wnt signaling by Sox proteins: XSox17 alpha/beta and XSox3 physically interact with beta-catenin. Mol Cell *4*, 487-498.